



universität  
wien

# DISSERTATION

Titel der Dissertation

„Probing of non-oncogene addiction targets in  
leukemia using advanced shRNAmir technology“

Verfasser

Mag. rer. nat. Thomas HOFFMANN

angestrebter akademischer Grad

Doctor of Philosophy (PhD)

Wien, 2015

Studienkennzahl lt. Studienblatt: A 094 490

Dissertationsgebiet lt. Studienblatt: Molekulare Biologie

Betreuerin / Betreuer: Dr. med. Johannes ZUBER

1

---

## Table of Contents

<b>Abstract</b>	<b>VI</b>
<b>Zusammenfassung</b>	<b>VIII</b>
<b>Acknowledgement</b>	<b>X</b>
<b>List of Figures</b>	<b>XII</b>
<b>Abbreviations</b>	<b>XIV</b>

<b>1</b>	<b>Introduction.....</b>	<b>1</b>
1.1	Cancer – a genetically complex and heterogeneous disease .....	1
1.2	Acute myeloid leukemia (AML) – a paradigm for chances and challenges in cancer therapy.....	3
1.3	Targeted cancer therapies exploiting oncogene addiction .....	6
1.4	Non-oncogene addiction (NOA) .....	9
1.5	Targeting cancer metabolism .....	11
1.6	RNAi – an experimentally programmable mechanism of gene suppression .....	16
1.7	Aims of the thesis.....	21

<b>2</b>	<b>Results.....</b>	<b>23</b>
2.1	An shRNAmir screen for identifying non-oncogene addiction targets in AML.....	23
2.1.1	Construction of a customized library for identifying druggable non-oncogene addiction targets in MLL/AF9-driven AML.....	23
2.1.2	Multiplexed comparative negative-selection shRNAmir screening in MLL/AF9;Nras <sup>G12D</sup> -driven AML and immortalized MEF .....	24
2.1.3	Primary hit-validation using single-shRNA assays.....	28
2.2	Characterization of Gart as a non-oncogene addiction target in AML .....	31
2.2.1	Extended genetic validation of RNAi-mediated Gart suppression effects.....	31
2.2.2	Probing the potency and leukemia-selectivity of Gart suppression .....	33
2.2.3	<i>In vivo</i> validation of Gart as a candidate non-oncogene addiction target in AML.....	37
2.3	Gart alterations and addiction in human leukemia .....	42
2.3.1	Gart is amplified and overexpressed in human leukemia .....	42
2.3.2	Human leukemias are broadly addicted to GART expression.....	45
2.4	Towards exploiting GART addiction for leukemia therapy .....	48
2.4.1	GART suppression promotes a rescuable IMP starvation in leukemia .....	48
2.4.2	Comparative analysis of available GART inhibitors.....	51
2.4.3	The AIRS component provides the most promising target for exploiting GART addiction .....	52
2.5	Improvements and new experimental strategies in shRNAmir technology.....	54
2.5.1	Establishment of an optimized miRNA backbone (miR-E).....	55
2.5.2	Development of a scalable shRNAmir reporter assay for quantifying target protein knockdown .....	58
2.5.3	Establishment of a system for multiplexed combinatorial shRNAmir screening.....	62
2.5.4	Establishment of an “all-in-one” allele for Tet-on regulatable ubiquitous gene suppression <i>in vivo</i> .....	65
<b>3</b>	<b>Discussion.....</b>	<b>71</b>
3.1	Fulfilling the promise of negative selection RNAi screening for cancer target discovery .....	71
3.2	GART – a non-oncogene addiction and candidate drug target in leukemia.....	78
<b>4</b>	<b>Material and Methods.....</b>	<b>85</b>

---

4.1	Cloning of shRNAs (miR-30 and miR-E).....	85
4.1.1	Shuttling of shRNAs from existing vectors .....	85
4.1.2	Cloning of miR-30 shRNAs from single stranded DNA oligos .....	86
4.1.3	Cloning of miR-E shRNAs from existing miR-30 vectors and oligos.....	87
4.2	Retroviral packaging.....	87
4.3	Lentiviral packaging.....	88
4.4	Retroviral and lentiviral transduction .....	88
4.5	Plasmids .....	89
4.6	Cell culture and cell lines .....	89
4.7	Multiplexed shRNA screening .....	89
4.8	Scoring of genes and hit calling .....	91
4.9	Fluorescence activated cell sorting (FACS) .....	92
4.10	Antibodies.....	92
4.11	Competitive proliferation assay .....	92
4.12	cDNA rescue studies .....	92
4.13	Western Blot.....	93
4.14	Doubling time .....	94
4.15	Cell cycle analysis by BrdU incorporation .....	95
4.16	FACS staining .....	95
4.17	Determination of IC <sub>50</sub> concentration of different compounds.....	95
4.18	Mice .....	96
4.19	Transplantation of leukemia cell for <i>in vivo</i> studies.....	96
4.20	Mass spectrometric analysis of metabolites .....	96
4.21	Medium throughput sensor assay .....	97
4.21.1	Generation of a stable reporter cell line.....	97
4.21.2	FACS based analysis of shRNA knockdown .....	98
4.22	Generation a new transgenic mouse line .....	99
4.22.1	Cloning of the all-in-one targeting construct.....	99
4.22.2	ECS targeting and verification of positive by southern blot.....	99
4.22.3	Backcrossing, genotyping and analysis of founder mice.....	102

4.23	Transduction and injection of fetal liver cells for leukaemogenesis studies .....	103
<b>5</b>	<b>Appendix .....</b>	<b>106</b>
5.1	Differential scores from 1133 analyzed genes .....	106
5.2	Control shRNAs used in the multiplexed RNAi screen .....	133
5.3	shRNAs used for validation experiments .....	134
<b>6</b>	<b>References.....</b>	<b>138</b>
<b>7</b>	<b>CV .....</b>	<b>166</b>

## Abstract

Acute myeloid leukemia (AML), the most common leukemia subtype accounting for 43% of leukemia deaths, arises from heterogeneous and dynamic patterns of driver mutations, most of which remain undruggable. Despite their diversity, individual mutations converge to dysregulate a limited number of cellular processes, which is thought to result in leukemia-specific dependencies. Strategies aimed at exploiting “non-oncogene addiction” to chromatin and cell-cycle regulators have recently shown promise in a wide range of AML subtypes. To accelerate the search for rapidly translatable non-oncogene addiction targets, we have constructed a custom shRNA library targeting 1133 candidate genes including known targets of established small-molecule inhibitors and tool compounds as well as potentially druggable genes that were found overexpressed in high-risk MLL-rearranged AML. Using multiplexed screens in an MLL-AF9;Nras<sup>G12D</sup>-driven AML mouse model and murine embryonic fibroblasts, we identify and validate a set of non-essential genes whose suppression triggers dramatic anti-leukemic effects. Strikingly, among the ten most potent leukemia-specific sensitivities, we identify five genes involved in diverse metabolic processes.

Both in the primary screen and secondary validation studies in murine and human AML contexts, shRNA-mediated suppression of GART, a tri-functional enzyme in *de novo* purine synthesis, turned out to be the most prominent leukemia-specific vulnerability. Remarkably, side-by-side comparisons to previously proposed and established targets (including BRD4, PLK1 and various metabolic targets), reveal that the potency and leukemia-specificity of these effects are unmatched. Interestingly, available antifolate inhibitors of GARTase (catalyzing the second GART-dependent enzymatic step), do not phenocopy the effects of shRNA-mediated GART suppression. In addition, several cDNA rescue experiments with mutated versions of Gart suggests that the GARTase activity does not represent the key bottleneck in AML and the AIRS activity should be targeted for a potential new therapy. Importantly, GART is located on chr21 in a region commonly amplified in pediatric B-ALL, suggesting that GART may have driver functions in iAMP21<sup>+</sup> and Down syndrome-associated leukemia. Furthermore, reanalysis of expression profiling studies reveal that GART is one of the most commonly overexpressed genes in a wide variety of hematopoietic and other malignancies. In summary, our study identifies inhibition of GART as promising strategy to therapeutically exploit the increased demand for nucleotide building blocks, which has been proposed as a hallmark of cancer cell metabolism.





## Zusammenfassung

Akute myeloische Leukämie (AML) ist die häufigste Form der Leukämie und verantwortlich für 43% aller Leukämiefälle. Sie entsteht durch das Zusammenspiel von heterogenen und dynamischen Mutationen von denen die meisten nicht gezielt inhibiert werden können. Trotz der großen Vielfalt an Mutationen werden davon nur einige wenige zelluläre Prozesse beeinflusst, was zur Entstehung von Leukämie spezifischen Abhängigkeiten führt die für eine klinische Intervention ausgenützt werden können. Vor allem im Bereich der Regulation des Chromatinstatus einer Zelle und bei der Regulation des Zellzyklus haben Strategien die diese Oncogen unabhängigen Schwachstellen von Krebszellen ausnützen schon vielversprechende Resultate in der klinischen Forschung gezeigt. Um die Entwicklung neuer Therapieansätze zu beschleunigen haben wir eine Sammlung von shRNAs gegen 1133 Gene zusammengestellt für die es entweder schon Inhibitoren gibt, die potentiell inhibierbar sind oder die in humanen Leukämien mit MLL Fusionsprotein dereguliert sind. Mittels einem gebündelten RNA Interferenz Screen in einem MLL-AF9;Nras<sup>G12D</sup>-AML Mausmodell und in immortalisierten Fibroblasten haben wir mehrere Gene identifiziert deren Inhibierung Leukämie spezifische Effekte zeigt. Interessanterweise sind unter den Top 10 Genen 5, die in grundlegende metabolische Prozesse in der Zelle involviert sind.

Sowohl im primären Screen, als auch bei der sekundären Validierung von top Genen in murinen und humanen Kontexten zeigt sich Gart, ein trifunktionales Enzym in der *de novo* Purinsynthese, als markanteste Schwachstelle. Parallele Vergleiche zu etablierten Genen wie BRD4, PLK1 und anderen metabolischen Genen zeigen, dass der Leukämie spezifische Effekt von Gart deutlich stärker ist als bei allen anderen bisher untersuchten Genen. Interessanterweise können Inhibitoren die die GARTfase Aktivität von Gart inhibieren, diese Effekte nicht reproduzieren. Zusammen mit Erkenntnissen aus Experimenten mit mutierten Gart-cDNAs deutet alles drauf hin, dass die AIRS Aktivität für neue AML Therapieansätze in Betracht gezogen werden sollte. Des weiteren liegt GART auf Chromosom 21, in einer Region die in pädiatrischen Leukämien oft amplifiziert ist, was bedeuten könnte, dass Gart auch zur Leukämieentstehung beiträgt. Die Analyse von publizierten Expressionsdaten zeigt, dass Gart im Gegensatz zu normalem Gewebe oft überexprimiert ist, besonders in hämatopoetischen Tumoren. Zusammenfassend kann man sagen, dass die Inhibition von Gart einen vielversprechenden neuen Therapieansatz darstellt, der drauf beruht den erhöhten Bedarf an Nukleotidbausteinen in Krebszellen auszunützen.



## Acknowledgements

First of all, I would like to thank Dr. Johannes Zuber for giving me the opportunity to work in his lab. His enthusiasm for science and the ability to assign the best fitting projects to every student and postdoc makes his lab a demanding but fun place to work. His relentless drive to answer new biological questions and his unbelievable disregard for sleep never ceases to amaze all of us.

Furthermore, I would like to thank all past and present members of the Zuber lab for many hours of scientific and nonscientific discussions and for making the lab an always buzzing environment, independent of the time of day or night.

I would like to thank my parents for making it possible for me to go to university and for all the support throughout the years. Although I had to scrape off remnants of exploding strawberry wine from the walls in my parent's basement and several floods on the terrace, my family always supported my decision to attend a school for chemistry and biochemistry and later to study molecular biology in Vienna.

At this point, I also want to thank my wonderful fiancé, and soon to be wife, Babsi. She had to endure many lonely evenings and weekends because I was running late, over and over again. She buffered numerous mood swings, caused by failed experiments or my general dissatisfaction with my situation as a whole. There is no way to sufficiently express my gratitude for your support over the last couple of years.

In addition, I would like to thank my PhD thesis committee members Daniel Gerlich and Stefan Nijman for many good suggestions early on in my PhD project and for reminding me several times to focus more on my main project.

I am also thankful to the staff from all the IMP scientific services and the CSF who make the IMP a perfect place to make good science. They always have an open ear for new ideas and try to make our experiments possible. Special thanks goes also to all animal care takers from the IMP/IMBA

mousehouse, especially Manuela. Their hard work and diligence enables us to perform animal experiments on the highest quality level possible.

Last but not least, I would like to thank all my friends for never giving up on me although I had to neglect them on many different occasions. Poker and movie nights never happened as often as I wanted to because I was usually too busy. Many of you encouraged me to keep going when I was in doubt but also reminded me that there are more things in life than just working all the time.

*“Progress in science relies on two prerequisites:  
good questions and good answers.”*

[Dr. Ernst-Ludwig Winnacker]

## List of Figures

Figure 1.1   Circos plot showing a panoramic view of genetic events leading to the pathogenesis of AML.....	5
Figure 1.2   Usage of metabolic pathways in different cell states .....	11
Figure 1.3   Endogenous miRNA pathway and entry points for synthetic RNAi triggers used for experimental RNAi .....	18
Figure 2.1   Schematic of the parallel multiplexed, negative-selection RNAi screen in RN2 and RMEF. ....	24
Figure 2.2   Correlation between replicates of the complete MLL-1000 library including all 9 subpools.....	25
Figure 2.3   Performance of control shRNAs in all subpools.....	26
Figure 2.4   A pooled, multiplexed RNAi screen identifies several AML specific vulnerabilities. .	27
Figure 2.5   Competitive proliferation assays for single shRNA validation. ....	29
Figure 2.6   Primary validation of shRNAs targeting top scoring genes. ....	30
Figure 2.7   Evaluation of additional Gart shRNAs in RN2 and RMEF. ....	31
Figure 2.8   Overexpression of a Gart cDNA completely rescues the lethal phenotype in RN2. ..	32
Figure 2.9   Analysis of cellular effects upon Gart knockdown. ....	35
Figure 2.10   Analysis of differentiation markers upon Gart knockdown. ....	36
Figure 2.11   Comparison of the effects of Gart knockdown to the effects of many proposed cancer targets. ....	37
Figure 2.12   Validation of Gart knockdown effects <i>in vivo</i> . ....	39
Figure 2.13   <i>In vivo</i> rescue of the Gart phenotype.....	41

Figure 2.14   GART is frequently amplified in human cancer. ....	43
Figure 2.15   Analysis of GART expression in cancer cell lines and normal tissue.....	44
Figure 2.16   Gart has no driver function in murine MLL/ENL and AML-Eto driven leukaemogenesis. .....	45
Figure 2.17   Evaluation of GART knockdown in human MOLM-13R cells. ....	46
Figure 2.18   Evaluation of GART suppression in various different human cell lines. ....	47
Figure 2.19   Proteins and intermediates involved in <i>de novo</i> purine synthesis.....	49
Figure 2.20   Mass spectrometric analysis of IMP levels upon Gart knockdown. ....	49
Figure 2.21   Hypoxanthine rescues the Gart knockdown phenotype. ....	50
Figure 2.22   IC <sub>50</sub> curves of different Gart inhibitors in RN2s and RMEFs. ....	52
Figure 2.23   cDNA rescue experiments with different Gart mutants identify AIRS as the bottleneck activity. ....	53
Figure 2.24   Restoration of a conserved motive in the miR-30 backbone enhances shRNA processing.....	56
Figure 2.25   Comparison of biological effects of miR-30 and miR-E embedded shRNAs.....	57
Figure 2.26   Sensor assay for medium throughput validation of shRNAs. ....	60
Figure 2.27   Vector and cloning scheme of a system for combinatorial RNA. ....	63
Figure 2.28   Biological effects of single and combinatorial shRNAs. ....	64
Figure 2.29   Generation of 3G-all-in-one shRNA transgenic mice.....	67
Figure 4.1   Schematic set-up of a wet transfer southern blot.....	101

## Abbreviations

A	ampere [unit]
ACN	acetonitril
ADP	adenosine diphosphate
AML	acute myeloid leukemia
APL	acute promyelocytic leukemia
ATP	adenosine tri-phosphate
ATRA	all-trans retinoic acid
B-ALL	B-cell acute lymphoblastic leukemia
BD	Becton Dickinson
BET	bromodomain and extraterminal domain family
bp	base pair
BSA	bovine serum albumin
CAG promotor	CMV early enhancer/chicken $\beta$ actin promotor
cDNA	complementary DNA
CDS	coding sequence
CIP	calf intestinal alkaline phosphatase
CML	chronic myeloid leukemia
CMML	chronic myelomonocytic leukemia
CO <sub>2</sub>	carbon dioxide
co-RNAi	combinatorial RNAi
CRISPR	clustered regularly interspaced short palindromic repeats
CTCL	cutaneous T cell lymphoma
DAPI	4',6-diamidino-2-phenylindole
DCA	dichloroacetate
DHFR	dihydrofolate reductase
DMEM	Dulbecco's modified eagle medium
DMSO	dimethyl sulfoxide
DNA	deoxyribonucleic acid
DNMT	DNA methyltransferases
dNTP	deoxynucleotide
dox	doxycycline
DR	drug resistance
DSB	double strand break
dsRNA	double stranded RNA
EGCG	epigallocatechin gallate

EGFR	epidermal growth factor receptor
ESC	embryonic stem cell
EtOH	ethanol
F	farad [unit]
FACS	fluorescence-activated cell sorting
FASN	fatty acid synthetase
FD	fold depletion
FDA	food and drug administration
FDG	fluorodeoxyglucose
FLC	fetal liver cell
fwd	forward
FT	farnesyl transferase
GDH	glutamine dehydrogenase
GFP	green fluorescent protein
GLS	glutaminase
Gy	gray [unit]
HBS	HEPES-buffered saline
HBSS	Hank's balanced salt solution
HDAC	histone deactylase
HEPES	4-(2-hydroxyethyl)-1-piperazineethanesulfonic acid
HPLC	high pressure liquid chromatography
HSPC	hematopoietic stem and progenitor cells
HTS	high throughput sampler
IC <sub>50</sub>	half maximal inhibitory concentration
IDT	integrated DNA technologies Inc.
IL	interleukin
IMDM	Iscove's modified eagle's media
IMP	inosine monophosphate
IRES	internal ribosome entry site
kDa	kilo Dalton
LC	liquid chromatography
LSC	leukemia stem cell
M	molar [unit, mol/l]
MCS	multiple cloning site
MCT1	monocarboxylate transporter 1
MeOH	methanol
miRNAs	micro-RNAs
mRNA	messenger RNA



---

MS	mass spectrometry
NOA	non-oncogene addiction
OA	oncogene addiction
PAM	protospacer adjacent motif
PCR	polymerase chain reaction
PEP	phosphoenolpyruvate
piRNA	piwi-interacting RNA
Pol II	RNA polymerase II
Pol-III	RNA polymerase III
Puro	Puromycin
qRT-PCR	quantitative reverse-transcription PCR
RAR $\alpha$	retinoic acid receptor alpha
rev	reverse
RISC	RNA-induced silencing complex
RNA	ribonucleic acid
RNAi	RNA interference
RNA-seq	RNA sequencing
RNR	ribonucleotide reductase
RPE	retinal pigment epithelium
rtTA	reverse Tet-transactivator
SCF	stem cell factor
SDS	sodium dodecyl sulfate
SFFV	strong spleen focus forming virus
shRNA <sup>mir</sup>	miRNA-embedded shRNA
shRNAs	short hairpin RNA
siRNA	short interfering RNA
SSC	saline sodium citrate
TBST	tris-buffered saline with Tween20
TGF- $\beta$	tumor growth factor beta
U	unit
UI	uninfected
UV-light	ultra violet light
V	volt [unit]
XPO5	exportin 5

Abbreviations of gene and protein names that are not listed here can be found in publicly accessible databases such as UCSC or UNIPROT.



# 1 Introduction

## 1.1 Cancer – a genetically complex and heterogeneous disease

Cancer is a complex malignant disease that can arise from almost every tissue in the human body. So far, more than 200 different cancer types are known. After cardiovascular diseases, cancer is the second most common cause of death worldwide (Bray, Ren, Masuyer, & Ferlay, 2013a). The most common cancer types include lung, colon, breast and prostate cancer, together accounting for almost 50% cancer deaths in the United States (Siegel, Miller, & Jemal, 2015).

Cancer is defined as an aberrant growth of cells with subsequent invasion of neighboring tissue or even spreading to another site in the body, called metastasis. Since cell growth is tightly controlled in healthy tissues, a cell has to acquire several new properties in order to be transformed into a cancer cell. Hanahan and Weinberg describe six “hallmarks of cancer” in their hallmark paper in 2000 (Hanahan, Weinberg, & Francisco, 2000), which include (I) self-sufficiency in growth signals, (II) loss of sensitivity to anti-growth signals, (III) loss of capacity for apoptosis and (IV) senescence. Beyond these features enabling cells to grow and replicate infinitely, cancer cells need to acquire (V) the ability to induce angiogenesis to supply newly formed tumor tissue with nutrients and oxygen. The last hallmark (VI) is the loss of contact inhibition, which enables cells to grow out of their normal boundaries and invade neighboring tissue. In 2011, the hallmarks of cancer were expanded and several new concepts were introduced (Hanahan & Weinberg, 2011). These include a reprogramming of energy metabolism, the evasion of immune surveillance, and the ability to recruit and utilize neighboring normal tissue for assembling the tumor microenvironment. Furthermore it has become apparent that tumorigenesis often involves various forms of cellular stress such as proteotoxic stress caused by aberrant activation of the heat shock response or DNA damage, as well as replication stress caused by fast and uncontrolled cell division (J. Luo, Solimini, & Elledge, 2009).

With development of advanced deep-sequencing technologies, a new era of cancer research began in 2008 (Bentley et al., 2008; Wheeler et al., 2008), and soon a case of acute myeloid leukemia (AML) described the first cancer genome (Ley et al., 2008). Meanwhile, deep-sequencing has been applied to identify cancer mutations in more than 20,000 whole cancer genomes and over 1 million individual tumors using targeted sequencing approaches (S. A. Forbes et al., 2014). Together, these efforts led to the identification of over 3 million individual protein coding mutations and more than 10,000 fusion proteins. While most of these mutations are regarded as “passenger mutations” that are not causative for the cancer phenotype (Pleasant et al., 2010), more than 500 recurrently mutated genes (i.e. almost 2% of all human genes) have been implicated as functionally relevant “cancer drivers” (Futreal et al., 2004). The main categories of driver lesions are activating mutations in proto-oncogenes and deactivating mutations or epigenetic silencing of tumor suppressor genes. Genomic instability can lead to DNA double strand breaks and, subsequently, chromosomal translocations that can result in the expression of fusion proteins, which due to their complex cellular effects can be viewed as a third driver category (Haber & Settleman, 2007; Stratton, Campbell, & Futreal, 2009).

Besides shedding light on the heterogeneity of cancer driver mutations, deep sequencing has also revealed that individual cancer genomes are extremely complex and typically involve several to dozens of driver mutations. Interestingly, it has been found that the number of driver mutations varies greatly among different tumor types. Melanomas, lung and colon tumors carry up to 200 protein altering mutations (Govindan et al., 2012). All these tumor types are associated with mutagens like UV-light or carcinogenic chemicals in tobacco smoke or the daily diet, partly explaining the phenomenon of extremely high mutation content. Cancers with defects in the DNA mismatch repair machinery are also prone to accumulate lots of mutations over time (Muzny et al., 2012; Palles et al., 2013). On the other end of the spectrum there are tumors with rather low complexity and only a few driver mutations. Many different leukemias fall into this category, together with most pediatric tumors and some very rare rhabdoid tumors (Donner, Wainwright, Zhang, & Biegel, 2007).

Cancer driver mutations do not occur all at once but accumulate over time and thereby slowly develop the malignant phenotype. It has been estimated that every single driver mutation mediates only a very small selective advantage to the cell (Bozic et al., 2010) but the combination of effects of several mutations favors the outgrowth of a tumor eventually (Fearon & Vogelstein,

1990; Nowell, 1976). Early studies estimated that 6-7 mutations are needed for cancer development (Armitage & Doll, 1954; Nordling, 1953) but more recent studies could show that in some contexts even 3 mutations are enough to transform a cell into a cancer cell (Tomasetti, Marchionni, Nowak, Parmigiani, & Vogelstein, 2015). Longitudinal and subclone analyses suggest, that the origin of cancer is laid by a small number of founder mutations, but the full-blown disease only breaks out when multiple mutations have been accumulated (Bozic et al., 2010). Another consequence of the stepwise accumulation of genetic aberrations is intratumoral heterogeneity. This means that one tumor mass can consist of groups of cells with partly different driver mutations which poses an additional challenge for the development of targeted therapies. A tumor can only be cured if all subclones are eradicated. It could be shown in several studies in leukemia and other tumors that if one subclone in the population is resistant to the treatment it will evade therapy and relapse eventually. Whole genome sequencing of AML samples before treatment and at the time of relapse revealed a clonal evolution of clones which have acquired new mutations, rendering them resistant to therapy (Ding et al., 2012).

These studies underline once more the importance of understanding the underlying mechanisms of cancerous transformation in order to be able to develop new therapies targeting common transforming events or newly acquired dependencies of all subclones.

## **1.2 Acute myeloid leukemia (AML) – a paradigm for chances and challenges in cancer therapy**

Recent advances in whole genome sequencing of many different human cancers reveal that genetic aberrations in tumors are extremely complex and heterogeneous. Even individual tumors are typically composed of a plethora of genetically diverse subclones. The first cancer genome (Ley et al., 2008), as well as many other key discoveries and paradigms in cancer biology, derive from studies in leukemia - a diverse group of blood cancers that affect approximately 300,000 new patients every year worldwide (Bray, Ren, Masuyer, & Ferlay, 2013b). Despite our advanced genetic knowledge, about 75% of leukemia patients cannot be cured with existing therapies, which is the fifth highest fatality rate of all major cancers (Bray et al., 2013b). In the ongoing search for better therapies two specific leukemia subtypes, chronic myeloid leukemia (CML) and acute promyelocytic leukemia (APL), have provided the first and still most impressive examples how targeted drugs can turn incurable cancer into a manageable condition (B J Druker et al., 2001; Huang et al., 1988). In both CML and APL, the presence of a druggable, functionally dominant oncogene

(BCR-ABL and PML-RARA, respectively), is the reason for the overall success. This is an exceptional scenario, since most leukemias (and other cancers) are genetically more complex. Functional co-operation of multiple driver mutations, most of which remain “undruggable”, impede the search for new therapy strategies even more.

Acute myeloid leukaemia (AML) is characterized by anomalous proliferation and differentiation of malignant myeloid progenitors, which rapidly accumulate and aggressively replace normal bone marrow resulting in severe hematopoietic insufficiency and frequently in peripheral hyperleukocytosis. The incidence of AML is about 3.7 in 100.000 (Greenlee, Hill-Harmon, Murray, & Thun, 2001). This means that approximately 12.000 men and women will be diagnosed with AML in the US per year (American Cancer Society. Cancer Facts and Figures 2005. Atlanta: American Cancer Society; 2005). Despite the growing amount of data trying to explain the causative mutations and mechanisms in AML, this knowledge has not yet translated into new therapies and the majority of patients will die from their disease (Rowe & Tallman, 2010). More than 100 driver mutations which occur in countless combinations have been identified since the sequencing of the first cancer genome. However, the functional relevance of identified alleles is still poorly understood (S. a. Forbes et al., 2009; Gilliland, Jordan, & Felix, 2004). In addition, recent studies in relapsed AML reveal that individual leukemias clonally evolve in a highly dynamic and adaptive process, which can alter their sensitivity to conventional and targeted therapies even during treatment (Walter et al., 2012; Welch et al., 2012). While the vast genetic complexity poses a daunting challenge for the development of targeted therapies, diverse driver mutations converge functionally to deregulate only a very limited number of cellular pathways and processes in order to establish the cancerous transformation. While only a minority of driver mutations is amenable to drug therapy, druggable key molecules in these convergent effector programs are predicted to provide alternative and more generally applicable therapeutic targets. The first main aberrant pathomechanism in leukemia is the deregulation of cytokine-dependent signaling pathways, which are commonly activated due to recurrent mutations in cell-surface receptors (e.g. FLT3, KIT, IL7R) or intracellular signaling molecules (e.g. KRAS, NRAS, ABL1, NF1, PTPN11, JAK2) (Figure 1.1). Based on the success of BCR-ABL inhibitors and our relatively advanced mechanistic understanding, signaling pathways have been a major focus in recent drug development, which has led to the identification of several potent inhibitors of signaling molecules (e.g. FLT3, BRAF, MEK, PI3K, JAK2). Although these compounds so far have shown limited success in the clinic, they might become valuable components in combinatorial strategies.

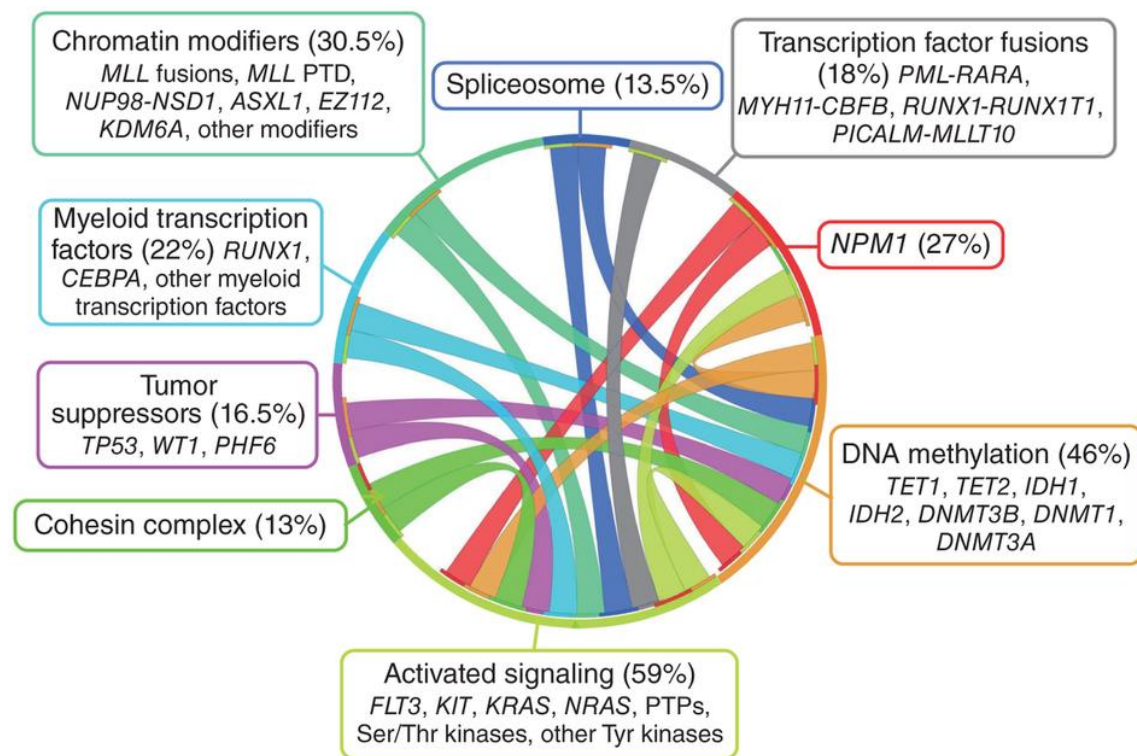


**Figure 1.1 | Circos plot showing a panoramic view of genetic events leading to the pathogenesis of AML.**

(S.-J. Chen, Shen, & Chen, 2013)

The second key event in leukemogenesis is the corruption of cell-fate programs and the establishment of aberrant self-renewal abilities in normal committed progenitor cells (Figure 1.1). This has been linked to mutations involving several transcriptional master regulators in hematopoiesis (e.g. AML1, GATA3, CEBPA, RARA, MLL, PAX5, IKZF1 and NOTCH1) (Pedersen-Bjergaard, Andersen, & Andersen, 2007). The great therapeutic potential of suppressing aberrant self-renewal programs has been demonstrated in genetically engineered mouse models (Demarest, Dahmane, & Capobianco, 2011; Horton et al., 2009; J Zuber et al., 2011) as well as in the clinical treatment of APL, where all-trans retinoic acid (ATRA) and arsenic trioxide synergize to degrade the PML-RARA fusion protein and induce durable remissions in >90% of patients (de Thé & Chen, 2010). While other drivers of this class remain undruggable and the downstream mechanisms involved in establishing aberrant self-renewal poorly understood, this process has been linked to global changes in the epigenetic landscape (J. Chen, Odenike, & Rowley, 2010). Several common oncogenes such as MYC, AML1-ETO, PML-RARA and MLL fusions proteins induce aberrant self-renewal, at least in part, through dysregulation of epigenetic pathways (Krivtsov et al., 2008; Villa et al., 2007; J Wang,

Hoshino, Redner, Kajigaya, & Liu, 1998). Moreover, recurrent somatic mutations in various epigenetic regulators involved in DNA methylation (e.g. DNMT3A, TET2, IDH1/2), histone methylation (e.g. MLL2, EZH2, SUZ12, JARID1A, UTX, ASXL1) and histone acetylation (e.g. CBP, p300) are among the most prominent and surprising findings of recent genome-sequencing studies in different leukemias (Dawson & Kouzarides, 2012; Geutjes, Bajpe, & Bernards, 2012; Shih, Abdel-Wahab, Patel, & Levine, 2012; Zhang et al., 2012). While the precise mechanisms underlying their prominent role in human leukemogenesis are still unknown, several mutations including TET2, DNMT3A and IDH1 have already been shown to promote self-renewal abilities in hematopoietic progenitors and may provide new therapeutic opportunities to target this program (Challen et al., 2011; Kunitomo et al., 2012; Sasaki et al., 2012).

Mouse models of AML have greatly facilitated the discovery of molecular key players in leukemogenesis and the evaluation of new therapeutic concepts. Currently, dozens of new lesion-based substances and even more drug combinations are pending to be evaluated. Performing such screenings directly in clinical trials is neither feasible nor ethically acceptable. *In vitro* models fail to engage decisive issues such as microenvironment, invasiveness and angiogenesis in AML. Most importantly, it has been observed that drug response programs and resistance mechanisms are often severely altered in tumor derived cell lines and completely missed in clonogenic survival assays (Schmitt, Rosenthal, & Lowe, 2000). Transgenic murine AML models provide intermediate experimental systems between cell culture and patient analysis that are experimentally tractable and take both malignant blasts and their microenvironment into account.

In the study at hand we use a MLL-AF9;Nras<sup>G12D</sup> driven AML mouse model as a means to discover new potential therapy strategies in this unique form of cancer. Cases of patients with complete remission after chemotherapy treatment show that a cure is generally possible but new and more focused treatments are needed in order to increase overall survival rates in AML patients (Ju, Hong, & Shin, 2014).

### **1.3 Targeted cancer therapies exploiting oncogene addiction**

Many studies show that cancer cells not only rely on genetic lesions for the establishment but also for the maintenance of the transformed state. This discovery has coined the term “oncogene addiction” (OA) and opened up a new way of thinking about targeted therapies (Weinstein & Joe, 2008). Despite setbacks in the development of new cancer therapies, the groundbreaking advances that oncogene-targeted therapies have provided in the treatment of some cancer subtypes



impressively showcases the validity and potential of exploiting oncogene addiction (J. Luo, Solimini, et al., 2009). The first major breakthrough was the development of Imatinib (Gleevec/Glivec), a small-molecule kinase inhibitor with potent activity against the oncogenic BCR-ABL fusion protein, the major driving oncogene in chronic myeloid leukemia (CML) (Schindler et al., 2000; Zimmermann, Buchdunger, Mett, Meyer, & Lydon, 1997). Since its discovery, Imatinib has changed the lives of tens of thousands of CML patients. With this new treatment option, the 5-year survival rate of CML has increased from 30% to 89%, thus transforming an almost untreatable disease into a manageable condition (Brian J Druker et al., 2006). Other examples of successful targeted therapy include Gefitinib (Iressa) and Erlotinib (Tarceva), both inhibiting the tyrosine kinase domain of epidermal growth factor receptor (EGFR) (Sharma, Bell, Settleman, & Haber, 2007). These drugs show efficacy in the treatment of certain forms of lung and breast cancer, as well as solid tumors such as pancreatic cancer.

The most dramatic improvement in the therapy of acute leukemias has been achieved by the discovery of all-trans retinoic acid (ATRA, Vesanoid, Tretinoin) and arsenic trioxide ( $\text{As}_2\text{O}_3$ ) as effective targeted agents in the treatment of acute promyelocytic leukemia (APL) (Tallman & Altman, 2008). APL is characterized by the presence of a chromosomal translocation between the long arms of chromosomes 15 and 17,  $t(15;17)(q22;q12)$ , resulting in a fusion oncoprotein that involves two transcriptional regulators (PML and  $\text{RAR}\alpha$ ) and promotes aberrant self-renewal capacities to myeloid progenitors (Z Chen & Chen, 1992). A combination of ATRA and  $\text{As}_2\text{O}_3$  has been found to trigger the degradation of the PML- $\text{RAR}\alpha$  fusion protein, leading to a rapid disease clearance by enforcing terminal differentiation of leukemic blasts. Using this combination therapy, a complete and durable remission can be achieved even without chemotherapy in about 90% of patients suffering from this otherwise highly fatal malignancy (de Thé & Chen, 2010).

Unfortunately, not all attempts to target oncogenes directly have led to such breakthroughs in the clinic. Following the example of Imatinib, a major focus of global drug development efforts has been on small-molecule inhibitors of kinases acting as direct drivers or downstream effectors in oncogenic signaling cascades. Kinases transfer phosphate groups, from mostly ATP, to serine, threonine and tyrosine residues of target proteins, and thereby act as cellular on and off switches that regulate the activity, cellular localization and binding ability of their target proteins. A small-molecule inhibitor binds the enzymatic pocket with higher affinity than the natural substrate, thus inhibiting the kinase function. However, due to structural similarities, kinase inhibitors typically bind and inhibit several kinases, which complicates the development of these agents and often

triggers side-effects. A major problem in the clinical use of kinase inhibitors is the rapid development of drug resistance, which can arise through various mechanisms including (1) mutations of the drug binding pocket that block the effective inhibitor binding, (2) compensatory mutations in other up- or downstream signaling molecules in the same pathway, and (3) the activation of compensatory parallel signaling pathways.

A prominent example for drug resistance caused by pocket mutations is Imatinib. Despite the fact that it has revolutionized the treatment of CML not all patients show longterm treatment benefits (Bhamidipati, Kantarjian, Cortes, Cornelison, & Jabbour, 2013). It was shown that a single point mutation in the ATP binding pocket can completely abrogate the binding of Imatinib to BCR-ABL. To conquer this problem, several second and third generation inhibitors were developed which are able to bind even BCR-ABL in imatinib resistant cells (Reddy & Aggarwal, 2012). In 2013, it was shown that the loss of NF1 in melanoma cells leads to resistance to the BRAF-V600E mutation specific inhibitors Sorafenib and Vemurafenib (Ascierto et al., 2012) (Whittaker et al., 2013). Rene Bernhards and his team showed in 2014 that resistance to BRAF-V600E inhibitors can also be mediated by aberrant activation of TGF- $\beta$  signaling in melanoma cells which is caused by loss or downregulation of SOX10 (Sun et al., 2014).

Beyond challenges in targeting oncogenic kinases, other efforts to develop targeted therapies exploiting oncogene addiction have mostly failed so far (Vivanco, 2014). The Ras oncogene is mutated in up to 33% of all cancers but so far there has been no inhibitor found which directly blocks mutated Ras (Baines, Xu, & Der, 2011). Strategies to inhibit farnesyl transferase (FT) in order to prevent Ras from being anchored to the cell membrane have shown only very weak therapeutic effects but high side effects because many proteins are substrates of FT (Russo, Loprevite, Cesario, & Ardizzone, 2004).

Besides the large number of mutations in tumor suppressor genes that remain unamenable to drug modulation, the structural properties of many oncogenes pose a challenge for the development of small-molecule inhibitors. One important example is MYC, which is amplified, mutated or overexpressed in more than 50% of human cancers. While MYC was long regarded as undruggable, several candidate molecules have been suggested as direct MYC inhibitors (Kiessling, Wiesinger, Sperl, & Berg, 2007; Huabo Wang et al., 2007). In addition, alternative approaches aimed at destabilizing the MYC (S. S. Wang et al., 2014) or blocking MYC transcription (Snyder, Ray, Blume, & Miller, 1991) have shown promise in pre-clinical studies.

Despite these advances, the vast majority of driver mutations remains undruggable to date, and the complexity of cancer genomes and the rapid development of drug resistance pose a daunting challenge for the development of more effective oncogene-targeted therapies.

#### **1.4 Non-oncogene addiction (NOA)**

The transformation of normal tissue into a cancerous state is accompanied by a plethora of regulatory changes within the cell, which can be direct or indirect consequences of genetic driver mutations. Importantly, despite the vast degree of genetic heterogeneity and complexity, individual driver mutations converge at the functional level to dysregulate a limited number of cellular processes. On the genetic level, this is reflected in the phenomenon of mutual exclusivity, which describes the observation that mutations with similar oncogenic functions almost never co-occur. In AML, several mutations are well known to be mutually exclusive, including mutations in (1) components of Ras signaling pathways such as FLT3, NRAS, KRAS and NF1 (Grossmann et al., 2013), (2) TET2 and IDH1/2, both leading to similar changes in DNA methylation (Figueroa et al., 2010), and (3) different mutations in components of the cohesion complex (Kon et al., 2013; Thol et al., 2014). The functional convergence of driver mutations and the common dysregulation of basic cellular processes is thought to create cancer-specific dependencies on genes that are not mutated or in any other way altered, but simply required for the survival of cancer cells. This phenomenon has been termed non-oncogene addiction (NOA) (J. Luo, Solimini, et al., 2009; Solimini, Luo, & Elledge, 2007).

While the concept of NOA has only been established a few years ago, some of the most promising candidate therapeutic targets currently pursued in pre-clinical and clinical studies exploit the phenomenon of NOA. Among numerous efforts, ongoing academic and commercial research is particularly focused on NOA targets in two cellular processes that are frequently altered in cancer: chromatin regulation and metabolism. The first and clinically most advanced chromatin-associated NOA targets are histone deacetylases (HDACs), a class of enzymes that erase histone acetylation marks (Mottamal, Zheng, Huang, & Wang, 2015; West & Johnstone, 2014). Vorinostat and Romidepsin are FDA-approved drugs applied in the treatment of cutaneous T cell lymphoma (CTCL), a class of non-Hodgkin lymphoma (Duvic et al., 2007; Piekarz et al., 2009). In addition, HDAC inhibitors are being clinically assessed in other cancer subtypes, e.g. Etenostat in melanoma (Gore et al., 2008), Panobinostat in prostate cancer (Younes et al., 2012), and Chidamide in solid tumors and lymphoma (Dong et al., 2012).

Another class of already FDA-approved chromatin-targeted therapeutics are inhibitors of DNA methyltransferases (DNMTs), which methylate cytosines at position 5, usually in the context of a CpG dinucleotide (Robertson & Jones, 2000). 60% of gene promoters contain CpG islands and, if methylated, the corresponding gene is usually only expressed at low levels due to decreased recognition by transcription factors (Y. Wang & Leung, 2004). These epigenetic alternations are reversible and it was shown that inhibition of DNA methylation can lead to reexpression of tumor suppressors in various cancer cells (Prendergast & Ziff, 1991). Vidaza (5-azacytidine) and Dacogen (decitabine or 5-aza-20-deoxycytidine) (Daskalakis et al., 2013; Issa et al., 2004) are approved for the treatment of myelodysplastic syndrome (MDS), AML and chronic myelomonocytic Leukemia (CMML). However, these two DNMT inhibitors are not selective towards specific DNMT classes and are associated with serious side-effects, like renal toxicity and myelotoxicity (P. W. Wijermans, Lübbert, Verhoef, Klimek, & Bosly, 2005; P. Wijermans et al., 2000) underlining once more the need for the development of more selective and specific inhibitors.

A recently discovered target that has shown promise in numerous cancer subtypes is BRD4, a chromatin reader that binds acetylated lysine residues on histones via two BET bromodomains and, in turn, recruits the pTEFB complex to promote transcriptional elongation (Moon et al., 2005). BRD4 was identified as a chromatin-associated NOA target using a genetic screen in an MLL/AF9;Nras<sup>G12D</sup>-driven mouse model of AML (Johannes Zuber, Shi, et al., 2011), which led to the testing of JQ1, a small-molecule BET bromodomain inhibitor (Filippakopoulos et al., 2010) in this disease context. Similar to effects observed after RNAi-mediated BRD4 suppression, JQ1 displayed strong anti-leukemic effects in a wide range of AML subtypes. At least in part, these effects are based on the requirement of BRD4 for transcription of MYC, which implicated JQ1 as the first pharmacologic approach to potently suppress this oncogene in hematologic malignancies. Meanwhile, BET inhibitors have been implicated as promising therapeutic avenue in a variety of cancers (Asangani et al., 2014; Lockwood, Zejnullahu, Bradner, & Varmus, 2012; Puissant et al., 2013), and a first clinical trial has reported single-agent activity in advanced hematologic cancers (Boi et al., 2015). Despite this rapid developments, the mechanistic basis for sensitivity and resistance to BET bromodomain inhibition remains poorly understood, and so far no predictive biomarker could be identified, which exemplifies a general problem commonly associated with NOA.

## 1.5 Targeting cancer metabolism

A second area of intense research aimed at exploiting NOA for cancer therapy is the study of cancer-specific changes and targets in cellular metabolism. Already in 1924, Otto Warburg discovered that cancer cells almost exclusively use glycolysis and subsequent fermentation of pyruvate to lactic acid, rather than mitochondrial oxidation as most other cells do under normoxic conditions (O. Warburg, K. Posener, 1924, Figure 1.2).

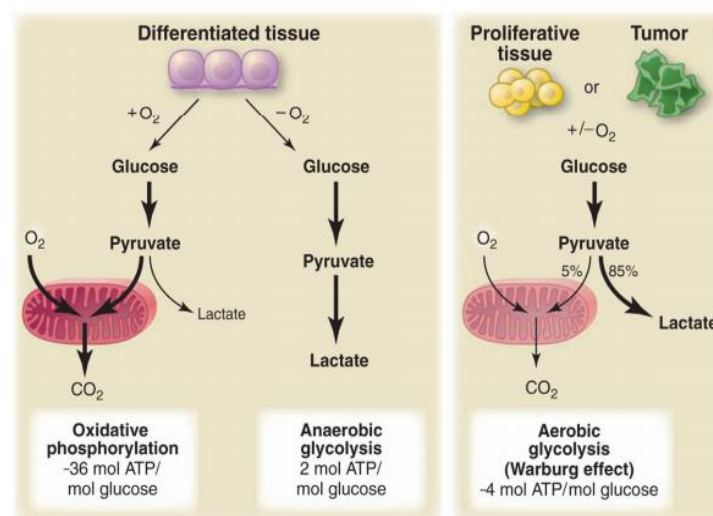


**Figure 1.2 | Usage of metabolic pathways in different cell states**

(Vander Heiden, M. G., Cantley, L.C., Thompson, 2009)

Aerobic glycolysis produces only two molecules of ATP per glucose molecule. In contrast, complete oxidation of one glucose molecule in the Krebs cycle produces 36 molecules of ATP. This leads to a massive increase in glucose consumption by upregulation of glucose transporters and glycolysis rates in cancer cells. This cancer-specific boost in glucose metabolism is also utilized in positron emission tomography (PET), a diagnostic imaging method involving injection of a radio-labelled glucose analog (Fluorodeoxyglucose, FDG) to visualize malignant tissues (Czernin & Phelps, 2002; Gambhir, 2002).

The mechanistic basis for the switch to anaerobic glucose metabolism (also called the “Warburg effect”) remains incompletely understood. One explanation, provided by Otto Warburg himself, could be the frequent damage of mitochondria in cancer that leads to impaired aerobic respiration and a subsequent reliance on glycolytic metabolism (Warburg, 1956). However, subsequent work showed that mitochondrial function is not impaired in most cancer cells (Fantin, St-Pierre, & Leder,

2006; Moreno-Sánchez, Rodríguez-Enríquez, Marín-Hernández, & Saavedra, 2007), suggesting that there has to be an alternative explanation for aerobic glycolysis in cancer cells. In 2010, it was shown that the Warburg effect is actually a favorable catabolic state for all rapidly dividing mammalian cells with a very high glucose uptake rate. While aerobic glycolysis is less efficient than mitochondrial respiration in terms of ATP yield per glucose uptake, it is more efficient in terms of the required solvent capacity (Vazquez, Liu, Zhou, & Oltvai, 2010).

An alternative mechanism that is currently discussed as the main reason for the “Warburg effect” is based on the strongly increased need of cancer cells for molecular building blocks for anabolic processes (Vander Heiden, M. G., Cantley, L.C., Thompson, 2009). In many cell types, the only molecules catabolized in larger quantities are glucose and glutamine. These two molecules have to supply all the necessary carbon, nitrogen, free energy, and reducing equivalents for the entire cell anabolism. Therefore it becomes clear that it would be a waste of resources if every glucose molecule would be oxidized to CO<sub>2</sub> via oxidative phosphorylation in the mitochondria. Instead, Pyruvate is fed directly into several biosynthetic pathways and is used to produce biomass (DeBerardinis et al., 2007).

The finding that glucose metabolism is vastly different in cancer cells has triggered multiple efforts to target these pathways for cancer treatment. Inhibitors of glucose transporters (GLUTs) such as Phloretin, WZB117 and Fasentin have shown anti-cancer activity in preclinical models (Y. Liu et al., 2012). Another glucose analog, 2-deoxyglucose (2-DG) also was tested in pre-clinical models, showing varying effects in different models (Kurtoglu et al., 2007; Zhong et al., 2008). Later studies showed no major activity in hypoxic cancer cells and revealed that 2-DG activates pro-survival pathways in cancer cells, actually contradicting the desired effect (Zhong et al., 2009) (Maher, Wangpaichitr, Savaraj, Kurtoglu, & Lampidis, 2007). In addition to the disappointing efficacy as a single compound, severe brain toxicity has been observed in several cases (Tennant, Durán, & Gottlieb, 2010). Lonidamine, an inhibitor of Hexokinase II catalyzing the first and rate limiting step in glycolysis, was tested in a Phase II clinical trial for the treatment of Glioblastoma multiforme (GBM) in combination with diazepam but it failed to show beneficial effects for treated patients (Oudard et al., 2003). Clinical phase II and III trials for the treatment of benign prostatic hyperplasia have been stopped after several patients suffered from hepatic adverse effects (Tennant et al., 2010) (ClinicalTrials.gov Identifiers: NCT00237536 and NCT00435448).

Other candidate targets investigated in glucose metabolism include phosphofructokinase (Clem et al., 2008), GAPDH (Ganapathy-Kanniappan, Kunjithapatham, & Geschwind, 2012) and lactate dehydrogenase (Le et al., 2010; M. Zhou et al., 2010). The monocarboxylate transporter 1 (MCT1) can be inhibited by AZD3965 and has shown activity in advanced solid tumors (Birsoy et al., 2013; Polański et al., 2014), as well as Dichloroacetate (DCA), a prescription drug for the treatment of lactic acidosis, which is now being explored as a cancer therapeutic based on its ability to inhibit pyruvate dehydrogenase kinase 1 (Michelakis, Webster, & Mackey, 2008).

One of the most studied genes in glucose metabolism is pyruvate kinase (PK). It comes in two splice forms PK-M1 and PK-M2 and it catalyzes the final step in glycolysis by transferring the phosphate group from phosphoenolpyruvate (PEP) to adenosine diphosphate (ADP) to yield adenosine triphosphate (ATP) and pyruvate. The M1 isoform is expressed in almost all adult tissues (Noguchi, Inoue, & Tanaka, 1986), whereas the M2 isoform is primarily expressed mainly during embryonic development (Jurica et al., 1998). Interestingly, it has been noted that highly proliferating tumor cells are reactivating PK-M2 expression which makes it a prime target for cancer treatment and a lot of research has been done in this direction (Goldberg & Sharp, 2012; Vander Heiden et al., 2010). However, several reports showed that the inhibition of PK-M2 alone is not enough for a cancer cell to die and that other metabolic pathways are compensating for the lower ATP levels (Cortés-Cros et al., 2013). It is even more interesting to note that the field has switched to investigate PK-M2 activators. It was shown, that the activation of PK-M2 leads to the formation and stabilization of the highly active tetrameric form of PK-M2 and impairs tumor-cell proliferation by interfering with anabolic metabolism (Anastasiou et al., 2012).

In addition to glucose metabolism, several other pathways have been explored as candidate targets for metabolic cancer therapy. Glutaminolysis is the second most important energy supply pathway in mammalian cells (Reitzer, Wice, & Kennell, 1979; Zielke, Zielke, & Ozand, 1984). Glutamine is the amino acid with the highest serum concentration, and cancer cells are thought to be particularly dependent on glutamine, which is converted to glutamate and further to  $\alpha$ -ketoglutarate and then fed into the Krebs cycle. This truncation of the Krebs cycle increases the abundance of acetyl-CoA in the cell (Parlo & Coleman, 1984), providing a building block for the synthesis of fatty acids and cholesterol, both highly demanded substances in dividing cells. Furthermore, each metabolized glutamine molecule yields one molecule of aspartate, which can be directly used for nucleic acid production and serine synthesis. Currently investigated strategies to exploit

the glutamine dependency of cancer cells include phenylacetate, which lowers circulating glutamine levels (Enns et al., 2007) and Epigallocatechin gallate (EGCG), a glutamine dehydrogenase (GDH) inhibitor found in the leaves of green and white tea (Chendong et al., 2009). Other efforts focus on the development of Glutaminase (GLS) inhibitors, which could block the hydrolysis of glutamine to glutamate (Hensley, Wasti, & Deberardinis, 2013; Jian Bin Wang et al., 2010; Xiang et al., 2015).

Another pathway explored for metabolic cancer targets is *de novo* lipid biosynthesis, which in mammals is usually carried out by a few specialized tissues including the liver, adipose tissue and the lactating breast. While all other tissues take up fatty acids and low density lipoproteins from the serum, cancer cells can acquire the ability to synthesize lipids *de novo*, which has been noted already in the 1950s (Medes, Thomas, & Weinhouse, 1953). Several strategies aimed at exploiting the addiction to *de novo* lipid biosynthesis have already been investigated. Inhibitors of fatty acid synthetase (FASN) such as Orlistat (Alli, Pinn, Jaffee, McFadden, & Kuhajda, 2005) have shown promising results in preclinical tests. Inhibitors of acetyl-CoA carboxylases (e.g. Sorafenib), enzymes producing malonyl-CoA as a key substrate for fatty acid synthesis, block lipid biosynthesis and stimulate  $\beta$ -oxidation at the same time, which in prostate cancer cells triggers apoptosis (Beckers et al., 2007). However, despite encouraging pre-clinical observations, strategies aimed at targeting lipid biosynthesis had so far little success in clinical trials, and are currently not intensely pursued anymore.

The first cancer drug to induce complete remission in children with acute lymphoblastic leukemia is directly targeting nucleotide metabolism (FARBER & DIAMOND, 1948). Although the exact mechanism was not known by the time, Aminopterin and its successor Methotrexate (Methotrexate) competitively inhibit dihydrofolate reductase (DHFR) and thereby the production of tetrahydrofolate, a metabolic intermediate used for the synthesis of purines, pyrimidines and other cellular components. The use of methotrexate resulted in one of the first cures of a solid tumor by chemotherapy in the late 1950s (LI, HERTZ, & BERGENSTAL, 1958), showing that nucleotide synthesis is a pathway worth studying as a cancer target that holds great promises for future therapies (Vander Heiden, 2011).

Most of the classic cytotoxic chemotherapies nowadays are taking advantage of the increased sensitivity of rapidly dividing cells to alterations in nucleotide metabolism. Fludarabine (Plunkett, Chubb, Alexander, & Montgomery, 1980) and Gemcitabine (Grindey, Hertel, & Plunkett, 1990) are



purine analogs that interfere with ribonucleotide reductase (RNR) and DNA polymerase and thereby inhibiting DNA synthesis. Furthermore, these compounds can be incorporated into cytidine which blocks further DNA replication and leads eventually to the induction of apoptosis. Hydroxyurea (Hydroxycarbamide) is an antineoplastic drug specifically decreasing the production of deoxyribonucleotides by inhibiting the chemical reaction catalyzed by RNR (Koç, Wheeler, Mathews, & Merrill, 2004). Since deoxyribonucleotides are needed for cell replication and repair cells induce apoptosis upon reaching critically low nucleotide levels.

Basically all chemotherapeutics used in the clinic at the moment exploit non oncogene addictions in various cancers. They target cancer specific sensitivities in DNA replication, DNA repair and nucleotide metabolism. The same principle applies for radiation therapy as well. Dividing cells are very sensitive to DNA damage and since only a small fraction of cells in normal tissues are dividing at any given moment, mainly tumor cells are targeted (Lomax, Folkes, & O'Neill, 2013).

The identification and development of new NOA targets and therapies is challenging in several ways. NOA targets are often not directly altered in cancer which means that they cannot be easily predicted from genetic or transcriptional information. NOA targets have to be identified through functional assays probing sensitivity. Besides screening available small-molecule inhibitors or large compound libraries, such systematic profiling studies can be performed using new functional genetic tools such as RNAi and CRISPR (Sidi Chen, Neville E. Sanjana, Kaijie Zheng, Ophir Shalem, Kyunghoon Lee, Xi Shi, David A. Scott, Jun Song, Jen Q. Pan, Ralph Weissleder, Hakho Lee, Feng Zhang, 2015; Johannes Zuber, Shi, et al., 2011). In contrast to oncogene-addiction therapies, the mechanistic basis of NOA effects and possible toxicities often remain elusive, which complicates the further development of these agents and their clinical application. Similarly, unlike in case of oncogene-addiction therapies where the presence of the mutation serves as a biomarker for assigning patient cohorts that will likely benefit from targeted therapy, the identification of predictive biomarkers for NOA-based therapeutics often can be very difficult. Due to these challenges, the truly comprehensive identification and mechanistic exploration of NOA targets heavily relies on functional genetic approaches, and recent developments in RNAi and CRISPR technology greatly facilitate these studies.

## 1.6 RNAi – an experimentally programmable mechanism of gene suppression

Over the past decade, RNA interference (RNAi) has rapidly emerged as a standard genetic tool for interrogating gene function. In cancer research, RNAi provides an increasingly robust tool to systematically probe candidate therapeutic targets through genetic screening, and comprehensively study their general and cancer-specific functions prior to drug development. RNAi exploits an endogenous mechanism of gene regulation that was discovered in the 1990s, and our advancing molecular understanding of this mechanism has helped to improve experimental RNAi over the years.

The first RNAi phenomenon was observed in 1990 when researchers inserted additional copies of the chalcone synthase gene, a key enzyme in flavonoid biosynthesis, into petunia plants in order to increase their purple color (Napoli, Lemieux, & Jorgensen, 1990). Contrary to the expected outcome, the resulting plants showed light purple or even white flowers, with up to 50-fold decreased levels of CHS. This experiment showed for the first time that one gene can influence the expression of other genes in trans, although the mechanism remained elusive at that time. Two years later a very similar phenomenon was described in the fungus *Neurospora crassa*, showing that homologous sequences can decrease mRNA levels of the endogenous gene (Romano & Macino, 1992). In 1995, Guo and Kemphues showed the first RNAi related effect in animals when they demonstrated that the introduction of sense and antisense RNA of the *par-1* gene leads to the degradation of the *par-1* RNA in *C. elegans* (Guo & Kemphues, 1995). However, it took another 3 years until Fire and Mellow discovered that neither sense, nor antisense RNA is responsible for this effect, but contaminating double stranded RNA (dsRNA) (Fire et al., 1998), a discovery that was awarded with the Nobel Prize for Physiology or Medicine in 2006.

Following this first description of the RNAi phenomenon, this mechanism of gene regulation was extensively studied in a variety of organisms. It is now believed that the mechanism of RNAi originally developed as a defense mechanism against viruses with a double stranded RNA genome, a RNA configuration that is normally not present in eukaryotic cells. In most animals three distinct RNAi pathways differing in the origin of precursor RNAs and in the mode of target silencing can be distinguished. The germline-specific piRNA pathway mainly processes precursor RNAs from uni- or bi-directionally transcribed piRNA clusters and is responsible for silencing of transposable ele-

ments in germ cells (Brennecke et al., 2007). Short interfering RNAs (siRNAs) mostly process exogenous dsRNA of viral origin, but also some endogenous siRNAs have been identified (Carthew & Sontheimer, 2009). The most ubiquitous RNAi pathway in mammals is based on expression of so-called micro-RNAs (miRNAs). To date, the human genome is known to encode more than 1000 miRNAs, which execute a plethora of regulatory functions.

The precursors of miRNAs (so-called pri-miRNAs) are transcribed as RNA polymerase II (Pol II)-dependent transcripts that can have a length up to several kilo bases. A nuclear protein complex called the micro-processor, consisting of Drosha and its cofactor Pasha (DGCR8 in humans), cleaves the base of stem-loop structures in pri-miRNAs to produce 80-120 bp long pre-miRNAs, which are subsequently exported into the cytoplasm by Exportin 5 (XPO5) (Filipowicz, Bhattacharyya, & Sonenberg, 2008). In the cytoplasm, Dicer, an endonuclease containing two RNase-III domains and two dsRNA binding domains, cleaves off the loop yielding 21-25 bp long mature miRNA duplexes. After cleavage, several other proteins and co-factors are recruited, together forming the RNA-induced silencing complex (RISC), which contains a protein from the argonaute (Ago) family as a key subunit. Subsequently, one of the two strands of the mature miRNA duplex, the so-called guide, is loaded onto the Ago protein and the other strand, the passenger, is released and degraded (Meister, 2013). Guide-loaded Ago proteins recognize target mRNAs through base pairing and suppress their expression through different mechanisms including mRNA cleavage, mRNA destabilization or translational repression (Bartel, 2009).

The discovery of RNAi as a new mechanism of gene regulation almost immediately triggered efforts to experimentally exploit RNAi pathways for loss-of-function genetic studies. Experimental RNAi utilizes synthetic mature miRNA duplexes that are designed to be fully complementary to a given target gene and program endogenous miRNA pathways to inhibit its expression.

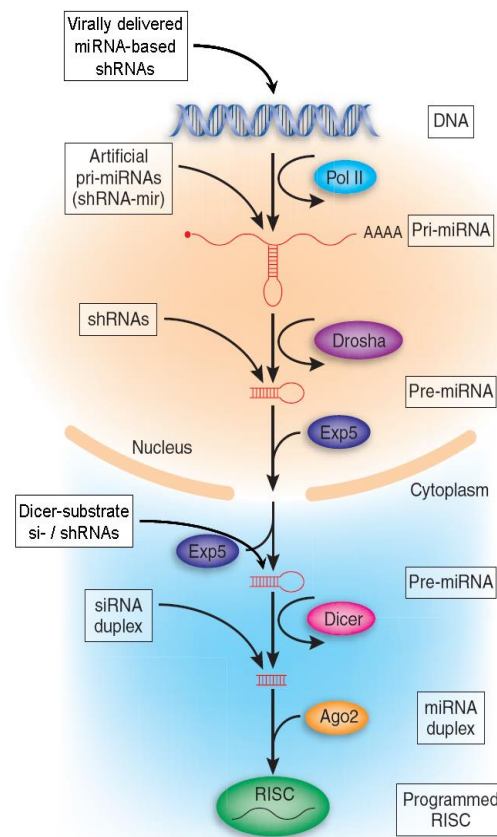


**Figure 1.3 | Endogenous miRNA pathway and entry points for synthetic RNAi triggers used for experimental RNAi**  
(Cullen, 2010)

Over the past years, a variety of experimental approaches has been established to utilize synthetic RNAi triggers entering miRNA pathways at different levels (Figure 1.3).

The most downstream entry point into the RNAi machinery is the direct transfection of double stranded RNA molecules into mammalian cells. While this method can induce gene silencing, dsRNAs trigger strong antiviral responses that can alter or even mask resulting phenotypes. This problem can be improved by transfection of 21-23 bp RNA duplexes with 2 bp overhangs on both ends (termed small interfering RNAs, siRNAs), which are directly loaded into RISC. While effective, target gene suppression using siRNAs is generally a transient phenomenon, because siRNA duplexes are diluted with each cell division (Yang, Tutton, Pierce, & Yoon, 2001). Depending on the growth rate, gene expression recovers after 96-120 hours or 3-5 cell divisions after transfection (Mocellin & Provenzano, 2004). Another limitation of siRNAs are sequence-dependent and -independent off-target effects. High amounts of transfected siRNA can overwhelm and eventually saturate the RNAi machinery with unpredictable effects on the cells under investigation (Jackson et al., 2006).

In addition, besides suppressing the intended target, high doses of transfected siRNAs are known to regulate many other genes with less complementarity (Jackson et al., 2003).

As an alternative to directly transfecting RISC-loadable RNA duplexes, the RNAi machinery can also be triggered by providing synthetic miRNA precursors mimicking endogenous miRNAs at different stages of processing (Figure 1.3). Besides RNA transfection, such precursors can be expressed from DNA vectors stably integrated into the genome, which enables stable or even regulatable RNAi (depending on the promoter). A broadly used approach involves the viral delivery of vectors stably transcribing simple stem-loop structures, so-called short-hairpin RNAs (shRNAs), from constitutive RNA polymerase-III (Pol-III) promoters (Thijn R Brummelkamp, Bernards, & Agami, 2002). Stem-loop shRNAs enter miRNA pathways as synthetic pre-miRNAs and can suppress target proteins as efficiently as siRNAs. However, several studies found that expression of simple stem-loop shRNAs can trigger general toxicities by interfering with endogenous miRNA processing (Grimm et al., 2006). In addition, a recent study investigating structural requirements of Dicer processing found that commonly used simple stem-loop shRNAs are associated with imprecise Dicer cleavage, resulting in the generation of a variety of cleavage products that increase the likelihood of off-target effects (Gu et al., 2012). These findings also exemplify that our advancing molecular understanding of miRNA processing still help to further improve experimental RNAi reagents.

As an alternative to Pol-III-driven stem-loop structures, shRNAs can be embedded into the context of endogenous miRNAs which, like natural miRNAs, can be expressed from polymerase-II (Pol-II) promoters and enter miRNA biogenesis as natural pri-miRNA (Zeng, Wagner, Cullen, & Carolina, 2002). The use of miRNA-embedded shRNAs (also termed “shRNAmirs”) is known to mitigate general toxicities associated with siRNAs or simple stem-loop shRNAs (Castanotto et al., 2007; McBride et al., 2008), and expression from Pol-II promoters facilitates the generation of versatile stable and tetracycline (Tet)-inducible shRNAmir expression systems. Furthermore, shRNAmirs like endogenous miRNAs can be placed in the 3'-untranslated region of protein-coding cDNAs (e.g. reporter genes), which enables a simple yet powerful setup to directly report and isolate shRNA-expressing cells (Stegmeier, Hu, Rickles, Hannon, & Elledge, 2005; Johannes Zuber, McJunkin, et al., 2011). The main limitation of early generations of shRNAmir-based RNAi systems was their relative ineffectiveness, and often dozens of candidates needed to be tested to identify one or two really potent shRNAmir. However, over the past years, a better understanding of miRNA processing requirements has led to dramatic improvements in the selection of effective target sites (Fellmann et al., 2011a) and the design of optimized miRNA backbones (Fellmann et al., 2013).

After implementing these improvements, the latest generation of shRNA<sub>mir</sub> designs has been validated to strongly (>90%) suppress the intended target protein in >60% of cases, even when expressed from a single genomic copy. At the same time, optimized shRNA<sub>mir</sub>s display a strong preference for RISC loading of the intended guide and do not interfere with endogenous miRNA processing (Fellmann et al., 2011a, 2013) which minimizes the risk of general or passenger strand-mediated off-target effects. Of note, while single-copy effectiveness (besides reducing off-target effects) is also an absolute prerequisite for the feasibility of pool-based screens, this criterion has not been rigorously tested in early stem-loop and shRNA<sub>mir</sub> libraries.

While these advances in shRNA<sub>mir</sub> technology dramatically improve the quality of shRNA<sub>mir</sub> libraries and the feasibility and power of high-throughput RNAi screens, the technology is still not perfect and still associated with some technical limitations: (1) Despite great improvements in the prediction and design of single-copy potent shRNA<sub>mir</sub>s, current libraries are still contaminated with shRNA<sub>mir</sub>s that do not trigger potent target knockdown, creating biases in the readout of large-scale screens that cannot be easily controlled. An ideal reagent for quantifying on-target effects and controlling for potential off-target, which can never be fully excluded, would be the generation of protein knockdown-validated shRNA<sub>mir</sub> libraries containing the same number (e.g. three) knockdown-validated shRNA<sub>mir</sub>s for every gene. (2) For the generation of such libraries, it would be desirable to establish assays to quantify the induced protein suppression in a standardized way. Importantly, simply quantifying mRNA levels does not report effects of shRNA<sub>mir</sub> effects on protein translation, and therefore fails to distinguish functional from very potent shRNA<sub>mir</sub>s. On the other hand, conventional immunoblot analyses are not scalable and depend on the availability of specific antibodies. (3) In principle, polycistronic expression of shRNA<sub>mir</sub>s enables systematic combinatorial RNAi (co-RNAi) screens, which could provide a genetic approach for identifying effective target combination. However, due to limitations in RNAi effectiveness and processing, such systems have remained challenging to establish. (4) An important limitation in multiplexed screens are PCR-biases in the deep-sequencing based quantification of library shRNAs. Besides my main project, during my PhD I have worked on addressing some of these questions and further improving shRNA<sub>mir</sub>-based technology (Fellmann et al., 2013), and results of these studies are summarized in section 2.5.1 “Establishment of an optimized miRNA backbone (miR-E)”.

## 1.7 Aims of the thesis

Over the past years, strategies aimed at exploiting non-oncogene addiction have emerged as a promising avenue for the development of targeted cancer therapies that are effective independent of the vast heterogeneity and complexity of cancer genomes. While some of the most promising targets pursued in pre-clinical and clinical studies belong to this class, non-oncogene addictions cannot be easily predicted but have to be identified and functionally evaluated through genetic or small-molecule based studies.

The main aim of my PhD project was to develop and apply high-throughput shRNAmir screens to systematically identify and characterize druggable non-oncogene addiction targets in an aggressive MLL/AF9;Nras<sup>G12D</sup>-driven mouse model of AML, which resembles the biology and aggressiveness of human MLL-rearranged AML. Specifically, I constructed a shRNAmir library comprising ~4000 sequence-verified shRNAs targeting ~1000 druggable candidate genes, including ~450 genes for which small-molecule inhibitors are already available. Systematic screening of this library in the AML model and immortalized embryonic fibroblasts revealed numerous leukemia-specific dependencies, including some known factors as well as novel candidate targets. As the top hit of the primary screen and extensive single-shRNA validation studies, we identify a strong leukemia-specific dependency on Gart, a trifunctional gene in *de novo* purine synthesis.

Further functional-genetic validation studies reveal that Gart suppression triggers potent anti-leukemic effects in both human and murine leukemia models *in vitro* and *in vivo*, which are of similar potency and superior specificity compared to some of the most promising non-oncogene addiction targets in AML. Quantification of purine synthesis metabolites reveals that partial Gart suppression leads to a severe depletion of IMP, the main product of *de novo* purine synthesis, which is not observed in other cell types and can be rescued through supplementation of hypoxanthine, a key substrate in purine salvage pathways. These findings suggest that leukemia cells are intrinsically addicted to fully functional *de novo* purine synthesis, while other cell types can compensate partial Gart suppression through salvage pathways that lack sufficient substrates in leukemia *in vitro* and *in vivo*. Using a series of genetic rescue studies we identify the AIRS component of Gart as the most promising enzymatic activity for exploiting leukemia-specific dependencies on *de novo* purine synthesis. Collectively, the results of my PhD thesis identify and validate Gart as a strong and highly leukemia-specific non-oncogene addiction that can be therapeutically exploited through AIRS inhibition. Since all available GART inhibitors target the folate-dependent GARTase

activity of GART, whose genetic ablation fails to recapitulate the addiction to GART as AIRS, our data strongly recommends the development of AIRS small-molecule inhibitors for targeted leukemia therapy.

From a technology perspective, this study illustrates that multiplexed shRNAir screens in genetically engineered cancer models provide a functional and promising approach to identify novel non-oncogene addiction targets. However, throughout my PhD project I encountered several remaining limitations of shRNAir technology, and the further optimization of this experimental tool eventually became a second major aim and focus of my work. Major achievements from my technology-focused projects include: (1) the development and validation of an optimized shRNAir backbone termed miR-E, which strongly improves the general shRNAir knockdown efficiency by 10-fold enhancing pri-miRNA processing; (2) the development of a scalable fluorescence-based shRNAir reporter assay, which enables the standardized testing of shRNAir-mediated protein knockdown and is currently applied for the generation of fully knockdown-validated shRNAir libraries; (3) the establishment and validation of an shRNAir-based co-RNAi system that enables the multiplexed evaluation of candidate targets in combination; (4) improvements in deep-sequencing readouts of multiplexed shRNAir screens.



## 2 Results

### 2.1 An shRNAmir screen for identifying non-oncogene addiction targets in AML

#### 2.1.1 Construction of a customized library for identifying druggable non-oncogene addiction targets in MLL/AF9-driven AML

To systematically identify non-oncogene addictions that might be exploitable for the development of target AML therapies, we curated a list of 1133 candidate genes including known targets of established small-molecule inhibitors and tool compounds (based on <http://www.drugbank.ca>) as well as potentially druggable genes that were found overexpressed in human and murine MLL/AF9-driven leukemia. To systematically probe this “MLL-1000” gene set for putative non-oncogene addiction targets, we designed a mouse shRNAmir library based on improved shRNAmir design rules (Fellmann et al., 2011b) and cloned it from on-chip synthesized oligo-nucleotide pools into TRMPV-Neo, a retroviral vector optimized for multiplexed negative-selection shRNAmir screening in Tet-on competent cancer models (Johannes Zuber, McJunkin, et al., 2011). All TRMPV-Neo-shRNAmir constructs were sequence-verified using high-throughput capillary sequencing, and a total of 4003 correct clones were combined at equimolar ratios in 9 sub-pools, each containing 242-1026 individual shRNAs. In addition to library shRNAs, each pool was supplemented at equimolar ratios with 32 control shRNAmirs (see Appendix 5.2) that had previously been characterized for their effects in MLL/AF9;Nras<sup>G12D</sup>-driven AML (Johannes Zuber, McJunkin, et al., 2011; Johannes Zuber, Rappaport, et al., 2011; Johannes Zuber, Shi, et al., 2011). Based on their known activity, three different classes of shRNAs were included: (1) shRNAs known to have no effects in MLL/AF9;Nras<sup>G12D</sup>-driven AML (neutral controls, n=17); (2) shRNAs targeting essential genes that are known to have detrimental effects in numerous models (essential controls, n=7); (3) shRNAs targeting established leukemia-specific dependencies (addiction controls,

n=8). The performance of such established control shRNAs provides a simple, yet powerful measure to assess the quality of multiplexed RNAi screens already at the level of primary deep-sequencing data.

### 2.1.2 Multiplexed comparative negative-selection shRNA<sup>mir</sup> screening in MLL/AF9;Nras<sup>G12D</sup>-driven AML and immortalized MEF

To systematically survey the “MLL-1000” library for leukemia-specific non-oncogene additions, we screened it in a multiplexed fashion in parallel in an established MLL/AF9;Nras<sup>G12D</sup>-driven AML mouse model, named RN2 (Johannes Zuber, McJunkin, et al., 2011) and Rosa26-rtTA-M2 mouse embryonic fibroblasts (RMEF) that have been immortalized through expression of large-T antigen (Johannes Zuber, McJunkin, et al., 2011).

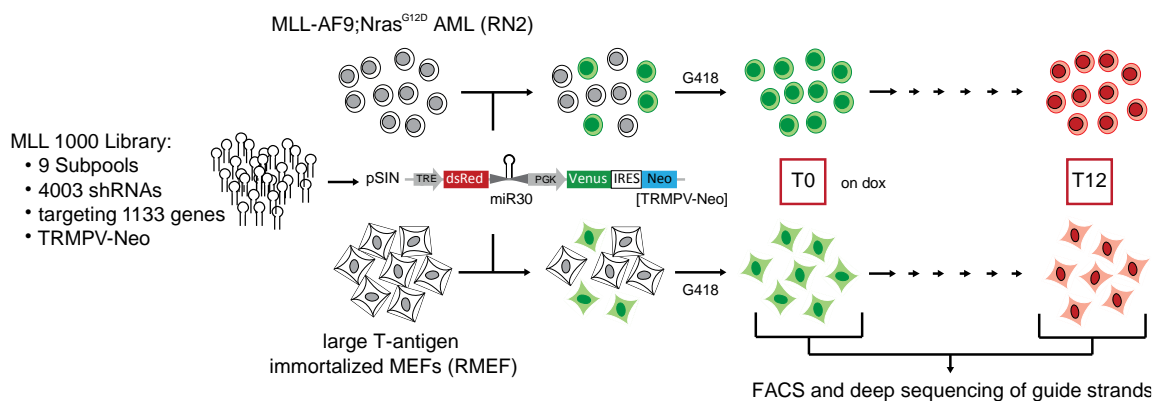


**Figure 2.1 | Schematic of the parallel multiplexed, negative-selection RNAi screen in RN2 and RMEF.**

RN2 and RMEF cells were retrovirally transduced in duplicates with the sequence verified shRNA library, MLL-1000, in 9 subpools using conditions that allow single-copy integration and a representation of >1000 cells per shRNA. After G418 selection (1 mg/mL) for 5-7 days, T0 samples were collected and shRNA-expression was induced with doxycycline (dox, 1 µg/mL). Cells were passaged for 12 days and sorted for shRNA expression (dsRed<sup>+</sup>/Venus<sup>+</sup>). Following genomic DNA extraction, Solexa sequencing libraries were generated using a custom PCR to determine the abundance of shRNAs at the indicated time points.

Both cell types stably express a reverse Tet-transactivator (rtTA), which enables Tet-on regulatable expression TRMPV-Neo-encoded shRNAs. Each of the nine library pools was transduced in two biological replicates into both RN2s and RMEFs using conditions that predominantly result in a single retroviral integration while ensuring a representation of each shRNA in approximately 1000 cells, which was maintained throughout the experiment (Figure 2.1).

Following G418 selection, a reference sample (T0) was obtained for each subpool and replicate, and deep-sequencing later confirmed that all shRNAs could be detected and their abundance

strongly correlated between both replicates (Figure 2.2 a), indicating that the library was sufficiently represented.

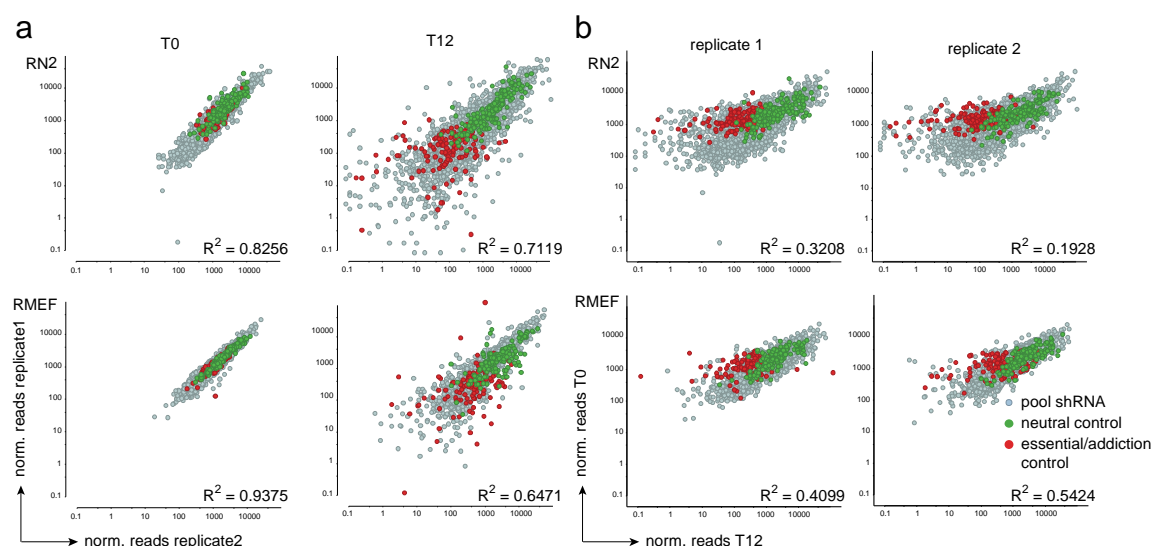


**Figure 2.2 | Correlation between replicates of the complete MLL-1000 library including all 9 subpools.**

(a) Correlation of normalized reads of all pools between two independent replicates at T0 and T12, in RN2 and in RMEF cells. Neutral and essential/addiction controls from all pools are highlighted as indicated. Abundance of positive control shRNAs (red) is decreased at T12. (b) Correlation of normalized reads of all pools between T0 and T12 in both replicates in RN2 and RMEF cells.

At T0, shRNAmir expression was induced by adding doxycycline (dox) to the media, and the cells were propagated for a total of 12 days in the presence of dox. Subsequently, shRNA-expressing cells (dsRed<sup>+</sup>/Venus<sup>+</sup>) were FAC-sorted as previously described (Johannes Zuber, McJunkin, et al., 2011), and a total of at least  $3 \times 10^6$  cells per replicate was used for determining the representation of the library at the end point (T12). To this end, shRNA guide strands were amplified from genomic DNA using primers that directly tag Illumina adaptors to the guide, and subsequently sequenced using a custom Illumina sequencing primer. For each subpool, read numbers for individual shRNAs were normalized to the total reads, and compared between replicates and between T0 and T12 to calculate the fold depletion value (FD, normalized reads T12/normalized reads T0; Figure 2.2 b). Comparisons of biological replicates of each pool at T12 showed a high correlation, indicating that the library was well preserved throughout the experiment and that effects were consistent (Figure 2.2 b). By contrast, reads at T0 and T12 correlated much less, and included control shRNAs showed the expected behavior (Figure 2.2 b).

First, we analyzed the behavior of control shRNAs in more detail. None of the 17 included neutral controls were depleted in either leukemia or MEF (Figure 2.3), while leukemia-specific addiction controls targeting Mcl1, Men1, Myb, Myc and Brd4 showed stronger depletion in leukemia, which was particularly clear for Mcl1 and Men1 shRNAs.

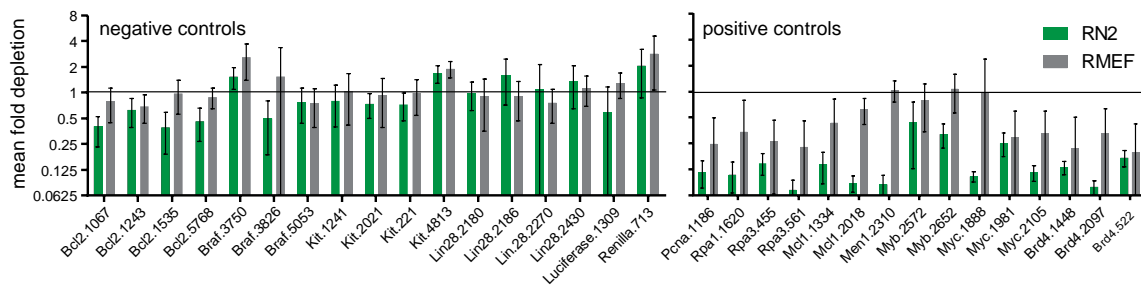


**Figure 2.3 | Performance of control shRNAs in all subpools.**

Mean fold depletion of spike-in controls from all 9 pools in RN2s and RMEFs. Values depict mean + SD and are plotted on a Log2 axis.

Besides strong depletion in leukemia, shRNAs targeting Myc and Brd4 were also depleted in MEF, which is in line with previous studies (Johannes Zuber, Shi, et al., 2011) and the known function of these genes in highly proliferating cells (H Wang, Mannava, & Grachtchouk, 2007). The leukemia-specific depletion of Myb shRNAs was lower than what could be expected from single-shRNA assays (J Zuber et al., 2011), indicating that some shRNAs might be false-negative. All 7 essential control shRNAs targeting the DNA replication factors PcnA, Rpa1 and Rpa3 were depleted in both contexts, albeit to varying degrees in individual replicates. Importantly, the depletion level of these shRNAs was generally stronger in leukemia than in RMEF, which might reflect difference in the proliferation and passaging of both cultures. To account for these differences in our final readout, we adjusted the fold-change levels classified as strong and weak effects to 10-fold or 3-fold in RN2 leukemia, and 5-fold or 2.5-fold in RMEF, respectively.

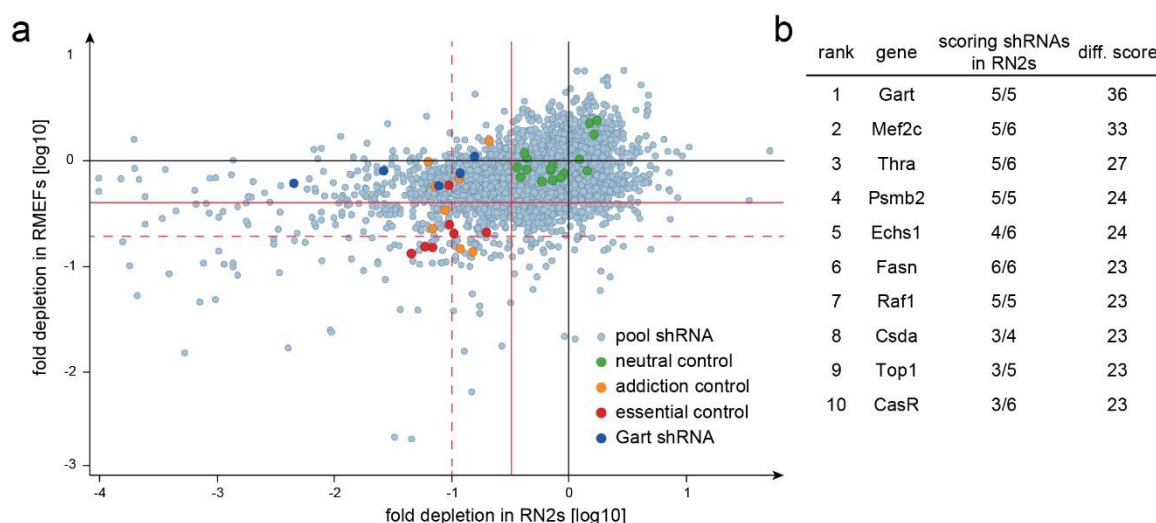


**Figure 2.4 | A pooled, multiplexed RNAi screen identifies several AML specific vulnerabilities.**

(a) The fold depletion of each shRNA was calculated by dividing the number of reads in the T12 samples by the number of reads in the T0 samples. Plotted is the geometric mean of 2 replicates in RN2 on the X-axis and RMEF on the Y-axis. The solid red line depicts the threshold for weak depletion (0.25 in RN2, 0.5 in RMEF) and the dotted line the threshold for strong depletion (0.1 in RN2, 0.25 in RMEF). GeoMean depletion of spike in control shRNAs is highlighted. (b) Table of the top 10 genes with the highest differential score. Gene scores were calculated by scoring 3 points for each hairpin showing weak depletion and 10 points for strong depletion. For the differential score, the gene score in RMEF was subtracted from the gene score in RN2.

We next analyzed the performance of library shRNAs (Figure 2.4 a). According to these thresholds, 64.3% (2574) of library shRNAs showed no major effect in leukemia and RMEF, consistent with the notions that (1) the majority of candidate target genes are neutral in both contexts and (2) a fraction of shRNAs in our library might be ineffective under single-copy conditions. Only 3.7% (149) of shRNAs showed an enrichment in either RN2 (FC>3-fold) or RMEF (FC>2.5-fold), suggesting that only few shRNAs can enhance proliferation and/or survival in these highly proliferative models. While interesting, these shRNAs were disregarded in further analyses. 1.25% (50) of shRNAs were strongly depleted in both RN2 and MEF, suggesting that they target essential genes. Indeed, in this group we identified multiple shRNAs targeting known essential genes involved in DNA replication (e.g. Mcm6, Top2a, and Pola1). Hence we found several subunits of the proteasome complex (e.g. Psma1, Psmb2, Psmd1, and Psmd2) and genes involved in basic cellular processes (e.g. Rrm1, Th, Kif11). By contrast, 5.8% (232) of shRNAs showed strong depletion in leukemia, while they were neutral in RMEF. These included several shRNAs targeting already known leukemia-specific dependencies, including Bcl2 (Glaser et al., 2012), Mef2c (Schüler et al., 2008), Hdac3 (Johannes Zuber, Shi, et al., 2011) and Cdk6 (Placke et al., 2014), which further supported the quality of our screen. The relative abundance of such leukemia-specific effects may reflect that (1) our library was biased for candidate genes highly expressed in MLL/AF9-driven leukemia, and (2)

that many of the targeted genes represent leukemia-specific non-oncogene addictions. To integrate this data at the gene level, we derived a semi-quantitative differential score that integrates all shRNAs for a given gene and reflects the different effects between RN2 and RMEF (Figure 2.4 b). In brief, we awarded three points for each shRNA with weak depletion and ten points for shRNAs with strong depletion. Then, we added all points for a given gene up and subtracted the score in RMEF from the score in RN2. Based on this scoring system, the second most prominent hit turned out to be Mef2c, a gene from the MADS (MCM1-agamous–deficient serum response factor) family of transcription factors. It was initially discovered as an important factor for myogenesis and vascular development (Black & Olson, 1998) but it is also known as a strong requirement in MLL-rearranged leukemia (Schwieger et al., 2009). The top hit of our screen was Gart, a tri-functional enzyme in *de novo* purine synthesis, for which all five shRNA contained in the library scored in the leukemia screen (3 strong, 2 weak), while none of them showed any depletion in RMEF (Figure 2.4 a).

### 2.1.3 Primary hit-validation using single-shRNA assays

After analyzing results from the multiplexed screen, several rounds of single-shRNA assays were performed to validate both the quality of the screen and identify leukemia-specific dependencies. For these studies we performed competitive proliferation assays using the same Tet-regulated shRNAmir expression vector in Tet-on competent leukemia RN2 and RMEF cells (Figure 2.5 a).

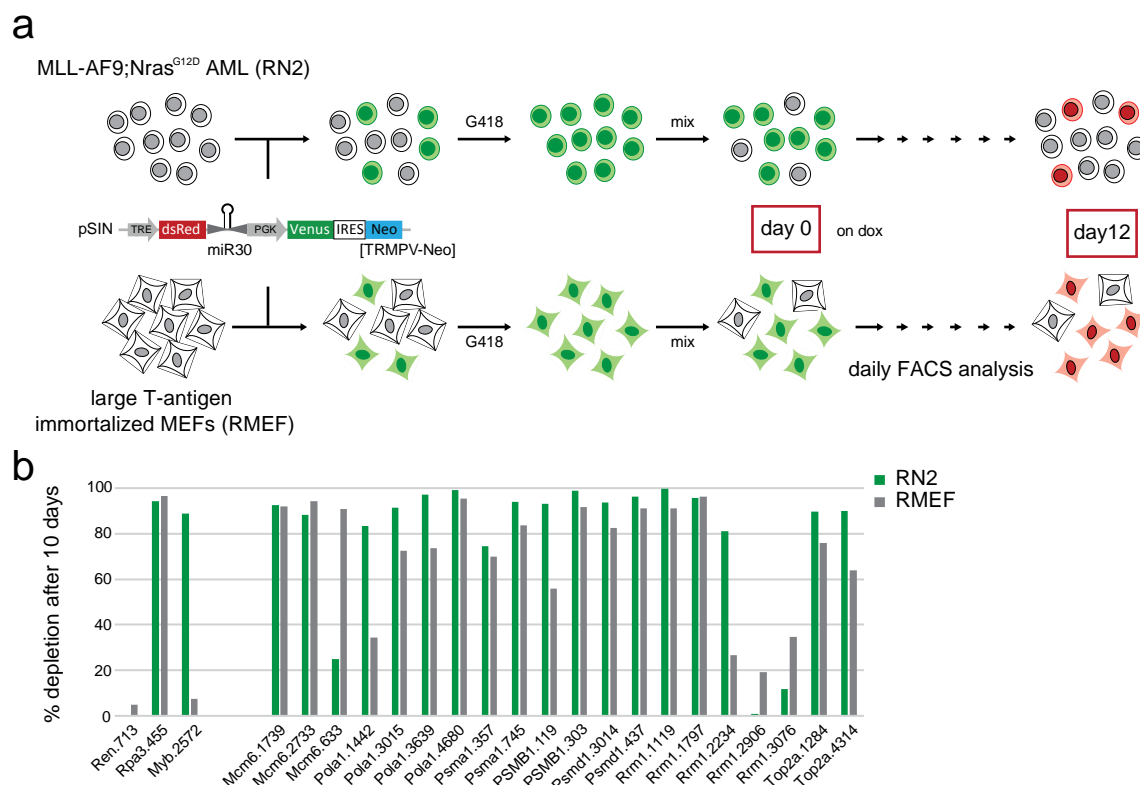


**Figure 2.5 | Competitive proliferation assays for single shRNA validation.**

a) Schematic of competitive proliferations assays for single shRNA validation. RN2 and RMEF cells are retrovirally transduced with TRMPV-Neo harboring single shRNAs and G418 selected (1 mg/mL) for 5-7 days. After complete selection wild type cells are mixed into each well, in a ratio 80:20 and shRNA expression is induced with doxycycline (1  $\mu$ g/mL). The relative ratio of shRNA<sup>+</sup> cells is monitored daily by FACS analysis, over the course of 12 days. (b) 20 shRNAs identified as essential in the screen were tested in single competitive proliferation assays in TRMPV-Neo. Percent depletion of shRNA<sup>+</sup> expressing cells after 10 days on dox, relative to day 2, is shown. Included are also a neutral shRNA Ren.713, an essential control Rpa3.455 and AML specific addition control Myb.2572. Most of the tested shRNAs show equally strong depletion in RN2s and RMEFs.

TRMPV-Neo vectors harboring individual shRNAs were transduced alongside with control shRNAs, and following drug selection transduced cells were mixed at a ratio of 80:20 with untransduced competitor cells. Subsequently, shRNAmir expression was induced by addition of dox, and the fraction of shRNA-expressing cells (dsRed<sup>+</sup>/Venus<sup>+</sup>) was followed over time using flow cytometry. While in case of a neutral shRNA the fraction of shRNA<sup>+</sup> and competitor cells would not change over time, shRNAs targeting a gene required for proliferation and/or survival would lead to a gradual depletion of shRNA<sup>+</sup> cells over time.

As a first step, we selected 20 shRNAs that showed depletion in both RN2 and RMEF cells in the original screen, and assayed them side-by-side with a neutral shRNA targeting Renilla luciferase

(Ren.713) (Johannes Zuber, McJunkin, et al., 2011), a positive control shRNA targeting the essential DNA replication factor Rpa3 (Rpa3.455) (McJunkin et al., 2011), and a leukemia-specific control targeting the transcription factor Myb (Myb.2572) (J Zuber et al., 2011), which behaved accordingly in single assays. Importantly, most of the tested shRNAs (75%) predicted to be generally deleterious based on the primary screen strongly depleted in both RN2 and RMEF cells (Figure 2.5 b), demonstrating that essential genes were accurately identified through multiplexed screening.

Next, we validated selected hits that were identified as leukemia-specific dependencies in our multiplexed screen. These studies included 2 shRNAs for the top 10 hits of our screen and 13 additional scoring genes of interest (Figure 2.6), for which we tested the strongest scoring shRNA from the primary screen.

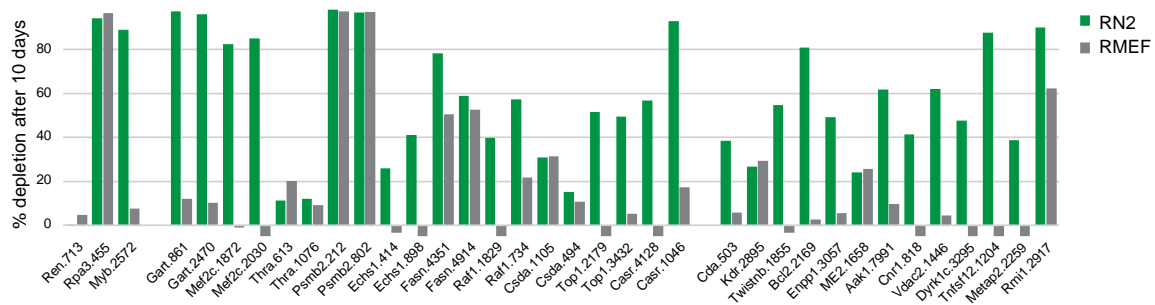


**Figure 2.6 | Primary validation of shRNAs targeting top scoring genes.**

Percent depletion of shRNA expressing cells on day 10 in competitive proliferation assays, relative to day 2, is shown. The same controls as in Figure 2.5 b were used (Ren.713, neutral control; Rpa3.457, essential control; Myb.2574, addition control). Y-axis is capped at -5% depletion because some shRNAs showed mild enrichment over 10 days.

In these assays, 21 of 28 tested shRNAs triggered inhibitory effects in RN2s that were less pronounced or absent in RMEF, indicating that the multiplexed screen accurately identified leukemia-specific dependencies in 75%. False-positive hits included shRNAs that did not trigger strong effects in either context (e.g. Thra) or were depleted in both leukemia and RMEF (e.g. Fasn, Casr). Like in the primary screen, the most prominent leukemia-specific dependencies included Mef2c and Gart, whose suppression showed very strong deleterious effects in AML cells, while being neutral in RMEF. In case of RNAi-mediated suppression of Gart, such highly context-specific phenotypes were very surprising. Based on its essential function in *de novo* purine synthesis, we would have predicted that Gart shRNAs would trigger similar effects like the many other shRNAs targeting essential genes that were established as controls (e.g. Rpa1, Rpa3, PcnA) or identified and validated in our screen (e.g. Mcm6, Rrm1, Pola1, Top2a). Based on the unexpected discrepancy to these known essential genes and the fact that Gart emerged as a clear top hit in both primary



screen and validation, we selected Gart for follow-up studies focused on its characterization of a candidate non-oncogene addiction target in AML.

## 2.2 Characterization of Gart as a non-oncogene addiction target in AML

### 2.2.1 Extended genetic validation of RNAi-mediated Gart suppression effects

To further investigate the specificity and potency of anti-leukemic effects following Gart suppression, we tested a total of seven Gart shRNAs (including all 5 scoring shRNAs from our library, and another 2, *de novo* designed shRNAs) in competitive proliferation assays (Figure 2.7).

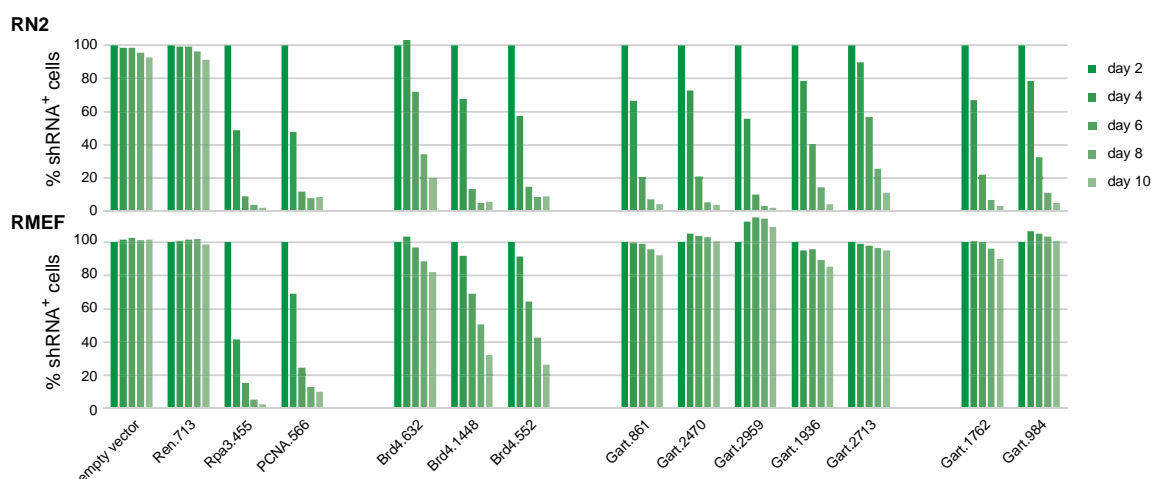


**Figure 2.7 | Evaluation of additional Gart shRNAs in RN2 and RMEF.**

Competitive proliferation assays of indicated Brd4 and Gart shRNAs in RN2 and RMEF. Depicted is the percentage of shRNA+ cells over time, relative to day 2 on dox in RN2 and RMEF. Compared to shRNAs targeting Brd4, shRNAs targeting Gart show a strong and specific depletion in RN2.

All seven shRNAs triggered deleterious effects in leukemia cells, which in light of the well-known variability in knockdown efficiency associated with miR-30-based shRNAs (Bassik et al., 2009; Fellmann et al., 2011a) is a remarkable consistency. These findings also indicate that partial suppression of Gart is sufficient to trigger anti-leukemic effects.

While consistent results of seven shRNAs strongly argue against biases due to off-target effects, we sought to confirm the presence of an on-target effect using cDNA rescue studies, which provide definitive evidence. To this end, we developed a two-vector competition assay that provides a sensitive and simple fluorescence-based readout for cDNA rescue studies in combination with Tet-inducible RNAi (Figure 2.8 a).

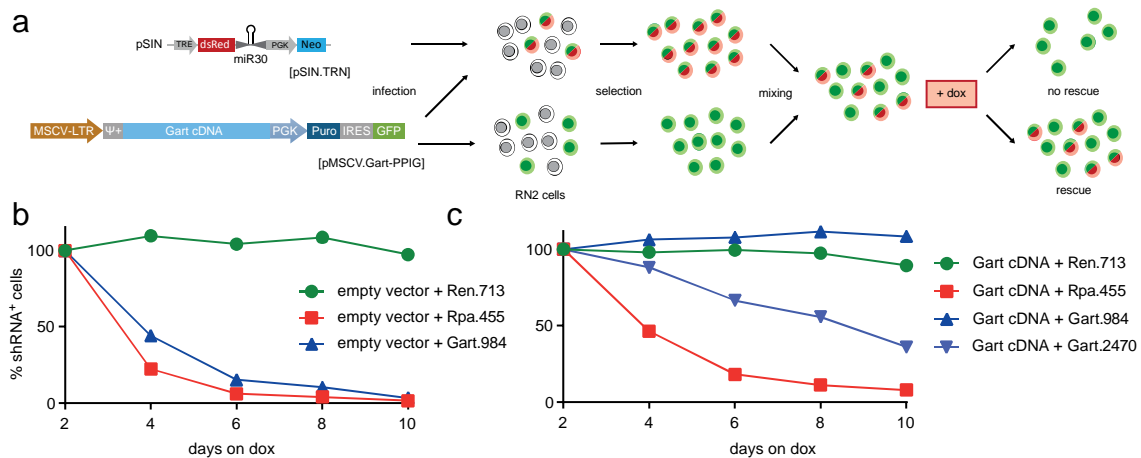


**Figure 2.8 | Overexpression of a Gart cDNA completely rescues the lethal phenotype in RN2.**

(a) Schematic depicting the cDNA rescue strategy. RN2 cells are either co-transduced with a red shRNA vector (TRN) and a MSCV-LTR driven cDNA expression vector additionally harboring a GFP cassette and a Puro selection marker or with the GFP vector alone. After selection for 5-7 days, cells are 50:50 mixed and cultured in dox containing medium. The ratio of GFP<sup>+</sup> and dsRed<sup>+</sup>/GFP<sup>+</sup> cells is followed over time by FACS analysis. (b) Rescue experiment with empty vector. Percentage of shRNA expressing cells over the course of 10 days on dox, relative to day 2 is shown. Both Rpa3.455 and Gart.984 deplete the cells over time. (c) Rescue experiment with full length Gart cDNA vector. Percentage of shRNA expressing cells over the course of 10 days on dox, relative to day 2 is shown. Gart.984 cannot deplete RN2s anymore, whereas a different Gart shRNA, Gart.2470, still depletes.

One retroviral vector delivers a constitute expression cassett which drives the expression of a RNAi-resistant cDNA, a Puromycin resistance gene, and a GFP reporter (pMSCV-cDNA-PGK-Puro-IRES-GFP; cDNA vector), while the other vector contains a neomycin resistance cassette and harbors a Tet-responsive element (TRE) driving expression of a miR-30 based shRNA in the 3'UTR of a red-fluorescent reporter (pSIN-TRE-miR-30-dsRed-PGK-Neo; shRNA vector). The cDNA expression vector is transduced either alone or together with the shRNA vector into Tet-on competent cells. Following drug selection, cells harboring only the cDNA vector are mixed in a 1:1 ratio with cells containing both constructs, and shRNA expression is induced through dox addition to the media. Cells expressing both the cDNA and the shRNA (dsRed<sup>+</sup>/GFP<sup>+</sup>) can be distinguished from cDNA-expressing competitor cells (GFP<sup>+</sup>), and their relative abundance followed over time serves as primary readout.

After developing this assay, it was applied to rescue phenotypes triggered by RNAi-mediated Gart suppression in our Tet-on competent MLL/AF9;Nras<sup>G12D</sup>-driven mouse model. Expression of a potent Gart shRNA (Gart.984) or an essential control (Rpa3.455) in the presence of an empty cDNA control vector triggered the same strong deleterious effects as in previous assays (Figure 2.8 b).

Expression of a murine Gart cDNA harboring a mutated Gart.984 target site (neutral to the encoded amino acid sequence) did not alter the effects of our neutral control shRNA (Ren.713) or an essential control (Rpa3.455). However, in cells expressing the Gart.984 shRNA, the presence of this cDNA completely rescued the deleterious RNAi phenotype, and even after extended culture over 10 days (usually leading to >95% loss of Gart shRNA<sup>+</sup> cells) we did not detect anti-leukemic effects of this shRNA anymore (Figure 2.8 c). Another potent Gart shRNA (Gart.2470) was still able to deplete RN2s over time, albeit with lesser strength than in single assays. The endogenous and the overexpressed Gart cDNA are both substrates for the second Gart shRNA (Gart2470) resulting in an overall attenuated effect. The effects of the essential shRNA Rpa3.455 is not influenced by the Gart cDNA. Collectively, these results conclusively demonstrated that the observed phenotypes are entirely due to on-target suppression of Gart.

### 2.2.2 Probing the potency and leukemia-selectivity of Gart suppression

After validating the anti-leukemic effects of RNAi-mediated Gart suppression in AML, we compared potency and leukemia-selectivity of these effects to other candidate therapeutic targets. As a first candidate target we selected Brd4, a chromatin reader of acetylated histones which is currently explored as a candidate therapeutic target in AML (Dawson et al., 2011; Toyoshima et al., 2012; Johannes Zuber, Shi, et al., 2011), other hematologic malignancies (Delmore et al., 2011) and solid cancers like glioblastoma (Cheng et al., 2013), neuroblastoma (Puissant et al., 2013), prostate cancer (Asangani et al., 2014) or non-small cell lung cancer (Lockwood et al., 2012). After its discovery as a non-oncogene addiction target in the same MLL/AF9;Nras<sup>G12D</sup>-driven AML model (Johannes Zuber, McJunkin, et al., 2011), the availability of small-molecule inhibitors of BET bromodomains has accelerated the pre-clinical and clinical development of this therapeutic concept, and only four years later clinical trials have reported single agent activity of these compounds in advanced hematologic cancers (Boi et al., 2015). When tested in comparative proliferation assays in RN2 and RMEF cells, three established Brd4 shRNAs of different potency (Johannes Zuber, Shi, et al., 2011) triggered the known strong deleterious effects in AML cells (Figure 2.7). While the weaker shRNA (Brd4.632) did not show major effects in RMEF, two more potent Brd4 shRNAs (Brd4.1448 and Brd4.552) also triggered clear deleterious effects in RMEF. By stark contrast, none of the three most potent Gart shRNAs identified in our study showed any depletion in RMEFs, while the strength of their anti-leukemic effects where in a similar range as the most potent Brd4 shRNAs.

Importantly, Gart was only partially suppressed at the onset of deleterious effects in AML (3d on dox), while there was no deleterious effect in RMEF even at later time points (5d on dox), when Gart protein knockdown was even more pronounced (Figure 2.9 a). In addition, we examined whether leukemia-specific effects are merely a consequence of different proliferation rates between our AML model and RMEF cells. However, the doubling time of both cell types was comparable (14 h in AML cells versus 15 h in RMEF; Figure 2.9 b), and BrdU-incorporation assays in growing cultures revealed that the fraction of cells in S-phase is comparable between both cell types (52% in AML cells vs. 55% in RMEF; Figure 2.9 c). Consistent with competitive proliferation assays, the S-phase fraction was dramatically reduced upon Gart suppression in AML, while being only minimally affected in RMEF cells (Figure 2.9 d).

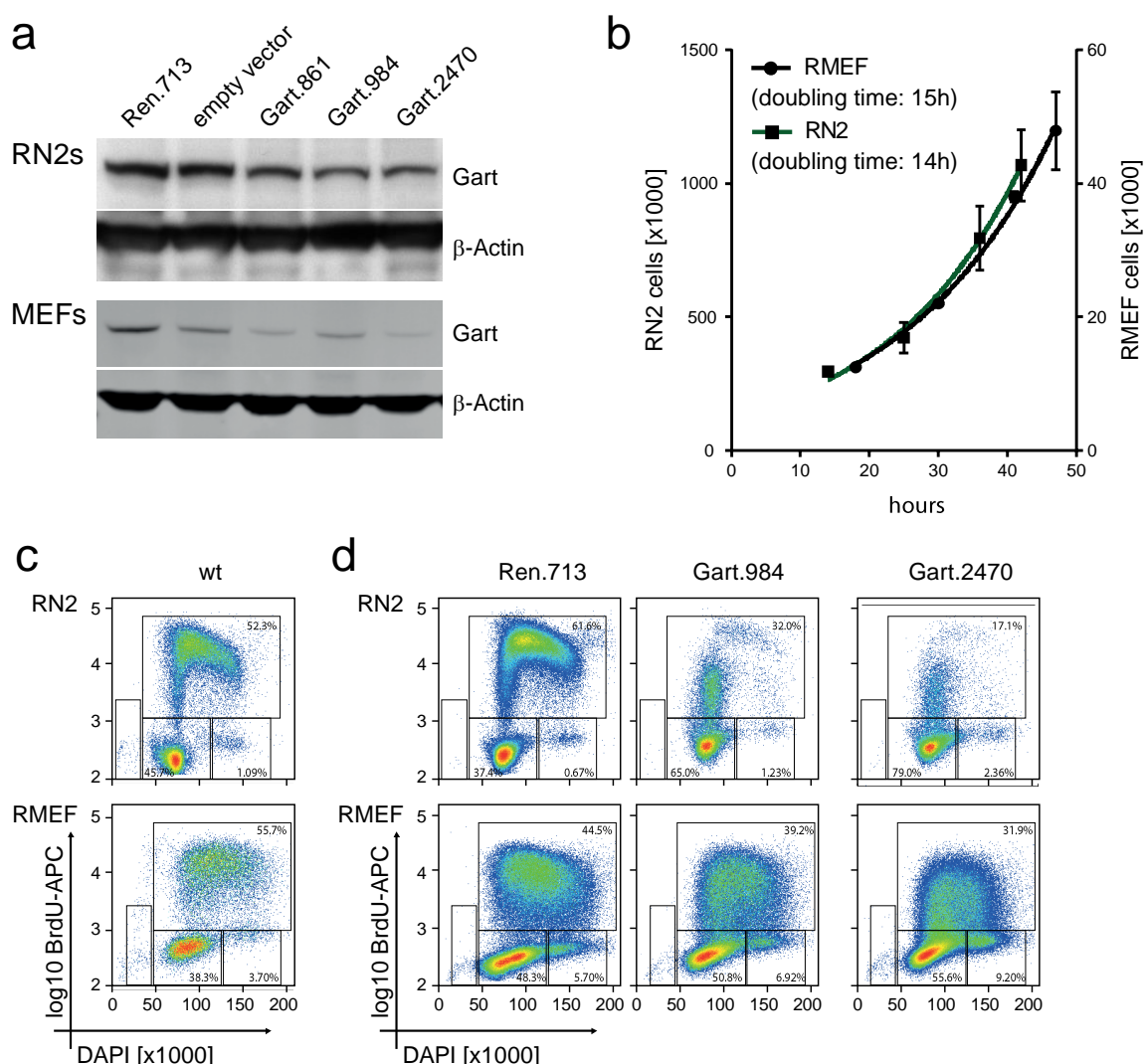


**Figure 2.9 | Analysis of cellular effects upon Gart knockdown.**

(a) Western blot of Gart following knockdown with the indicated shRNAs. Whole cell lysates from sorted, shRNA<sup>+</sup> RN2 and RMEF were prepared after 3d and 5d on dox respectively. β-Actin is used as protein loading control. (b) Growth curves of RN2s and RMEFs. 150.000 RN2s and 10.000 RMEFs were seeded into 24 well plates and cell numbers were determined (Guava Merck Millipore) every 12-14 hours over the course of 48 hours. All measurements were done in triplicates and doubling times were calculated using a nonlinear fit function for exponential growth. (c) RN2 and RMEF cells were cultured for 3 days at normal density and then the cells were pulsed with BrdU for 45min. Representative FACS blots of antibody staining for incorporated BrdU and DNA content are shown. Percentage of cells in S-Phase, G1 and G2/M is indicated in the respective gates. (d) Same assay as in c), but RN2 and RMEF cells were transduced with shRNAs in TRMPV-Neo and selected for 7 days with G418 (1 mg/ml) and cultured on dox for 3 days before the assay was performed.

The major effects of Gart on the cell cycle of AML cells were accompanied by a loss of c-Kit, a leukemia stem cell (LSC) marker in MLL/AF9-driven AML models (Krivtsov et al., 2006), and an upregulation of the myeloid differentiation marker Cd11b (Figure 2.10).

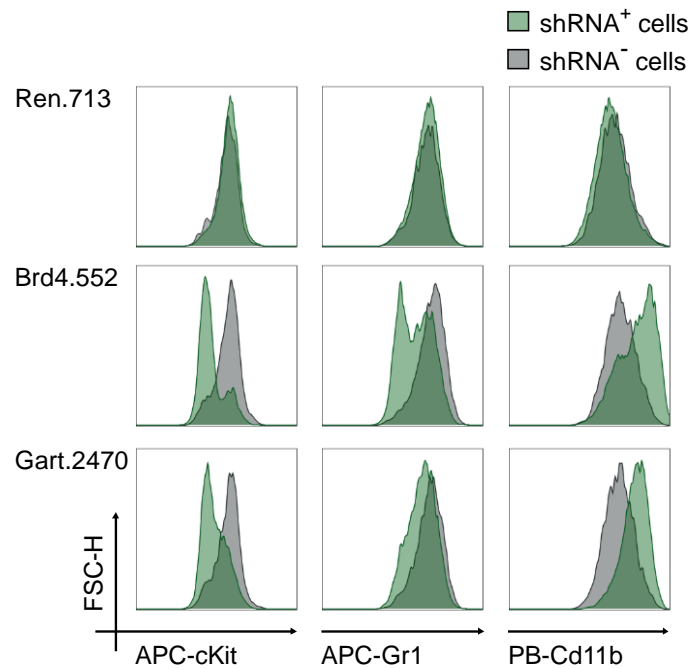


**Figure 2.10 | Analysis of differentiation markers upon Gart knockdown.**

G418 selected TRMPV-Neo cells were mixed with wild type cells and treated with dox for 72 h (1  $\mu$ g/mL). Cells were FACS stained for the indicated differentiation markers and shRNA<sup>+</sup> and shRNA<sup>-</sup> cells in each well were compared.

Of note, the neutrophilic marker Gr-1, which is upregulated upon suppression of MLL-AF9 or its downstream targets Myb and Myc (Johannes Zuber et al., 2009) while lost upon monocytic differentiation triggered inhibition of Brd4 (Johannes Zuber, Shi, et al., 2011) was not affected by Gart inhibition. Together, these results indicate that Gart suppression primarily triggers a robust G1 arrest that is accompanied by a loss of LSCs in our model.

In addition to Brd4, we compared the effects of Gart suppression to knockdown validated shRNAs (Figure 2.11 and 2.26 d) targeting several genes that have been proposed as promising therapeutic targets for cancer therapy – i.e. Atm (Khalil, Tummala, Chakarov, Zhelev, & Lane, 2012), several isoforms of Pik3 (Jabbour, Ottmann, Deininger, & Hochhaus, 2014; P. Liu, Cheng, Roberts, & Zhao, 2009), Mtor (Advani, 2010), Plk1 (Lan et al., 2012), Glis (Xiang et al., 2015), Dhfr (Schweitzer, Dicker, & Bertino, 1990), Phgdh (Zogg, 2014) and Pdk1 (Raimondi & Falasca, 2011).

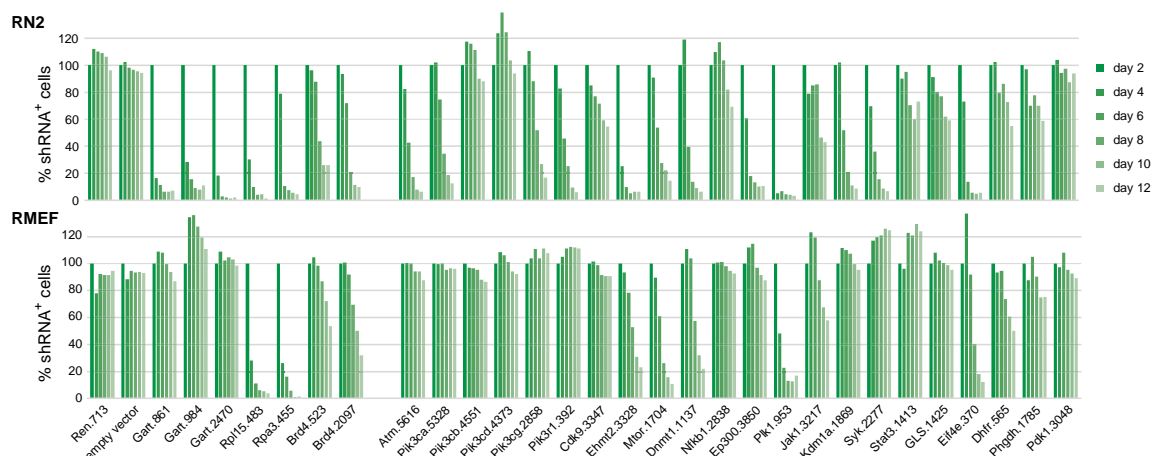


**Figure 2.11 | Comparison of the effects of Gart knockdown to the effects of many proposed cancer targets.**

Competitive proliferation assay with neutral controls (Ren.713 and empty vector), essential controls (Rpl15.483 and Rpa3.455) and addition controls (Gart.861, Gart.984, Gart.2470, Brd4.523 and Brd4.2097) and 22 sensor validated shRNAs against proposed drug targets. All shRNAs were tested in TRMPV-Neo-miR-E except the two Brd4 shRNAs, which were tested in miR-30. Percentage of shRNA<sup>+</sup> cells over time, relative to day 2 on dox in AML and RMEF is shown. Gart shows the highest differential effect in RN2s and RMEF.

However, suppression of many of these targets showed no, or only very mild effects in RN2s (Cdk9, Nfkb1, Glis, Phgdh and Pdk1). Furthermore some of the tested shRNAs showed highly toxic effects in both cell lines (Ehmt2, Mtor, Dnmt1, Eif4e and Dhfr). Interestingly, also suppression of Plk1, a kinase involved in cell cycle regulation, rapidly depleted RN2s and RMEFs. Many potent inhibitors of Plk1 have been developed in the last years (Schöffski, 2009) and Volasertib, developed by Boehringer Ingelheim, has completed phase II clinical trials already (Rudolph et al., 2009). Only a few genes showed leukemia specific effects in our assay (Atm, some Pik3 isoforms, Kdm1a, Ep300 and Syk) but none of them reached the level of specificity shown by Gart. Together, these findings characterize Gart as a non-oncogene addiction target in leukemia, whose suppression effects match those of promising targets pursued in the clinic, while being selective at an unprecedented level.

### 2.2.3 *In vivo* validation of Gart as a candidate non-oncogene addiction target in AML

While Gart emerged as strong and selective AML dependency in both, our multiplexed screen and extensive validation studies, all these experiments have been performed in tissue culture, which may introduce biases in cancer dependencies. Such biases might be particularly relevant when studying non-oncogene addiction to metabolic targets, since nutrient supply and growth conditions are vastly different between standard cell culture and conditions *in vivo* (Jang, Kim, & Lee,

2013). To investigate whether AML cells are addicted to Gata *in vivo*, we took advantage of a previously established Tet-on RNAi approach for validating candidate targets in fully established leukemia in mice (Johannes Zuber, McJunkin, et al., 2011). Specifically, we transplanted Tet-on competent MLL/AF9;Nras<sup>G12D</sup> leukemia cells transduced with TRMPV-Neo constructs encoding Gata and control shRNAs into syngeneic CD45.1<sup>+</sup> recipient mice, and triggered shRNA expression upon disease onset in bioluminescent imaging by supplementing the drinking water with dox (Figure 2.12 a).



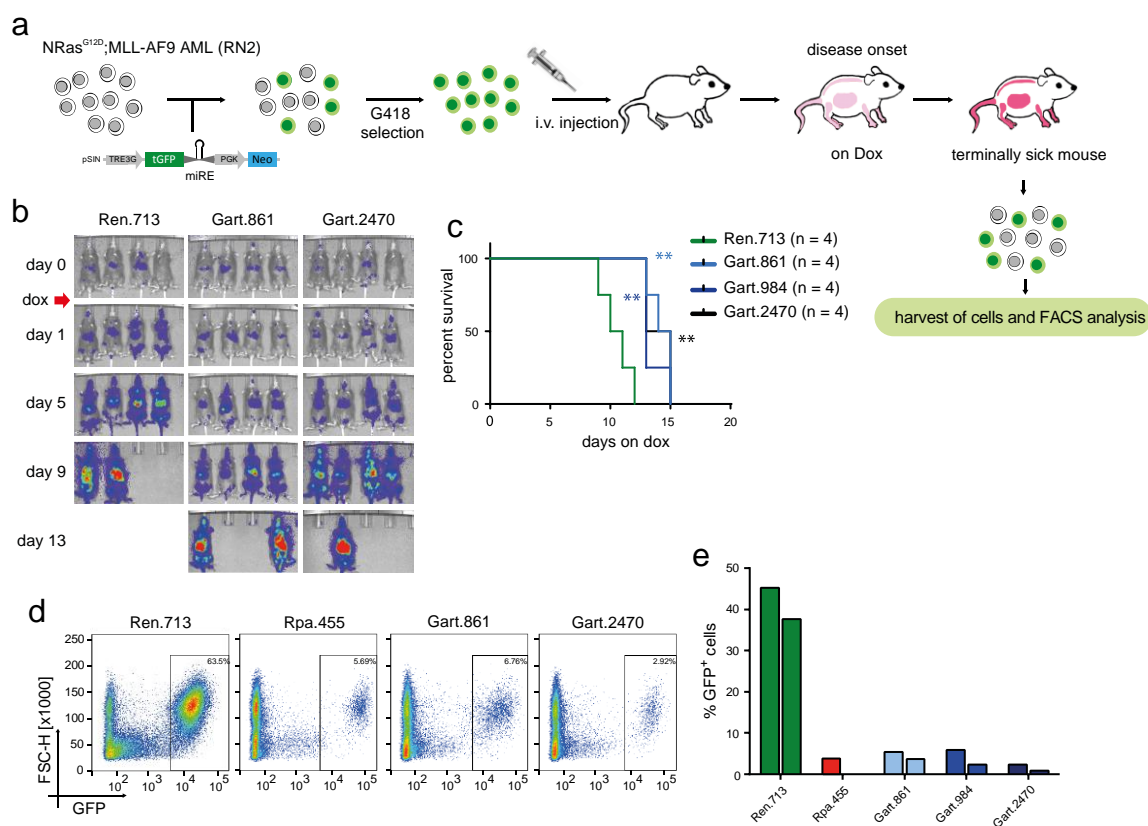


**Figure 2.12 | Validation of Gart knockdown effects *in vivo*.**

(a) Schematic of the *in vivo* transplantation assay. RN2 cells are infected with TGmPNe harboring different hairpins. Cells are selected with G418 for 7 days (1 mg/ml). 2.5 × 10<sup>6</sup> were injected into sublethally irradiated Rag<sup>-/-</sup> mice (5.5Gy, 18 h before injection). Mice were monitored using bioluminescent imaging every other day and upon disease onset dox was supplied in the drinking water (4 mg/ml). Spleen and bone marrow of terminally diseased mice were harvest and analyzed using flow cytometry. (b) Bioluminescent images of Rag<sup>-/-</sup> mice transplanted with RN2 cells, transduced with the indicated shRNA in the vector TGmPNe. Doxycycline was administered via drinking water upon disease onset (day 0, 4 mg/ml). The scale is identical for all images (counts, min: 25, max 30.000) except for day 0 where the min. threshold is 17. (c) Kaplan-Meier survival curves of recipient Rag<sup>-/-</sup> mice depicted in 2b transplanted with RN2 harboring 3 different Gart shRNAs and Ren.713 shRNAs. Statistical significance was determined using the Log-rank (Mantel-Cox) test (\*\*, *p* < 0.01). (d) Representative flow cytometry plots of leukemic cells harvested from spleens of terminally sick mice depicted in 2b. The shown cell population is the fraction of transplanted Ly5.1<sup>+</sup> cells and the percentage of shRNA<sup>+</sup> cells is indicated. (e) Quantification of FACS analysis depicted in (d). 2 mice/condition are shown (for Rpa.455 there is only one value available).

Compared to control mice transplanted with AML cells expressing a neutral Ren.713 control shRNA, expression of two independent Gart shRNAs resulted in delayed disease progression in bioluminescent imaging (Figure 2.12 b) and a significant survival benefit (Figure 2.12 c). Of note, the scale of these effects was similar to effects seen after suppressing Brd4 in the same model (Johannes Zuber, Shi, et al., 2011).

In addition to bioluminescent imaging and overall survival, the TGMPNe-based RNAi system allows for direct quantification of shRNA<sup>+</sup> leukemia cells at a terminal disease stage through co-expressed

fluorescent reporters, which provides a more sensitive readout for the assessment of leukemia-specific dependencies that takes in account cell populations that have evaded shRNA-expression (Johannes Zuber, McJunkin, et al., 2011). While most leukemia cells isolated from terminally diseased recipients of TRMPV-Ren.713 transduced AML cells showed strong shRNA expression, shRNA<sup>+</sup> cells were strongly depleted in case of Rpa3.455 and two independent Gart shRNAs (Figure 2.12 d and e), demonstrating that AML cells expressing these shRNAs were outcompeted by shRNA<sup>-</sup> cells *in vivo*. To further validate the addiction to Gart *in vivo* as an on-target RNAi effects, we transplanted AML cells harboring a Tet-inducible dsRed-shRNA expression cassette together with constitutively expressed Gart and control cDNAs into syngeneic recipients, and initiated shRNA expression upon disease onset in bioluminescent imaging. Expression of fully functional Gart (3x wt Gart) or a Gart cDNA harboring mutations in all enzymatic pockets (3x mut. Gart) showed no major effects on disease progression and overall survival (Figure 2.13 a and c), co-expression of the functional protein completely rescued the effects of Gart suppression *in vivo*, while no such effects were observed when expressing an enzymatically dead Gart cDNA (Figure 2.13 a and c).

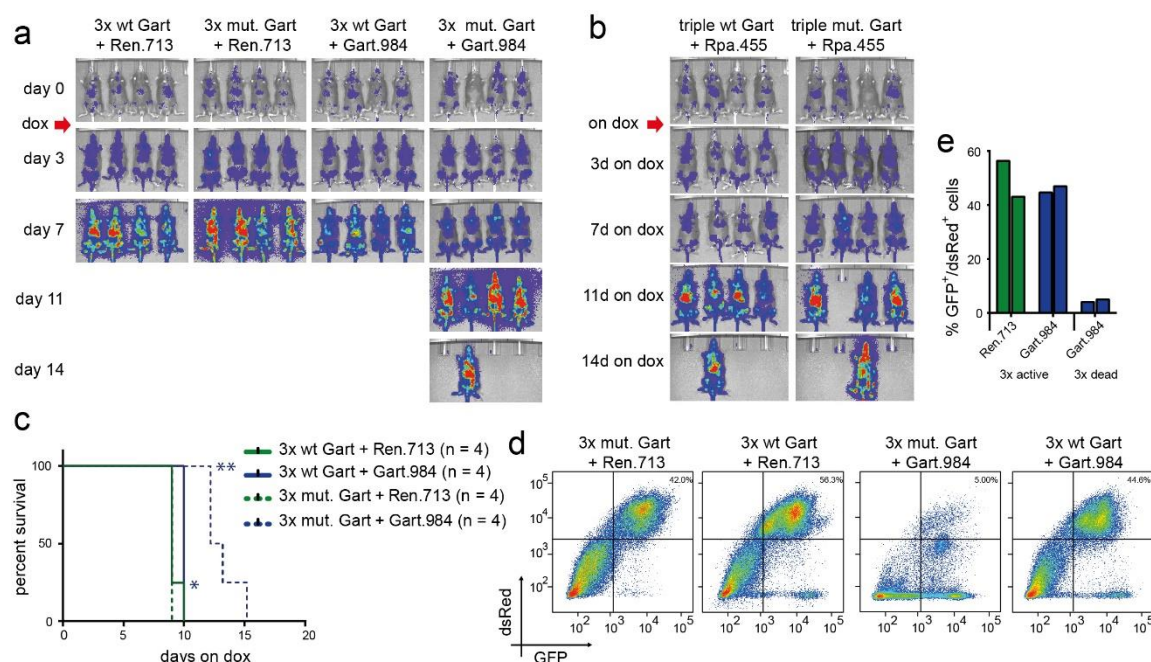


**Figure 2.13 | *In vivo* rescue of the Gart phenotype.**

(a), (b) Bioluminescent imaging of Rag<sup>-/-</sup> mice transplanted with  $2.0 \times 10^6$  RN2 cells co-transduced with shRNAs in TRN and either a 3x wt or a 3x mutant Gart cDNA. Doxycycline was administered via the drinking water upon disease onset (day 0, 4 mg/ml). The scale is identical for all images (counts, min: 25, max 30.000) except for day 0 where the min. threshold is 17. (c) Kaplan–Meier survival curves of recipient Rag<sup>-/-</sup> mice depicted in (a). Survival curves of mice transplanted with leukemia cells harboring the Gart shRNA were compared to Ren.713 using a Log-rank (Mantel-Cox) test (\*,  $p = 0.04$ ; \*\*,  $p = 0.0082$ ). (d) Representative flow cytometry plots of leukemic cells harvested from spleens of terminally sick mice depicted in (a). The shown population is the fraction of transplanted, Ly5.1<sup>+</sup> cells and the percentage of cDNA<sup>+</sup>/shRNA<sup>+</sup> (GFP<sup>+</sup>/dsRed<sup>+</sup>) cells is indicated in the corner of the gate. (e) Quantification of FACS analysis depicted in (a) and (b). 2 mice/condition are shown.

Importantly, expression of wildtype and mutant Gart cDNAs had no impact on the survival benefit promoted by expression of an essential control shRNA (Rpa3.455; Figure 2.13 b). FACS analysis of cells harvested from terminally sick mice showed that mice with an enzymatically dead Gart cDNA and a Gart shRNA succumb to RN2s cells which have silenced shRNA expression (Figure 2.13 d and e). In contrast, when a functional cDNA is expressed, there is no negative selection on Gart shRNA expression anymore. Together, these results demonstrate that AML cells are addicted to Gart *in vivo*, ruling out the possibility that the observed effects are culture medium based *in vitro* artefacts.

## 2.3 Gart alterations and addiction in human leukemia

### 2.3.1 Gart is amplified and overexpressed in human leukemia

After validating Gart as a leukemia-specific dependency in MLL/AF9;Nras<sup>G12D</sup>-driven murine AML, we wondered about the role of GART in human AML. In humans, GART is located on the long arm of chromosome 21 (21q22.11). Interestingly, Down-syndrome patients carrying a trisomy 21, while having no increased risk of developing cancer overall and a reduced risk of developing solid tumors (Hasle, Clemmensen, & Mikkelsen, 2000), have a 10-20-fold increased risk of developing leukemia (both AML and ALL), and a 500-fold increased risk of developing acute megakaryoblastic leukemia (Hitzler, 2007). In addition, a focal amplification of chromosome 21 (so-called iAMP21) typically involving 47 protein coding genes including GART, has been identified as a recurrent copy-number alteration and a poor prognostic marker in B-ALL patients (Li et al., 2014; Rand et al., 2011) (Figure 2.14 a).

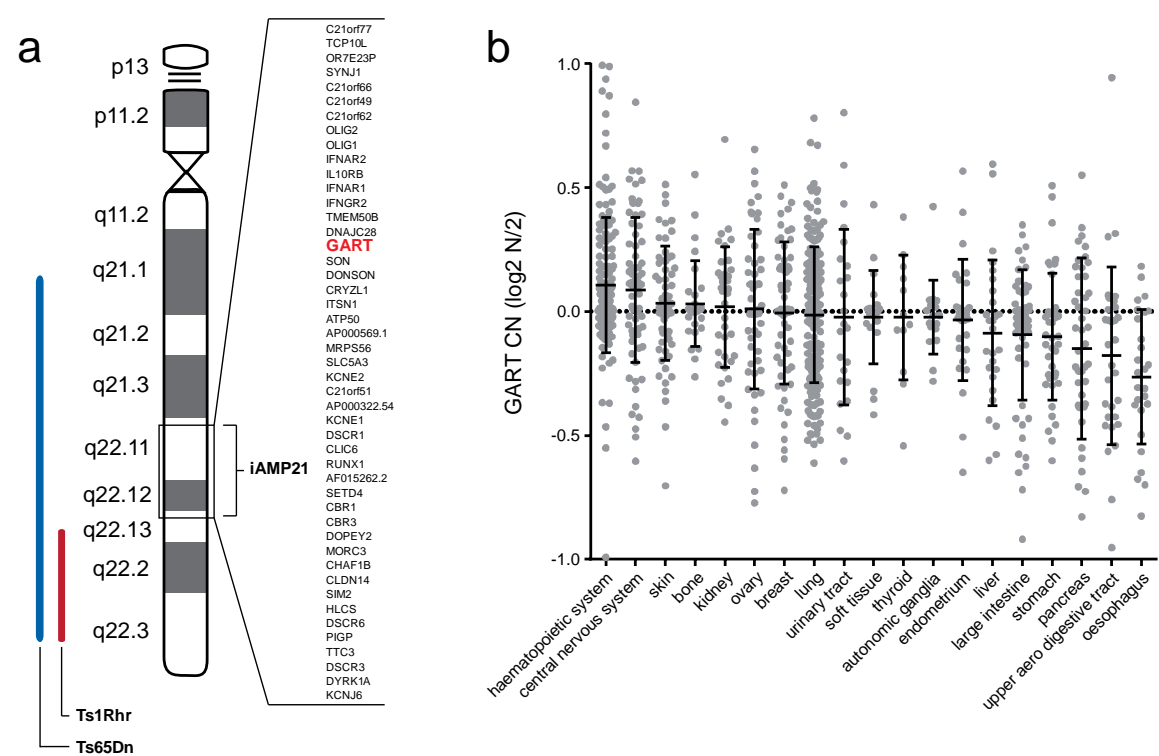


**Figure 2.14 | GART is frequently amplified in human cancer.**

(a) Schematic of chromosome 21. The frequently amplified area iAMP21 and the 47 protein coding genes therein are indicated. Blue and red bars indicate orthologous areas on mouse chromosomes 16 amplified in 2 trisomy 21 mouse models. Only Ts65Dn contains a Gart amplification. (b) Analysis of GART-copy number alterations in 1036 human cell lines. Only datasets with more than 10 cell lines are shown. Error bars indicate mean + SD.

In addition to this B-ALL-specific prognostic marker, a systematic analysis of 1036 human cancer cell lines revealed that GART copy number gains are common in leukemia (Barretina et al., 2012) (Figure 2.14 b). Moreover, transcriptional profiling of this large cell line panel showed that GART expression is significantly higher in hematopoietic malignancies compared to solid tumors (Figure 2.15 a). Similar results were observed in a recent RNA-seq analysis of 675 cancer cell lines (Klijn et al., 2014), where hematopoietic cancers were again showing significantly higher GART transcript levels than solid tumors (Figure 2.15 b).

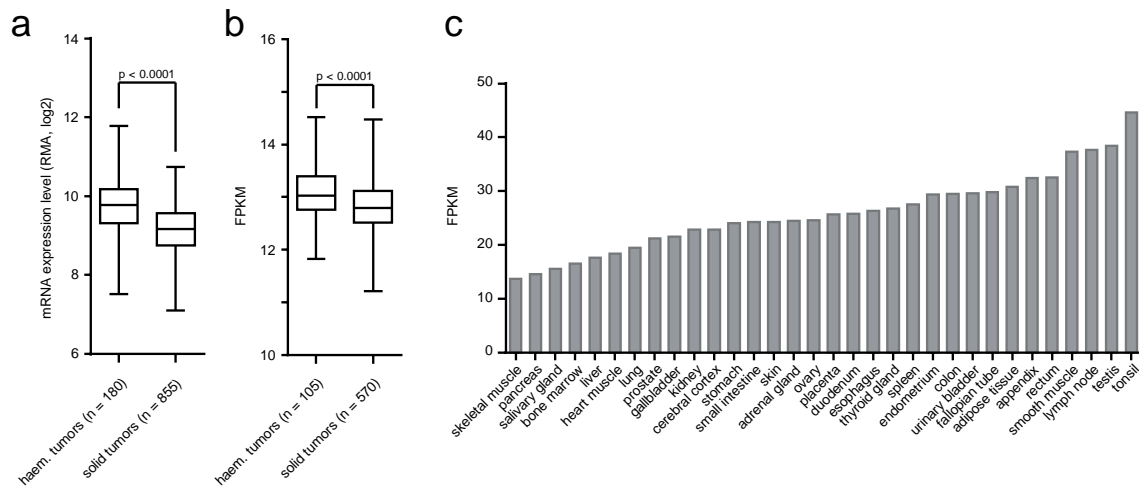


**Figure 2.15 | Analysis of GART expression in cancer cell lines and normal tissue.**

(a), (b) Comparison of GART gene expression in hematopoietic and solid tumors. Panel (a) contains data from CCLE (Barretina et al., 2012) and panel (b) published data from Klijn et. al. (Klijn et al., 2014). Box plots show median, and whiskers min and max values. Statistical significance was determined by applying a t-test to compare datasets. (c) Expression of GART in normal tissues. Data extracted from human protein atlas (<http://www.proteinatlas.org>)

RNA-seq analysis of normal tissues shows no particularly strong GART expression in bone marrow (Fig. 2.15 c). Together, these analyses reveal that GART is commonly amplified and overexpressed in hematopoietic malignancies, raising the possibility that GART might act as an oncogene in this context.

While several candidates have been proposed, the driver mechanisms of trisomy 21- and iAMP21-associated leukemias remain incompletely understood, and despite its frequent involvement in amplifications and its common overexpression, GART has not been discussed as a candidate driver. A recent study has used a mouse model harboring triplication of a syntenic region involving 31 genes to identify overexpression of HMGN1, a nucleosome remodeling protein on 21q22, as a candidate driver mechanism in B-ALL (A. a Lane et al., 2014). Importantly, the triplication in this model does not involve all common iAMP21 genes and excluded GART and others (Fig. 2.14 a). To functionally explore GART overexpression as a candidate driver mechanism, we performed leukemogenesis assays using two established AML models based on expression of common fusion proteins (MLL/ENL and AML1/ETO9a), which have been used previously to investigate cooperating oncogenes (Johannes Zuber et al., 2009). Specifically, fetal liver-derived hematopoietic stem and progenitor cells (HSPC) were transduced with two MSCV-based retroviral vectors, one expressing either fusion protein linked to Luciferase, and the other expressing GFP either alone or together

with a murine Gart cDNA or Nras<sup>G12D</sup>, which is known to strongly cooperate with both fusion proteins (Johannes Zuber et al., 2009). While enforced expression of Nras<sup>G12D</sup> led to the expected strong acceleration of leukaemogenesis in both models (Figure 2.16), co-expression of Gart did not lead to shorter onset and survival times in either model, suggesting that it does not act as a potent oncogene in concert with these two fusion proteins.

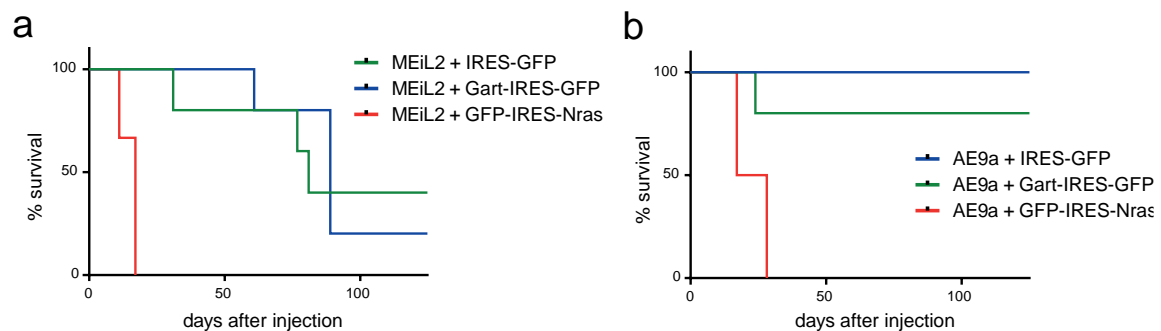


**Figure 2.16 | Gart has no driver function in murine MLL/ENL and AML-Eto driven leukaemogenesis.**

(a), (b) Kaplan Meier survival curves of mice injected with fetal liver cells (FLC) cotransduced with a retroviral vector carrying an oncogenic fusion protein coupled to luciferase expression (MLL/ENL, AML1-ETO) and a vector carrying either Gart or Nras<sup>G12D</sup> cDNA coupled to GFP expression as well as an empty control vector. Expression of a Gart cDNA in combination with a fusion protein did not accelerate leukaemogenesis in comparison to an empty control vector (IRES-GFP).

Importantly, this does not exclude the possibility that Gart overexpression promotes leukemogenesis and aggressiveness in other genetic contexts.

### 2.3.2 Human leukemias are broadly addicted to GART expression

While GART's potential role as a direct driver remains to be explored, the more relevant question to our work was whether other leukemia contexts are functionally addicted to GART to a similar degree as our mouse model. As a first step into exploring this question, we performed Tet-RNAi competition assays in Tet-on competent MOLM-13 cells (J Zuber et al., 2011), which harbor an occult chromosome insertion (ins[11;9][q23;p22p23]) leading to expression of an MLL/AF9 fusion protein (Matsuo et al., 1997), resembling the defining oncogene in our genetically engineered mouse model. RNAi-mediated suppression of GART (Figure 2.17 a) triggered rapid depletion of shRNA<sup>+</sup> MOLM-13 cells (Figure 2.17 b).

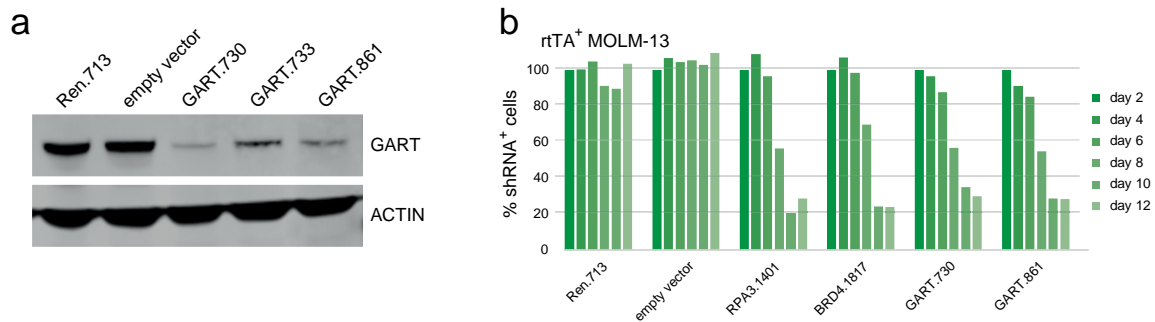


**Figure 2.17 | Evaluation of GART knockdown in human MOLM-13R cells.**

(a) GART western blot of whole cell lysates from rtTA<sup>+</sup> MOLM-13 cells, transduced with the indicated shRNAs in TRMPV-Neo. shRNA<sup>+</sup> cells were sorted after 5 days on dox. ACTIN is used as protein loading control. (b) Quantification of shRNA<sup>+</sup> cells in representative competitive proliferation assays with human rtTA<sup>+</sup> MOLM-13 cells. All values are relative to day 2 on dox and a time course over 12 days is shown.

Like in our mouse model, the scale of these effects were comparable with an essential control shRNA targeting RPA3 and a potent shRNA targeting BRD4, which is well-established as a non-oncogene addiction target in MOLM-13 and other human AML lines (Johannes Zuber, Shi, et al., 2011).

After validating addiction to GART in MOLM-13 cells, we expanded validation studies to 15 hematopoietic cancer lines involving different driver mutations and tissue contexts. To facilitate straight-forward shRNAir-based competition assays in human cell lines, we constructed a simple lentivirus constitutively expressing GFP together with optimized miR-E-embedded shRNAirs (Fellmann et al., 2013) from a strong spleen focus forming (SFFV) promotor (González-Murillo et al., 2010) (Figure 2.18 a).



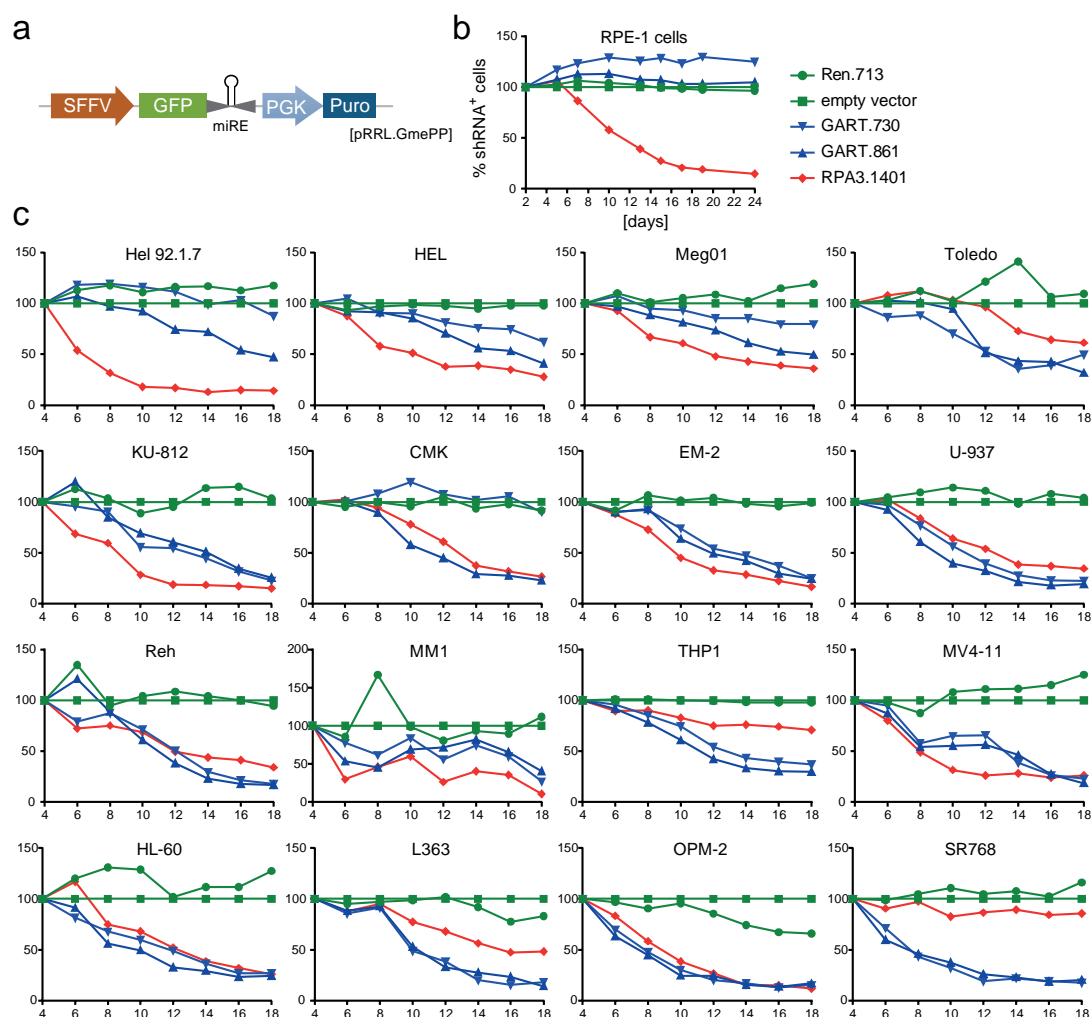


**Figure 2.18 | Evaluation of GART suppression in various different human cell lines.**

(a) Vector scheme of the lentiviral vector GmePP. (b) Quantification of shRNA<sup>+</sup> cells in representative competitive proliferation assays in human, non-transformed RPE-1 cells. Cells were infected with shRNAs in the lenti viral vector GmePP under S2 biosafety conditions. The percentage of shRNA<sup>+</sup> cells was determined by FACS over a course of 24 days and normalized to day 2 after transduction and empty vector. (c) Same assay as (b) with 16 different human, haematopoietic cancer cell lines. Values are normalized to day 4 and empty vector. Cell lines are sorted from high GART expression (top left corner) to low GART expression (lower right corner).

This simple lentivirus ensures both high-titer packaging and optimal shRNAmir expression and processing, and has meanwhile been successfully used for validation studies in human cancer lines by many labs. To control for generally lethal effects of GART suppression, we first performed competition assays in non-transformed RPE-1 cells, which are near-diploid epithelial cells isolated from retinal pigmented epithelium (Bodnar et al., 1998; Jiang et al., 1999). While RPE-1 cells expressing a potent RPA3 shRNA strongly depleted over time (as expected in this highly proliferative cell line), expression of two potent GART shRNAs was fully tolerated over an extended culture period of 24 days (Figure 2.18 b) similar to the neutral behavior observed in murine fibroblasts (RMEF). By stark

contrast, GART suppression was detrimental in all 15 analyzed hematopoietic cancer cell lines (Figure 2.18 c). In 11 out of the 16 cell lines the effects of GART suppression were similar or even stronger compared to the effects of RPA3 suppression, while in five cell lines the effects were weaker. Importantly, strong effects were not associated with a specific hematopoietic lineage, suggesting that addiction to GART affects diverse subtypes of hematopoietic cancers. It appears that cells with very high GART expression (Figure 2.18 c, top row) or even harboring an additional copy of chromosome 21 (HEL 92.1.7, HEL, Meg01, CMK) are less sensitive to GART suppression. Despite this, still all of the cell lines responded, indicating that addiction to GART is not primarily determined by aberrant expression states but a more general trait of hematopoietic cancers.

## 2.4 Towards exploiting GART addiction for leukemia therapy

### 2.4.1 GART suppression promotes a rescuable IMP starvation in leukemia

As a tri-functional enzyme, GART catalyzes three of ten steps in *de novo* purine synthesis, a linear pathway converting ribose-5-phosphate to inosine monophosphate (IMP), which provides the common source for the synthesis of all adenine- and guanine-containing molecules (A. N. Lane & Fan, 2015) (Figure 2.19).

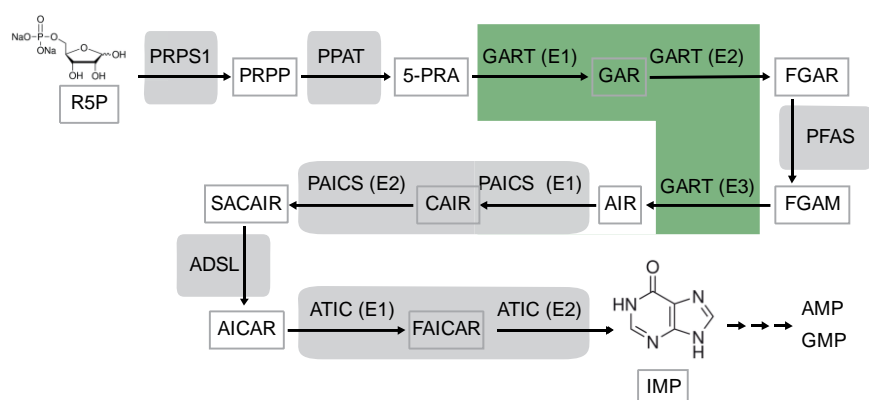


**Figure 2.19 | Proteins and intermediates involved in *de novo* purine synthesis.**

The schematic shows 11 enzymatic steps from ribose-5-phosphate (R5P) to inosine monophosphate (IMP). The product of the first step also used for other cellular processes, while all other products are unique in this pathway. Enzymes are indicated in filled boxes, intermediates are indicated with grey frames. PRPP, 5-Phosphoribosyl pyrophosphate; 5-PRA, 5-Phosphoribosylamine; GAR, Glycinamide ribotide; FGAR, Formylglycinamide ribotide; FGAM, Formylglycinamide ribotide; AIR, 5-Aminoimidazole Ribotide; CAIR, Carboxyaminoimidazole Ribotide; SACAIR, 5-Aminoimidazole-4-(N-succinylcarboxamide) Ribotide; AICAR, 5-Aminoimidazole-4-carboxamide Ribotide; FAICAR, 5-Formamionimidazole-4-carboxamide Ribotide;

To investigate how RNAi-mediated GART suppression affects cellular levels of this central molecule, we established a mass spectrometry-based assay to quantify IMP levels in different cellular contexts. In GART-addicted MLL/AF9;Nras<sup>G12D</sup>-driven leukemia cells, partial suppression of GART using two independent shRNAs triggered a highly significant 4-8-fold reduction of intracellular IMP levels (Figure 2.20 a).

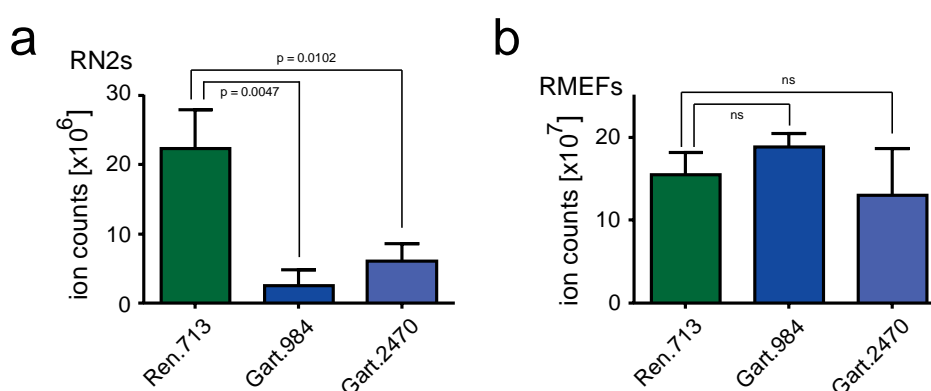


**Figure 2.20 | Mass spectrometric analysis of IMP levels upon Gart knockdown.**

(a) Mass spectrometric analysis of IMP levels in RN2s expressing different shRNAs in TRMPV-Neo (miR-E). shRNA<sup>+</sup> cells were sorted after 3 days on dox. Per biological sample, metabolites from 3\*10<sup>6</sup> cells were extracted and the mean of two technical replicates was determined. The analysis was conducted in biological triplicates. Statistical significance was determined using a t-test, n = 3, mean + SD, (b) IMP levels of RMEFs.

Remarkably, these effects were not observed in insensitive RMEF cells, in which IMP levels were unaffected despite similar or even stronger GART protein suppression (Figure 2.20 b). These results indicate that a partial GART suppression results in a drop of IMP specifically in cells that are addicted to full GART expression.

In addition to *de novo* synthesis starting from ribose-5-phosphate, cells can produce IMP from hypoxanthine in a reaction catalyzed by the hypoxanthine-guanine phosphoribosyltransferase (HGPRT), a key enzyme in purine salvage pathways (Ao et al., 2008). To investigate how this pathway affects the leukemia-specific addiction to Gart, we performed competitive proliferation assays in MLL/AF9;Nras<sup>G12D</sup> leukemia cells with and without media supplementation with hypoxanthine. While Gart suppression in the absence of hypoxanthine triggered the known deleterious effects, addition of hypoxanthine completely rescued this phenotype and leukemia cells expressing two independent Gart shRNA showed no depletion over nine days of culture (Figure 2.21 a).

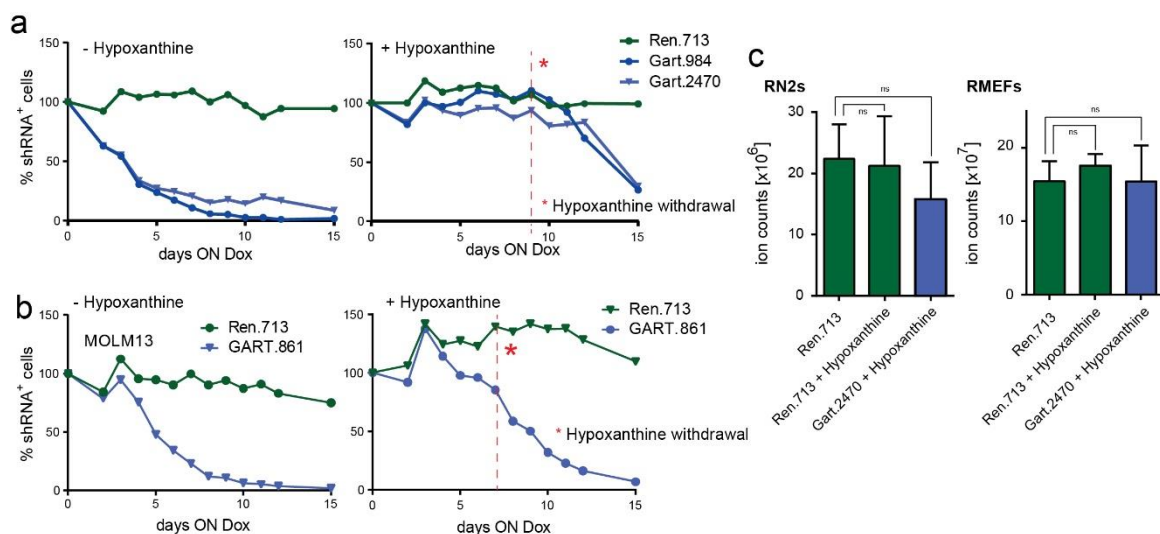


**Figure 2.21 | Hypoxanthine rescues the Gart knockdown phenotype.**

a) Competitive proliferation assays were performed with RN2s cells, transduced with the indicated shRNAs in TRMPV-Neo. Together with dox, half of the cells was cultured in the presence of hypoxanthine (100  $\mu$ M) for 9 days. After 9 days of Hypoxanthine treatment, the compound was washed out and cells were cultured with dox only for another 6 days. Percent shRNA<sup>+</sup> cells, relative to day 0 on dox is shown. (b) MOLM13R cells were assayed as in (a) and hypoxanthine was withdrawn after 7 days. (c) Mass spectrometric analysis of IMP levels in RN2s expressing different shRNAs in TRMPV-Neo (miR-E). shRNA<sup>+</sup> cells were sorted after 6 days on dox and on hypoxanthine (100  $\mu$ M). Per biological sample, metabolites from 3\*10<sup>6</sup> cells were extracted and the mean of two technical replicates was determined. The analysis was conducted in biological triplicates. The same Ren.713 values as in Figure 2.20 were used. Statistical significance was determined using a t-test, n = 3, mean + SD.

Upon withdrawal of hypoxanthine, we again observed a rapid depletion of Gart-shRNA<sup>+</sup> cells, and similar effects were also observed in human MOLM-13 AML cells (Figure 2.21 b). To explore how hypoxanthine supplementation affects IMP levels in Gart-addicted and non-addicted cells, we quantified IMP in leukemia and RMEF cells expressing a potent Gart or control shRNA. While hypoxanthine addition did not alter IMP levels in any control shRNA expressing cells or RMEFs expressing a potent Gart shRNA, it restored IMP levels in addicted leukemia cells upon Gart suppression (Figure 2.21 c). Together, these results suggest that the leukemia-specific sensitivity to partial Gart suppression is associated with an inability to utilize salvage pathways for compensating a reduction in *de novo* purine synthesis. Importantly, while in tissue culture this metabolic bottleneck can be rescued through hypoxanthine supply, our validation studies in mice (Figure 2.12 and 2.13) suggest that hypoxanthine levels *in vivo* are insufficient to compensate for a reduction of *de novo* purine synthesis. It should also be noted that the availability of a rescue strategy for mitigating the consequences of GART suppression may turn out useful in clinical treatment regimens.

#### 2.4.2 Comparative analysis of available GART inhibitors

After establishing compelling genetic evidence that leukemia cells are addicted to GART, we sought to investigate how this phenomenon can be exploited for targeted leukemia therapy. Several small-molecule GART inhibitors are already available, which was the main reason why GART was included as a “drugged” target in our focused shRNAmir library. All available agents are antifolates inhibiting the 10-formyltetrahydrofolate-dependent activity of the GARTase component of GART with varying selectivity. The most specific GART inhibitor currently known is Lometrexol (DDATHF), an anti-folate with high selectivity for the GARTase component of GART (Beardsley, Moroson, Taylor, & Moran, 1989). Another potent GARTase inhibitor is Pemetrexed (Alimta), which also has activity on other folate-dependent enzymes including thymidylate synthase and dihydrofolate reductase (DHFR) (Taylor et al., 1992). Another even more unspecific way to inhibit GARTase is provided by Methotrexate, a widely used competitive DHFR inhibitor that leads to a global reduction of intracellular tetrahydrofolate levels (Khan, Tripathi, & Mishra, 2012; Meyer, Miller, Rowen, Bock, & Rutzky, 1950).

To investigate whether any of the compounds would recapitulate the strong leukemia-specific effects of RNAi-mediated GART suppression, we determined proliferation-based IC<sub>50</sub> values side-by-side in MLL/AF9;Nras<sup>G12D</sup> AML cells and RMEFs (Figure 2.22).

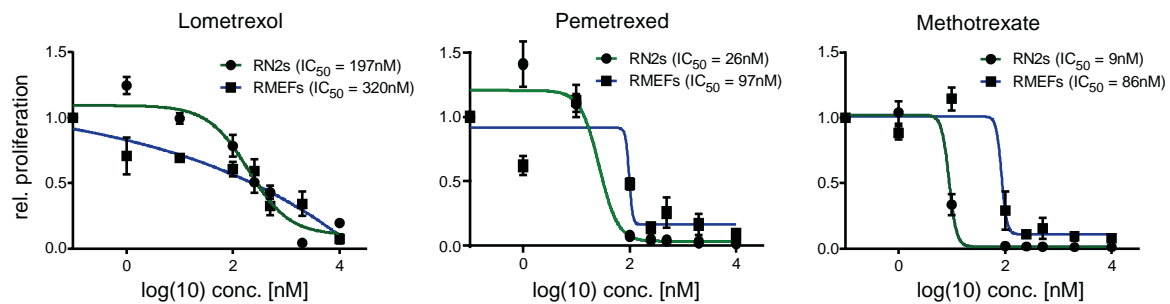


**Figure 2.22 | IC<sub>50</sub> curves of different GART inhibitors in RN2s and RMEFs.**

Relative proliferation of RN2 and RMEF cells after 48 culture in the presence of Pemetrexed, Lometrexol or Methotrexate at the indicated concentrations. For each condition three biological triplicates were prepared and IC<sub>50</sub> concentrations were calculated using a nonlinear fit model. Error bars depict mean + SD.

In these assays, the most selective GARTase inhibitor Lometrexol showed strong anti-proliferative effects in both leukemia and RMEF cells, and IC<sub>50</sub> values in leukemia were only slightly below those in RMEF (197 nM vs. 320 nM). Similarly, Pemetrexed showed strong inhibitory effect in both contexts that were slightly more leukemia-specific (26 nM vs. 97 nM), while the general anti-folate Methotrexate showed the highest difference in sensitivity between leukemia and RMEF (9 nM vs. 86 nM). These relatively similar anti-proliferative effects of these agents and, in particular, the inverse correlation between their GARTase selectivity and the leukemia-specificity of their effects reveals that small-molecule inhibition of GARTase fails to recapitulate the potent leukemia-specific effects of RNAi-mediated GART suppression. These results suggest that inhibiting the GARTase activity is insufficient to exploit the addiction to GART for targeted leukemia therapy.

#### 2.4.3 The AIRS component provides the most promising target for exploiting GART addiction

Translating the leukemia-specific addiction to GART observed using genetic approaches into a small-molecule based targeted therapy is complicated by the peculiarity that the GART protein catalyzes three druggable enzymatic activities in *de novo* purine synthesis. To rigorously probe which enzymatic pocket represents the most promising target for therapeutically exploiting the addiction to GART, we performed three independent genetic rescue experiments involving different mutants of GART or its subdomains (Figure 2.11). The applied experimental strategy was similar to previous cDNA rescue experiments showing that expression of an RNAi-resistant Gart cDNA fully rescued the effects of inducible Gart-shRNAs in competitive proliferation assays in our Tet-on competent AML mouse model (Figure 2.8). Here, we expressed three RNAi-resistant Gart cDNAs each harboring a single mutation that destroyed one of the enzymatic activities (Figure

2.23 a) to study which activity loss would impair the rescue potential most strongly. Expression of an RNAi-resistant cDNA encoding the wild type protein again fully rescued the effects of a potent Gart shRNA, and mutants deficient for the GARS and GARTfase function showed a rescue potential that was only slightly reduced compared to the wild type (Figure 2.23 b). By stark contrast, expression of an RNAi-resistant Gart variant harboring a defective AIRS component was unable to rescue the effects of RNAi-mediated Gart suppression, and cells expressing this variant depleted comparable to control cells expressing a cDNA harboring loss-of-function mutations in all three enzymatic domains (Figure 2.23 b).

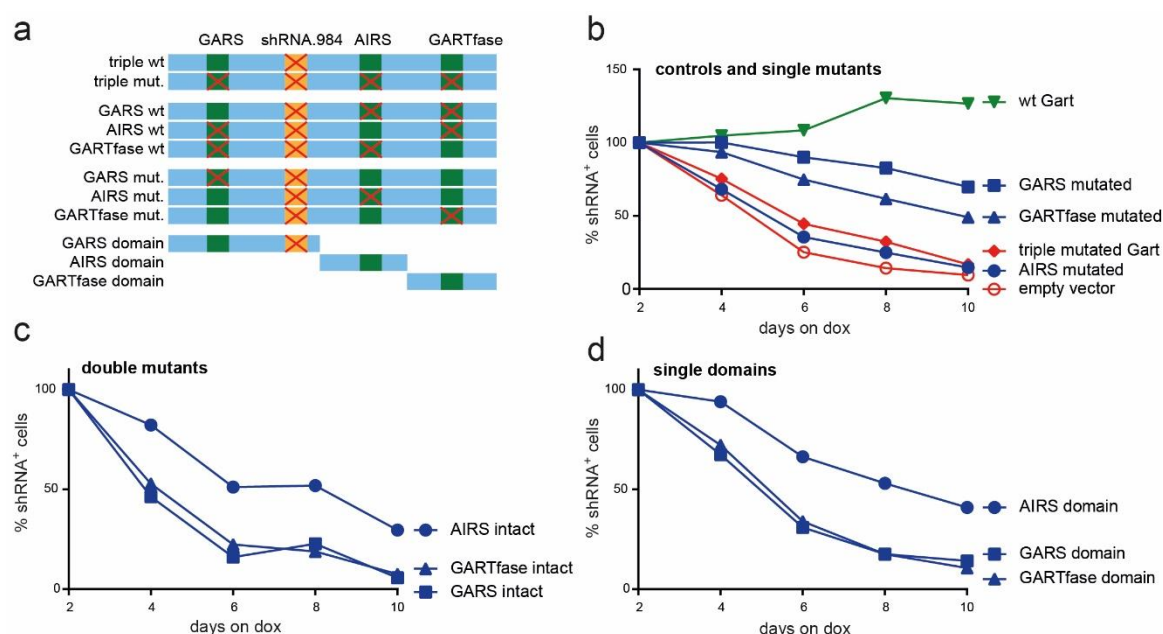


**Figure 2.23 | cDNA rescue experiments with different Gart mutants identify AIRS as the bottleneck activity.**

(a) Schematic depicting all Gart mutants used for a series of rescue experiments. The shRNA target site for Gart.984 was mutated in all cDNAs. Furthermore, one or two of the three enzymatic activities GARS, AIRS and GARTfase were rendered inactive by point mutations. One set of experiments was carried out with only the individual functional domains of Gart. (b), (c), (d) Series of cDNA rescue experiments showing the percentage of shRNA expressing cells over the course of 10 days on dox, relative to day 2. The respective cDNA and shRNA combination used is indicated next to the last time point of each condition.

In a subsequent rescue experiment, we expressed Gart cDNAs harboring inactivating mutations in two of the three catalytic pockets to identify the enzymatic activity whose restoration would provide the strongest rescue for the suppression of the entire protein. While expression of double-mutants encoding only an intact GARS or GARTfase activity did not rescue the anti-leukemic effects of RNAi-mediated Gart suppression, restoring the AIRS activity partially rescued this phenotype (Figure 2.23 c). Lastly, we expressed synthetic cDNAs encoding each of the three enzymatic

Gart domains individually, and again observed that expression of GARS and GARTase had no effect, while expression of the isolated AIRS domain partially rescued the detrimental effects of RNAi-mediated suppression of endogenous Gart (Figure 2.23 d). Together, these rescue experiments provide compelling evidence that the anti-leukemic effects of partial Gart suppression are largely caused by an enzymatic bottleneck in the AIRS component. Therefore, small-molecule inhibition of AIRS is predicted to provide a promising strategy for therapeutically exploiting the addiction to GART and *de novo* purine biosynthesis in leukemia therapy. These findings provide strong genetic support for the development of selective AIRS inhibitors, which according to our colleagues at Boehringer Ingelheim is structurally feasible.

## 2.5 Improvements and new experimental strategies in shRNAmir technology.

The analysis of my multiplexed shRNAmir screen and subsequent extensive validation studies indicated that miR-30-based negative-selection screening accurately identified leukemia-specific dependencies in the model. However, during my project I encountered several areas where existing shRNAmir technology could be further improved. While previous efforts to derive better shRNAmir design rules have led to a substantial improvement in overall shRNAmir potency (Fellmann et al., 2011a), I encountered several genes where only one or two shRNAs produced sufficient target protein knockdown. Furthermore, the identification of potent shRNAmirs mainly relied on conventional immunoblot analysis (which depends on the availability of specific antibodies), or the quantification of mRNA suppression levels, which is insufficient to assess shRNAmir effects on translation that are very relevant for quantifying actual effects at the protein level. At later stages of my project, I realized the potential of shRNAmirs to perform systematic combinatorial loss-of-function experiments, which could provide a powerful system for genetically exploring targeted therapies in combination. Through working on a candidate target involved in very basic cellular processes such as purine synthesis, I also realized Tet-on regulatable shRNAmir expression in transgenic mice throughout all tissues could provide a unique system for studying target suppression effects in adult tissues in order to explore therapeutic windows and possible toxicities associated with non-oncogene addiction targets. During my PhD, the further optimization of shRNAmir technology became a second major focus, and projects addressing the aforementioned questions are summarized below.



### 2.5.1 Establishment of an optimized miRNA backbone (miR-E)

In collaboration with Mirimus, a small biotechnology company at Cold Spring Harbor Laboratories developing shRNAmir reagents, we took a systematic approach to optimize the experimental miR-30 backbone, which has become the most commonly used shRNAmir expression system worldwide. In comparison to the natural MIR30A, the experimental miR-30 backbone contains three major modifications (Figure 2.24 a): 1. The experimental miR-30 stem has no bulge and harbors the intended guide on the opposite strand. 2. Two conserved base pairs flanking the loop were changed from CU/GG to UA/UA. 3. To facilitate shRNA cloning, XhoI/EcoRI restriction sites were introduced into regions flanking the basal stem, which in case of the 3' region turned out to be highly conserved in evolution. To test whether restoration of these features could improve miR-30 processing, we modified them to the natural and various alternative configurations, and tested the resulting miR-30 variants using a reporter-assay I established in the laboratory (see also chapter 2.5.2 “Development of a scalable shRNAmir reporter assay for quantifying target protein knockdown”).

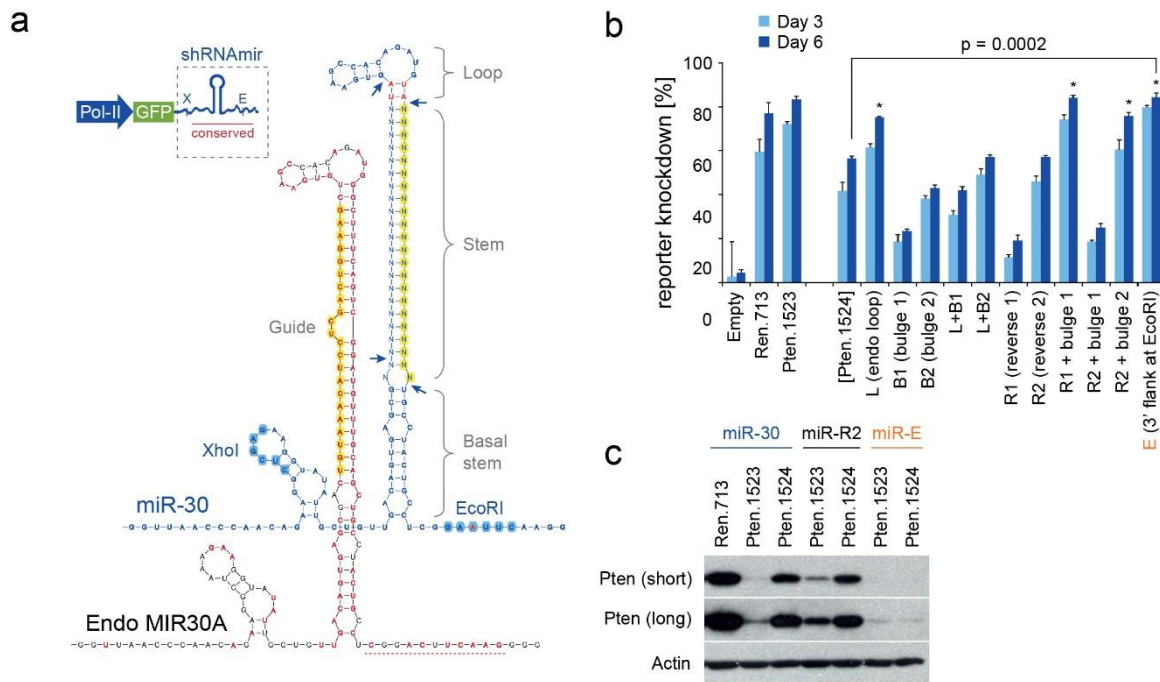


**Figure 2.24 | Restoration of a conserved motive in the miR-30 backbone enhances shRNA processing.**

(a) Comparison of sequence and predicted structure of the endogenous human MIR30A (black) and the experimental miR-30 backbone (blue). In MIR30A, conserved nucleotides are printed in dark red, the guide strand is highlighted in yellow, and a conserved region 3' of the basal stem is underlined. In the experimental miR-30, variable target dependent nucleotides are shown as "N", the guide strand is highlighted in yellow, restriction sites used for shRNA cloning are highlighted in blue, and all conserved nucleotides that are altered compared to MIR30A are printed in red. Arrows indicate canonical Drosha and Dicer cleavage sites. (b) Reporter-based evaluation of shRNA backbone variants. Reporter cells expressing dTomato tagged with target sites of the probed shRNAs were transduced at single copy with LMN vectors expressing the indicated shRNAs. All tested backbone variants contain Pten.1524. dTomato fluorescence intensity of shRNA-expressing cells was quantified at the indicated time points. Values represent means of biological triplicates; error bars represent the SEM. Asterisks, backbone variants that show a highly significant ( $p < 0.001$ ) increase in knockdown potency at day 6 compared to miR-30 Pten.1524. (c) Western blot for Pten with whole cell lysates from NIH 3T3 fibroblasts expressing the indicated shRNAs from miR-30, miR-R2, or miR-E under single-copy conditions. Short and long exposures are shown; miR-30-based Ren.713 served as negative control.

In these assays, several variants of an established Pten shRNA known to trigger intermediate Pten knockdown showed significantly increased efficiency (Figure 2.24 b). Besides a configuration closely resembling the natural MIR30A, the strongest improvement was achieved through restoring a conserved ACNNC motif 3' of the basal stem. Use of an optimized backbone termed miR-E, in which we restored the ACNNC motif by repositioning shRNA cloning sites, improved the knockdown efficacy of both intermediate and potent established miR-30 shRNAs (Figure 2.24 c). Importantly, combining the miR-E design with other favorable modifications identified in our primary assay did not result in any further increase of knockdown levels. This, together with the fact that the miR-E design is very simple to implement in existing miR-30 reagents through PCR subcloning, prompted us to focus further validation studies on the miR-E backbone. As a first step, 11 miR-30

shRNAs targeting mouse Dnmt3a were converted to the miR-E design and tested using reporter assays side-by-side in both configurations (Figure 2.25 a).

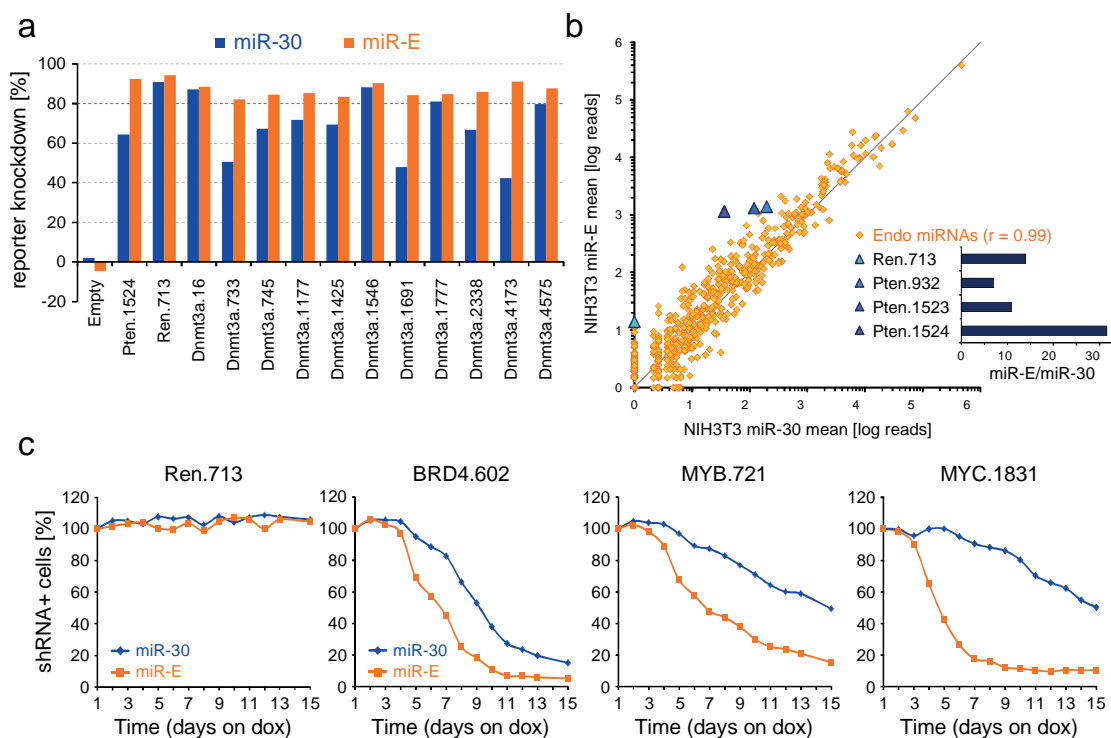


**Figure 2.25 | Comparison of biological effects of miR-30 and miR-E embedded shRNAs.**

(a) Reporter-based quantification of knockdown efficiency of various Dnmt3a shRNAs expressed from either the miR-30 or miR-E backbone under single-copy conditions. Mouse embryonic fibroblasts expressing a dTomato reporter tagged with target sites of the probed shRNAs were transduced at single copy with the indicated shRNAs. An empty vector, Ren.713 and Pten.1524 shRNAs served as controls. (b) Deep-sequencing analysis of mature small RNAs of endogenous mouse microRNAs and synthetic shRNAs. Compared are read numbers of mature small RNAs in NIH 3T3s transduced at single copy with LMP expressing one of four shRNAs from either miR-E (y axis) or miR-30 (x axis). Values for endogenous miRNAs are means of four replicates.  $r$ , Pearson correlation coefficient. Endo miRNAs, endogenous microRNAs. The inset shows the fold change in mature small RNA levels when expressing the indicated shRNAs from miR-E compared to miR-30. (c) Competitive proliferation assays evaluating established shRNAs targeting genes known to be essential in MOLM-13 leukemia cells. Tet-ON competent MOLM-13 cells were infected with a vector conditionally expressing the indicated shRNAs from the miR-30 or miR-E backbone and Ren.713 as neutral control. Infected cells were mixed with uninfected cells, and the percentage of shRNA expressing cells was monitored upon shRNA induction by doxycycline (dox).

While only 4 out of 11 shRNAs triggered more than 80% dTomato protein knockdown in the miR-30 configuration, all 11 shRNAs triggered at least 80% knockdown in the miR-E design, demonstrating that restoring the ACNNC motif can convert ineffective into potent shRNAmir reagents.

As the main factor underlying this major improvement, we found that the miR-E configuration was associated with a strong increase in pri-miRNA processing efficiency, leading to 10 to 30-fold higher levels of mature miRNAs (Figure 2.25 b). Importantly, mature miRNA duplexes produced

from the miR-E backbone rank high but do not exceed or alter levels of endogenous miRNAs, indicating that there are no toxicities due to overloading of the endogenous processing machinery. To confirm that miR-E-based shRNA are more effective in experimental assays we tested several shRNAmirs targeting genes required for survival in AML cells in the miR-30 and miR-E designs side-by-side. Competitive proliferation assays revealed that in all cases miR-E shRNAs triggered more potent anti-proliferative effects in AML, while expression of a neutral control shRNA displayed no negative effect in either design (Figure 2.25 c). Subsequently, we implemented the miR-E backbone into more than 20 lenti- and retroviral vectors for conditional and constitutive shRNAmir expression, and following our publication (Fellmann et al., 2013) these vectors have been supplied to over 100 laboratories worldwide, who appreciate the easy implementation and substantial improvement of this new shRNAmir system. In addition, the first miR-E based multiplexed RNAi screens have impressively showcased the improvement provided by miR-E, mostly owing to the fact that the majority of predicted shRNAmir trigger strong target knockdown in this configuration.

### 2.5.2 Development of a scalable shRNAmir reporter assay for quantifying target protein knockdown

The identification of shRNAs triggering potent knockdown of the intended target protein is a prerequisite for most RNAi applications. While the efficacy of individual shRNAs can be evaluated through different approaches, available assays remain laborious and are not scalable to validate shRNAs for larger gene sets at the same time. The gold standard for validating knockdown efficiency is immunoblotting of the respective target protein. However, for many genes there are no suitable antibodies available, while in other cases their testing turns out to be expensive and laborious. As a frequently used alternative, quantitative reverse-transcription PCR (qRT-PCR) can be used to quantify the suppression of the target mRNA, distinguishing dysfunctional from functional shRNAs. However, due to the fact that both endogenous and experimental miRNAs can trigger gene suppression via mRNA degradation and translational inhibition, qRT-PCR analysis does not accurately monitor effects on the protein level, and the most potent shRNAs for a given gene cannot be easily identified using this approach.

In order to establish a standardized and scalable method for quantifying protein suppression effects of individual shRNAs, I developed a FACS-based reporter assay enabling the side-by-side testing of many shRNAs targeting different genes in one single experiment (Fellmann et al., 2013). To this end, I constructed a reporter vector containing an SFFV-driven dTomato fluorescent protein

and a Blasticidin resistance gene, which in its 3'-UTR carries the target sites of several validated control shRNAs (Ren.713, Bcl2.906, p53.1224, Pten1523/24 and Luc.1309) and a multiple cloning site (MCS) (Figure 2.26 a). The site is used to insert synthetic DNA cassettes harboring up to forty 22-bp shRNA binding sites, which are readily available through gene synthesis products such as gBlocks (Integrated DNA Technologies Inc.). Resulting vectors are then used to generate stable cell lines expressing dTomato with many artificial shRNA binding sites in its 3'-UTR, and following Blasticidin selection these cells are transduced with individual experimental and control shRNAs expressed in standard shRNA vectors in conjunction with GFP (Figure 2.26 b). Subsequently, the protein knockdown efficiency of each shRNA can be quantified based on suppression of the dTomato reporter in flow cytometry analysis.

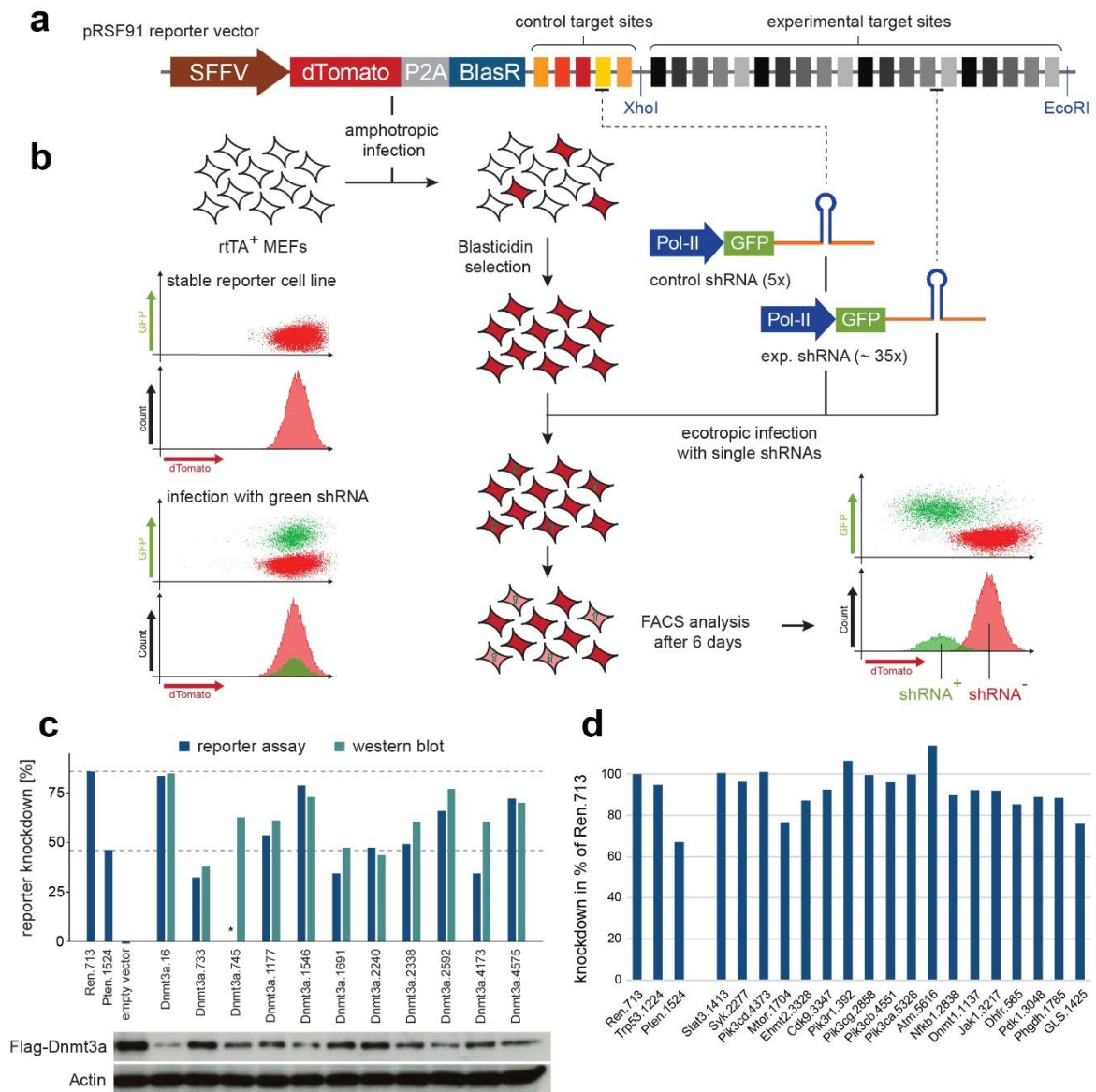


**Figure 2.26 | Sensor assay for medium throughput validation of shRNAs.**

(a) The retroviral reporter vector harbors a SFFV driven red fluorescent reporter (dTomato) and a Blasticidin selection cassette (BlasR). Located in the 3'UTR of dTomato are target sites for shRNAs with known potency (Ren.713, Luci.1309, Trp53.1224, Bcl2.906, Pten.1523/1524) and a XhoI/EcoRI cloning site for the insertion of additional experimental target sites. Typically, a DNA fragment containing up to 40 shRNA target sites is generated using gene synthesis (e.g. gBlocks Gene Fragments, IDT), and introduced using directional cloning. (b) Schematic depicting the experimental workflow of a reporter assay. A reporter vector containing control and experimental shRNA target sites is transduced into reporter cells (typically rtTA expressing mouse or chicken embryonic fibroblasts) using amphotropic (or VSV-G pseudotyped) packaging (to keep reporter cells naive to ecotropic transduction). Following selection using Blasticidin (2  $\mu$ g/ml) and/or FACS, dTomato positive reporter cells are infected at single-copy with individual control and experimental shRNAs expressed from any shRNAmir expression vector co-expressing GFP (e.g. LMP, LMN, LEPG, LENG). Flow cytometry is used to analyze reporter cells at different stages of the assay. The graphs show dot plots and histograms of the same cell populations. dTomato levels are quantified (typically 3 and 6 days after infection), and compared between shRNA expressing (GFP<sup>+</sup>) and shRNA negative (GFP<sup>-</sup>) cells. As final readout, the relative reporter knockdown is calculated for each sample, and compared to included controls of known knockdown potency. (c) Side-by-side comparison of knockdown potencies of a set of Dnmt3a shRNAs determined using the reporter assay or western blotting in NIH3T3 cells expressing Flag-tagged Dnmt3a. Western blot signal intensities were normalized to  $\beta$ -Actin, and the knockdown level quantified

relative to the empty vector control. Pearson correlation between the two data sets:  $r = 0.87$ ,  $p < 0.001$ . Asterisk, Dnmt3a.745 shRNA was not analyzed in this reporter assay. (d) Sensor validation of 18 shRNAs targeting proposed cancer targets. Knockdown relative to Renilla strength in the respective assay, on day 6 after infection is shown. shRNAs with known potency were used as controls (Trp53.1224 and Pten.1524).

To investigate whether dTomato reporter suppression correlates with endogenous protein knockdown, a set of Dnmt3 shRNAs was tested side-by-side in the reporter assay and in Western blot analysis. Western blot signal intensities were normalized to  $\beta$ -Actin, and the knockdown levels quantified relative to empty vector control. These assays revealed a strong correlation between protein suppression levels observed using both methods (Pearson  $r = 0.87$ ,  $p < 0.001$ , Figure 2.26 c) validating that the reporter assay provides an accurate surrogate method to assess the knockdown efficiency of endogenous protein targets in a standardized and scalable way.

In order to be able to test many shRNAs against larger genes sets, I further optimized and simplified the reporter assay following its publication. Specifically, the cloning of reporter constructs was optimized for Gibson cloning (Gibson et al., 2009). Specially designed overhangs on gBlocks containing the experimental target sites omit the need for restriction digest and purification of inserts. Furthermore, after confirming that the target site position in the artificial 3'-UTR has no major influence on the accuracy of the assay, reporter vectors were expanded to contain target-site cassettes spanning 2000 bp, which enable the parallel testing of 80 shRNAs. Retrovirus production, infection and FACS analysis were scaled to a 96-well format, which substantially reduced the required DNA amount and work load per assay. As a first high-throughput application, we used this assay to identify protein knockdown-validated human and mouse shRNAmirs for a set of 80 established target genes of available small-molecule inhibitors. Figure 2.26 d exemplifies results from testing of 18 shRNAs targeting proposed human drug target genes, which were compared to three controls shRNAs of known knockdown potency (Ren.713, Trp53.1224 and Pten.1524). Only the best shRNA for each gene is shown and all knockdown values are normalized to Ren.713 in their respective assays in order to make a comparison over independent reporter lines possible.

Following its successful application in identifying knockdown-validated shRNAmirs for over 200 genes, we are currently planning to expand the use of this assay for generating much larger collections of truly knockdown-validated shRNAmir libraries, which will be performed in a collaborative effort with three laboratories in Germany. In preparation for these large-scale assays, I have devised several possible improvements that we are currently investigating. First of all, the handling of adherent murine reporter cells is time consuming and comes with the disadvantage that shRNAs targeting essential genes might have detrimental effects on the reporter cells. A possible

work around is the use of suspension cells of non-mammalian origin (Winding & Berchtold, 2001). Second, following the establishment of the miR-E backbone we noticed that the dynamic range of the assay is often insufficient to identify the best among several highly effective shRNAs, since shRNAs above a certain potency level trigger very strong dTomato suppression that cannot be further enhanced. To solve this problem, we are currently trying to further expand the dynamic range by the use of different promoters and fluorescent proteins.

### 2.5.3 Establishment of a system for multiplexed combinatorial shRNAmir screening

The vast majority of new cancer therapeutics fail in clinical trials, mostly due to lack of efficacy as single agents. While the use of targeted agents in combination has long been proposed as a possible solution to this problem, the testing of drug combinations in conventional well-by-well approaches is complex and expensive, since it requires advanced pipetting robotics and automated cell culture facilities to manage the hundreds of thousands of possible drug combinations. One way to overcome this problem could be the use of combinatorial RNA (co-RNAi). However, existing co-RNAi strategies based on co-transduction of si- or shRNAs still have substantial technical limitations (Castanotto et al., 2007; Lambeth, Van Hateren, Wilson, & Nair, 2010) and do not allow for pool-based studies.

Inspired by improvements of shRNAmir reagents and multiplexed genetic screening technology, I sought to develop a multiplexed co-RNAi system that combines validated shRNAmir libraries with an innovative cloning and DNA-barcoding strategy to quantify co-RNAi effects through deep-sequencing. For developing such a system, miRNA-based shRNAs such as miR-E provide a decisive advantage, since they can be expressed as a polycistron, mimicking a common configuration of endogenous miRNA transcripts. The use of sensor-validated shRNAs of comparable potency will not only maximize knockdown efficacies, but also improve the equal processing of both shRNAs.



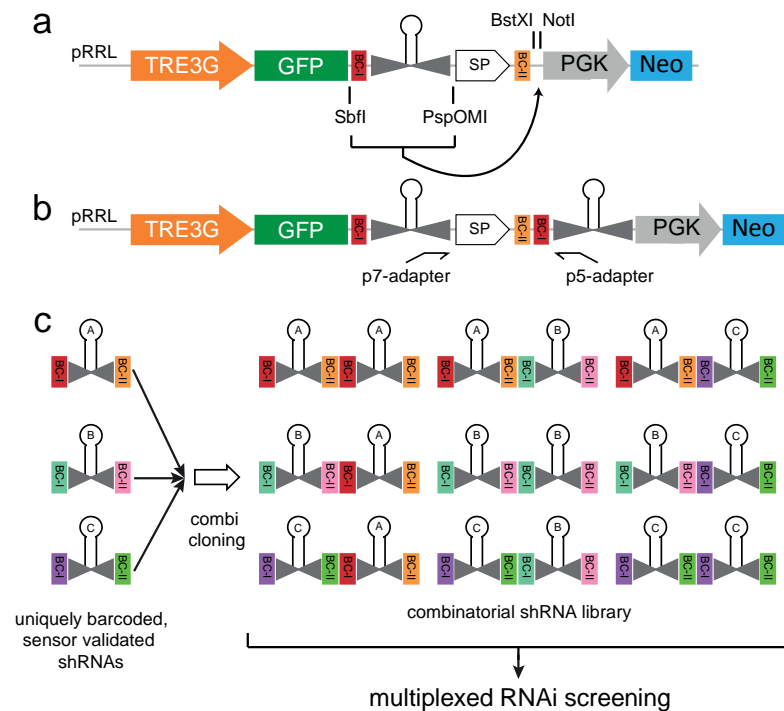


**Figure 2.27 | Vector and cloning scheme of a system for combinatorial RNAi.**

(a) Vector scheme depicting the barcoding and the cloning strategy for combinatorial RNAi. In a first step shRNAs are uniquely marked with two 6N barcodes flanking the miR-E cassette in pRRL.TRE3G.GFP.miR-E.PGK.Neo. To create tandem shRNAs, the barcoded shRNA is digested with SbfI/PspOMI and cloned into BstXI/NotI of the same vector. SP, Solexa sequencing primer binding site. (b) Vector scheme depicting the tandem shRNA vector and the PCR strategy for the amplification of fused barcodes in order to identify shRNA combinations in a multiplexed screening setup. The primers add p5 and p7 adapters to the amplicon, producing a “flow cell ready” product. SP, Solexa sequencing primer binding site. (c) Schematic of three uniquely barcoded shRNAs giving rise to 9 shRNA combinations upon combinatorial cloning. Each tandem can be identified by the fused barcodes between the two miR-E cassettes. For larger comprehensive screens 100 shRNAs can be combined, resulting in 10.000 different combinations.

To establish a system that could be used for multiplexed, combinatorial RNAi studies I designed lentiviral expression vector that contains a TRE3G driven GFP fused to a miR-E cassette and a PGK-Neo selection cassette (Figure 2.27 a). The miR-E cassette is flanked by two 6N barcodes, marking every validated shRNA uniquely. In order to produce a combinatorial library, barcoded shRNAs are pooled and one half of the DNA is digested with the restriction enzymes SbfI and PspOMI to create the insert. The other half of the pooled DNA is opened with BstXI and NotI creating the backbone. The ligation of these two products creates tandem shRNAs in every possible combination (Fig. 2.27 b and c). Every combination can be identified by the fused barcodes in between the two shRNA cassettes. A PCR strategy was devised to amplify the fused barcodes from genomic DNA. At the same time, the Illumina sequencing adaptors p5 and p7 are added during the amplification to generate a flow-cell ready PCR product.

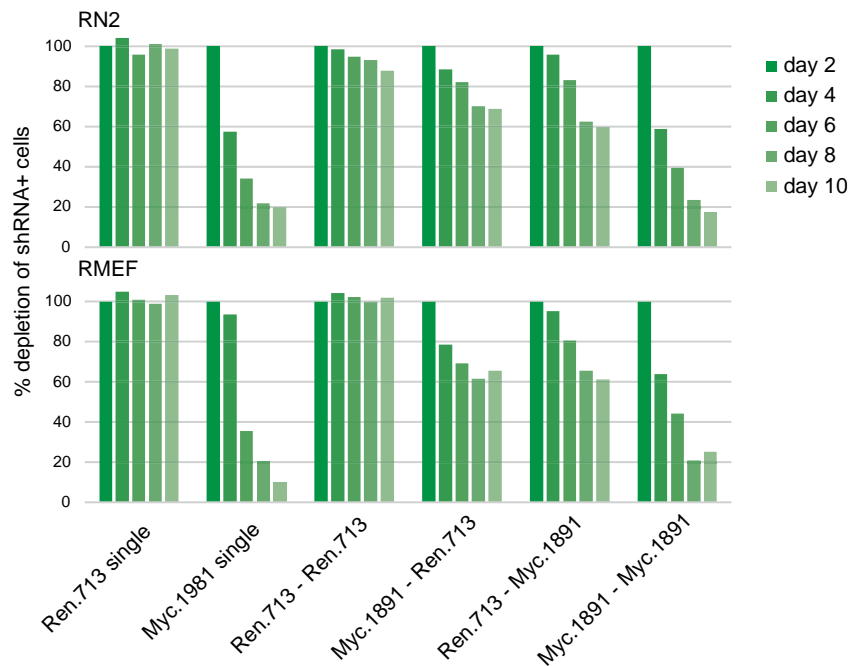


**Figure 2.28 | Biological effects of single and combinatorial shRNAs.**

Competitive proliferation assay in RN2s and RMEFs using Ren.713 and Myc.1891 in single and indicated tandem configuration. Percent depletion of shRNA<sup>+</sup> cells over time, relative to day 2 on dox is shown. The deleterious effect of the Myc shRNA is reduced when expressed in tandem configuration with a neutral shRNA but the effect is rescued with two Myc shRNAs.

To test this vector we cloned a detrimental shRNA (Myc.1891) into the single construct and in combination with a neutral Ren.713 shRNA. RN2s and RMEFs were infected and after 7 days of selection, competitive proliferation assays were performed (Figure 2.28). The results of these assays led to several important conclusions about this co-RNAi system: (1) Tandem expression of two Ren.713 shRNAs has no detrimental effect on either cell type. (2) As expected, a combinatorial cassette encoding one Myc and one Renilla shRNA has weaker effects than expression of a single Myc shRNA, because only one shRNA will be processed from each transcript. (3) The effects of Myc.1891 placed in the first or second position in combination with Ren.713 are the same, demonstrating that both positions in the tandem shRNA setup are processed equally. (4) Expression of two identical Myc shRNAs leads to exactly the same depletion dynamics as observed in Myc single constructs. These results have several ramifications for future combinatorial screens. One general concern in the use of validated shRNA libraries is that shRNAs which show a phenotype as a single shRNA would then score in combination with every shRNA from the library. However, in our setting we could show that tandem expression with a neutral shRNA strongly reduces single shRNA effects and therefore only real synergistic combinations will be detrimental to their host cell. At

the same time, single effective shRNAs can be identified through tandem constructs expressing two shRNAs targeting the same gene serving as a perfect internal positive control. Together, these results validate our vector system as a promising reagent for performing multiplexed co-RNAi screens. Following the generation of knockdown validated shRNA libraries covering a large number of established drug targets, we have constructed a first version of a pooled co-RNAi library, which we are currently screening in several cancer models.

#### 2.5.4 Establishment of an “all-in-one” allele for Tet-on regulatable ubiquitous gene suppression *in vivo*

Organ toxicities are another major reason why many new targeted agents fail in pre-clinical and clinical trials. As soon as tool compounds are available, animal models provide an important experimental system to evaluate such toxicities prior to studies in humans. However, for the increasing number of genetically identified targets the evaluation of possible toxicities in normal tissues is far more challenging, since such effects cannot be easily predicted from cell culture-based studies. At the same time, phenotypes of conventional knock-out mice may overestimate such effects, since a complete loss of a gene throughout development may not recapitulate the consequences of gene suppression in adult tissues. This problem is illustrated by the fact that many well-established drug targets are embryonic lethal in knockout studies. Ideally, genetically identified targets could be tested genetically for suppression effects in adult tissues prior to expensive and time-consuming drug development campaigns.

A recently developed system that could fulfill this promise is the generation of transgenic mice harboring Tet-on regulatable shRNAmir cassettes that can be induced in adult tissues (McJunkin et al., 2011; Premssirut et al., 2011). However, available systems either suffer from leakiness or do not allow for truly ubiquitous shRNAmir expression in all adult tissues. One problem of current systems is that TRE-driven shRNAmir expression cassette and the required reverse Tet-transactivator (rtTA) are expressed from two independent loci, increasing the chances that the system becomes dysfunctional in certain tissues due to locus silencing. This is even the case when those transgenic alleles are knocked-in into loci that have been described as generally accessible, indicating that truly ubiquitous “safe-harbor” loci remain to be found in the mouse genome. Another improvement could be provided by the use of so-called “all-in-one” Tet-on expression cassettes that harbor both the TRE-shRNAmir and the rtTA transgene in one ubiquitously accessible locus.

In an effort to establish such a system for the evaluation of effects triggered by ubiquitous suppression of Gata and other candidate targets, I designed an all-in-one construct containing a TRE3G-driven GFP-miR-E cassette, a CMV early enhancer/chicken  $\beta$  actin (CAG) -driven rtTA, and PGK-Puromycin resistance cassette (needed for selection of correctly inserted ESC clones), which was flanked by lox511 sites (Figure 2.28 a).

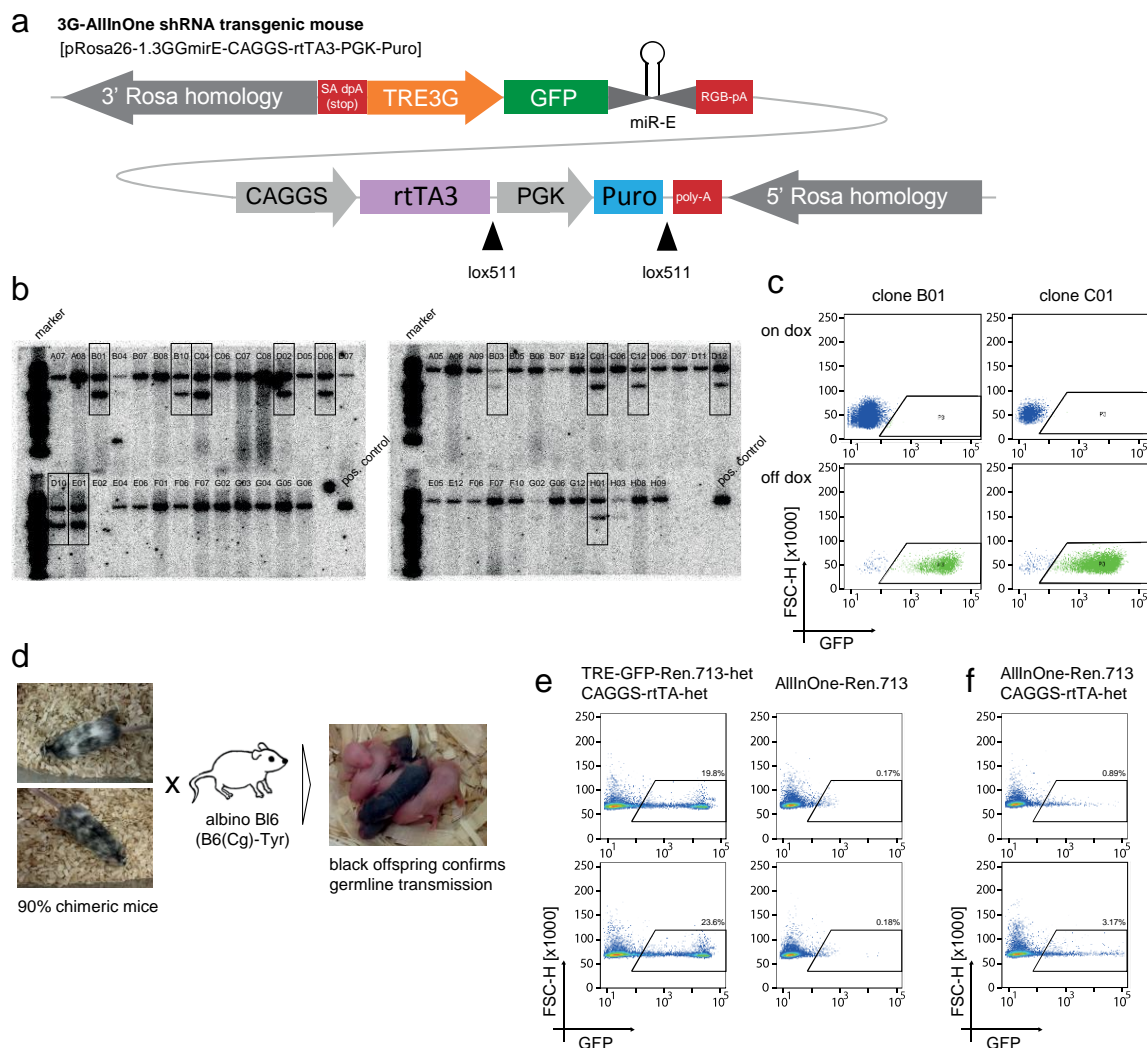


**Figure 2.29 | Generation of 3G-all-in-one shRNA transgenic mice.**

(a) Vector scheme depicting the targeting vector for the production of a new generation of inducible shRNA transgenic, all-in-one mice containing an inducible GFP-miR-E cassette, a CAGGS driven rtTA3 and 3' and 5' homology arms for targeting the cassette into the Rosa locus. Additionally, a PGK-Puro cassette flanked by lox511 sites was added to enable selection of positive embryonic stem cell (ESC) clones after the targeting. (b) Southern blot analysis of pre-selected ESC clones using a radioactive labelled probe specific for the Rosa locus. Genomic DNA of each clone was digested with BamHI, resulting in a 5826 bp wt band and a 3094 bp targeted band. (c) Representative FACS analysis of two clones that tested positive in the southern blot. Each clone was split into two wells and one of them was cultured for 48 hours with dox (1  $\mu$ g/ml). Homogeneous and strong GFP expression was observed on dox, but no leakiness off dox. (d) Representative pictures of chimeric mice resulting from the injection of targeted B6 ESCs into albino B6 embryos. Mice with the highest chimerism were bred to albino B6 and black offspring were genotyped for the targeting cassette in order to determine the first generation founders. (e) FACS analysis of whole bone marrow after 4 days on dox. Two TRE-GFP-miR-E<sup>het</sup>/CAGGS-rtTA<sup>het</sup> and two AllInOne.Ren.713 mice were analyzed. In contrast to the control mice, there was no GFP induction in the hematopoietic system of the all-in-one mice. (f) FACS analysis of whole bone marrow after 4 days on dox from all-in-one mice crossed to a CAGGS-rtTA. The additional rtTA allele slightly improved the induction but it is still only a fraction of the control mice depicted in (e).

As the most well-established ubiquitous locus, we decided to knock this cassette into the Rosa26 locus (Friedrich & Soriano, 1991) in reverse orientation, which has been shown to provide more robust transgene expression (C. M. Chen, Krohn, Bhattacharya, & Davies, 2011). For testing purposes, we first used a construct containing a neutral Ren.713 control shRNA. The final construct was targeted into the Rosa26 locus of 5B3 C57BL/6 embryonic stem cells (provided by Ross Dickins, WEHI, Australia) using homologous recombination, and correct targeting was confirmed for several Puromycin-resistant clones using Southern blotting (Figure 2.28 b). To test the induction of the Tet-regulatable shRNAmir expression cassette, positive clones were grown in dox-containing media for 48h. FACS analysis showed almost 100% induction, reported by GFP expression (Figure 2.28 c). Clones with the strongest GFP expression were selected for injection into albino C57BL/6 blastocysts, and several chimeric mice were born with varying chimerism from 15% up to 95%. The best chimera from each clone was crossed to an albino C57BL/6 mouse, and black offspring of these breedings were genotyped to confirm germline transmission of the transgenic allele (Figure 2.28 d). Subsequently, positive founders were bred to C57BL/6 mice to expand the colony.

To test inducibility of the all-in-one Tet expression cassette *in vivo*, two transgenic mice harboring an all-in-one Ren.713 expression cassette were supplied with dox water for 4 days. As a control, conventional mice harboring a conventional Tet-RNAi system in two separate alleles, namely a TRE-GFP.Ren.713 cassette in the Collagen-A1 locus and a CAGGS-rtTA3 transgene (Premisrirut et al., 2011), were put on dox water for the same period of time. Inducibility of the TRE-GFP-shRNAmir expression cassette was tested after 4 days of dox treatment using flow cytometry of bone marrow cells, which in the conventional system are known to show mosaic induction due to transgene silencing. These effects were confirmed in our analysis, since bone marrow cells isolated from conventional Tet-RNAi transgenic mice were GFP-positive in only about 20% (Figure 2.28 e). Unfortunately, GFP induction levels were even worse in our newly generated transgenic mice, indicating that the all-in-one expression cassette in the Rosa26 locus is predominantly silenced in the hematopoietic compartment. To confirm that this result is not due to specific silencing of the CAGGS-rtTA3 element, another allele of CAGGS-rtTA3 was crossed in but could not substantially increase the inducibility of the TRE3G-GFP-miR-E cassette (Figure 2.28 f).

While transgenic *in vivo* RNAi provides a unique and promising tool to probe the side effects of newly identified candidate targets prior to drug development, there is still no satisfying system providing robust and truly ubiquitous shRNAmir expression in all adult tissues. The described all-

in-one system was another attempt to tackle this problem by combining the latest advances in shRNAir technology with a novel approach to express all transgenic elements for the same locus. While it could be demonstrated that the Rosa26-targeted cassette works extremely well in ESC, during development this cassette is apparently prone to epigenetic silencing. This example highlights the need for identifying true “safe harbor loci” in the mouse genome, which following our experience using the Rosa26 locus is currently pursued as a project in our laboratory. More generally, the aforementioned efforts to further develop shRNAir reagents illustrate that RNAi technology, despite major progress in the past years, can still be improved in many aspects. Given the unique potential of RNAi in the discovery and validation of candidate therapeutic targets, resolving remaining limitations should remain a priority.





## 3 Discussion

### 3.1 Fulfilling the promise of negative selection RNAi screening for cancer target discovery

Following the discovery of RNAi, over the past years our mechanistic understanding of small RNA-based gene regulation has rapidly evolved, which also has led to continuous improvements of the application of RNAi as an experimental tool. What started out with the discovery of an ancient pathogen defense mechanism has rapidly developed into a versatile genetic tool that is applicable in almost all common model organisms. In 2003, the first large-scale siRNA screen led to the identification of new modulators of TRAIL induced apoptosis (Aza-Blanc et al., 2003). Following this initial success, Dharmacon introduced the first genome-scale siRNA library in 2005.

Since its discovery, RNAi has inspired translational researchers as a unique genetic tool for identifying candidate targets for cancer therapy. In 2007, Whitehurst and colleagues performed a high-throughput siRNA screen to identify genes whose suppression sensitizes non-small lung cancer cells to Paclitaxel treatment (Whitehurst et al., 2007). While these and other early siRNA screens revealed some new candidate targets, it also became clear that siRNA screening has several limitations for the study of therapeutic targets in cancer. First of all, the knockdown effect is only transient and cannot be observed for more than a few days before the transfected siRNAs dilute out. Furthermore, transfected siRNAs can reach very high levels in cells, potentially saturating the whole machinery and resulting in cellular toxicity (Fedorov et al., 2006). It also became clear that off-target effects (OTE) are highly concentration dependent, so the efficient transfection of one siRNA can downregulate dozens of transcripts that are complementary to its seed region (Jackson et al., 2006). Another limitation of siRNA screens, especially for large-scale screens in multiple contexts, is that they cannot be performed in a pool-based (multiplexed) fashion but must be conducted in a well-by-well setup.

The need for better RNAi screening systems led to the development of vector-based RNAi reagents. In 2004, a first retroviral library comprising over 20,000 so-called stem-loop shRNAs targeting 8000 human genes was developed and used to identify new factors in the p53 pathway (Berns et al., 2004; T. R. Brummelkamp et al., 2004). From then on, numerous RNAi screens were performed in various scales and biological systems, and the technology was constantly improved. One major milestone was the implementation of next generation sequencing-based readouts, which greatly facilitated the feasibility and robustness of pool-based screens (Bassik et al., 2009; Silva et al., 2008; Johannes Zuber, McJunkin, et al., 2011). Despite these rapid developments, the critical review and cross-comparison of RNAi-screening datasets revealed substantial shortcomings associated with this technology. One major concern was the lack of overlap that could be observed in independent screens asking similar biological questions. For example, between 2009 and 2011 five screens investigating the HIV host-virus interaction were published, but not a single gene overlapped between the hit lists (Brass et al., 2008; König et al., 2008; Lu et al., 2011; Rato et al., 2010; H. Zhou et al., 2008). Furthermore, in cancer research, many of the first candidate targets identified in large-scale negative selection RNAi screens failed to validate in academic and commercial research. Prominent examples include a series of papers describing STK33 and TBK1 as synthetic-lethal targets in Kras-mutant cancer (Barbie et al., 2009; Scholl et al., 2009). Independent testing by researchers at Amgen could not reproduce the effects of STK33 suppression (Babij et al., 2011), and BRD-8899, a potent STK33 inhibitor developed based on the initial claims, was meanwhile given up as a cancer therapeutic (T. Luo et al., 2012). Similarly, the KRAS-specific effects of TBK1 inhibition turned out to be not reproducible by various academic and commercial laboratories (Muvaffak et al., 2014).

Based on these and other examples, it became clear that RNAi reagents need to be further improved to truly enable large-scale RNAi screening, especially in a multiplexed setup. One major limitation was the lack of design algorithms to reliably predict shRNAs that are effective when expressed from a single genomic integration, which is an absolute prerequisite for the feasibility of pool-based shRNA screens. However, early shRNA libraries have not been rigorously tested to fulfill this criterion and, ultimately, turned out to predominantly contain shRNAs that are ineffective under single-copy conditions (Bassik et al., 2009; Fellmann et al., 2011a). As one possible solution, several groups proposed the use of ultra-complex libraries containing up to 30 shRNAs per gene (Bassik et al., 2009). However, the use of such complex libraries poses additional challenges, especially for the design and readout of large-scale screens. In addition to the inefficacy of shRNA

libraries under single-copy conditions, the expression of simple stem-loop shRNAs from strong Pol-III promoters (a commonly used system) turned out to be associated with toxicities due to interference with endogenous miRNA processing (McBride et al., 2008). Furthermore, due to our poor understanding of miRNA processing at the time of their development, several features introduced in simple stem-loop shRNAs turned out to be associated with inaccurate miRNA processing and aberrant passenger strand loading, which strongly increases the frequency of OTE (Auyeung, Ulitsky, McGeary, & Bartel, 2013).

While the development of improved shRNA design algorithms remained complicated due to our incomplete understanding of miRNA processing requirements, the introduction of microRNA embedded shRNAs (shRNAmir) helped to improve several of these problems and established a more versatile RNAi reagent (Fellmann & Lowe, 2014). The fact that shRNAmirs can be transcribed from Pol-II promoters enables the expression from a variety of ubiquitous, tissue-specific and Tet-regulatable promoters, and the positioning of shRNAmirs in the 3'-UTR of reporter genes enables to directly monitor and isolate shRNA expressing cells, which turned out to be particularly useful for the study of genetic dependencies (Johannes Zuber, McJunkin, et al., 2011). While simple stem-loop based shRNA reagents have not been further developed over the past years, major efforts have been undertaken to further improve the efficiency and specificity of shRNAmirs. Using large-scale testing of shRNAmirs knockdown efficiencies, design algorithms of shRNAmirs have been dramatically improved through the definition of so-called sensor rules (Fellmann et al., 2011a). Importantly, sensor-based shRNAmirs do not only suppress their intended target more efficiently, but also show a strong bias for RISC loading of the intended guide strand, which strongly reduces passenger-mediated off-target effects. More recently, a better understanding of miRNA processing requirements has led to the development of an optimized shRNAmir backbone called miR-E (Fellmann et al., 2013), which (in combination with sensor rules) yields single-copy efficient shRNAmirs in over 60% and thereby enables the generation of single-copy effective libraries.

Following the steady improvement of shRNAmir technology, pool-based shRNAmir screens aimed at the identification of cancer vulnerabilities have been increasingly successful. A multiplexed screen using a focused miR-30 based shRNAmir library comprising ~1100 shRNAs targeting 243 chromatin- regulators led to the identification of BRD4 as a candidate therapeutic target in AML and a strategy to suppress MYC in leukemia (Johannes Zuber, Shi, et al., 2011). Notably, BRD4 has meanwhile been found as a strong leukemia dependency in several other multiplexed shRNA screens by independent laboratories (Hoffman et al., 2014; Sroczynska et al., 2014) which also

illustrates the improved robustness of next-generation RNAi screens. Together, these findings have triggered great interest in the evaluation of BET bromodomain inhibitors as therapeutic agents in AML. After several of these compounds have shown strong anti-leukemic activity in pre-clinical models (Boi et al., 2015), clinical trials are already underway and one of these studies has recently reported good tolerance and single-agent activity of the BET inhibitor OTX015 in the treatment advanced hematologic cancers (Coudé et al., 2015). This rapid development less than five years after the initial screen demonstrates the potential of advanced RNAi technology as a target discovery tool.

Besides these advances in shRNAmir-based RNAi, over the past years several alternative approaches have been discovered to explore gene function (Mohr, Smith, Shamu, & Neumüller, 2014). A revolutionary development was the discovery of the CRISPR/Cas9 system, a bacterial immune defense mechanism that can be repurposed for targeted mutagenesis and genome editing (Cong et al., 2013; Prashant Mali et al., 2013). CRISPR is based on expression of the Cas9 nuclease and a guide RNA. The Cas9 protein binds the guide RNA and uses it as a probe to find complementary regions in the genome. The most commonly used CRISPR/Cas9 variant is derived from *Streptococcus pyogenes*, which needs a certain protospacer adjacent motif (PAM) at the 3' end of the recognition site. This three nucleotide NGG motif slightly limits the design space but, nevertheless, genome-wide libraries can easily be generated (Shalem et al., 2014; Sidi Chen et al., 2015).

This system has many different applications in various fields of molecular biology, but it defined a quantum leap for translational cancer research (P Mali, Esvelt, & Church, 2013). CRISPR/Cas9-mediated mutagenesis enables researchers to rapidly introduce genomic mutations resulting in hetero- or homozygous gene loss. Furthermore, in combination with homologous recombination, recurrent mutations in cancer can be precisely modelled in animal models (Heckl et al., 2014; Inui et al., 2014; Xue et al., 2014). Furthermore, modified versions of the CRISPR system can be used to mediate gene knockdown (Qi et al., 2013) or even gene activation (Gilbert et al., 2013). Similar to RNAi the CRISPR/Cas9 system can also be applied in multiplexed screening setups, where deep-sequencing of the sgRNAs serves as the final readout.

Despite the multitude of applications there are some technical limitations to the system. Due to the nature of the target sequence, off-target effects are quite frequent and can mask or distort the real phenotype, a phenomenon that is also observed in RNAi. This problem was partly solved by the development of a Cas9 version which only nicks one DNA strand, called Cas9-nickase (Ran

et al., 2013). In combination with a tandem guide RNA the system is much more specific, because double strand breaks (DSB) only occur at double nicked sites. However, similar to RNAi, each phenotype has to be confirmed with several independent guide RNAs to rule out off-target effects. Another limitation is that the Cas9 protein has to be introduced into cells, which in some systems can be challenging since the Cas9 cDNA consists of more than 4000 base pairs.

Although it is a versatile tool in many research areas, there are some concerns how CRISPR/Cas9 can be used for target discovery and validation. In contrast to RNAi, CRISPR/Cas9 mutagenesis produces irreversible hetero- or homozygous knockout states and does not allow for the generation of hypomorphic gene states, which are relevant for the discovery and study of candidate therapeutic targets. Most established targeted therapies reduce the activity of their target protein to a certain degree, but rarely trigger a complete loss of function. In contrast, using RNAi it is even possible to simulate varying compound affinity and dosage effects by the use of shRNAs of different knockdown potency. Unlike shRNA-based RNAi, the CRISPR/Cas9 system also does not allow to directly report cells harboring the intended genetic perturbation. This is particularly problematic for studies of essential target genes, because affected cell populations might die off before the intended assay even started.

There is no doubt that CRISPR/Cas9 can be used for large, multiplexed positive selection screens where a large fraction of the experimental cells are expected to deplete and only a few genetic events lead to survival of a given condition, for example resistance to a drug (T. Wang, Wei, Sabatini, & Lander, 2014). However, it is less well-established whether the CRISPR/Cas9 system can be applied for negative selection where only a few clones out of a large population are expected to deplete. A substantial fraction of mutations introduced by CRISPR/Cas9 leads to no phenotype because of synonymous mutations, or small non-frame shifting insertions and deletions. Importantly, once a gene is mutated, the recognition site is destroyed and the guide RNA cannot bind anymore, which inevitably leads to a substantial background of non-deleterious mutants in multiplexed negative selection screens.

In conclusion, advanced RNAi and the CRISPR/Cas9 system are both powerful genetic tools with partly complementary applications. Each system comes with specific strengths and weaknesses, and depending on the biological question and the chosen readout one or the other may represent the better tool. However, it is safe to predict that both techniques will keep being subject to

change and development, and it is very likely that they will yield a plethora of new discoveries within the next years.

The MLL-1000 shRNAmir screen described in my PhD thesis presents another well-controlled and successful application of next-generation RNAi technology for probing candidate targets for the treatment of AML. Focusing our custom-built library on 1133 drugged or druggable genes enabled screening at high representation and provided a shortcut for identifying vulnerabilities that can be quickly translated into small-molecule inhibitor therapies. All 9 subpools were analyzed in duplicates and the correlation between the replicates showed that the library could be well represented at all time points. The addition of more than 30 control shRNAs with known effects on RMEFs and RN2s provided another measure to assess the overall screen performance and estimate the magnitude of depletion effects. With a few exceptions, all control shRNAs performed as expected throughout all subpools, which demonstrates the overall quality of the screen. As the most important quality measure, we performed extensive single-shRNA validation studies. As a first estimate, we tested 20 shRNAs predicted to be deleterious in both cell types based on the multiplexed screen. Indeed, 15 of these shRNAs validated to strongly deplete both RN2 and RMEF cells, which is far above validation rates in previously reported multiplexed screens (J. Luo, Emanuele, et al., 2009).

After integrating results from the single shRNA to the gene level, shRNAs covering all top leukemia-specific hits were tested in single competition assays. About 65% of all tested shRNAs validated to have strong leukemia-specific effects, again demonstrating a high validation rate of our high-throughput multiplexed screen. False-positive hits are, at least in part, based on PCR biases introduced during the amplification of guide strands from complex DNA templates. As we have gained more experience with datasets from pooled negative selection screens it has become clear that deep-sequencing based readouts help to identify candidate genes with sufficient accuracy, but do not provide an exact quantification of the scale of biological effects. To date, these can only be quantified using single-shRNA validation assays, which should be viewed as an integral part of every multiplexed screen. However, during the course of my project, I have derived several strategies to reduce PCR biases in the deep-sequencing based readout of multiplexed screens. As a first measure, I have systematically tested different polymerases, priming strategies and cycling protocols, which led to the establishment of an optimized protocol that reduces PCR biases and

thereby improves hit calling. This new protocol will soon be published (Rathert & Roth et al., *Nature*, in press), and has already been implemented as the standard strategy for reading out multiplexed miR-E-based screens in our and numerous other laboratories.

Further possible improvements for upcoming screening ventures in the laboratory are: (1) The implementation of the miR-E backbone (Fellmann et al., 2013) will increase the number of phenotype inducing hairpins per gene. More working shRNAs per gene, will most likely produce more high confidence hits. (2) Newly designed, focused libraries will be designed with 8 instead of 4-6 shRNAs per gene. (3) To increase the statistical power of hit calling even more, future screens will be performed in biological triplicates and not duplicates, as described in the MLL-1000 screen.

While Gart emerged as a clear top hit in both the primary screen and single-shRNA validation studies and, subsequently, was followed up in great detail (as discussed below), the MLL-1000 screen identified several additional leukemia-specific dependencies that define novel candidate targets for non-oncogene addiction therapies. The transcription factor Mef2c, which was identified as the second top hit is well established as a dependency in MLL-rearrange leukemia (Canté-Barrett, Pieters, & Meijerink, 2013) and, therefore, serves as a control for the quality of the MLL-1000 screen. Interestingly, two of the genes in the top 10 list are involved in fatty acid metabolism. While the two tested Fasn shRNAs (fatty acid synthase) showed toxicity in RN2s and RMEFs, shRNAs targeting Echs1 showed weaker yet highly leukemia specific effects. Echs1 encodes for the enoyl coenzyme A hydratase which catalyzes the second step of the mitochondrial fatty acid beta-oxidation pathway (Agnihotri & Liu, 2003). While there are only few publications describing its role in cancer, it could be shown that suppression of ECHS1 inhibits the proliferation of hepatocellular carcinoma (X. Zhu et al., 2013) and gastric cancer cells (X.-S. Zhu et al., 2014). Topoisomerase I (Top1), an enzyme responsible for the removal of supercoiled DNA during replication and transcription (J. C. Wang, 2002), was also identified as a leukemia-specific vulnerability. While Top1 inhibitors like Irinotecan (M. Isomura, 1991) and Camptothecin (Adams et al., 2006) are already used in the treatment of solid tumors, to our knowledge these agents have never been tested in leukemia. The calcium sensing receptor (Casr) was identified as a leukemia-specific dependency and validated with one strong and one medium shRNA in single shRNA assays. Casr is a class C G-protein coupled receptor that senses extracellular levels of calcium ions (Brennan et al., 2013) and has been implicated both as an oncogene and a tumor suppressor, depending on the cellular context (Singh, Promkan, Liu, Varani, & Chakrabarty, 2013). Further down the list of leukemia-specific

dependencies there is Twistnb, a recently discovered DNA-dependent RNA polymerase that catalyzes the transcription of DNA into ribosomal RNA precursors as a component of RNA polymerase I (Kosan & Kunz, 2002). Enpp1 is another poorly understood gene that was identified as a leukemia-specific dependency in our study. Enpp1 is a member of the ecto-nucleotide pyrophosphatase/phosphodiesterase family and can cleave a variety of substrates, including phosphodiester bonds of nucleotides and nucleotide sugars and pyrophosphate bonds of nucleotides and nucleotide sugars. Mutations in Enpp1 are associated with susceptibility to type 2 diabetes (Tang et al., 2014) and one study identified it as a potential facilitator of breast cancer bone metastases by comparing expression profiles of different metastatic clones (Lau et al., 2013). While these additional candidates are interesting and, potentially, translationally relevant, their nomination as candidate therapeutic targets will require additional functional validation studies *in vitro* and *in vivo*, which within the framework of this project were only performed for GART.

### **3.2 GART – a non-oncogene addiction and candidate drug target in leukemia**

Over the past years, non-oncogene addictions (NOAs) are increasingly recognized as promising targets for cancer therapy (J. Luo, Emanuele, et al., 2009; Silva et al., 2008; Solimini et al., 2012, 2007). In principle, conventional chemotherapy already provides an example how targeting cancer-specific vulnerabilities can be exploited for the development of clinical cancer therapies. In addition to chemotherapeutics, some of the most promising targets currently pursued in pre-clinical and clinical studies (e.g. KDM1A, BRD4, PLK1 and others) fall into this category. Most of these established NOA targets, as well as additional candidates such as Chk1 (Zehan Chen et al., 2006) and PK-M2 (Christofk et al., 2008) were derived through hypothesis-driven approaches. More recently, large-scale negative selection screens have provided an experimental approach to identify NOAs in a systematic and unbiased way, and first candidate targets have already been identified using these approaches. For example, an siRNA screen led to the identification of ATM as a critical kinase in tumors deficient for the Fanconi anemia pathway (Kennedy et al., 2007), and heat shock factor 1 (HSF1) was found to be essential in Ras and p53-induced tumorigenesis (Dai, Whitesell, Rogers, & Lindquist, 2007).

While the malignant transformation of cells is accompanied by changes in various cellular pathways, two basic cellular functions have been implicated and intensely studied as a source of exploitable NOAs: 1. changes in the epigenetic landscape and chromatin regulation, and 2. cancer-



specific changes in basic cell metabolism. While chromatin-associated addictions have already led to the development of effective and, in some cases, FDA-approved targeted therapies, the exploitation of metabolic dependencies has yet to fulfill its promise. Long after the first description of the Warburg effect in the 1920s (O Warburg, K Posener, 1924), enzymes involved in glycolysis regained interest as candidate therapeutic targets based on the discovery that PK-M2 acts as a cancer-specific isoform of pyruvate kinase (reviewed in Mazurek, Boschek, Hugo, & Eigenbrodt, 2005). Meanwhile, several other candidate targets in glycolysis have been described (Lew & Tolan, 2012). Another milestone further fueling the interest in cancer metabolism was the identification of phosphoglycerate dehydrogenase (PHGDH), which catalyzes the first step in serine synthesis, as a candidate therapeutic target in breast cancer (Possemato et al., 2011). Despite numerous proposed candidates, efforts to exploit metabolic addictions have not yet led to major breakthroughs in clinical cancer therapy.

Here we have identified Gart as a strong and highly context-specific NOA in AML. Among 1133 genes probed in the MLL-1000 screen, Gart showed clearly the strongest leukemia-specific effects, both in the pooled screen and in consecutive single shRNA validation studies. Remarkably, all seven Gart shRNAs tested in our study triggered potent anti-leukemic effect, which not only demonstrates on-target specificity, but also suggests that leukemia cells are hypersensitive to partial Gart suppression. The strengths of these effects was comparable with the strongest known addictions in this model including Myb and Brd4, and outcompeted the effects observed after suppressing established metabolic and other candidate targets using validated shRNAs. At the same time, the effects were extremely leukemia-specific, and even the most potent shRNAs targeting Gart did not trigger any detrimental effects in immortalized non-hematopoietic cell lines, which is in contrast to well-established and, in some cases, clinically pursued targets such as Brd4, Dhfr, Plk1, Mtor, Ehmt2 and others. Based on our in-depth genetic analyses, the strength and leukemia-specificity of Gart suppression is superior to all known therapeutic targets in this AML model.

The leukemia-specificity of these effects was also recapitulated in cell cycle analysis, which revealed that partial Gart suppression triggers an S-phase arrest in leukemia cells, while there was no such effect in fibroblasts despite comparable or even stronger knockdown levels. After identifying and extensively validating Gart as a NOA in cell culture, we carefully validated this phenomenon *in vivo*, which seemed particularly important for a metabolic target. Similar to *in vitro* stud-

ies, AML cells expressing Gart shRNAs were rapidly eliminated from the population, demonstrating that established AML *in vivo* is dependent on full Gart expression. Furthermore, the addiction to Gart could be fully rescued *in vitro* and *in vivo* through expression of an RNAi-resistant Gart cDNA, eliminating any concern that the observed effects are unspecific or off-target.

Following studies in murine models, suppression of GART validated to trigger strong anti-proliferative effects in a wide variety of human leukemia cell lines, which were comparable suppression of the essential RPA3 gene and not observed in immortalized non-hematopoietic RPE-1 cells. Interestingly, while GART is overexpressed in a variety of hematological malignancies and commonly involved in focal or large amplifications of chromosome 21, neither its genomic amplification nor high (or low) GART expression levels correlated with the sensitivity to GART suppression. In addition, overexpression of murine Gart did not accelerate two well-established AML mouse model, indicating that it has no general driver function in AML leukemogenesis. Together, these results suggest that the sensitivity to GART suppression is not dependent on high expression levels or a potential driver function of amplified GART, which also means that these parameters cannot serve as a clinical biomarker.

Mammalian cells employ two pathways for the production of inosine monophosphate (IMP), which is needed as essential purine building block in basic cellular processes: IMP can be synthesized via the *de novo* purine synthesis pathway, or it can be salvaged from RNA or DNA or other high energy compounds like GDP or ADP (Adam, 2005). In eukaryotes, six different enzymes catalyze the ten steps of *de novo* purine synthesis (Figure 2.19) in a fully linear pathway via intermediates that are unique to this pathway and not used for any other cellular processes (Adam, 2005). GART is the only tri-functional enzyme in the pathway, catalyzing the steps 2, 3 and 5 (Welin et al., 2010). The GART protein comprises 1010 amino acids, which are structured in three distinct domains, each catalyzing one step of *de novo* purine synthesis. The N-terminal GARS domain uses one molecule of glycine and ATP to transform phosphoribosylamine (5-PRA) into glycinamide ribonucleotide (GAR). The C-terminal GARTase unit mediates the third pathway step, the production of N-formylglycinamide ribonucleotide (FGAR) from GAR, which is dependent on 10-formyltetrahydrofolate as a cofactor and, therefore, can be targeted using anti-folate inhibitors. The middle domain is called AIRS and transforms formylglycinamide ribonucleotide (FGAM) and ATP to aminoimidazole ribonucleotide (AIR).

The peculiarity of a tri-functional enzyme catalyzing three steps in one metabolic pathway already implies that individual synthesis steps are tightly coupled. In addition, recent studies suggest that the six enzymes involved in *de novo* purine synthesis can be compartmentalized in a higher structure called the “Purinosome”, which is formed in the cytosol in response to low purine levels (An, Kumar, Sheets, & Benkovic, 2008). Through a better channeling of substrates, the close interaction between these six enzymes is thought to provide a mechanism for boosting the output of the pathway (Deng et al., 2012). However, the structural composition and cellular function of this “Purinosome” remain poorly explored and, in part, speculative. However, this structure truly exists and functions as a mechanism to boost purine production, it would be conceivable that differences in the ability to form this compartment would lead to a particular sensitivity to GART suppression.

As alternatives to *de novo* synthesis, free purines can be obtained from diet or recycled from nucleic acids and nucleotides. Mammalian purine salvage pathways involve two key enzymes: HPRT catalyzes the conversion of hypoxanthine and guanine to IMP and GMP, respectively, while APRT is responsible for the conversion of adenine to AMP (reviewed in Nyhan, 2005). The main advantage of purine salvage is that these pathways require very little energy compared to the energy-consuming *de novo* synthesis. Interestingly, the addition of leukemia cells to full GART expression can be completely rescued through supply of hypoxanthine, which directly fuels IMP production via the salvage pathway. This suggests that leukemia cells, in contrast to immortalized RMEF and RPE-1 cells, are unable to compensate the partial suppression of *de novo* purine synthesis through salvage pathways. In line with this model, mass spectrometry revealed that, in AML cells, Gart suppression results in a severe reduction of IMP that can be rescued through addition of hypoxanthine. Strikingly, similar or even stronger Gart suppression did not alter IMP levels in MEFs, indicating that the salvage pathway compensates for a partial loss of *de novo* synthesis in this context. These remarkable functional differences in a basic metabolic process such as purine synthesis cannot simply be explained through expression differences in relevant enzymes, as these are all expressed at similar levels in both cell types. Similarly, it remains unclear which purine-dependent cellular process is mainly responsible for the anti-leukemic effects observed after GART suppression and IMP depletion. In preliminary analyses, GART suppression also triggers a substantial reduction of AMP and GMP levels specifically in AML cells. A surprising observation in these measurements was that overall AMP levels, unlike any other metabolite, appear to be much

higher in AML compared to RMEF cells. Whether this hints towards ATP and cellular energy levels as main effector of GART addiction remains to be determined.

In the discussion of possible effector mechanisms it should be mentioned that several purine anti-metabolites, including 6-Mercaptopurine (Lennard & Lilleyman, 1989; Paton, Ekert, Waters, Matthews, & Toogood, 1982), 6-Thioguanine (Nelson, Carpenter, Rose, & Adamson, 1975), Fludarabine (Ricci, Tedeschi, Morra, & Montillo, 2009) and others, are well-established chemotherapeutics that together account for almost 20% of all FDA-approved cancer drugs (Parker, 2009). It is generally assumed that all these agents mainly act through their misincorporation into DNA, which interferes with DNA replication and transcription, and ultimately triggers cell death. Very interestingly, all these purine anti-metabolites are mainly effective and clinically used in the treatment of various hematopoietic malignancies, while they show little activity in solid tumors. Importantly, such strong efficacy biases are quite unusual compared to other chemotherapeutics, and cannot be easily explained through the very general toxicity mechanism such as DNA misincorporation and consecutive damage. Instead, it is conceivable that all purine antimetabolites interfere with *de novo* purine synthesis. Indeed, 6-Thioguanine and 6-Mercaptopurine have already been shown to potently inhibit PPAT, the first and rate limiting step in purine synthesis (Nelson et al., 1975; Zaza et al., 2010). Based on our genetic findings, the inhibition of *de novo* purine synthesis could provide a much better explanation for the particular effectiveness of these agents in hematologic malignancies.

After identifying and validating GART as a leukemia-specific NOA using genetic approaches, we sought to test pharmacological approaches for exploiting this dependency for AML therapy. All available GART inhibitors are anti-folate inhibitors of the GARTase component, of which we selected three well-established compounds with varying specificity towards GART. Pemetrexed (Alimta), an anti-folate inhibitor approved for the treatment of mesothelioma and non-small-cell lung cancer (Muhsin, Gricks, & Kirkpatrick, 2004; Taylor et al., 1992) has known activity against several folate-dependent enzymes including thymidylate synthase (its main target), dihydrofolate reductase (DHFR), and GARTase (Shin et al., 1997). In our tests, leukemia cells were slightly more sensitive than RMEFs, although these differences did not mirror the extreme difference observed following genetic GART suppression. Similarly, Lometrexol (DDATHF), a more specific GARTase inhibitor (Beardsley et al., 1989) that has already been evaluated in several clinical trials (Roberts et al., 2000; Sessa et al., 1996), displayed slightly lower IC<sub>50</sub> values in leukemia compared to RMEF

cells. The strongest differential effect was observed for Methotrexate, a well-established anti-folate that is approved for the treatment of several autoimmune disorders and cancer subtypes (Khan et al., 2012; Meyer et al., 1950), which mainly acts through inhibition of DHFR and therefore interferes with all folate-dependent reactions (Rajagopalan et al., 2002). Together, the activity profiles of the three inhibitors suggest that inhibition of GARTase using available anti-folates does not reproduce the strong leukemia-specific effects of genetic GART suppression, indicating that alternative ways need to be explored to exploit this addiction for clinical therapy.

One possible explanation for the failure of GARTase inhibitors could be that this enzymatic activity is not the step that creates a bottleneck under lower GART protein levels. To rigorously test this possibility and identify the enzymatic activity that seems most promising for the development of NOA therapies, we performed three independent yet complimentary cDNA rescue experiments. Strikingly, all three experiments clearly reveal that AIRS is the major bottleneck and most promising activity for the development of GART inhibitors for leukemia therapy. Unfortunately, while AIRS contains an enzymatic pocket that is highly amenable to small-molecule inhibition, there are no known inhibitors or tool compounds to inhibit this activity. Our unbiased multiplexed screen and in-depth genetic validation studies establish GART/AIRS as one of the strongest leukemia-specific NOA targets known to date. These findings, also in light of the remarkable potency and specificity of these effects in comparison with already established leukemia targets, make a strong case for the development of small-molecule AIRS inhibitors, which we will pursue together with our partners at Boehringer Ingelheim. Once available, AIRS inhibitors could provide a first strategy to exploit bottlenecks in the supply of nucleotide building blocks, which has been proposed as a NOA in cancer cell metabolism. From a more general perspective, this study illustrates the power of advanced RNAi tools to systematically identify candidate NOA targets and rigorously test their potential as a therapeutic target prior to expensive and costly drug development campaigns.



## 4 Material and Methods

### 4.1 Cloning of shRNAs (miR-30 and miR-E)

#### 4.1.1 Shuttling of shRNAs from existing vectors

In order to shuttle a shRNA from one vector to another, 20 µg of shRNA containing plasmid are digested with 1 µl of XhoI (R0146L, New England Biolabs) and 1 µl of EcoRI (R3101L, New England Biolabs), in a 35 µl reaction (NEB smart cut buffer) for 2 h at 37 °C. After the digest, the sample is mixed with 6x loading dye and loaded on a 2% agarose gel. Gel electrophoresis is performed for approx. 30 min at 120 V and the shRNA band at 110 bp is cut out and purified (Qiagen, gel purification kit).

5 µg of the target vector are digested under the same conditions. After the digest 1 µl CIP (M0290S, New England Biolabs) is added and incubated at 37 °C for 30 min. Then, the backbone is purified over a column (Quiagen, PCR purification kit).

After measuring the DNA concentration (Nanodrop, ThermoScientific), 300 ng backbone and insert in a molar ratio 1:3 are combined in a 20 µl ligation reaction with 1 µl of ligase (New England Biolabs, M0202L) and 2 µl of 10x ligase buffer. The ligation is incubated for at least 1 h or overnight at 16 °C.

For the transformation, 2 µl of ligation reaction are combined with 20 µl of competent bacteria (XL10-Gold or Stbl-3) and incubated on ice for 5 min. After a 45 s heatshock at 42 °C, the reaction is incubated another 2 min on ice. Then, the reaction is spread on a LB-Amp plate and the plate is put overnight in a 37 °C bacterial incubator. 2-3 single colonies are picked, and after DNA isolation

(Qiagen, mini prep kit) the shRNA cassette is sequenced with the sequencing primer SH (5' - TGTTTGAATGAGGCTTCAGTAC - 3')

#### 4.1.2 Cloning of miR-30 shRNAs from single stranded DNA oligos

Alternatively, shRNAs can also be cloned from *de novo* designed DNA oligos. 97 mers are ordered as 4 nmol “ultramers” from www.idtdna.com. The oligos are dissolved in 120 µl of ddH<sub>2</sub>O which will give a stock concentration of 1 µg/µl. (97mers have a MW of ≈30 kDa = 120 µg). For each oligo one PCR reaction is set up:

Reagent	Volume (µl)	Final	
ddH <sub>2</sub> O	33		
10x PCR Buffer	5	1X	
10x PCR Enhancer	5	1X	
MgSO <sub>4</sub> (50 mM)	1	1 mM	
dNTP (10 mM)	1.5	0.25 mM each	
Fwd Primer (10 µM)	1.5	0.3 µM	5'miR30- <b>XhoI</b>
Rev Primer (10 µM)	1.5	0.3 µM	3'miR30- <b>EcoRI</b>
Template 0.01 -0.1 ng/µl	1		
Pfx DNA polymerase	0.5	1.25 U	
<b>Total</b>	<b>50</b>		

ZUB-SH-miR30XhoF\_new: 5' – TACAATACTCGAGAAGGTATATTGCTGTTGACAGTGAGCG - 3

SH-miR30EcoR\_new: 5' – ACTTAGAAGAATTCCGAGGCAGTAGGCA - 3

In order to avoid contamination, the PCR reagent mix should be prepared in a designated DNA free area. Hence, a water-only control has be included in each round of PCR to ensure that all used reagents are plasmid free. For the PCR the following conditions are used:

Temperature (°C)	Time	Cycles
94 (Initial Denaturing)	2 min	1
94 (Denaturing)	15 s	33
54 (Annealing)	30 s	
68 (Extension)	25 s	
68 (Final Extension)	5 min	1
4 (Storage)	∞	-



To confirm successful oligo amplification 4 µl of the PCR reaction are run on a 2% (weight/vol) agarose gel, which should show a single 125 bp band. In some instances there is an unspecific band just below 200 bp, which will be excluded from further cloning procedures through gel purification of the desired lower band.

At this point, a fraction of each PCR can be pooled if several shRNAs are cloned at the same time. After the column purification of the PCR the shRNAs are cloned in the same way as described in chapter 4.1.1.

#### 4.1.3 Cloning of miR-E shRNAs from existing miR-30 vectors and oligos

Existing shRNAs can be easily transferred from miR-30 into the miR-E backbone. Therefore the same PCR reaction as described in chapter 4.1.2 is used, but with the following miR-E specific primers:

Fwd Primer 5' miRE-XhoI 5' – TACAATACTCGAGAAGGTATATTGCTGTTGACAGTGAGCG - 3'

Rev Primer 3' miRE-EcoRI 5' – TTAGATGAATTCTAGCCCCCTGAAGTCCGAGGCAGTAGGCA - 3'

The same primers can also be used when cloning shRNAs from oligos, as described in chapter 4.1.2.

## 4.2 Retroviral packaging

All retroviral packaging was performed using the PlatinumE (PlatE) cell line (Cell Biolabs) according to established protocols (Fellmann et al., 2013). In brief: PlatE cells were cultured in DMEM, supplemented with 10% FBS, 20 mM glutamate, 10 mM sodium pyruvate, 100 U ml<sup>-1</sup> penicillin and 100 µg ml<sup>-1</sup> streptomycin. The cells were split in a 1:5 ratio every other day to avoid 100% confluence. The cells can be used for up to 40 – 50 passages. After this time or when decreasing titers are observed, a fresh vial with a low passage number is thawed.

For the transfection, nearly confluent PlatE plates were split 1:2 and the CaCl<sub>2</sub> transfection was performed approximately 8 hours later. 500 µl of 2x HBS buffer (280 mM NaCl, 50 mM HEPES, 1.5 mM Na<sub>2</sub>HPO<sub>4</sub>, 12 mM Dextrose and 10 mM KCl) was prepared in a clear FACS tube. A second tube, containing 20 µg of plasmid DNA, 10 µg GagPol helper DNA, 417.5 µl H<sub>2</sub>O and 62.5 µl 2M CaCl<sub>2</sub> was prepared as well. Afterwards, the DNA containing solution is added drop wise to the 2x HBS while an electrical pipetting aid is used to blow bubbles into the mixture. A fine precipitate forms

that is added directly onto the cells 15 minutes after the bubbling. In order to increase transfection efficiency, 2.5 µl 100 mM chloroquine is added to each 10 cm plate.

12-14 h after the transfection the medium is changed to remove the chloroquine and 24 h after transfection, the medium is changed carefully to the target medium because transfected cells detach easily. Virus containing supernatant can be harvested 3-4 times every 6-8 hours. Highest titers are observed between 32-60 hours post transfection. The virus supernatant can be stored in the fridge for 1-2 weeks or at -80 °C for several months, but freeze/thawing cycle reduce the titer by approx. 50 %.

### 4.3 Lentiviral packaging

293 FT packaging cells (Life Technologies) are cultured in DMEM and split in a ratio 1:5 every other day to avoid 100% confluence. In the morning before the transfection, Cell culture plates are coated with 2% gelatin (1 h, 37 °C). After 1 h the liquid gelatin is removed nearly confluent 293 FT plates are split 1:2 and the cells are transferred onto the coated plates. 6 – 8 hours later, the 293 FT cells should be around 90% confluent and the CaCl<sub>2</sub> transfection was performed as follows: 500 µl of 2x HBS buffer (280 mM NaCl, 50 mM HEPES, 1.5 mM Na<sub>2</sub>HPO<sub>4</sub>, 12 mM Dextrose and 10 mM KCl) was prepared in a clear FACS tube. A second tube, containing 15 µg of plasmid DNA, 7 µg pcDNA3.GP.4xCTE, 1 µg pMD.G VSVG, 5 µg pRSV.Rev, 417.5 µl H<sub>2</sub>O and 62.5 µl 2M CaCl<sub>2</sub> was prepared as well. Afterwards, the DNA containing solution is added drop wise to the 2x HBS while an electrical pipetting aid is used to blow bubbles into the mixture. A fine precipitate forms that is added directly onto the cells 15 minutes after the bubbling. In order to increase transfection efficiency, 2.5 µl 100 mM chloroquine is added to each 10 cm plate.

From this step on, the cells have to be transferred to a bio safety S2 lab and adequate safety precautions have to be taken. After 12 h the media is changed to the target media and 8h after this, the first viral supernatant can be harvested. If more virus supernatant is needed, a second and a third harvest can be done every 8 hours. The virus supernatant can be stored in the fridge for several weeks or at -80 °C for several months.

### 4.4 Retroviral and lentiviral transduction

Prior to infection, the virus supernatant is filtered through a 0.45 µm syringe filter or spun for 10 min at 4000 rpm in order to get rid of floating or dead plate or 293 FT cells. In the case of adherent

cells, cells should be sparsely (20 – 30 % confluence) plated 6 hours prior to infection and the virus supernatant is put directly on the cells. When suspension cells are infected, 1 ml of cells is mixed with 2-3 ml of virus supernatant. To increase infection efficiency, polybrene can be added to media (stock: 4 mg/ $\mu$ l, use 1:1000). For cells which are difficult to infect, spin occultation (30 min, 1500 rpm) and multiple infections cycles can be done.

## 4.5 Plasmids

The shRNA library used in the screen was cloned into TRMPV-Neo (pSIN-TRE-dsRed-miR-30-PGK-Venus-IRES-NeoR). The same vector was used for validation of essential genes and top ranked shRNAs. For further validation several shRNAs were cloned into the miR-E version of TRMPV-Neo (pSIN-TRE-dsRed-miR-E-PGK-Venus-IRES-NeoR). For the cDNA rescue studies TRN (pSIN-TRE-dsRed-miR-30-PGK-NeoR) and pMSCV-CDS-PGK-Puro-IRES-GFP were used. For the *in vivo* validation Gart and control shRNAs were cloned into TGmPNe (pSIN-TRE3G-tGFP-miR-E-PGK-NeoR). Human leukemia cell lines were infected with the lentiviral vector GmEPP (pRRL-SFFV-GFP-miR-E-PGK-PuroR).

## 4.6 Cell culture and cell lines

PlatE, 293FT, RMEFs and RPE-1 cells were cultured in DMEM (Gibco-Invitrogen) supplemented with 10% FBS, 20 mM Glutamate, 10 mM sodium pyruvate 100 U ml<sup>-1</sup> penicillin and 100  $\mu$ g ml<sup>-1</sup> streptomycin. RN2s and the human leukemia cell lines MOLM-13, MV4-11, OPM2, MEG01, HEL9217, TOLEDO, SR786, THP1, U937, EM2, HEL, HL60 and MM1 were cultured in RPMI 1640 (Gibco-Invitrogen) supplemented with 10% FBS, 20 mM glutamate, 10 mM sodium pyruvate, 100 U ml<sup>-1</sup> penicillin and 100  $\mu$ g ml<sup>-1</sup> streptomycin. Reh cells were cultured in RPMI supplemented with 10% FBS, but without penicillin and streptomycin. KU812, CMK and L363 were RPMI 1640 (Gibco-Invitrogen) supplemented with 20% FBS, 20 mM glutamate, 10 mM sodium pyruvate, 100 U ml<sup>-1</sup> penicillin and 100  $\mu$ g ml<sup>-1</sup> streptomycin.

## 4.7 Multiplexed shRNA screening

A custom shRNA library targeting 1133 chromatin-regulating mouse genes was designed using up-to-date miR-30-adapted predictions (6 shRNAs per gene) and constructed by PCR-cloning from a pool of oligonucleotides synthesized on 55k customized arrays (Agilent Technologies or Integrated

DNA Technologies) (Johannes Zuber, Shi, et al., 2011). After sequence verification, 4003 shRNAs were pooled in 9 subpools:

	# of shRNAs
DGG1	398
DGG2	399
DGG3	397
DGG4	396
DGG5	396
DGG6	242
MLLRA	394
MLLRB	354
MLLDT	1027
$\Sigma$	4003

These pools were transduced in duplicates into MLL-AF9/Nras<sup>G12D</sup> leukemia cells (RN2) and immortalized fibroblasts (RMEF) using conditions that predominantly lead to a single retroviral integration and represent each shRNA in a calculated number of >1000 cells. To ensure library representation, a total of twenty million cells was infected per subpool, with a transduction efficiency of 2-3 %. For the larger MLLDT pool fifty million cells were infected. Throughout drug selection with 1 mg/ml G418 the same cell number was maintained at each passage to preserve library representation. After 7 days of selection T0 samples were acquired bei FAC-sorting (4-6 million GFP<sup>+</sup> cells per replicate and subpool) using a FACSArialI (BD Biosciences).

The fully selected cells were cultured in dox containing media (1 µg/ml) for 12 days. To obtain T12 samples, around 1-3\*10<sup>6</sup> GFP<sup>+</sup>/dsRed<sup>+</sup> double positive cells were sorted per replicate. Genomic DNA from T0 and T12 samples was isolated by two rounds of phenol extraction using PhaseLock tubes (5prime) followed by isopropanol precipitation. Deep sequencing libraries were generated by PCR amplification of shRNA guide strands using primers that tag the product with standard Illumina adapters and a sample specific 4N barcode (p7+Loop: CAAGCAGAAGACGGCAT-ACGANNNTAGTGAAGCCACAGATGTA; p5+miR30: AATGATACGGCGACCAC-CGACTAAAGTAGCCCCTTGAATTC). For each sample, DNA from at least one million cells was used as template in multiple parallel 50 µl PCR reactions, each containing 0.5 µg template, 1x AmpliTaq Gold buffer, 0.2 mM of each dNTP, 2 mM MgCl<sub>2</sub>, 0.3 µM of each primer and 2.5 U AmpliTaq Gold (life technologies), which were run using the following cycling parameters:

Temperature (°C)	Time	Cycles
95 (Initial Denaturing)	10 min	1
95 (Denaturing)	30 s	32
52 (Annealing)	45 s	
72 (Extension)	60 s	
72 (Final Extension)	7 min	1
4 (Storage)	∞	-

PCR products (117 bp) were combined for each sample, column purified using QIAquick PCR purification kit (Qiagen) and further purified on a 1% agarose gel (QIAquick gel extraction kit, Qiagen). Libraries were analyzed on an Illumina Genome Analyzer at a final concentration of 10 pM; 22 nucleotides of the guide strand were sequenced using a custom primer (miR30EcoRISeq, TAGCCCCTTGAATTCCGAGGCAGTAGGCA). To provide a sufficient baseline for detecting shRNA depletion in experimental samples, we aimed to acquire > 500 reads per shRNA in the sequenced shRNA pool to compensate for disparities in shRNA representation inherent in the pooled plasmid preparation or introduced by PCR biases. With these conditions, we acquired baselines of >500 reads for 4003 shRNAs. Sequence processing was performed using a customized Galaxy platform (Goecks, Nekrutenko, & Taylor, 2010). For each shRNA and condition, the number of matching reads was normalized to the total number of library-specific reads per lane and imported into a database for further analysis (Access 2003, Microsoft).

#### 4.8 Scoring of genes and hit calling

For the hit calling in the RNAi screen, the fold depletion for each shRNA was calculated by dividing the normalized read counts at T12 by the normalized read counts at T0. Furthermore, the geometric mean of the values from both replicates was determined. Based on the performance of spike in control shRNAs, thresholds for weak and strong depletion were determined.

	Weak fold depletion	Strong fold depletion
RN2	3	10
RMEF	2.5	5

Based on this threshold we scored 3 points for each weak depleting shRNA and 10 points for each strong depleting shRNA. In order to obtain the differential score, scores from all shRNAs for one gene were added up and the value in RMEFs was subtracted from the value in RN2s.

## 4.9 Fluorescence activated cell sorting (FACS)

FACS was performed on FACS Aria machines (Becton Dickinson). For the RNAi screen T0 samples GFP<sup>+</sup> cells were sorted and for western blots, samples for mass spectrometric analysis and RNAi screen T12 samples GFP<sup>+</sup>/dsRed<sup>+</sup> double positive cells were sorted.

## 4.10 Antibodies

For western blot, we used antibodies against Gata (HPA002119, Atlas Antibodies) and  $\beta$ -Actin (A3854, Sigma-Aldrich). Secondary antibodies were anti-mouse (926-32210, LI-COR<sup>®</sup>) and anti-rabbit (926-32211, LI-COR<sup>®</sup>). For FACS we used the following antibodies: APC anti-mouse CD117 (c-Kit, 105812, BioLegend), APC anti-mouse Ly-6G/Ly-6C (Gr-1, 108412, BioLegend) and Brilliant Violet 421 anti-mouse CD11b (Mac-1, 101236, BioLegend).

## 4.11 Competitive proliferation assay

Competitive proliferation assays using shRNAs in TRMPV-Neo and TRMPV-Neo-miR-E were performed as follows: MLL-AF9/Nras<sup>G12D</sup> (RN2) cells, RMEFs or cells of a Tet-ON competent variant of the human leukemia MOLM- transduced and selected with G418 (1 mg/ml, 10131-027, Invitrogen) for 7 days. At the start of the assay, 20% of wildtype cells were mixed in each well and the exact ratio was determined by FACS (Guava, Merck milipore). From then on, cells were cultured in dox containing media (1  $\mu$ g/ml) and the percentage of shRNAs expressing cells was assayed every day for RN2s and every other day for RMEFs over the course of 12 days.

The competitive proliferation assays with human cancer cell lines and RPE-1 cells were performed with the constitutive lentiviral vector GmEPP. The infection efficiency was measured 2 days after infection and then the percentage of GFP<sup>+</sup> cells was determined every other day of the course of 18 days (24 days for RPE-1 cells).

## 4.12 cDNA rescue studies

For all cDNA rescue studies, RN2 cells were cotransduced with the cDNA containing vector (pMSCV-CDS-PGK-Puro-IRES-GFP) and the shRNA contain vector (pSIN-TRE-dsRed-miR-30-PGK-NeoR) and in parallel they were also infected with the cDNA vector alone. The cotransduced cells were selected for 7 days with G418 1 mg/mL and Puro 4  $\mu$ g/ml. The single infected cells were selected with 4  $\mu$ g/ml for 7 days. On day 0 of the assay, all cells were spun down (1500 rpm, 5

min) and resuspended in fresh media to get rid of the antibiotics. Single and double infected cells were mixed in a 1:1 ratio and cultured in dox containing media (1  $\mu\text{g}/\text{ml}$ ) for 10 days. The ratio of GFP<sup>+</sup> and GFP<sup>+</sup>/dsRed<sup>+</sup> cells was measured every day by flow cytometry (Guava, MerckMilipore).

### 4.13 Western Blot

Proteins extraction for western blot was usually performed from 3-5 million cells per sample. The cell pellets were pipetted up and down with 60  $\mu\text{L}$  ice cold extraction buffer (1:1 mix of Tween20 buffer, 50mM HEPES pH7.5, 150mM NaCl, 10mM EDTA, 0.2% Tween20 and NP40-Buffer: 1% NP40, 50mM Tris pH7.5, 150mM NaCl, 10mM EDTA plus cOmplete, Mini, EDTA-free Protease Inhibitor Cocktail, 04693159001, Roche Diagnostics GmbH) until the whole pellet is dissolved. After 10 min on ice, all samples were centrifuged and the protein concentration on the supernatant was determined by Bradford assay.

A BSA standard solution with 10 mg/ml was prepared and diluted to obtain the following standards:

	BSA mg/mL	$\mu\text{l}$ Stock	$\mu\text{l}$ water
Std. 1	0.00	0	1000
Std. 2	0.25	25	975
Std. 3	0.50	50	950
Std. 4	0.75	75	925
Std. 5	1.00	100	900
Std. 6	1.50	150	850
Std. 7	2.00	200	800

The Bradford reagent is diluted 1:10 with distilled water (working solution) and a suitable amount of cuvettes is prepared with 1mL working solution each. 10  $\mu\text{l}$  of each standard and each sample is pipetted into the cuvettes and quickly mixed with a 200  $\mu\text{l}$  Pipette.

A Nanodrop spectrometer (Thermo Scientific Inc.) is used to make the standard curve and measure all samples after incubation of 5 min at RT. Samples with values outside of the range of the standard curve have to be diluted and measured again.

For the SDS page electrophoresis, 20 µg of protein in 10 µl are used and 10 µl 2x NuPage LDS sample buffer (NP0007, Life Technologies) is added. After incubation at 95 °C for 5 min the samples are cooled down on ice and loaded on a 4-12 % acrylamide gel (NuPAGE® Novex® 4-12% Bis-Tris Gels, 1.0 mm, 12 well, NP0335BOX, Invitrogen). 5 µl of protein marker are loaded on one side of the gel (MagicMark, Western Protein Standard, 20-220 kDa, LC5602, Invitrogen).

The gel is run at about 80 mA for the first 30 - 45 min and then at 150 mA until the front runs out (Running buffer: NuPage NuPAGE MOPS SDS Running Buffer, NP0001, Invitrogen).

For the transfer, the gel is soaked in transfer buffer (10x transferbuffer: 144.13 g Glycine, 30.28g Tris base in 1l of H<sub>2</sub>O; 1x transferbuffer: 100ml 10x transferbuffer, 1 ml 20% SDS, 150ml Methanol in 1l of H<sub>2</sub>O) for a maximum of 10 min and a piece of FL membrane (IPFL00010, Millipore) is activated in 100% methanol, rinsed in H<sub>2</sub>O and soaked in transfer buffer for 5 – 15 min. The layers of the sandwich are assembled as follows:

Black side → foam → 3x Whatmann papers → gel → membrane → 3Whatman → foam → read side (wet all in transfer buffer). The transfer is run at 400 mA const. for 1 h (2 h for 2 blots) in the cold room.

After the transfer the membrane is stained with PonceauS to check for equal loading and air bubbles. Therefore the membrane is rinsed in H<sub>2</sub>O and then soaked in undiluted PonceauS (P7170-1l, Sigma-Aldrich) for 15-20 seconds. Then the membrane is destained under running tap water. Marker bands can be marked with pencil and then the membrane is completely destained in TBS-T for few minutes. The destained membrane is incubated in Lycor Blocking agent (927-40000, LICOR) for 45 min and then the first AB, diluted in 15 ml Lycor Blocking agent + 150 µL 20% Tween is applied overnight, at 4°C. The membrane is rinsed and washed twice TBS-T for 15mins each.

The secondary antibody is diluted 1:15.000 in 15 ml Lycor Blocking agent + 150 µL 20% Tween and the blot is incubated for 30 min at RT. The blot is washed twice in TBS-T for 15 min and then it is scanned with an Odyssey CLx scanner (Licor Inc.).

#### **4.14 Doubling time**

In order to determine the doubling time for RN2s and RMEFs, 150.000 or 10.000 cells respectively, were seeded into 24 well plates and cell numbers were determined (Guava Merck Millipore) every



12-14 hours over the course of 48 hours. For all conditions, three biological replicates were prepared and doubling times were calculated using a nonlinear fit function for exponential growth (GraphPad Prism).

#### **4.15 Cell cycle analysis by BrdU incorporation**

Prior to the BrdU assay, TRMPV-Neo transduced and fully selected RN2 and RMEFs were cultured in dox containing media (1  $\mu\text{g}/\text{ml}$ ) for 3 days. For the BrdU labeling the BrdU stock (10 mg/ml BrdU solution) is diluted to a 1 mM and 10  $\mu\text{l}$  are added directly to each ml of tissue culture medium. After 60 min  $2 \times 10^6$  cells per sample are spun down (2000 rpm, 5 min, 4 °C). The pellet is washed by adding 1 ml of staining buffer per tube and centrifuged again at 2000 rpm for 5 min. The pellet is resuspended in 100  $\mu\text{l}$  of BD Cytofix/Cytoperm Buffer and incubated for 25 min at RT. After Washing the cells with 1 ml 1x BD Perm/Wash Buffer, the cells are incubated with 100  $\mu\text{l}$  of BD Cytofix/Cytoperm Plus Buffer for 10 min on ice. The cells are washed and refixed with 100  $\mu\text{l}$  of BD Cytofix/Cytoperm Buffer for 5 min at RT. After another washing cycle, the pellet is resuspended in 100  $\mu\text{l}$  of diluted DNase (300  $\mu\text{g}/\text{ml}$ ) to expose the incorporated BrdU. After 1h at 37 °C, cells are washed and resuspended in 50  $\mu\text{l}$  of BD Perm/Wash Buffer containing 1:50 diluted APC anti-BrdU. After 20 min of incubation at RT, the cells are washed and resuspended in 1 ml of staining buffer. 2  $\mu\text{l}$  of DAPI (1 mg/ml) is added to each sample and then the cells are ready for FACS analysis.

#### **4.16 FACS staining**

For the FACS staining of RN2s to check for expression levels of surface markers fully selected cells were mixed with 50% wt cells and then cultured in dox containing media (1  $\mu\text{g}/\text{ml}$ ) for 3 days. The cells are spun down (1500 rpm, 5 min) and washed twice with FACS buffer (PBS + 5% FBS). FACS antibodies are diluted 1:500 in FACS buffer and the staining is usually done in 40  $\mu\text{l}$  of volume in a 96 well plate. After incubation for 20min at 4 °C, the cells are washed twice and resuspended in 600  $\mu\text{l}$  FACS buffer for the FACS measurement. Stained samples were analyzed on a LSR Fortessa (BD) flow cytometer. Data analysis was performed using FlowJo software (Treestar).

#### **4.17 Determination of IC<sub>50</sub> concentration of different compounds**

To determine the IC<sub>50</sub> of different compounds 200.000 RN2s or 40.000 RMEFs were seeded into 24 well plates. The compounds were added in the concentrations 1, 10, 100, 250, 500, 2000 and

10000 nM. Three wells per concentration are prepared and a DMSO control is also done to be able to calculate the relative proliferation at the end. After 48h hours of incubation cell numbers in each well are determined by flow cytometry (Guava, MerckMilipore). The relative proliferation is calculated by division of the cell number in each well by the cell number in the DMSO control wells. IC<sub>50</sub> concentrations were calculated in GraphPad prism, using a nonlinear fit function.

#### 4.18 Mice

For leukemia transplantation studies B6-Rag2<sup>-/-</sup> Ly 5.1 mice (Morse, 1992; Shinkai et al., 1992) between 8 and 12 weeks of age were used. Targeted ESC clones were injected into albino-BL6 mice (B6(Cg)-Tyr<sup>c-2J</sup>/J) (Townsend, Witkop, & Mattson, 1981) and later backcrossed to standard C57BL/6J. CAGGS-rtTA mice (Premsrirut et al., 2011) were used to add another allele of rtTA to the all-in-one mice.

All animals were maintained in the pathogen-free animal facility of the Research Institute of Molecular Pathology in Vienna. All animal experiments were carried out according to valid project licenses, which were approved and regularly controlled by the Austrian Veterinary Authorities.

#### 4.19 Transplantation of leukemia cell for *in vivo* studies

Retrovirally transduced and fully selected MLL-AF9/Nras<sup>G12D</sup> leukemia cells (RN2) were transplanted by tail-vein injection of  $2 \times 10^6$  cells into sub-lethally (5.5 Gy, 16h before the transplantation) irradiated RAg2<sup>-/-</sup> B6/SJL (CD45.1) recipient mice. For whole-body bioluminescent imaging, mice were intraperitoneally injected with 50 mg kg<sup>-1</sup> D-Luciferin (Goldbio), and after 5 min, analyzed using an IVIS Spectrum system (Caliper LifeSciences). For the induction of shRNA expression in transduced cells, dox was supplied with the drinking water, upon disease onset (4 mg/ml)

#### 4.20 Mass spectrometric analysis of metabolites

For the extraction of metabolites,  $3 \times 10^6$  sorted cells were centrifuged at 1500 rpm for 5 min at 4 °C. The pellet is washed once with ice cold PBS and then the cells are snap frozen in liquid nitrogen. At this point the samples can be stored at -80 °C.

The cell pellets were extracted using a MeOH:ACN:H<sub>2</sub>O (2:2:1, v/v) solvent mixture. A volume of 1 ml of cold solvent was added to each pellet, vortexed for 30 s, and incubated in liquid nitrogen for 1 min. The samples were then allowed to thaw at room temperature and sonicated for 10 min.

This cycle of cell lysis in liquid nitrogen combined with sonication was repeated three times. To precipitate proteins, the samples were incubated for 1 h at  $-20^{\circ}\text{C}$ , followed by 15 min centrifugation at 13.000 rpm at  $4^{\circ}\text{C}$ . The resulting supernatant was removed and evaporated to dryness in a vacuum concentrator. The dry extracts were then reconstituted in 100  $\mu\text{l}$  of ACN:H<sub>2</sub>O (1:1, v/v), sonicated for 10 min, and centrifuged 15 min at 13.000 rpm and  $4^{\circ}\text{C}$  to remove insoluble debris. The supernatants were transferred to HPLC vials and stored at  $-80^{\circ}\text{C}$  prior to LC/MS analysis (Ivanisevic et al., 2013).

LC/MS was performed using a TSQ Vantage triple quadrupole mass spectrometer (Thermo Scientific) coupled to an UltiMate 3000 XRS HPLC system (Dionex, Thermo Scientific). Metabolites were separated using a gradient between 5% mobile phase A (10 mM ammonium acetate in water; pH 7.0) to 95 % A in phase B (acetonitrile) using a ZIC-HILIC column (150 x 1mm, 3.5  $\mu\text{m}$ , 200 Å) employing a flow rate of 100  $\mu\text{l}/\text{min}$ . Metabolites were quantified using precursor ion scanning in negative ion mode. Before analysis, 80  $\mu\text{l}$  of acetonitrile was added to 20  $\mu\text{l}$  of each sample and 10  $\mu\text{l}$  were injected on the column. Each experiment was measured in technical duplicates.

## 4.21 Medium throughput sensor assay

### 4.21.1 Generation of a stable reporter cell line

In order to design the target linker for the reporter construct, mRNA target sites of all shRNAs to be tested are collected and 2 extra bases are added on both sides of each shRNA, according to their unique surrounding mRNA context. The DNA fragments are strung together to a maximum of 1900bp, and the following sequences have to be avoided: CTCGAG (XhoI), GAATTC (EcoRI), AATAAA and ATTAAA (both polyA signals). If one of these sequences occurs somewhere throughout the sequence, the order of shRNAs has to be changed, or if it occurs in one target site, this shRNA has to be skipped. Hence, flanks with cloning sites are added:

5' flank: CAGGAATTTTGTTTAATATAACTCGAG

3' flank: GAATTCCAATTGACGCGTCTGGAACAATC

The DNA is ordered as a gBlock (Integrated DNA technologies) and cloned into the sensor vector pRSF91-SFFV-dTomato-P2A-BlastaR-[XhoI/EcoRI-MCS] using XhoI/EcoRI and standard cloning protocols.

Once the construct is cloned and sequence verified a stable reporter cell lines is generated. The vector is used for amphotropic packaging to keep reporter cells “Eco-naïve” to ensure subsequent shRNA infections using ecotropic packaging. In brief: Plat-A packaging cells are transfected cells with the reporter construct and a GagPol helper plasmid (pCMV-GagPol, CellBiolabs). RMEFs are infected under S2 lab safety conditions because of the amphotropic nature of the virus. Infected cells can be sorted or selected with Blasticidin (2 µg/mL) in order to obtain a clean, dTomato<sup>+</sup> population.

#### 4.21.2 FACS based analysis of shRNA knockdown

All shRNAs to be tested have to be cloned into a constitutive GFP vector like pLENG (pMSCV-miR-E-PGK-Neo-IRES-GFP) as described in chapter 4.1. Transfection and infection is done as described in 4.2 and 4.4 but it is recommended to scale the assay down to 96 well format if a larger set of shRNAs is tested at the same time. The following controls have to be included as a measure to check the quality of each round of sensor assays:

- pLENG.empty (no knockdown)
- pLENG.Renilla.713 (~90-95% knockdown, optimal shRNA)
- pLENG.Trp53.1224 (~90-95% knockdown, optimal shRNA)
- LMN.Pten.1524 (medium strength knockdown, miR-30).

Two days after the infection, the cells are analyzed for the first time, using a LSR Fortessa (BD) flow cytometer equipped with a 96 well High Throughput Sampler (HTS, BD™). The infection efficiency should not be higher than 15 -20 % to ensure single copy infection of all constructs. For every sample the dTomato value of the GFP<sup>+</sup> [P3] cells and the GFP<sup>-</sup> [P4] cell is measured. Hence, the dTomato value of uninfected (UI) wt RMEFs is determined as well at each time point. The knockdown of each shRNA is determined with the following formula:

$$\% \text{ knockdown} = 100 - \frac{\text{mean } dTom [P3] - \text{mean } dTom [UI]}{\text{mean } dTom [P4] - \text{mean } dTom [UI]} * 100$$

6 days after the infection, the second and final time point is measured and the knockdown is calculated. It proved to be practical to normalize the knockdown of each shRNA to the knockdown of Ren.713, the strongest shRNA available, to make the system comparable between different assays and reporter lines.

## 4.22 Generation a new transgenic mouse line

### 4.22.1 Cloning of the all-in-one targeting construct

The targeting constructs for the all-in-one shRNA transgenic mice were constructed using conventional cloning techniques. In brief, dsDNA linkers were used to insert additional restriction sites into pRosa26-1.CAGGS-rtTA3-PGK-Puro. At the same time, the vector C3GGmiR-E (ColFLP-TRE3G-GFP-miR-E) was constructed from cTGM (ColFLP-TRE.GFP.miR-30) (Premisrirut et al., 2011). In a last step the TRE3G-GFP-miR-E cassette from C3GGmiR-E was shuttled into pRosa26-1.CAGGS-rtTA3-PGK-Puro to obtain the complete all-in-one targeting construct: pRosa26-1.3GGmiR-E-CAGGS-rtTA3-PGK-Puro. One version was cloned with the neutral shRNA Ren.713 and one with the experimental shRNA Gart.984.

### 4.22.2 ECS targeting and verification of positive by southern blot

For the targeting, 5B3 ESCs were used. This clone was derived from a parental B6 ES cell line called Bruce4 (Hughes et al., 2007) and contains a landing pad for FlpE mediated recombination in the ColA1 locus which is not relevant for the targeting at hand.

The ESCs are cultured on a layer of irradiated DR4 feeder cells (Tucker, Wang, Dausman, & Jaenisch, 1997) for at least 3 or 4 days prior to electroporation. 3 hours before the electroporation, the ECS media is changed and tissue culture plates are coated with 0.1% gelatin for the feeder depletion. The stem cells are washed, trypsinized cells and resuspended in 10 ml ESC medium. The cell suspension is put onto 10cm gelatin coated plates. After approx. 45 min the feeders will reattach, while the ES cells remain detached and can be carefully removed from the plate. The ES cells are resuspended in 10ml DPBS, counted and  $12 \times 10^6$  cells in 0.8 ml DPBS are prepared in per targeting construct. 20  $\mu$ g of linearized targeting vector is added to the cells and the mixture is carefully transferred to an electroporation cuvette without introducing bubbles (0.4 cm gap, Biorad). The electroporation is ran at 250 V and 500  $\mu$ F which usually results in a time constant between 5 and 6 seconds. After the electroporation, the cuvette is placed on RT for 5 minutes and then the cells are diluted in pre-warmed Hyclone medium and distribute across 5-6 plates. Two days after the electroporation the cells are put on selection media (75  $\mu$ g/ml Hygromycin B and 0.75  $\mu$ g/ml Puromycin) for 7 - 10 days. The Media has to be changed every day and the selection is continue selection until clones are apparent.

2 days prior to picking clones, feeders are plated onto 5 gelatin coated 96-well plates. Single, well-shaped and non-differentiated colonies are picked under the microscope by gently detaching them with a P20 pipetman. Each clones is transferred to a 96 well U-bottom plate with 15  $\mu$ l of trypsin. Once the ESC clones are dissociated, the trypsin is stopped with 100ul of ESC media and the clones are distributed to 5 96 well plates. The medium is changed every day and 4 out of 5 plates are frozen when most of the cells near confluence. For the freezing, the cells are trypsinized and then 55  $\mu$ l media, 55  $\mu$ l FBS and 15  $\mu$ l DMSO is added to each well. Each plate is sealed with tape and wrapped in green paper towels and aluminum wrap and quickly transferred to  $-80^{\circ}\text{C}$ .

The plate for the southern blot is washed twice with PBS and then incubated with 50  $\mu$ l proteinase K solution (4.5 ml lysis buffer, 10 mM Tris, pH 7.5, 10 mM EDTA, pH 8.0, 10 mM NaCl, 0.5% N-Lauroylsarcosine + 0.5 ml Proteinase K, 10 mg/ml stock) overnight at  $56^{\circ}\text{C}$ . On the next day, 98.5  $\mu$ l 100%, ice cold EtOH and 1.5  $\mu$ l 5M NaCl are added to each well. The solution gets milky and should turn clear after slightly shaking the plate. After 30 min of incubation at RT the plate is spun at maximum speed for 5 min. the supernatant is carefully decanted and each well is washed with 100  $\mu$ l 70 % EtOH after 10 min of centrifugation, the supernatant is decanted again. The plate is air dried until the EtOH is evaporated completely but should not be overdried. The precipitated DNA is resuspend in 45  $\mu$ l TE or  $\text{H}_2\text{O}$  and shaken on  $37^{\circ}\text{C}$  for 6 – 10 hours before the plate is frozen at  $-80^{\circ}\text{C}$  until further use.

In preparation for the southern blot, 5-10  $\mu\text{g}$  of the genomic DNA is digested with 10 U of BamHI (R3136L, New England Biolabs) over night. Loading dye is added to the wells and then they are loaded on a large agarose gel (Biorad chambers, 900 ml of 1% agarose). The gel is run at 90 V for the first hour and then at 120 V for 2 hours. At this point a gel photo can be taken under a trans-illuminator to confirm complete digest of the genomic DNA. The gel is transferred to a suitable container and incubated in depurination solution (0.25 M HCl) for 30mins while slowly shaking. The gel is washed once with  $\text{ddH}_2\text{O}$  and then incubated with denaturation solution (0.5 M NaOH, 1.5 M) for another 30 min. The gel is incubated in neutralization solution (0.5 M Tris pH7.5, 1.5 M NaCl) for 30 min and washed once in  $\text{ddH}_2\text{O}$ .

During the neutralization step, one piece of membrane (Millipore Immobilon NY+; INYCOO010) and six Whatman papers (Whatman® cellulose chromatography papers: Sigma-Aldrich, Z270857) of the size of the gel are prepared. The membrane is soaked in monoQ and then equilibrated for 10 min in 20x SSC (150 mM NaCl, 300 mM  $\text{Na}_3\text{Citrate}$ ).

The blot is assembled as depicted in Figure 4.1. After the gel is turned upside down, the loading slots and all excess gel is cut away. It is important to carefully remove air bubbles between the gel and the membrane before the absorbent paper is stacked on top. The edges can be sealed with parafilm to ensure that the capillary force acts on the gel and does not bypass the gel.

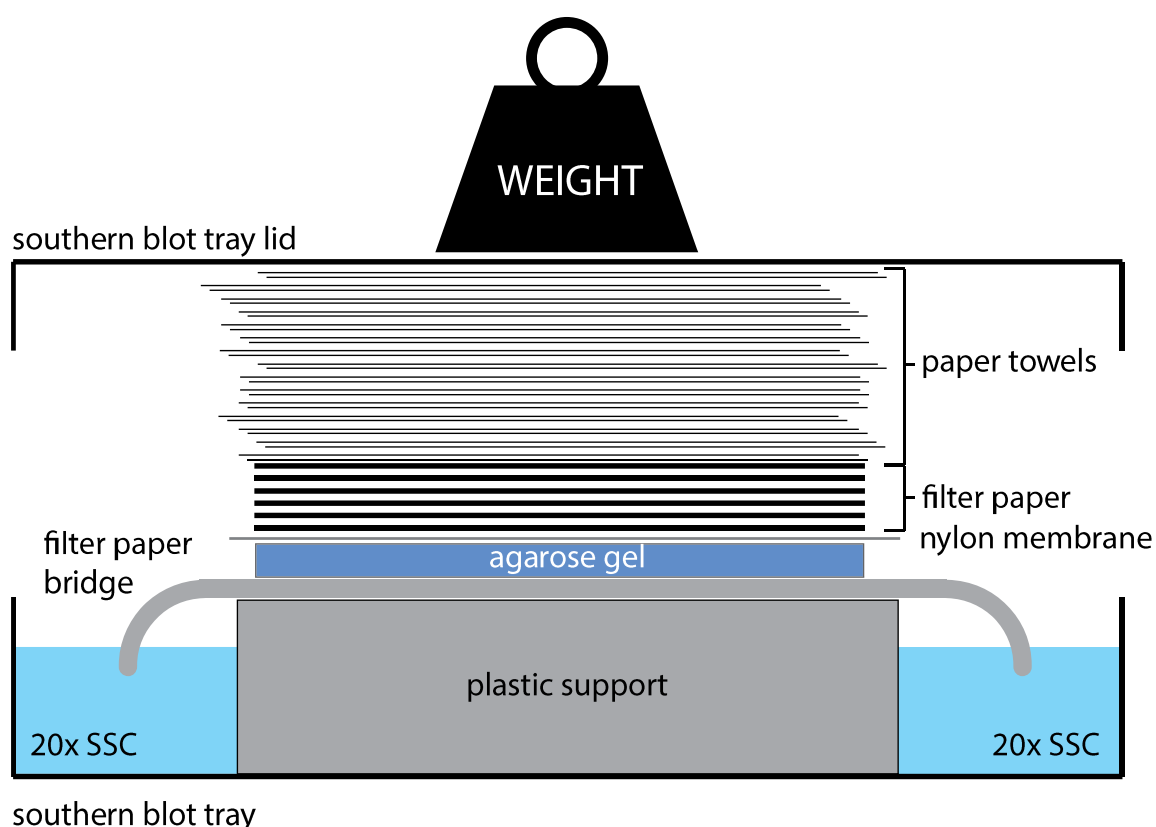


**Figure 4.1 | Schematic set-up of a wet transfer southern blot.**

Depicted is the schematic setup of a wet transfer southern blot. It is important that air bubbles between the gel and the nylon membrane are carefully removed. The edges of the gel can be sealed with parafilm in order to bypassing buffer. Image modified from <http://www.gibthai.com/userfiles/image/technote/Southern%20Blot-1.jpg>

On the next day, the membrane is dried for 1 h 80 °C and subsequently cross-linked using a Stratagene 1800 UV-cross linker (auto cross-link settings).

The membrane is carefully transferred to a hybridization tube and prehybridized with 15 ml hybridization buffer (Perfect Hyb Plus, H7033-125ml, Sigma) at 65°C for 30 min rolling in the hybridization oven.

The probe binding outside of the 5' Rosa26 homology arm can be PCR amplified from mouse genomic DNA or cut from suitable plasmids.

>Rosa26\_southern\_probe

```
TTTGAGAGCAGGGTTGGGAGGCCTCTCCTGAAAAGGGTATAAACGTGGATAGGCAACCC
AGGCAAAAAGGGGAGACCAGAGTAGGGGGAGGGGAAGAGTCCTGACCCAGGGAAGCATT
AAAAAGGTAGTGGGGTCGACTAGATGAAGGAGAGCCTTTCTCTCTGGGCAAGAGCGGTG
AATGGTGTGTAAAGGTAGCTGAGAAGACGAAAAGGGCAAGCATCTTCCTGCTACCAGGC
TGGGGAGGCCCCAGGCCACGACCCCGAGGAGAGGGGAACGCAGGGAGACTGAGGTGACCC
TTCTTT
```

For the labelling of the probe, 50 ng of purified DNA added to a labeling kit tube (Stratagene Prime it, random primer labeling kit) and filled up to 42 µl. The mixture is transferred to a tube with screw able cap and boiled sample for 5-10 min to denature the template.

After cooling the sample down on ice, the mixture is transferred to a lab dedicated for work with radioactivity and 3 µl of polymerase and 5 µl radioactivity ([ $\alpha$   $^{32}$ P] dCTP, NEG513H250UC). After 15 min at 37 °C the labelled probe is purified by using illustra probe quant Columns according to manufacturer's protocol. After the labelling the probe is added directly into the hybridization solution and the membrane is hybridized overnight at 65 °C.

On the next day, the radioactive hybridization solution is disposed of in an appropriate container and the membrane is rinsed and then washed for 20 min with low stringency buffer (2x SSC, 0.1% SDS). The still radioactive wash buffer is discarded and the membrane is washed for 20 min with medium stringency buffer (2x SSC, 0.1% SDS). If necessary, the blot can be washed with high stringency buffer (2x SSC, 0.1% SDS) but usually washing twice is enough.

The membrane is dried for a few minutes on paper towels and then wrapped in saran wrap and prepared for exposure to a phosphor-imager screen. The screen is scanned after 6-12hours, depending on the strength of the signal (Typhoon, GE Healthcare Life Sciences).

Positive clones were thawed, expanded and tested for their shRNA induction *in vitro*. 3-4 clones per construct were submitted for injection into blastocysts from albino-BL6 mice.

#### 4.22.3 Backcrossing, genotyping and analysis of founder mice

Resulting chimeric mice with more than 75% chimerism were back crossed to albino-BL6 in order to confirm germline transmission of the targeted transgenic cassette. Black offspring were genotyped for the CAGGS promotor and the respective shRNA with the following primers:



CAGGS genotyping:

- CAGGS\_geno\_fwd CAATGCCCTGGCTCACAAATAC
- CAGGS\_geno\_rev1 GTAACGCGGAACTCCATATATGG

shRNA genotyping:

- Ren.713\_fwd AAGCATTATAATTCCTATGCCTAC
- Gart.984\_fwd TAAACTCCAACACTTTTGGGCT
- shRNA\_geno\_rev CACCCTGAAAACCTTGCCCC

A standard touch down PCR protocol is used to amplify the respective PCR products. Positive mice were supplied with dox in the drinking water (4 mg/ml) and bone marrow (BM) and spleen cells were harvested after 4 days. GFP induction in the harvested cells was analyzed by flow cytometry using a LSR Fortessa (BD) flow cytometer.

In order to increase induction efficiency an allele of CAGGS-rtTA was crossed into the all-in-one.Ren.713 mouse strain. Offspring was genotyped for the all-in-one cassette as described above and for CAGGS-rtTA with the following primers:

- SApA For1 CTGCTGTCCATTCCTTATTC
- Ch8 Rev2 CGAAACTCTGGTTGACATG
- Ch8 For1 TGCCTATCATGTTGTCAAA

The wild type band appears at 363 bp, whereas the CAGGS-rtTA band is only 330 bp in length. Dox treatment and induction analysis was done as described above.

### 4.23 Transduction and injection of fetal liver cells for leukaemogenesis studies

Fetal liver cells (FLCs) from embryos at embryonic day 13.5 and 14.5 were harvested, cultured and transduced according to established protocols (Johannes Zuber, McJunkin, et al., 2011). In brief, approximately 3 – 4 mice can be injected with the cells from one embryo. FLCs are cultured in B-cell media (BCM: 450 ml DMEM, 450 ml IMDM, 10 ml 100x penicillin-streptomycin, 100 ml FBS, 20 ml 200 mM L-Glutamine and 3.4 µl 14.3M β-mercaptoethanol) supplemented with IL-3 2 ng/ml, IL-6 2 ng/ml and SCF 10 ng/ml. Four rounds of spin infection with the respective retroviral vectors are done every 6-8 hours, starting 20 h after thawing.

On the fourth day the infection efficiency is analyzed by flow cytometry and if the infection is successful, the recipient mice are irradiated with 5.5 Gy. On the next day, cells are collected, spun down and resuspended in HBSS (Hank's Balanced Salt Solution, 14170138, Invitrogen). The recipient mice are irradiated again with 5.5 Gy and then each mouse is intravenously injected with 200  $\mu$ l of cell suspension. For the first two weeks after irradiation and injection the mice are provided with antibiotics in the drinking water (ciprofloxacin 125 mg/l + sucrose 20 g/l) to shield them from infections until their immune system has recovered. Disease progression is monitored weekly, by bioluminescent imaging, as described in Chapter 4.19.

## 5 Appendix

### 5.1 Differential scores from 1133 analyzed genes

rank	gene	Entrez ID	shRNAs	RN2 score	MEF score	differential score
1	Gart	14450	5	36	0	36
2	Mef2c	17260	6	36	3	33
3	Thra	21833	6	36	9	27
4	Psmb2	26445	5	50	26	24
5	Echs1	93747	6	33	9	24
6	Fasn	14104	6	39	16	23
7	Raf1	110157	5	29	6	23
8	Csda	56449	4	23	0	23
9	Top1	21969	5	23	0	23
10	Casr	12374	6	23	0	23
11	Cda	72269	3	23	3	20
12	Kdr	16542	5	26	6	20
13	Twistnb	28071	5	23	3	20
14	Acy1	109652	4	20	0	20
15	Bcl2	12043	4	20	0	20
16	Enpp1	18605	4	20	0	20
17	ME2	107029	4	20	0	20
18	Aak1	269774	5	20	0	20
19	Cnr1	12801	6	20	0	20
20	Vdac2	22334	5	19	0	19
21	Mdm2	17246	4	26	9	17
22	Kcmf1	74287	4	23	6	17
23	Dyrk1c	13548	3	20	3	17
24	Gdi1	14567	3	20	3	17
25	Spry2	24064	3	20	3	17
26	Tnfsf12	21944	3	20	3	17

27	Cacnb1	12295	5	23	6	17
28	Hdac3	15183	5	23	6	17
29	Metap2	56307	6	30	13	17
30	Avpr1a	54140	4	20	3	17
31	Ccnd3	12445	4	20	3	17
32	Pola2	18969	4	20	3	17
33	Rmi1	74386	4	20	3	17
34	Kif18a	228421	5	20	3	17
35	Plcd1	18799	5	20	3	17
36	Rap2b	74012	5	20	3	17
37	Acsf4	50790	6	22	6	16
38	Mcm6	17219	5	43	29	14
39	Kif11	16551	6	40	26	14
40	Pla2g10	26565	6	23	9	14
41	Dhps	330817	4	20	6	14
42	Etv6	14011	4	20	6	14
43	Igf1r	16001	6	20	6	14
44	Gfi1	14581	3	16	3	13
45	Pcdhgc5	93724	3	16	3	13
46	Plod3	26433	2	13	0	13
47	Btd	26363	4	16	3	13
48	Cdk6	12571	5	16	3	13
49	Kcnmb2	72413	5	16	3	13
50	Pctk1	18555	3	13	0	13
51	Stat1	20846	6	16	3	13
52	6330527006 Rik	76161	4	13	0	13
53	C130039016 Rik	238317	4	13	0	13
54	Clec9a	232414	4	13	0	13
55	Dgkd	227333	4	13	0	13
56	Fryl	72313	4	13	0	13
57	Hoxa5	15402	4	13	0	13
58	Il12rb1	16161	4	13	0	13
59	Lig3	16882	4	13	0	13
60	Xylt1	233781	4	13	0	13
61	Adam10	11487	5	13	0	13
62	Bcl7a	77045	5	13	0	13
63	Ep300	328572	5	13	0	13
64	Hivep2	15273	5	13	0	13
65	Kcnq5	226922	5	13	0	13
66	Lcn2	16819	5	13	0	13
67	Rhoh	74734	5	13	0	13

68	Src	20779	5	13	0	13
69	Mme	17380	6	13	0	13
70	Rrm1	20133	5	30	19	11
71	EG277089	277089	2	13	3	10
72	Bclp2	229687	1	10	0	10
73	Cd6	12511	1	10	0	10
74	Pitpnm1	18739	1	10	0	10
75	Plcb2	18796	1	10	0	10
76	Ptpn18	19253	1	10	0	10
77	Sept10	103080	1	10	0	10
78	Slc12a5	57138	1	10	0	10
79	Avpr1b	26361	5	23	13	10
80	PSMB1	19170	5	23	13	10
81	Mcm7	17220	3	13	3	10
82	Pan3	72587	3	13	3	10
83	Pde4dip	83679	3	13	3	10
84	Tk1	21877	3	13	3	10
85	Vamp1	22317	3	13	3	10
86	Ccdc45	320162	4	13	3	10
87	Chd9	109151	4	13	3	10
88	Clcnkb	56365	4	13	3	10
89	Ggps1	14593	4	13	3	10
90	H6pd	100198	4	13	3	10
91	Fas	14102	2	10	0	10
92	Gas1	14451	2	10	0	10
93	Hexa	15211	2	10	0	10
94	Htatip2	53415	2	10	0	10
95	Lima1	65970	2	10	0	10
96	Rgs6	50779	2	10	0	10
97	Wnt10b	22410	2	10	0	10
98	Arid1b	239985	5	13	3	10
99	Dhfr	13361	5	13	3	10
100	Nqo2	18105	5	13	3	10
101	Prkaa1	105787	5	13	3	10
102	Rarb	218772	5	13	3	10
103	Slc1a3	20512	5	13	3	10
104	Stk39	53416	5	13	3	10
105	Twist1	22160	5	13	3	10
106	Cacna1g	12291	6	13	3	10
107	Mtap	66902	6	13	3	10
108	Ptpn1	19246	6	13	3	10
109	Soat1	20652	6	13	3	10
110	Tgfbr1	21812	6	13	3	10

111	Arf3	11842	3	10	0	10
112	Bcat1	12035	3	10	0	10
113	Cerk	223753	3	10	0	10
114	Hmx3	15373	3	10	0	10
115	Klf5	12224	3	10	0	10
116	Slc22a4	30805	3	10	0	10
117	Slfn1	20555	3	10	0	10
118	Smchd1	74355	3	10	0	10
119	Wrnip1	78903	3	10	0	10
120	Akt3	23797	4	10	0	10
121	Ar	11835	4	10	0	10
122	Atp1a1	11928	4	10	0	10
123	Cacna1h	58226	4	10	0	10
124	Ecgf1	72962	4	10	0	10
125	Klrk1	27007	4	10	0	10
126	Rbks	71336	4	10	0	10
127	Smg7	226517	4	10	0	10
128	Arg2	11847	5	10	0	10
129	Aspa	11484	5	10	0	10
130	Brd2	14312	5	10	0	10
131	Cldn15	60363	5	10	0	10
132	Grem1	23892	5	10	0	10
133	Il21r	60504	5	10	0	10
134	Lrp2	14725	5	10	0	10
135	Pdf	68023	5	10	0	10
136	Pgr	18667	5	10	0	10
137	Ppard	19015	5	10	0	10
138	Ppp3r1	19058	5	10	0	10
139	Tlr2	24088	5	10	0	10
140	Tnfrsf1a	21937	5	10	0	10
141	Trib2	217410	5	10	0	10
142	Cacna1d	12289	6	10	0	10
143	Cacnb4	12298	6	10	0	10
144	Cd44	12505	6	10	0	10
145	Gprc5a	232431	6	10	0	10
146	Nnt	18115	6	10	0	10
147	Ppp2r5c	26931	6	10	0	10
148	Prkcb1	18751	6	10	0	10
149	Ptpn4	19258	6	10	0	10
150	Camk2d	108058	4	9	0	9
151	Prkce	18754	5	9	0	9
152	Pts	19286	6	9	0	9
153	Ube1x	22201	4	20	12	8

154	Gusb	110006	2	20	13	7
155	Ntrk3	18213	2	13	6	7
156	Bckdha	12039	1	10	3	7
157	Cd97	26364	1	10	3	7
158	Centd3	106952	1	10	3	7
159	Pgam1	18648	1	10	3	7
160	RP23-448C18	n.a.	1	10	3	7
161	Syt17	110058	1	10	3	7
162	Vnn3	26464	1	10	3	7
163	Gab3	210710	3	13	6	7
164	Siah2	20439	3	13	6	7
165	Cacna1a	12286	5	16	9	7
166	Pdxk	216134	6	16	9	7
167	Fgd4	224014	4	13	6	7
168	Cdc42ep3	260409	2	10	3	7
169	Clcn1	12723	2	10	3	7
170	F3	14066	2	10	3	7
171	Flot2	14252	2	10	3	7
172	Fn1	14268	2	10	3	7
173	L1cam	16728	2	10	3	7
174	Ncf1	17969	2	10	3	7
175	Ttll3	101100	2	10	3	7
176	Ucp1	22227	2	10	3	7
177	Flt4	14257	5	13	6	7
178	Parp1	11545	5	13	6	7
179	Ap1s2	108012	3	10	3	7
180	Braf	109880	3	10	3	7
181	Ccr1	12768	3	10	3	7
182	Cx3cr1	13051	3	10	3	7
183	Dhodh	56749	3	10	3	7
184	EG408196	408196	3	10	3	7
185	Cdk9	107951	6	13	6	7
186	Pla2g4a	18783	6	13	6	7
187	Srd5a2	94224	6	13	6	7
188	Casp1	12362	4	10	3	7
189	Dach1	13134	4	10	3	7
190	Elovl6	170439	4	10	3	7
191	Gm9234	668548	4	10	3	7
192	Lig1	16881	4	10	3	7
193	Prg3	53856	4	10	3	7
194	Rxrg	20183	4	10	3	7
195	Tm7sf3	67623	4	10	3	7
196	Vegfa	22339	4	10	3	7

197	Cacnb2	12296	5	10	3	7
198	Cant1	76025	5	10	3	7
199	Cd1d1	12479	5	10	3	7
200	Chst11	58250	5	10	3	7
201	Crp	12944	5	10	3	7
202	Fgf2	14173	5	10	3	7
203	Lmo2	16909	5	10	3	7
204	Man1b1	227619	5	10	3	7
205	Senp6	215351	5	10	3	7
206	Snx5	69178	5	10	3	7
207	Tpsb2	17229	5	10	3	7
208	Adcyap1	11516	6	10	3	7
209	Akp5	11650	6	10	3	7
210	Cd33	12489	6	10	3	7
211	Cysltr1	58861	6	10	3	7
212	Ghr	14600	6	10	3	7
213	Mmp8	17394	6	10	3	7
214	Npc1l1	237636	6	10	3	7
215	Ppp1cc	19047	6	10	3	7
216	Rarres1	109222	6	10	3	7
217	Hdac1	433759	4	16	10	6
218	Ptger3	19218	4	9	3	6
219	Cox7a1	12865	2	6	0	6
220	Hipk3	15259	5	9	3	6
221	Fdps	110196	6	9	3	6
222	Btg1	12226	3	6	0	6
223	Cpne8	66871	4	6	0	6
224	Eea1	216238	5	6	0	6
225	Mical1	171580	5	6	0	6
226	Prss16	54373	5	6	0	6
227	Rnf220	66743	5	6	0	6
228	Hint1	15254	6	6	0	6
229	Lrp1	16971	6	6	0	6
230	Mapk3	26417	6	6	0	6
231	Mmp13	17386	6	6	0	6
232	Pck1	18534	6	6	0	6
233	Pde2a	207728	6	6	0	6
234	Psat1	107272	6	6	0	6
235	Was	22376	6	6	0	6
236	Map2k7	26400	6	13	9	4
237	Mttp	17777	6	13	9	4
238	Sparc	20692	6	13	9	4
239	Clcn2	12724	5	13	9	4



240	Cacna1f	54652	6	10	6	4
241	Dlg4	13385	6	10	6	4
242	Hck	15162	6	10	6	4
243	Jun	16476	6	10	6	4
244	Pim1	18712	6	10	6	4
245	Syk	20963	6	10	6	4
246	Trpm4	68667	3	13	9	4
247	2810407C02R ik	69227	5	10	6	4
248	Ghrhr	14602	5	10	6	4
249	Hsf1	15499	5	10	6	4
250	Rhoa	11848	5	10	6	4
251	Slc38a1	105727	5	10	6	4
252	Slpi	20568	5	10	6	4
253	Tgfb1	21803	5	10	6	4
254	Ccbl1	70266	4	10	6	4
255	Txnrd1	50493	4	10	6	4
256	Dio2	13371	3	10	6	4
257	Dsp	109620	3	10	6	4
258	Ifngr2	15980	3	10	6	4
259	Jak3	16453	3	10	6	4
260	Ogg1	18294	3	10	6	4
261	Pygl	110095	3	10	6	4
262	Dnmt1	13433	6	26	22	4
263	Cdc42ep1	104445	2	10	6	4
264	Dnase1	13419	2	10	6	4
265	Park2	50873	2	10	6	4
266	Plxnd1	67784	2	10	6	4
267	Ddx5	13207	4	16	13	3
268	Itga7	16404	2	6	3	3
269	Hdac6	15185	6	16	13	3
270	Nt5e	23959	6	16	13	3
271	Th	21823	6	16	13	3
272	1110003E01R ik	68552	3	6	3	3
273	Kcne3	57442	3	6	3	3
274	Myh8	17885	3	6	3	3
275	Adcy4	104110	1	3	0	3
276	BC100530	10003468 4	1	3	0	3
277	Ckm	12715	1	3	0	3
278	Ctsd	13033	1	3	0	3
279	Cxcr4	12767	1	3	0	3
280	Gsr	14782	1	3	0	3

281	Ilk	16202	1	3	0	3
282	Reep3	28193	1	3	0	3
283	Serpinb2	18788	1	3	0	3
284	Slc16a3	80879	1	3	0	3
285	Slc28a2	269346	1	3	0	3
286	Unc5a	107448	1	3	0	3
287	Wbp2	22378	1	3	0	3
288	Mgst1	56615	4	6	3	3
289	Rac2	19354	4	6	3	3
290	Cyth2	19158	5	6	3	3
291	Dpysl2	12934	5	6	3	3
292	Galns	50917	5	6	3	3
293	Mapk1	26413	5	6	3	3
294	Mmp3	17392	5	6	3	3
295	Pggt1b	225467	5	6	3	3
296	Spen	56381	5	6	3	3
297	Tnfrsf1b	21938	5	6	3	3
298	Cdc25b	12531	6	6	3	3
299	Cdk7	12572	6	6	3	3
300	Dpyd	99586	6	6	3	3
301	Il5	16191	6	6	3	3
302	Pitpna	18738	6	6	3	3
303	Prkab1	19079	6	6	3	3
304	Cxcl14	57266	2	3	0	3
305	Entpd1	12495	2	3	0	3
306	Esr2	13983	2	3	0	3
307	Fut4	14345	2	3	0	3
308	Lypla3	192654	2	3	0	3
309	Mark2	13728	2	3	0	3
310	Phyh	16922	2	3	0	3
311	Ppp3ca	19055	2	3	0	3
312	Rock2	19878	2	3	0	3
313	Slc25a25	227731	2	3	0	3
314	Arhgap25	232201	3	3	0	3
315	Dgkg	110197	3	3	0	3
316	Gnaq	14682	3	3	0	3
317	Hpgd	15446	3	3	0	3
318	Klrb1b	17058	3	3	0	3
319	Mtm1	17772	3	3	0	3
320	Nkg7	72310	3	3	0	3
321	Nln	75805	3	3	0	3
322	Shmt1	20425	3	3	0	3

323	5430427019 Rik	71398	4	3	0	3
324	Atp8b4	241633	4	3	0	3
325	Chd1	12648	4	3	0	3
326	Crabp2	12904	4	3	0	3
327	Decr1	67460	4	3	0	3
328	Epha7	13841	4	3	0	3
329	Fuca1	71665	4	3	0	3
330	Igf2bp3	140488	4	3	0	3
331	Itga4	16401	4	3	0	3
332	Mtap2	17756	4	3	0	3
333	Plekho1	67220	4	3	0	3
334	Prkaca	18747	4	3	0	3
335	Satb1	20230	4	3	0	3
336	Spn	20737	4	3	0	3
337	Ssbp2	66970	4	3	0	3
338	Trap1	68015	4	3	0	3
339	Abl2	11352	5	3	0	3
340	Acat3	224530	5	3	0	3
341	Bhmt	12116	5	3	0	3
342	Bmp2k	140780	5	3	0	3
343	Cd40	21939	5	3	0	3
344	Chd2	244059	5	3	0	3
345	D12Ertd551e	52635	5	3	0	3
346	Fgf1	14164	5	3	0	3
347	Gsk3b	56637	5	3	0	3
348	Hmga2	15364	5	3	0	3
349	Hmgcr	15357	5	3	0	3
350	Hook3	320191	5	3	0	3
351	Il1b	16176	5	3	0	3
352	Jmjd1c	108829	5	3	0	3
353	Lss	16987	5	3	0	3
354	Masp2	17175	5	3	0	3
355	Mmp11	17385	5	3	0	3
356	Nr5a1	26423	5	3	0	3
357	Olr1	108078	5	3	0	3
358	Phf17	269424	5	3	0	3
359	Pik3cg	30955	5	3	0	3
360	Ppara	19013	5	3	0	3
361	Prg2	19074	5	3	0	3
362	Prlr	19116	5	3	0	3
363	Ptgis	19223	5	3	0	3
364	Rock1	19877	5	3	0	3

365	Stag2	20843	5	3	0	3
366	Zbtb10	229055	5	3	0	3
367	Zcchc7	319885	5	3	0	3
368	Bcat2	12036	6	3	0	3
369	Dapk1	69635	6	3	0	3
370	Flt3	14255	6	3	0	3
371	Gamt	14431	6	3	0	3
372	Gcdh	270076	6	3	0	3
373	Hs3st3a1	15478	6	3	0	3
374	Icam1	15894	6	3	0	3
375	Kcnma1	16531	6	3	0	3
376	Nfkb1	18033	6	3	0	3
377	Odc1	18263	6	3	0	3
378	Pde7a	18583	6	3	0	3
379	Pdgfra	18595	6	3	0	3
380	Ptgs1	19224	6	3	0	3
381	Siglece	83382	6	3	0	3
382	Sstr5	20609	6	3	0	3
383	Ugcg	22234	6	3	0	3
384	Xrcc4	108138	6	3	0	3
385	Btk	12229	6	10	9	1
386	Cacna1s	12292	6	10	9	1
387	Esrrg	26381	6	10	9	1
388	Vdac1	22333	6	10	9	1
389	Rap1ga1	110351	4	10	9	1
390	Impdh1	23917	6	20	19	1
391	Pola1	18968	5	43	43	0
392	Psmc2	21762	4	40	40	0
393	Psma1	26440	5	40	40	0
394	Psmc1	70247	6	40	40	0
395	Top2a	21973	5	33	33	0
396	Hsp90ab1	15516	6	26	26	0
397	Napsa	16541	2	13	13	0
398	Centa1	231821	3	13	13	0
399	Gstk1	76263	3	13	13	0
400	Prss12	19142	3	13	13	0
401	Ncam1	17967	4	13	13	0
402	Il2ra	16184	5	13	13	0
403	Fn3k	63828	1	10	10	0
404	Nmur1	14767	1	10	10	0
405	Slc15a3	65221	1	10	10	0
406	Adam23	23792	2	10	10	0
407	Ctbs	74245	2	10	10	0

408	Mag	17136	2	10	10	0
409	Nrg4	83961	3	10	10	0
410	Thyn1	77862	4	10	10	0
411	Cacna2d1	12293	6	10	10	0
412	Por	18984	6	9	9	0
413	BC011248	224823	2	6	6	0
414	Phip	83946	3	6	6	0
415	Smpd2	20598	3	6	6	0
416	Rdx	19684	5	6	6	0
417	Ccnd1	12443	6	6	6	0
418	Gfra1	14585	6	6	6	0
419	Hyal2	15587	6	6	6	0
420	Mapk14	26416	6	6	6	0
421	Ptger4	19219	6	6	6	0
422	Sts	20905	6	6	6	0
423	Cyp4a10	13117	1	3	3	0
424	Dusp3	72349	1	3	3	0
425	EG209324	209324	1	3	3	0
426	Fez1	235180	1	3	3	0
427	Id1	15901	1	3	3	0
428	Kcnh7	170738	1	3	3	0
429	Krt23	94179	1	3	3	0
430	Myo7a	17921	1	3	3	0
431	Penk1	18619	1	3	3	0
432	Pld4	104759	1	3	3	0
433	Psen1	19164	1	3	3	0
434	Slc11a1	18173	1	3	3	0
435	Tpm4	326618	1	3	3	0
436	Tspan17	74257	1	3	3	0
437	Acsl1	14081	2	3	3	0
438	Anxa3	11745	2	3	3	0
439	Bmx	12169	2	3	3	0
440	F10	14058	2	3	3	0
441	Gstm4	14865	2	3	3	0
442	Hoxa9	15405	2	3	3	0
443	Hp	15439	2	3	3	0
444	Inpp1	16332	2	3	3	0
445	Kynu	70789	2	3	3	0
446	Myl3	17897	2	3	3	0
447	Pik3r5	320207	2	3	3	0
448	Prl	19109	2	3	3	0
449	Rab7l1	226422	2	3	3	0
450	Sepx1	27361	2	3	3	0

451	Soat2	223920	2	3	3	0
452	Stk10	20868	2	3	3	0
453	Stk4	58231	2	3	3	0
454	Vps26b	69091	2	3	3	0
455	Abcd2	26874	3	3	3	0
456	Cftr	12638	3	3	3	0
457	Clec11a	20256	3	3	3	0
458	Gna14	14675	3	3	3	0
459	Hexb	15212	3	3	3	0
460	Hoxa4	15401	3	3	3	0
461	Hoxa7	15404	3	3	3	0
462	Ltb4dh	67103	3	3	3	0
463	Mkl1	223701	3	3	3	0
464	Nucb2	53322	3	3	3	0
465	Pira3	18726	3	3	3	0
466	Pon3	269823	3	3	3	0
467	Sec16b	89867	3	3	3	0
468	Serpina3c	16625	3	3	3	0
469	Setd5	72895	3	3	3	0
470	Sh3bp1	20401	3	3	3	0
471	Tcf4	21413	3	3	3	0
472	Tfpi2	21789	3	3	3	0
473	Zfp36l2	12193	3	3	3	0
474	Amt	434437	4	3	3	0
475	Cbr1	12408	4	3	3	0
476	Cd244	18106	4	3	3	0
477	Cyp3a16	13114	4	3	3	0
478	Dusp6	67603	4	3	3	0
479	Erg	13876	4	3	3	0
480	Esr1	13982	4	3	3	0
481	Hsd17b1	15485	4	3	3	0
482	Map3k1	26401	4	3	3	0
483	Pah	18478	4	3	3	0
484	Pla2g2a	18780	4	3	3	0
485	Ret	19713	4	3	3	0
486	Tctex1d1	67344	4	3	3	0
487	Zhx2	387609	4	3	3	0
488	Adcy2	210044	5	3	3	0
489	Arsa	11883	5	3	3	0
490	Caml	12328	5	3	3	0
491	Col19a1	12823	5	3	3	0
492	Cpt2	12896	5	3	3	0
493	Gba	14466	5	3	3	0

494	Gpx3	14778	5	3	3	0
495	Hif1an	319594	5	3	3	0
496	Hsd3b1	15492	5	3	3	0
497	Il6	16193	5	3	3	0
498	Impdh2	23918	5	3	3	0
499	Mapk10	26414	5	3	3	0
500	Pomc	18976	5	3	3	0
501	Ptk2b	19229	5	3	3	0
502	Ramp1	51801	5	3	3	0
503	Rnf170	77733	5	3	3	0
504	Adcy7	11513	6	3	3	0
505	Alox15	11687	6	3	3	0
506	Car2	12349	6	3	3	0
507	Car4	12351	6	3	3	0
508	Dapp1	26377	6	3	3	0
509	Hdac2	15182	6	3	3	0
510	Hsd3b2	15493	6	3	3	0
511	Il1r2	16178	6	3	3	0
512	Mtap1a	17754	6	3	3	0
513	Nr1i3	12355	6	3	3	0
514	Nr3c1	14815	6	3	3	0
515	Pde1b	18574	6	3	3	0
516	Pnpo	103711	6	3	3	0
517	Ptgdr	19214	6	3	3	0
518	Tyr	22173	6	3	3	0
519	1200002N14 Rik	71712	2	0	0	0
520	1700010I14Ri k	66931	3	0	0	0
521	4632428N05 Rik	74048	2	0	0	0
522	8430406I07Ri k	74528	5	0	0	0
523	A130092J06Ri k	241303	3	0	0	0
524	A830007P12R ik	227612	1	0	0	0
525	A930008G19 Rik	77938	3	0	0	0
526	Abcb1	18671	5	0	0	0
527	Abcc2	12780	2	0	0	0
528	Abhd5	67469	1	0	0	0
529	Abhd6	66082	3	0	0	0
530	Adipor1	72674	2	0	0	0

531	Agtr1a	11607	4	0	0	0
532	Agtr2	11609	1	0	0	0
533	Akna	100182	1	0	0	0
534	Alox5	11689	5	0	0	0
535	Alox5ap	11690	1	0	0	0
536	Amd1	11702	4	0	0	0
537	Anpep	16790	4	0	0	0
538	Aoah	27052	2	0	0	0
539	Apoc4	11425	1	0	0	0
540	Arhgef6	73341	3	0	0	0
541	Art1	11870	5	0	0	0
542	Atp1b1	11931	3	0	0	0
543	Atp6v1a	11964	1	0	0	0
544	Baz2b	407823	2	0	0	0
545	Bc022224	192970	5	0	0	0
546	BC061194	381350	1	0	0	0
547	BC117090	10003885 4	1	0	0	0
548	Bcar1	12927	1	0	0	0
549	Bmp2	12156	5	0	0	0
550	Bmpr1a	12166	5	0	0	0
551	Bst1	12182	3	0	0	0
552	C3ar1	12267	3	0	0	0
553	Cacna1i	239556	4	0	0	0
554	Cacna2d2	56808	2	0	0	0
555	Cacnb3	12297	4	0	0	0
556	Cacng1	12299	3	0	0	0
557	Camk2a	12322	6	0	0	0
558	Capns1	12336	1	0	0	0
559	Car1	12346	6	0	0	0
560	Car5a	12352	3	0	0	0
561	Cat	12359	6	0	0	0
562	Ccdc61	232933	1	0	0	0
563	Ccdc80	67896	2	0	0	0
564	Ccl3	20302	2	0	0	0
565	Ccl6	20305	1	0	0	0
566	Ccl9	20308	2	0	0	0
567	Ccr2	12772	4	0	0	0
568	Ccr4	12773	2	0	0	0
569	Ccr5	12774	4	0	0	0
570	Cd1d2	12480	1	0	0	0
571	Cd302	66205	1	0	0	0
572	Cd4	12504	2	0	0	0



573	Cd40lg	21947	5	0	0	0
574	Cd70	21948	1	0	0	0
575	Cd86	12524	2	0	0	0
576	Cd96	84544	4	0	0	0
577	Cdk5	12568	5	0	0	0
578	Cdk8	264064	6	0	0	0
579	Ceacam2	26367	1	0	0	0
580	Celsr3	107934	2	0	0	0
581	Ces1	12623	3	0	0	0
582	Cflar	12633	2	0	0	0
583	Cfp	18636	1	0	0	0
584	Chd7	320790	1	0	0	0
585	Chi3l4	104183	1	0	0	0
586	Chia	81600	2	0	0	0
587	Chst12	59031	2	0	0	0
588	Clec4a2	26888	2	0	0	0
589	Clec4b1	69810	2	0	0	0
590	Clec4b2	381809	1	0	0	0
591	Clec4n	56620	2	0	0	0
592	Clstn2	64085	2	0	0	0
593	Cmas	12764	3	0	0	0
594	Cnn2	12798	2	0	0	0
595	Cp	12870	5	0	0	0
596	Cpm	70574	1	0	0	0
597	Crot	74114	4	0	0	0
598	Csta	209294	2	0	0	0
599	Ctbp2	13017	4	0	0	0
600	Ctgf	14219	1	0	0	0
601	Ctsb	13030	1	0	0	0
602	Ctsg	13035	3	0	0	0
603	Cxcl10	15945	2	0	0	0
604	Cybb	13058	2	0	0	0
605	Cyp1b1	13078	3	0	0	0
606	Dhrs1	52585	1	0	0	0
607	Dok3	27261	1	0	0	0
608	Dpep1	13479	2	0	0	0
609	EG433016	433016	2	0	0	0
610	Egf	13645	3	0	0	0
611	Eml5	319670	3	0	0	0
612	Emr1	13733	1	0	0	0
613	Erbb2	13866	5	0	0	0
614	Es1	13884	1	0	0	0
615	Esrra	26379	2	0	0	0

616	Evl	14026	1	0	0	0
617	F5	14067	2	0	0	0
618	Fbp1	14121	1	0	0	0
619	Fbxo40	207215	2	0	0	0
620	Fcgr2b	14130	2	0	0	0
621	Fcgr3	14131	1	0	0	0
622	Fgfr1	14182	3	0	0	0
623	Fgr	14191	2	0	0	0
624	Fkbp1a	14225	4	0	0	0
625	Flna	192176	1	0	0	0
626	Fmn12	71409	4	0	0	0
627	Fpr-rs2	14289	1	0	0	0
628	Ganc	76051	2	0	0	0
629	Gdpd4	233537	2	0	0	0
630	Gli1	14632	2	0	0	0
631	Glo1	109801	5	0	0	0
632	Gm7308	640703	5	0	0	0
633	Gmip	78816	1	0	0	0
634	Gnpda1	26384	6	0	0	0
635	Gns	75612	1	0	0	0
636	Gpc1	14733	3	0	0	0
637	Gpr109a	80885	6	0	0	0
638	Gpr44	14764	1	0	0	0
639	Gria3	53623	3	0	0	0
640	Grn	14824	1	0	0	0
641	Gsn	227753	1	0	0	0
642	Gzma	14938	3	0	0	0
643	H2afy	26914	5	0	0	0
644	Hdac9	79221	6	0	0	0
645	Hgf	15234	3	0	0	0
646	Hipk4	233020	2	0	0	0
647	Hk3	212032	2	0	0	0
648	Hmgcl	15356	2	0	0	0
649	Hnmt	140483	2	0	0	0
650	Homer3	26558	1	0	0	0
651	Hoxa10	15395	3	0	0	0
652	Hoxa11	15396	1	0	0	0
653	Hprt1	15452	5	0	0	0
654	Hpse	15442	1	0	0	0
655	Hsd11b1	15483	6	0	0	0
656	Hsd17b11	114664	5	0	0	0
657	Hsp90aa1	15519	5	0	0	0
658	Hyal1	15586	4	0	0	0

659	Hyal5	74468	5	0	0	0
660	Idua	15932	2	0	0	0
661	Ifng	15978	6	0	0	0
662	Ifngr1	15979	1	0	0	0
663	Igf2r	16004	1	0	0	0
664	Igsf6	80719	3	0	0	0
665	Ikzf2	22779	4	0	0	0
666	Il10rb	16155	1	0	0	0
667	Il13ra1	16164	2	0	0	0
668	Il2rg	16186	5	0	0	0
669	Iqgap1	29875	1	0	0	0
670	Itgam	16409	2	0	0	0
671	Itgb2	16414	2	0	0	0
672	Itgb5	16419	1	0	0	0
673	Kit	16590	1	0	0	0
674	Kng2	385643	6	0	0	0
675	Lamp2	16784	2	0	0	0
676	Lbp	16803	2	0	0	0
677	Lck	16818	4	0	0	0
678	LOC624461	624461	1	0	0	0
679	Lpl	16956	1	0	0	0
680	Lrp4	228357	2	0	0	0
681	Lrrc58	320184	2	0	0	0
682	Lrrk2	66725	4	0	0	0
683	Lst1	16988	1	0	0	0
684	Ly86	17084	4	0	0	0
685	M6prbp1	66905	2	0	0	0
686	Marcks	17118	1	0	0	0
687	Meis1	17268	2	0	0	0
688	Mett5d1	76894	3	0	0	0
689	Mif	17319	6	0	0	0
690	Mmp2	17390	6	0	0	0
691	Mmp9	17395	4	0	0	0
692	Mrpl33	66845	1	0	0	0
693	Ms4a6b	69774	3	0	0	0
694	Ms4a6d	68774	3	0	0	0
695	Mtmr11	194126	1	0	0	0
696	Naglu	27419	2	0	0	0
697	Ncf4	17972	1	0	0	0
698	Nid1	18073	5	0	0	0
699	Nos3	18127	4	0	0	0
700	Nqo1	18104	6	0	0	0
701	Nr0b1	11614	6	0	0	0

702	Nr1h2	22260	3	0	0	0
703	Ntrk2	18212	2	0	0	0
704	Nudt9	74167	4	0	0	0
705	Oprl1	18389	1	0	0	0
706	Orm2	18406	1	0	0	0
707	Otc	18416	5	0	0	0
708	Otud4	73945	4	0	0	0
709	P39688-2	14360	5	0	0	0
710	Padi2	18600	1	0	0	0
711	Pank1	75735	5	0	0	0
712	Pbx3	18516	5	0	0	0
713	Pctp	18559	5	0	0	0
714	Pde4a	18577	2	0	0	0
715	Pftk1	18647	4	0	0	0
716	Pglyrp1	21946	1	0	0	0
717	Phka2	110094	3	0	0	0
718	Pi16	74116	2	0	0	0
719	Pitpnc1	71795	4	0	0	0
720	Pkib	18768	1	0	0	0
721	Plagl2	54711	1	0	0	0
722	Plaur	18793	2	0	0	0
723	Pld1	18805	2	0	0	0
724	Plec1	18810	1	0	0	0
725	Pmaip1	58801	5	0	0	0
726	Ppfibp1	67533	5	0	0	0
727	Ppm1l	242083	3	0	0	0
728	Ppp3r2	19059	6	0	0	0
729	Prdx5	54683	5	0	0	0
730	Prom1	19126	4	0	0	0
731	Ptger1	19216	4	0	0	0
732	Ptger2	19217	5	0	0	0
733	Ptgs2	19225	1	0	0	0
734	Ptov1	84113	1	0	0	0
735	Ptpn2	19276	1	0	0	0
736	Qk	19317	3	0	0	0
737	Rab3d	19340	1	0	0	0
738	Rab4b	19342	1	0	0	0
739	Ramp2	54409	6	0	0	0
740	Rcan3	53902	3	0	0	0
741	Rel1	100532	1	0	0	0
742	Rgs19	56470	2	0	0	0
743	Rhog	56212	1	0	0	0
744	Rhou	69581	1	0	0	0

745	Rnf43	207742	2	0	0	0
746	Rod1	230257	4	0	0	0
747	Rxrb	20182	5	0	0	0
748	Ryr1	20190	6	0	0	0
749	S100a1	20193	1	0	0	0
750	Scnn1a	20276	1	0	0	0
751	Sfpi1	20375	1	0	0	0
752	Sgip1	73094	4	0	0	0
753	Sgsh	27029	1	0	0	0
754	Slc13a3	114644	1	0	0	0
755	Slfn2	20556	3	0	0	0
756	Smad1	17125	4	0	0	0
757	Smpdl3a	57319	1	0	0	0
758	Sord	20322	4	0	0	0
759	Sorl1	20660	1	0	0	0
760	Sort1	20661	1	0	0	0
761	Spata13	219140	3	0	0	0
762	Sqle	20775	6	0	0	0
763	Srd5a1	78925	4	0	0	0
764	Stat5b	20851	5	0	0	0
765	Stfa3	20863	2	0	0	0
766	Sult1a1	20887	4	0	0	0
767	Sult1e1	20860	6	0	0	0
768	Supt3h	109115	5	0	0	0
769	Tacr3	21338	4	0	0	0
770	Tbc1d14	100855	4	0	0	0
771	Tbc1d9	71310	2	0	0	0
772	Tead2	21677	1	0	0	0
773	Tgfb2	21808	2	0	0	0
774	Thbd	21824	4	0	0	0
775	Thbs1	21825	6	0	0	0
776	Tinagl	94242	1	0	0	0
777	Tktl1	83553	2	0	0	0
778	Tlr1	21897	2	0	0	0
779	Tlr4	21898	4	0	0	0
780	Tmem132a	98170	1	0	0	0
781	Tmem2	83921	3	0	0	0
782	Tmem46	219134	3	0	0	0
783	Tnfaip2	21928	1	0	0	0
784	Tnrc18	231861	2	0	0	0
785	Tph1	21990	6	0	0	0
786	Tppp3	67971	1	0	0	0
787	Trhde	237553	5	0	0	0

788	Trib1	211770	1	0	0	0
789	Tsc22d2	72033	5	0	0	0
790	Tyrobp	22177	1	0	0	0
791	Ugp2	216558	3	0	0	0
792	Utx	22289	5	0	0	0
793	Vldlr	22359	1	0	0	0
794	Vps54	245944	3	0	0	0
795	Xiap	11798	5	0	0	0
796	Zc3h12c	244871	5	0	0	0
797	Zc3h14	75553	2	0	0	0
798	Zcchc2	227449	3	0	0	0
799	Zfp532	328977	1	0	0	0
800	Il2rb	16185	5	9	10	-1
801	Nos1	18125	5	10	12	-2
802	Acadsb	66885	6	0	3	-3
803	Cdk2	12566	6	0	3	-3
804	Crat	12908	6	0	3	-3
805	Cyth3	19159	6	0	3	-3
806	Igfbp3	16009	6	0	3	-3
807	Il1r1	16177	6	0	3	-3
808	Mat1a	11720	6	0	3	-3
809	Nt5m	103850	6	0	3	-3
810	Pmf1	67037	6	0	3	-3
811	Pnp1	18950	6	0	3	-3
812	Ppp5c	19060	6	0	3	-3
813	Procr	19124	6	0	3	-3
814	Rxra	20181	6	0	3	-3
815	Slc6a1	232333	6	0	3	-3
816	Thrb	21834	6	0	3	-3
817	Abl1	11350	5	0	3	-3
818	Ache	11423	5	0	3	-3
819	Aldh7a1	110695	5	0	3	-3
820	Arid4b	94246	5	0	3	-3
821	Atp2c1	235574	5	0	3	-3
822	Csf1r	12978	5	0	3	-3
823	Flt1	14254	5	0	3	-3
824	Galnt2	108148	5	0	3	-3
825	Hnf4a	15378	5	0	3	-3
826	Larp1	73158	5	0	3	-3
827	Neu2	23956	5	0	3	-3
828	Pde5a	242202	5	0	3	-3
829	Prkcd	18753	5	0	3	-3
830	Ptgir	19222	5	0	3	-3

831	Ramp3	56089	5	0	3	-3
832	Rara	19401	5	0	3	-3
833	Serpinb5	20724	5	0	3	-3
834	Serpinb6a	20719	5	0	3	-3
835	Sgk3	170755	5	0	3	-3
836	Snca	20617	5	0	3	-3
837	Spr	20751	5	0	3	-3
838	Yes1	22612	5	0	3	-3
839	Akr1b1	11677	4	0	3	-3
840	B4galnt1	14421	4	0	3	-3
841	Cd163	93671	4	0	3	-3
842	Cpeb2	231207	4	0	3	-3
843	Dpp4	13482	4	0	3	-3
844	Hnf1a	21405	4	0	3	-3
845	Itgb8	320910	4	0	3	-3
846	Jak2	16452	4	0	3	-3
847	Nos2	18126	4	0	3	-3
848	Pcm1	18536	4	0	3	-3
849	Pde9a	18585	4	0	3	-3
850	Pnmt	18948	4	0	3	-3
851	Rapsn	19400	4	0	3	-3
852	Sdc2	15529	4	0	3	-3
853	Top1mt	72960	4	0	3	-3
854	Wdr26	226757	4	0	3	-3
855	Xpc	22591	4	0	3	-3
856	Agxt	11611	3	0	3	-3
857	Alas1	11655	3	0	3	-3
858	Aldh3a2	11671	3	0	3	-3
859	Apaf1	11783	3	0	3	-3
860	BC051070	229688	3	0	3	-3
861	Bcl2a1b	12045	3	0	3	-3
862	Capn2	12334	3	0	3	-3
863	Cd80	12519	3	0	3	-3
864	Crip1	12925	3	0	3	-3
865	Dnmt3l	54427	3	0	3	-3
866	Ebf1	13591	3	0	3	-3
867	Ebi3	50498	3	0	3	-3
868	Epha2	13836	3	0	3	-3
869	Evi2b	216984	3	0	3	-3
870	Fdx1	14148	3	0	3	-3
871	Fgl2	14190	3	0	3	-3
872	Gas7	14457	3	0	3	-3
873	Gca	227960	3	0	3	-3

874	Gm2a	14667	3	0	3	-3
875	Hopx	74318	3	0	3	-3
876	Hspg2	15530	3	0	3	-3
877	Pilrb2	381678	3	0	3	-3
878	Sh3bp5	24056	3	0	3	-3
879	Tmem176b	65963	3	0	3	-3
880	Tnf	21926	3	0	3	-3
881	Trio	223435	3	0	3	-3
882	Tshr	22095	3	0	3	-3
883	Vcam1	22329	3	0	3	-3
884	Calcr	12311	6	3	6	-3
885	Ikbkb	16150	6	3	6	-3
886	Mefv	54483	6	3	6	-3
887	Mmp12	17381	6	3	6	-3
888	Mmp25	240047	6	3	6	-3
889	Nrp1	18186	6	3	6	-3
890	Sult2b1	54200	6	3	6	-3
891	2310039D24R ik	75704	2	0	3	-3
892	4930418G15R ik	69312	2	0	3	-3
893	Adprh	11544	2	0	3	-3
894	Cadm1	54725	2	0	3	-3
895	Cd28	12487	2	0	3	-3
896	Cd300lf	246746	2	0	3	-3
897	Cd37	12493	2	0	3	-3
898	Cd93	17064	2	0	3	-3
899	Cdk5r1	12569	2	0	3	-3
900	Cspg4	121021	2	0	3	-3
901	Ctsh	13036	2	0	3	-3
902	Dgat1	13350	2	0	3	-3
903	Dhrs9	241452	2	0	3	-3
904	Dmc1	13404	2	0	3	-3
905	Dusp7	235584	2	0	3	-3
906	Ednrb	13618	2	0	3	-3
907	Ets2	23872	2	0	3	-3
908	Fcgr4	246256	2	0	3	-3
909	Gda	14544	2	0	3	-3
910	Gpsm3	106512	2	0	3	-3
911	Gsta3	14859	2	0	3	-3
912	Id2	15902	2	0	3	-3
913	Il1rn	16181	2	0	3	-3
914	Il7r	16197	2	0	3	-3



915	Lgals3	16854	2	0	3	-3
916	Lilrb3	18733	2	0	3	-3
917	Lin7a	108030	2	0	3	-3
918	Mmp19	58223	2	0	3	-3
919	Ms4a4b	60361	2	0	3	-3
920	Ms4a4d	66607	2	0	3	-3
921	Naip4	17940	2	0	3	-3
922	Nedd9	18003	2	0	3	-3
923	Olfml2b	320078	2	0	3	-3
924	Orm1	18405	2	0	3	-3
925	Plod1	18822	2	0	3	-3
926	Ppm1m	67905	2	0	3	-3
927	Pvr	52118	2	0	3	-3
928	Scn10a	20264	2	0	3	-3
929	Skap2	54353	2	0	3	-3
930	Slfn4	20558	2	0	3	-3
931	Tmem43	74122	2	0	3	-3
932	Vnn1	22361	2	0	3	-3
933	Bace1	23821	5	3	6	-3
934	Cdk4	12567	5	3	6	-3
935	Col4a1	12826	5	3	6	-3
936	Hdac8	70315	5	3	6	-3
937	Hoxa3	15400	5	3	6	-3
938	Hpd	15445	5	3	6	-3
939	Mogat2	233549	5	3	6	-3
940	Sfrs15	224432	5	3	6	-3
941	Tyms	22171	5	3	6	-3
942	Avpr2	12000	4	3	6	-3
943	Fxyd2	11936	4	3	6	-3
944	Myo6	17920	4	3	6	-3
945	Ptpr	19279	4	3	6	-3
946	Rarg	19411	4	3	6	-3
947	Tex14	83560	4	3	6	-3
948	Abcc1	17250	6	6	9	-3
949	Rac1	19353	6	6	9	-3
950	Xdh	22436	6	10	13	-3
951	2310005N03 Rik	66359	3	3	6	-3
952	Alad	17025	3	3	6	-3
953	Hmox1	15368	3	3	6	-3
954	Ptpn22	19260	3	3	6	-3
955	1700012H17R ik	242297	1	0	3	-3

956	1700055N04 Rik	73458	1	0	3	-3
957	Adcy9	11515	1	0	3	-3
958	AHNAK	66395	1	0	3	-3
959	Apoc2	11813	1	0	3	-3
960	Arhgap9	216445	1	0	3	-3
961	Bpi	329547	1	0	3	-3
962	Camk1	52163	1	0	3	-3
963	Camp	12796	1	0	3	-3
964	Cd52	23833	1	0	3	-3
965	Cdk2ap2	52004	1	0	3	-3
966	Cdkn1c	12577	1	0	3	-3
967	Col1a1	12842	1	0	3	-3
968	Cotl1	72042	1	0	3	-3
969	Ctsz	64138	1	0	3	-3
970	Cxcr6	80901	1	0	3	-3
971	Dcxr	67880	1	0	3	-3
972	Dok2	13449	1	0	3	-3
973	EG631922	631922	1	0	3	-3
974	Fcer1g	14127	1	0	3	-3
975	Fmo5	14263	1	0	3	-3
976	G0s2	14373	1	0	3	-3
977	Htr1d	15552	1	0	3	-3
978	Il18rap	16174	1	0	3	-3
979	Inmt	21743	1	0	3	-3
980	Kcnj9	16524	1	0	3	-3
981	Krt80	74127	1	0	3	-3
982	Lgals2	107753	1	0	3	-3
983	LOC382044	382044	1	0	3	-3
984	Lrrc33	224109	1	0	3	-3
985	Ltb4r1	16995	1	0	3	-3
986	Man2b1	17159	1	0	3	-3
987	Mettl7b	71664	1	0	3	-3
988	Ms4a4c	64380	1	0	3	-3
989	Ncf2	17970	1	0	3	-3
990	Nod2	257632	1	0	3	-3
991	Orm3	18407	1	0	3	-3
992	Parp3	235587	1	0	3	-3
993	Pgd	110208	1	0	3	-3
994	Polm	54125	1	0	3	-3
995	Ralb	64143	1	0	3	-3
996	S100a10	20194	1	0	3	-3
997	Satb2	212712	1	0	3	-3

998	Sh2d3c	27387	1	0	3	-3
999	Tcfef	21425	1	0	3	-3
1000	Tcn2	21452	1	0	3	-3
1001	Tmem176a	66058	1	0	3	-3
1002	Tnip1	57783	1	0	3	-3
1003	Tom1	21968	1	0	3	-3
1004	Tpp1	12751	1	0	3	-3
1005	Ddx39	68278	5	6	9	-3
1006	Cacna1c	12288	5	13	16	-3
1007	Fpr1	14293	2	3	6	-3
1008	Nudt4	71207	2	3	6	-3
1009	Pkm2	18746	2	3	6	-3
1010	Pltp	18830	2	3	6	-3
1011	Sept5	18951	2	3	6	-3
1012	Abat	268860	6	16	19	-3
1013	Atp2a3	53313	3	6	9	-3
1014	Slc5a11	233836	3	6	9	-3
1015	Slc6a13	14412	3	13	16	-3
1016	S100a9	20202	2	10	13	-3
1017	Ddr1	12305	6	0	6	-6
1018	Ephx2	13850	6	0	6	-6
1019	Hsd17b10	15108	6	0	6	-6
1020	Map2k1	26395	6	0	6	-6
1021	Serpina6	12401	6	0	6	-6
1022	Vdac3	22335	6	0	6	-6
1023	Arg1	11846	5	0	6	-6
1024	Crabp1	12903	5	0	6	-6
1025	Egfr	13649	5	0	6	-6
1026	Mgmt	17314	5	0	6	-6
1027	Pklr	18770	5	0	6	-6
1028	Ptrn3	19152	5	0	6	-6
1029	Runx2	12393	5	0	6	-6
1030	Sstr1	20605	5	0	6	-6
1031	Accs	329470	4	0	6	-6
1032	Apex1	11792	4	0	6	-6
1033	Edn3	13616	4	0	6	-6
1034	Igfbp7	29817	4	0	6	-6
1035	Nin	18080	4	0	6	-6
1036	Nr1i2	18171	4	0	6	-6
1037	Cysltr2	70086	6	3	9	-6
1038	G6pdx	14381	6	3	9	-6
1039	8430410A17R ik	232210	3	0	6	-6

1040	B4galt6	56386	3	0	6	-6
1041	C3	12266	3	0	6	-6
1042	Cd180	17079	3	0	6	-6
1043	Dbnidd2	52840	3	0	6	-6
1044	Ela2	50701	3	0	6	-6
1045	Isl2	104360	3	0	6	-6
1046	Mst1	15235	3	0	6	-6
1047	Mylk	107589	3	0	6	-6
1048	Naga	17939	3	0	6	-6
1049	Oas1a	246730	3	0	6	-6
1050	Rab31	106572	3	0	6	-6
1051	Acpp	56318	5	3	9	-6
1052	Folh1	53320	5	3	9	-6
1053	Oat	18242	5	3	9	-6
1054	Pfkfb1	18639	5	3	9	-6
1055	Aip	11632	2	0	6	-6
1056	Atp6v1b2	11966	2	0	6	-6
1057	Atp6v1e1	11973	2	0	6	-6
1058	Capg	12332	2	0	6	-6
1059	Csrp2	13008	2	0	6	-6
1060	Daglb	231871	2	0	6	-6
1061	Dapk2	13143	2	0	6	-6
1062	Fes	14159	2	0	6	-6
1063	Mknk1	17346	2	0	6	-6
1064	Pde8a	18584	2	0	6	-6
1065	Pxn	19303	2	0	6	-6
1066	Slc31a2	20530	2	0	6	-6
1067	Slc36a1	215335	2	0	6	-6
1068	Slfn3	20557	2	0	6	-6
1069	Akt1	11651	5	10	16	-6
1070	Grb2	14784	6	13	19	-6
1071	Prep	19072	5	13	19	-6
1072	Gatm	67092	6	3	10	-7
1073	Il12b	16160	6	3	10	-7
1074	Sat1	20229	4	3	10	-7
1075	Clk1	12747	6	6	13	-7
1076	Ceacam1	26365	3	3	10	-7
1077	Evi2a	14017	3	3	10	-7
1078	Ms4a6c	73656	3	3	10	-7
1079	Hagh	14651	5	6	13	-7
1080	Lta4h	16993	4	6	13	-7
1081	AU018778	234564	2	3	10	-7
1082	BC025575	217219	2	3	10	-7

1083	Camk2b	12323	2	3	10	-7
1084	Ccl5	20304	2	3	10	-7
1085	Pilra	231805	2	3	10	-7
1086	Ptafr	19204	2	3	10	-7
1087	Ptplad2	66775	2	3	10	-7
1088	Atp6v0d1	11972	3	16	23	-7
1089	Cpd	12874	2	13	20	-7
1090	Myo1f	17916	1	3	10	-7
1091	Pdpk1	18607	6	0	9	-9
1092	Cdc2a	12534	5	0	9	-9
1093	Pparg	19016	5	0	9	-9
1094	Tspo	12257	5	0	9	-9
1095	Lgals1	16852	4	0	9	-9
1096	Ntrk1	18211	4	0	9	-9
1097	Prdx2	21672	6	3	12	-9
1098	Met	17295	5	10	19	-9
1099	Ms4a1	12482	5	0	10	-10
1100	C78409	216441	3	0	10	-10
1101	Dnahc8	13417	3	0	10	-10
1102	Eif4e	13684	3	0	10	-10
1103	Pld3	18807	3	0	10	-10
1104	Fhit	14198	6	3	13	-10
1105	Pde3b	18576	5	3	13	-10
1106	Chi3l3	12655	2	0	10	-10
1107	Ldlr	16835	4	3	13	-10
1108	Tnfsf10	22035	4	3	13	-10
1109	Pde3a	54611	6	6	16	-10
1110	Hsd11b2	15484	1	0	10	-10
1111	LOC100041146	100041146	1	0	10	-10
1112	Mgam	232714	1	0	10	-10
1113	Pilrb1	170741	1	0	10	-10
1114	Rab27a	11891	1	0	10	-10
1115	Riok3	66878	1	0	10	-10
1116	Pcbd1	13180	5	0	12	-12
1117	Dtymk	21915	4	0	12	-12
1118	Qpct	70536	6	0	13	-13
1119	Mmp16	17389	5	0	13	-13
1120	Sumf2	67902	4	0	13	-13
1121	Wee1	22390	6	3	16	-13
1122	Neu1	18010	3	0	13	-13
1123	Padi4	18602	3	0	13	-13
1124	Pgf	18654	3	0	13	-13

1125	Sqrdl	59010	3	0	13	-13
1126	Ctnna1	12385	5	3	16	-13
1127	Psmb5	19173	4	3	16	-13
1128	Il27	246779	2	0	13	-13
1129	Dnajc10	66861	3	3	16	-13
1130	Pdgfrb	18596	5	0	16	-16
1131	Tnk2	51789	6	3	20	-17
1132	Gpi1	14751	4	0	19	-19
1133	Frap1	56717	5	3	33	-30

## 5.2 Control shRNAs used in the multiplexed RNAi screen

shRNA	control type	97mer sequence
Bcl2.1067	Neutral ctrl	TGCTGTTGACAGTGAGCGCACACACCTGATTTTAACTTCTAGTGAA-GCCACAGATGTAGGAAGTTAAAATCAGGTGTGTTGCCTACTGCCTCGGA
Bcl2.1243	Neutral ctrl	TGCTGTTGACAGTGAGCGCCAAGTGTTCGGTGTAACATAAATAGTGAA-GCCACAGATGTATTAGTTACACCGAACACTTGATGCCTACTGCCTCGGA
Bcl2.1535	Neutral ctrl	TGCTGTTGACAGTGAGCGCTGCCCCACCCCTGGCATCTTTAGTGAA-GCCACAGATGTAAAGATGCCAGGGGTGGGGCAGTGCCCTACTGCCTCGGA
Bcl2.5768	Neutral ctrl	TGCTGTTGACAGTGAGCGCCAGGAAAAGGTTGAAATATAATAGTGAA-GCCACAGATGTATTATATTTCAACCTTTTCTGTTGCCTACTGCCTCGGA
BRAF.3750	Neutral ctrl	TGCTGTTGACAGTGAGCGCTAGCATAATGACAATTATTTATAGTGAA-GCCACAGATGTATAAATAATTGTCATTATGCTAATGCCTACTGCCTCGGA
BRAF.3826	Neutral ctrl	TGCTGTTGACAGTGAGCGCCCCATTGTTTCTTCCAACTATAGTGAA-GCCACAGATGTATAAGTTGGAAGAAACAATGGGATGCCTACTGCCTCGGA
BRAF.5053	Neutral ctrl	TGCTGTTGACAGTGAGCGCTAGGGTGATGTCTCACTTGAATAGTGAA-GCCACAGATGTATTCAAGTGAGACATCACCTATTGCCTACTGCCTCGGA
Kit.1241	Neutral ctrl	TGCTGTTGACAGTGAGCGCTTCCGTGACATTCAACGTTTATAGTGAA-GCCACAGATGTATAAACGTTGAATGTCACGGAAGTGCCCTACTGCCTCGGA
Kit.2021	Neutral ctrl	TGCTGTTGACAGTGAGCGCCACCCTGGTCATTACAGAATATAGTGAA-GCCACAGATGTATATTCTGTAATGACCAGGGTGGTGCCTACTGCCTCGGA
Kit.221	Neutral ctrl	TGCTGTTGACAGTGAGCGCCAGATGGACTTTCAAGACCTATAGTGAA-GCCACAGATGTATAGGTCTTGAAAGTCCATCTGATGCCTACTGCCTCGGA
Kit.4813	Neutral ctrl	TGCTGTTGACAGTGAGCGCTTGGATATTCTTGAAAGTTTATAGTGAA-GCCACAGATGTATAAACTTTCAAGAATATCCAAGTGCCCTACTGCCTCGGA
Lin28.2180	Neutral ctrl	TGCTGTTGACAGTGAGCGCAGCGTGATGGTTGATAGCTAATAGTGAA-GCCACAGATGTATTAGCTATCAACCATCACGCTATGCCTACTGCCTCGGA
Lin28.2186	Neutral ctrl	TGCTGTTGACAGTGAGCGCATGGTTGATAGCTAAAGGAAATAGTGAA-GCCACAGATGTATTTCCTTTAGCTATCAACCATCTGCCTACTGCCTCGGA
Lin28.2270	Neutral ctrl	TGCTGTTGACAGTGAGCGCAACGGGACAAATGCAATAGAATAGTGAA-GCCACAGATGTATTCTATTGCATTGTCCCGTTTTGCCTACTGCCTCGGA
Lin28.2430	Neutral ctrl	TGCTGTTGACAGTGAGCGCTGGCCTAGTTGTGTAAATATATAGTGAA-GCCACAGATGTATATATTTACACAACCTAGGCCACTGCCTACTGCCTCGGA
Luciferase.1309	Neutral ctrl	TGCTGTTGACAGTGAGCGCCCGCCTGAAGTCTCTGATTAATAGTGAA-GCCACAGATGTATTAATCAGAGACTTCAGGCGGTTGCCTACTGCCTCGGA
Renilla.713	Neutral ctrl	TGCTGTTGACAGTGAGCGCAGGAATTATAATGCTTATCTATAGTGAA-GCCACAGATGTATAGATAAGCATTATAATTCCTATGCCTACTGCCTCGGA
Pcna.1186	essential ctrl	TGCTGTTGACAGTGAGCGCATCAATGATCTTGACGCTAAATAGTGAA-GCCACAGATGTATTTAGCGTCAAGATCATTGATGTGCCTACTGCCTCGGA
Rpa1.1620	essential ctrl	TGCTGTTGACAGTGAGCGCCCGCATGATCTTATCGGCAAATAGTGAA-GCCACAGATGTATTTGCCGATAAGATCATGCGGTTGCCTACTGCCTCGGA

Rpa3.455	essential ctrl	TGCTGTTGACAGTGAGCGCGGACTCCTATAATTTCTAATTAGTGAA- GCCACAGATGTAATTAGAAATTATAGGAGTCGCTTGCCCTACTGCCTCGGA
Rpa3.561	essential ctrl	TGCTGTTGACAGTGAGCGCAAAAGTGATACTTCAATATATTAGTGAA- GCCACAGATGTAATATATTGAAGTATCACTTTTATGCCTACTGCCTCGGA
Myc.1888	essential ctrl	TGCTGTTGACAGTGAGCGCGAAACGACGAGAACAGTTGAATAGTGAA- GCCACAGATGTATTCAACTGTTCTCGTCGTTTCCTGCCTACTGCCTCGGA
Myc.1891	essential ctrl	TGCTGTTGACAGTGAGCGCACGACGAGAACAGTTGAAACATAGTGAA- GCCACAGATGTATGTTCAACTGTTCTCGTCGTTTGCCCTACTGCCTCGGA
Myc.2105	essential ctrl	TGCTGTTGACAGTGAGCGCCTGCCTCAAACCTTAAATAGTATAGTGAA- GCCACAGATGTATACTATTTAAGTTTGAGGCAGTTGCCTACTGCCTCGGA
Mcl1.1334	addiction ctrl	TGCTGTTGACAGTGAGCGCAAGAGTCACTGTCTGAATGAATAGTGAA- GCCACAGATGTATTCAATTCAGACAGTGACTCTTCTGCCTACTGCCTCGGA
Mcl1.2018	addiction ctrl	TGCTGTTGACAGTGAGCGCGGACTGGTTATAGATTATATAATAGTGAA- GCCACAGATGTATTATAAATCTATAACCAGTCCATGCCTACTGCCTCGGA
Men1.2310	addiction ctrl	TGCTGTTGACAGTGAGCGCCACCCTCATCCTCTAATTCAATAGTGAA- GCCACAGATGTATTGAATTAGAGGATGAGGGTGATGCCTACTGCCTCGGA
Myb.2572	addiction ctrl	TGCTGTTGACAGTGAGCGCTCCATGTATCTCAGTCACTAATAGTGAA- GCCACAGATGTATTAGTGACTGAGATACATGGAATGCCTACTGCCTCGGA
Myb.2652	addiction ctrl	TGCTGTTGACAGTGAGCGCCCCAAGTAATACTTAATGCAATAGTGAA- GCCACAGATGTATTGCATTAAGTATTACTTGGGATGCCTACTGCCTCGGA
Brd4.1448	addiction ctrl	TGCTGTTGACAGTGAGCGCCACAATCAAGTCTAAACTAGATAGTGAA- GCCACAGATGTATCTAGTTTACTTGGATTGTGCTGCCTACTGCCTCGGA
Brd4.2097	addiction ctrl	TGCTGTTGACAGTGAGCGCCTAAGTCTAGATATCAACAAATAGTGAA- GCCACAGATGTATTGTTGATATCTAGACTTAGCTGCCTACTGCCTCGGA
Brd4.552	addiction ctrl	TGCTGTTGACAGTGAGCGCCCATGGATATGGGAACAATATAGTGAA- GCCACAGATGTATTGTTCCCATATCCATGGGTTGCCTACTGCCTCGGA

### 5.3 shRNAs used for validation experiments

shRNA	species	97mer
Aak1.7991	mouse	TGCTGTTGACAGTGAGCGCCTCCTCTAATTTAGTCTTTAATAGTGAA GCCACAGATGTATTAAAGACTAAATTAGAGGAGATGCCTACTGCCTCGGA
Atm.5616	mouse	TGCTGTTGACAGTGAGCGCAACAGTGAAATTCCTCAGTTATAGTGAA GCCACAGATGTATAACTGGAGAATTTCACTGTTTTGCCTACTGCCTCGGA
Bcl2.2169	mouse	TGCTGTTGACAGTGAGCGCCAGTAGAAATTATATGCATTATAGTGAA GCCACAGATGTATAATGCATATAATTTCTACTGCTGCCTACTGCCTCGGA
Brd2.1739	mouse	TGCTGTTGACAGTGAGCGCCCCACCGATGATATTGTCTCTATAGTGAA GCCACAGATGTATAGGACAATATCATCGGTGGGCTGCCTACTGCCTCGGA
Brd4.1448	mouse	TGCTGTTGACAGTGAGCGACACAATCAAGTCTAAACTAGATAGTGAA GCCACAGATGTATCTAGTTTACTTGGATTGTGCTGCCTACTGCCTCGGA
BRD4.1817	human	TGCTGTTGACAGTGAGCGACAGCAGAACAAACAAAGAAATAGTGAA GCCACAGATGTATTTCTTTGGTTGTTCTGCTGGTGCCTACTGCCTCGGA
Brd4.2097	mouse	TGCTGTTGACAGTGAGCGACTAAGTCTAGATATCAACAAATAGTGAA GCCACAGATGTATTTGTTGATATCTAGACTTAGCTGCCTACTGCCTCGGA
Brd4.523	mouse	TGCTGTTGACAGTGAGCGATCCCTGATTACTATAAGATTATAGTGAA GCCACAGATGTATAATCTTATAGTAATCAGGGAGTGCCTACTGCCTCGGA
Brd4.552	mouse	TGCTGTTGACAGTGAGCGCCCATGGATATGGGAACAATATAGTGAA GCCACAGATGTATATTGTTCCCATATCCATGGGTTGCCTACTGCCTCGGA
BRD4.602	mouse	TGCTGTTGACAGTGAGCGACAGGACTTCAACACTATGTTTTAGTGAA GCCACAGATGTAAAACATAGTGTGAAGTCCTGGTGCCTACTGCCTCGGA
BRD4.602	mouse	TGCTGTTGACAGTGAGCGACAGGACTTCAACACTATGTTTTAGTGAA GCCACAGATGTAAAACATAGTGTGAAGTCCTGGTGCCTACTGCCTCGGA
Brd4.632	mouse	TGCTGTTGACAGTGAGCGCCACTATGTTTACAAATGTTTATAGTGAA GCCACAGATGTATAACAATTTGTAAACATAGTGTGCCTACTGCCTCGGA
Casr.1746	mouse	TGCTGTTGACAGTGAGCGCTACATGGACTACGAACATTTATAGTGAA GCCACAGATGTATAAATGTTCTAGTCCATGTAATGCCTACTGCCTCGGA
Casr.4128	mouse	TGCTGTTGACAGTGAGCGCCACCATTAAAGTTGAGTCTAATAGTGAA GCCACAGATGTATTAGACTCAACTTTAATGGTGGTGCCTACTGCCTCGGA
Cda.503	mouse	TGCTGTTGACAGTGAGCGCACGGCTCTTGGAAGACTTCATTAGTGAA GCCACAGATGTAATGAAGTCTTCCAAGAGCCGTTTGCCCTACTGCCTCGGA

Cdk9.3347	mouse	TGCTGTTGACAGTGAGCGCCAGCTACAGTGACTTACTATTAGTGAA GCCACAGATGTAATAGTAAGTACACTGTAGCTGTTGCCTACTGCCTCGGA
Cnr1.818	mouse	TGCTGTTGACAGTGAGCGCAACCAACATTACAGAGTTCTATAGTGAA GCCACAGATGTATAGAACTCTGTAATGTTGGTTGTGCCTACTGCCTCGGA
Csda.1105	mouse	TGCTGTTGACAGTGAGCGCCAGGGTGACCTAAAGAATTAATAGTGAA GCCACAGATGTATTAATTCTTTAGGTCACCTGCTGCCTACTGCCTCGGA
Csda.494	mouse	TGCTGTTGACAGTGAGCGCAACCGAAATGACACCAAAGAATAGTGAA GCCACAGATGTATTCTTTGGTGTCAATTCGGTTTGCCTACTGCCTCGGA
Dhfr.565	mouse	TGCTGTTGACAGTGAGCGCACGAGTTCAAGTACTTCCAAATAGTGAA GCCACAGATGTATTTGGAAGTACTTGAACCTCGTTTGCCTACTGCCTCGGA
Dnmt1.1137	mouse	TGCTGTTGACAGTGAGCGCCCCGAAGATCAACTACCAAATAGTGAA GCCACAGATGTATTTGGTGAGTTGATCTTCGGGATGCCTACTGCCTCGGA
Dyrk1c.3295	mouse	TGCTGTTGACAGTGAGCGCCACAGAGAATGGGTAATTC AATAGTGAA GCCACAGATGTATTGAATTACCCATTCTCTGTGTTGCCTACTGCCTCGGA
Echs1.414	mouse	TGCTGTTGACAGTGAGCGCACCGGTCATCGCAGCTGTCAATAGTGAA GCCACAGATGTATTGACAGCTGCGATGACCGGTTTGCCTACTGCCTCGGA
Echs1.898	mouse	TGCTGTTGACAGTGAGCGCCACTGAGAAGTGGCAGCTATATAGTGAA GCCACAGATGTATATAGCTGCCAGTTCTCAGTGGTGCCTACTGCCTCGGA
Ehmt2.3328	mouse	TGCTGTTGACAGTGAGCGATGGGACATCAAGAGCAAGTATTAGTGAA GCCACAGATGTAATACTTGCTCTTGATGTCCAGTGCCTACTGCCTCGGA
Eif4e.370	mouse	TGCTGTTGACAGTGAGCGCTCCAGTTGTCTAGTAATTTAATAGTGAA GCCACAGATGTATTAAATTACTAGACAAC TGGATTGCCTACTGCCTCGGA
Enpp1.3057	mouse	TGCTGTTGACAGTGAGCGCAAGAATTAGATGTGTCATAATAGTGAA GCCACAGATGTATTAGTGACACATCTAATTCCTATGCCTACTGCCTCGGA
Epi300.3850	mouse	TGCTGTTGACAGTGAGCGCCTGAAGTATTTGACAAGAAATAGTGAA GCCACAGATGTATTTCTTGTTCAAATACTTCAGATGCCTACTGCCTCGGA
Fasn.4351	mouse	TGCTGTTGACAGTGAGCGCCTGAAGGATGTT CAGACCAAATAGTGAA GCCACAGATGTATTTGGTCTGAACATCCTTCAGGTGCCTACTGCCTCGGA
Fasn.4914	mouse	TGCTGTTGACAGTGAGCGCTCGGTGTATCCTGCTGTCCAATAGTGAA GCCACAGATGTATTGGACAGCAGGATACACCGAATGCCTACTGCCTCGGA
Gart.1762	mouse	TGCTGTTGACAGTGAGCGCCTCGACCTCAGTACAAC TGAATAGTGAA GCCACAGATGTATTACGTTGTACTGAGGTCGAGCTGCCTACTGCCTCGGA
Gart.2470	mouse	TGCTGTTGACAGTGAGCGCAAGAATCTGATTGAAACCATATAGTGAA GCCACAGATGTATATGGTTTCAATCAGATTCTTATGCCTACTGCCTCGGA
Gart.2713	mouse	TGCTGTTGACAGTGAGCGCACCAGGGTAATTAATCACA AATAGTGAA GCCACAGATGTATTTGTGATTAATTACCCTGGTGTGCCTACTGCCTCGGA
Gart.2959	mouse	TGCTGTTGACAGTGAGCGCACCGTACACTTTGTGCTGAATAGTGAA GCCACAGATGTATTACGCGACAAAGTGTACGGTATGCCTACTGCCTCGGA
GART.730	human	TGCTGTTGACAGTGAGCGACCTCAGGTTTCTAATGATCTATAGTGAA GCCACAGATGTATAGATCATTAGAAACCTGAGGGTGCCTACTGCCTCGGA
GART.733	human	TGCTGTTGACAGTGAGCGCCAGGTTTCTAATGATCTATTATAGTGAA GCCACAGATGTATAATAGATCATTAGAAACCTGATGCCTACTGCCTCGGA
GART.861	human	TGCTGTTGACAGTGAGCGACCCAAAAGTTCTAGAGTTTAATAGTGAA GCCACAGATGTATTAAACTCTAGAACTTTTGGGCTGCCTACTGCCTCGGA
Gart.861	mouse	TGCTGTTGACAGTGAGCGCTTCTAAGGACTTGTTAGTAAATAGTGAA GCCACAGATGTATTTACTAACAAGTCCTTAGAAATGCCTACTGCCTCGGA
Gart.984	mouse	TGCTGTTGACAGTGAGCGACCCAAAAGTGTGGAGTTTAATAGTGAA GCCACAGATGTATTAAACTCCAACACTTTTGGGCTGCCTACTGCCTCGGA
Gls.1425	mouse	TGCTGTTGACAGTGAGCGCTTGCAATAGGATATTACTTAATAGTGAA GCCACAGATGTATTAAAGTAATATCCTATTGCAAATGCCTACTGCCTCGGA
Jak1.3217	mouse	TGCTGTTGACAGTGAGCGATGCCAAAGAATAAGAACAAAATAGTGAA GCCACAGATGTATTTTGTCTTATTCTTTGGCAGTGCCTACTGCCTCGGA
Kdm1a.1869	mouse	TGCTGTTGACAGTGAGCGCAGGCTTGGACATTAAACTGAATAGTGAA GCCACAGATGTATTCAGTTTAATGTCCAAGCCTTTGCCTACTGCCTCGGA
Kdr.2895	mouse	TGCTGTTGACAGTGAGCGCAGCCTCATGTCTGAACTCAATAGTGAA GCCACAGATGTATTGAGTTCAGACATGAGGGCTCTGCCTACTGCCTCGGA
Mcm6.2733	mouse	TGCTGTTGACAGTGAGCGCTAGGCTTCTTGTAATAGTGAA GCCACAGATGTATTCAATAGTACAAGAAGCCTATTGCCTACTGCCTCGGA
Mcm6.663	mouse	TGCTGTTGACAGTGAGCGCTTCCTTCTAGACACTAATAAATAGTGAA GCCACAGATGTATTTATTAGTGTCTAGAAGGAACTGCCTACTGCCTCGGA
ME2.1658	mouse/ human	TGCTGTTGACAGTGAGCGCCAGGAAGTTTCTGCTAACATATAGTGAA GCCACAGATGTATATGTTAGCAGAAACTTCCTGATGCCTACTGCCTCGGA



Mef2c.1872	mouse	TGCTGTTGACAGTGAGCGCTGCCTCAGTGATACAGTATAATAGTGAA GCCACAGATGTATTATACTGTATCACTGAGGCAATGCCTACTGCCTCGGA
Mef2c.2030	mouse	TGCTGTTGACAGTGAGCGCTTGACAGTTCAACGTTATTTATAGTGAA GCCACAGATGTATAAATAACGTTGAACCTGCAACTGCCTACTGCCTCGGA
Metap2.2259	mouse	TGCTGTTGACAGTGAGCGCAAGGAGTTTGATCAAAGGCAATAGTGAA GCCACAGATGTATTGCCTTTGATCAAACCTCTTTGCCTACTGCCTCGGA
Mtor.1704	mouse	TGCTGTTGACAGTGAGCGCCACAGCTGAAGAAAAGATATATAGTGAA GCCACAGATGTATATATCTTTCTTCAGCTGTGGATGCCTACTGCCTCGGA
MYB.721	human	TGCTGTTGACAGTGAGCGACTGGACGAACGTAAATGCTATAGTGAA GCCACAGATGTATAGCATTATCAGTTTCGTCCAGGTGCCTACTGCCTCGGA
Myc.1888/ MYC.1831	mouse/ human	TGCTGTTGACAGTGAGCGAGAAACGACGAGAACAGTTGAATAGTGAA GCCACAGATGTATTCAACTGTTCTCGTCGTTTCTGCCTACTGCCTCGGA
Myc.1891/ MYC.1834	mouse/ human	TGCTGTTGACAGTGAGCGCACGACGAGAACAGTTGAAACATAGTGAA GCCACAGATGTATGTTTCAACTGTTCTCGTCGTTTGCCTACTGCCTCGGA
Nfkb1.2838	mouse	TGCTGTTGACAGTGAGCGACAGGTATTTGACATACTAAATTAGTGAA GCCACAGATGTAATTTAGTATGTCAAATACCTGCTGCCTACTGCCTCGGA
PCNA.566	mouse/ human	TGCTGTTGACAGTGAGCGATCGGGTGAATTTGCACGTATATAGTGAA GCCACAGATGTATATACGTGCAAATTCACCCGACTGCCTACTGCCTCGGA
Pdk1.3048	mouse	TGCTGTTGACAGTGAGCGACAGGGTTTTTAGCTAATACTATAGTGAA GCCACAGATGTATAGTATTAGCTAAAAACCCTGGTGCCTACTGCCTCGGA
Phgdh.1785	mouse	TGCTGTTGACAGTGAGCGCCCCGCTCAACTGTGACCTATATAGTGAA GCCACAGATGTATATAGGTCACAGTTGAGCGGGTTGCCTACTGCCTCGGA
Pik3ca.5328	mouse	TGCTGTTGACAGTGAGCGCACACTTTGTGTTACTTAGATATAGTGAA GCCACAGATGTATATCTAAGTAACACAAAGTGTTCCTACTGCCTCGGA
Pik3cb.4551	mouse	TGCTGTTGACAGTGAGCGACACATGGAAATCTTTAATTTATAGTGAA GCCACAGATGTATAAATTAAGATTTCCATGTGGTGCCTACTGCCTCGGA
Pik3cd.4373	mouse	TGCTGTTGACAGTGAGCGACCAACTCTGAAATAGGAAATAGTGAA GCCACAGATGTATTTCTTATTTTCAAGTTGGTGGTGCCTACTGCCTCGGA
Pik3cg.2858	mouse	TGCTGTTGACAGTGAGCGCCACGACAACATTATGATCTATAGTGAA GCCACAGATGTATAGATCATAATGTTGTGCTGTTGCTACTGCCTCGGA
Pik3r1.392	mouse	TGCTGTTGACAGTGAGCGCCAAGTTGTCAAAGAAGATAATTAGTGAA GCCACAGATGTAATTATCTTCTTTGACAACCTGATGCCTACTGCCTCGGA
Plk1.953	mouse	TGCTGTTGACAGTGAGCGCCAGAAGATGCTTCAGACAGATAGTGAA GCCACAGATGTATCTGTCTGAAGCATCTTCTGGATGCCTACTGCCTCGGA
Pola1.1442	mouse	TGCTGTTGACAGTGAGCGCCACAGCTTCCACAGAATTTAATAGTGAA GCCACAGATGTATTAATTTCTGTGGAAGCTGTGGTGCCTACTGCCTCGGA
Pola1.3015	mouse	TGCTGTTGACAGTGAGCGCTACGAAAGACATGGTACAGAATAGTGAA GCCACAGATGTATTCTGTACCATGTCTTTCGTATTGCCTACTGCCTCGGA
Pola1.3649	mouse	TGCTGTTGACAGTGAGCGCTTGACAGAACTTGACAATTTATAGTGAA GCCACAGATGTATAAATTGTCAAGTTTCTGCAATTGCCTACTGCCTCGGA
Pola1.4680	mouse	TGCTGTTGACAGTGAGCGCAGGCGAGAAATGCTACTTTATAGTGAA GCCACAGATGTATAAAGTAGCAATTTCTGCCCTGTGCCTACTGCCTCGGA
Psma1.357	mouse	TGCTGTTGACAGTGAGCGCCAGACTGTTATGCAACTTTATAGTGAA GCCACAGATGTAATAAAGTTGCATAACAGTCTGGTGCCTACTGCCTCGGA
Psma1.745	mouse	TGCTGTTGACAGTGAGCGCTCCATTGGAATCGTTGGTAAATAGTGAA GCCACAGATGTATTTACCAACGATTCCAATGGAATGCCTACTGCCTCGGA
PSMB1.119	mouse/ human	TGCTGTTGACAGTGAGCGCACGGAGGTACTGTATTGGCAATAGTGAA GCCACAGATGTATTGCCAATACAGTACCTCCGTTTGCCTACTGCCTCGGA
PSMB1.303	mouse/ human	TGCTGTTGACAGTGAGCGCAGCAAGATTAAAGATGTACAATAGTGAA GCCACAGATGTATTGTACATCTTTAATCTTGCTTTGCCTACTGCCTCGGA
Psmb2.212	mouse	TGCTGTTGACAGTGAGCGCCAAGATGTTTAAAGATGAGTGATAGTGAA GCCACAGATGTATCACTCATCTTAACATCTTGTTCCTACTGCCTCGGA
Psmb2.802	mouse	TGCTGTTGACAGTGAGCGCTTGATAGATGGTTAATTCAAATAGTGAA GCCACAGATGTATTTGAATTAACCATCTATCAAGTGCCTACTGCCTCGGA
Psmd1.3014	mouse	TGCTGTTGACAGTGAGCGCTTCGAGTATATCGATGACTAATAGTGAA GCCACAGATGTATTAGTCATCGATATACTCGAAGTGCCTACTGCCTCGGA
Psmd1.437	mouse	TGCTGTTGACAGTGAGCGCAACGTCAATGATAACTCTGAATAGTGAA GCCACAGATGTATTCAGAGTTATCATTTGACGTTGTGCCTACTGCCTCGGA
Pten.1523	mouse	TGCTGTTGACAGTGAGCGACCAGCTAAAGGTGAAGATATATAGTGAA GCCACAGATGTATATATCTTACCTTTAGCTGGCTGCCTACTGCCTCGGA

Pten.1524	mouse	TGCTGTTGACAGTGAGCGACAGCTAAAGGTGAAGATATATTAGTGAA GCCACAGATGTAATATATCTTCACCTTTAGCTGGTGCCTACTGCCTCGGA
Raf1.1829	mouse	TGCTGTTGACAGTGAGCGCGACATGAAATCCAACAATATATAGTGAA GCCACAGATGTATATATTGTTGGATTTTCATGTCTTGCCTACTGCCTCGGA
Raf1.734	mouse	TGCTGTTGACAGTGAGCGCCAGGAACACAAAGGTAAGAAATAGTGAA GCCACAGATGTATTTCTTACCTTTGTGTTCCCTGGTGCCTACTGCCTCGGA
Rap2b.878	mouse	TGCTGTTGACAGTGAGCGCACCCATGATCCTGGTAGGCAATAGTGAA GCCACAGATGTATTGCCTACCAGGATCATGGGTATGCCTACTGCCTCGGA
Rmi1.2917	mouse	TGCTGTTGACAGTGAGCGCAAGAATAGTGATGGACTGACATAGTGAA GCCACAGATGTATGTCAGTCCATCACTATTCTTTTGCCTACTGCCTCGGA
Rpl15.483	mouse	TGCTGTTGACAGTGAGCGCGGCTATGTCATTTACAGGATTTAGTGAA GCCACAGATGTAAATCCTGTAAATGACATAGCCTTGCCTACTGCCTCGGA
Rrm1.1119	mouse	TGCTGTTGACAGTGAGCGCCTGGGACTAATGGCAATTCTATAGTGAA GCCACAGATGTATAGAATTGCCATTAGTCCCAGCTGCCTACTGCCTCGGA
Rrm1.1797	mouse	TGCTGTTGACAGTGAGCGCCAGAGGCACACTTATCAAATATAGTGAA GCCACAGATGTATATTTGATAAGTGTGCCTCTGGTGCCTACTGCCTCGGA
Rrm1.2234	mouse	TGCTGTTGACAGTGAGCGCCAGATTGTGAATCCTCACTTATAGTGAA GCCACAGATGTATAAGTGAGGATTCACAATCTGATGCCTACTGCCTCGGA
Rrm1.3076	mouse	TGCTGTTGACAGTGAGCGCAAGCAATTACTCATCAGCTAATAGTGAA GCCACAGATGTATTAGCTGATGAGTAATTGCTTGTGCCTACTGCCTCGGA
Stat3.1413	mouse	TGCTGTTGACAGTGAGCGATCAGAGGGTCTCGGAAATTTATAGTGAA GCCACAGATGTATAAATTTCCGAGACCCTCTGAGTGCCTACTGCCTCGGA
Syk.2277	mouse	TGCTGTTGACAGTGAGCGAAGCAAAGGACATAAAGAGAAATAGTGAA GCCACAGATGTATTTCTCTTTATGTCTTTGCTGTGCCTACTGCCTCGGA
Thra.1076	mouse	TGCTGTTGACAGTGAGCGCCAGCGAGTTTACCAAGATCATTAGTGAA GCCACAGATGTAATGATCTTGGTAAACTCGCTGATGCCTACTGCCTCGGA
Thra.613	mouse	TGCTGTTGACAGTGAGCGCCCGTTTATCACTACCGCTGTATAGTGAA GCCACAGATGTATACAGCGGTAGTGATAACCGGTTGCCTACTGCCTCGGA
Tnfsf12.1204	mouse	TGCTGTTGACAGTGAGCGCAATGGATATTAAAGAGAATAATAGTGAA GCCACAGATGTATTATTCTCTTTAATATCCATTTTGCCTACTGCCTCGGA
Top1.2179	mouse	TGCTGTTGACAGTGAGCGCAGCGAAGATTCTATCTTATAATAGTGAA GCCACAGATGTATTATAAGATAGAATCTTCGCTGTGCCTACTGCCTCGGA
Top1.3432	mouse	TGCTGTTGACAGTGAGCGCACCATTCTTTGTACCCTTTAATAGTGAA GCCACAGATGTATTAAAGGGTACAAAGAATGGTCTGCCTACTGCCTCGGA
Top2a.1284	mouse	TGCTGTTGACAGTGAGCGCTTGGATCAACATGTCAATTAATAGTGAA GCCACAGATGTATTAATTGACATGTTGATCCAAATGCCTACTGCCTCGGA
Top2a.4314	mouse	TGCTGTTGACAGTGAGCGCCAGCGGAAACTGAACAGTCAATAGTGAA GCCACAGATGTATTGACTGTTTCAGTTTCCGCTGGTGCCTACTGCCTCGGA
Trp53.1224	mouse	TGCTGTTGACAGTGAGCGCCCACTACAAGTACATGTGTAATAGTGAA- GCCACAGATGTATTACACATGTACTTGTAGTGGATGCCTACTGCCTCGGA
Twistnb.1855	mouse	TGCTGTTGACAGTGAGCGCAAAGCCTATAAAGTCAATCAATAGTGAA GCCACAGATGTATTGATTGACTTTATAGGCTTTGTGCCTACTGCCTCGGA
Vdac2.1446	mouse	TGCTGTTGACAGTGAGCGCAACATGACAAATTATGAATAATAGTGAA GCCACAGATGTATTATTCATAATTTGTCATGTTTTGCCTACTGCCTCGGA

## 6 References

- Adam, T. (2005). Purine de novo Synthesis – Mechanisms and Clinical Implications, *13*(4), 177–181.
- Adams, D. J., Wahl, M. L., Flowers, J. L., Sen, B., Colvin, M., Dewhirst, M. W., ... Wani, M. C. (2006). Camptothecin analogs with enhanced activity against human breast cancer cells. II. Impact of the tumor pH gradient. *Cancer Chemotherapy and Pharmacology*, *57*(2), 145–154. doi:10.1007/s00280-005-0008-5
- Advani, S. H. (2010). Targeting mTOR pathway: A new concept in cancer therapy. *Indian Journal of Medical and Paediatric Oncology : Official Journal of Indian Society of Medical & Paediatric Oncology*, *31*(4), 132–136. doi:10.4103/0971-5851.76197
- Agnihotri, G., & Liu, H. W. (2003). Enoyl-CoA hydratase: Reaction, mechanism, and inhibition. *Bioorganic and Medicinal Chemistry*. doi:10.1016/S0968-0896(02)00333-4
- Alli, P. M., Pinn, M. L., Jaffee, E. M., McFadden, J. M., & Kuhajda, F. P. (2005). Fatty acid synthase inhibitors are chemopreventive for mammary cancer in neu-N transgenic mice. *Oncogene*, *24*(1), 39–46. doi:10.1038/sj.onc.1208174
- An, S., Kumar, R., Sheets, E. D., & Benkovic, S. J. (2008). Reversible compartmentalization of de novo purine biosynthetic complexes in living cells. *Science (New York, N.Y.)*, *320*(5872), 103–106. doi:10.1126/science.1152241
- Anastasiou, D., Yu, Y., Israelsen, W. J., Jiang, J.-K., Boxer, M. B., Hong, B. S., ... Vander Heiden, M. G. (2012). Pyruvate kinase M2 activators promote tetramer formation and suppress tumorigenesis. *Nature Chemical Biology*, *8*(10), 839–847. doi:10.1038/nchembio.1060
- Ao, L., Liu, S. X., Yang, M. S., Fong, C. C., An, H., & Cao, J. (2008). Acrylamide-induced molecular mutation spectra at HPRT locus in human promyelocytic leukaemia HL-60 and NB4 cell lines. *Mutagenesis*, *23*(4), 309–315. doi:10.1093/mutage/gen016

- Armitage, P., & Doll, R. (1954). The Age Distribution of Cancer and a Multi-Stage Theory of Carcinogenesis. *British Journal of Cancer*, VIII(I), 1–12.
- Asangani, I. a, Dommeti, V. L., Wang, X., Malik, R., Cieslik, M., Yang, R., ... Chinnaiyan, A. M. (2014). Therapeutic targeting of BET bromodomain proteins in castration-resistant prostate cancer. *Nature*, 510(7504), 278–282. doi:10.1038/nature13229
- Ascierto, P. a, Kirkwood, J. M., Grob, J.-J., Simeone, E., Grimaldi, A. M., Maio, M., ... Mozzillo, N. (2012). The role of BRAF V600 mutation in melanoma. *Journal of Translational Medicine*. doi:10.1186/1479-5876-10-85
- Auyeung, V. C., Ulitsky, I., McGeary, S. E., & Bartel, D. P. (2013). Beyond secondary structure: Primary-sequence determinants license Pri-miRNA hairpins for processing. *Cell*, 152(4), 844–858. doi:10.1016/j.cell.2013.01.031
- Aza-Blanc, P., Cooper, C. L., Wagner, K., Batalov, S., Deveraux, Q. L., & Cooke, M. P. (2003). Identification of modulators of TRAIL-induced apoptosis via RNAi-based phenotypic screening. *Molecular Cell*, 12(3), 627–637. doi:10.1016/S1097-2765(03)00348-4
- Babij, C., Zhang, Y., Kurzeja, R. J., Munzli, A., Shehabeldin, A., Fernando, M., ... Dussault, I. (2011). STK33 Kinase Activity Is Nonessential in KRAS-Dependent Cancer Cells. *Cancer Research*, 71(17), 5818–5826. doi:10.1158/0008-5472.CAN-11-0778
- Baines, A. T., Xu, D., & Der, C. J. (2011). Inhibition of Ras for cancer treatment: the search continues. *Future Medicinal Chemistry*. doi:10.4155/fmc.11.121
- Barbie, D. a, Tamayo, P., Boehm, J. S., Kim, S. Y., Moody, S. E., Dunn, I. F., ... Hahn, W. C. (2009). Systematic RNA interference reveals that oncogenic KRAS-driven cancers require TBK1. *Nature*, 462(7269), 108–112. doi:10.1038/nature08460
- Barretina, J., Caponigro, G., Stransky, N., Venkatesan, K., Margolin, A. a., Kim, S., ... Garraway, L. a. (2012). The Cancer Cell Line Encyclopedia enables predictive modelling of anticancer drug sensitivity. *Nature*. doi:10.1038/nature11003
- Bartel, D. P. (2009). MicroRNAs: Target Recognition and Regulatory Functions. *Cell*, 136(2), 215–233. doi:10.1016/j.cell.2009.01.002
- Bassik, M. C., Lebbink, R. J., Churchman, L. S., Ingolia, N. T., Patena, W., LeProust, E. M., ... McManus, M. T. (2009). Rapid creation and quantitative monitoring of high coverage shRNA libraries. *Nature Methods*, 6(6), 443–445. doi:10.1038/nmeth.1330
- Beardsley, G. P., Moroson, B. A., Taylor, E. C., & Moran, R. G. (1989). A new folate antimetabolite, 5,10-dideaza-5,6,7,8-tetrahydrofolate is a potent inhibitor of de novo purine synthesis. *Journal of Biological Chemistry*, 264(1), 328–333.

- Beckers, A., Organe, S., Timmermans, L., Scheys, K., Peeters, A., Brusselmans, K., ... Swinnen, J. V. (2007). Chemical inhibition of acetyl-CoA carboxylase induces growth arrest and cytotoxicity selectively in cancer cells. *Cancer Research*, 67(17), 8180–8187. doi:10.1158/0008-5472.CAN-07-0389
- Bentley, D. R., Balasubramanian, S., Swerdlow, H. P., Smith, G. P., Milton, J., Brown, C. G., ... Smith, A. J. (2008). Accurate whole human genome sequencing using reversible terminator chemistry. *Nature*, 456(7218), 53–59. doi:10.1038/nature07517
- Berns, K., Hijmans, E. M., Mullenders, J., Brummelkamp, T. R., Velds, A., Heimerikx, M., ... Bernards, R. (2004). A large-scale RNAi screen in human cells identifies new components of the p53 pathway. *Nature*, 428(6981), 431–437. doi:10.1038/nature02371
- Bhamidipati, P. K., Kantarjian, H., Cortes, J., Cornelison, a M., & Jabbour, E. (2013). Management of imatinib-resistant patients with chronic myeloid leukemia. *Therapeutic Advances in Hematology*, 4(2), 103–117. doi:10.1177/2040620712468289
- Birsoy, K., Wang, T., Possemato, R., Yilmaz, O. H., Koch, C. E., Chen, W. W., ... Sabatini, D. M. (2013). MCT1-mediated transport of a toxic molecule is an effective strategy for targeting glycolytic tumors. *Nature Genetics*, 45(1), 104–8. doi:10.1038/ng.2471
- Black, B. L., & Olson, E. N. (1998). Transcriptional control of muscle development by myocyte enhancer factor-2 (MEF2) proteins. *Annual Review of Cell and Developmental Biology*, 14, 167–196. doi:10.1146/annurev.cellbio.14.1.167
- Bodnar, A. G., Ouellette, M., Frolkis, M., Holt, S. E., Chiu, C. P., Morin, G. B., ... Wright, W. E. (1998). Extension of life-span by introduction of telomerase into normal human cells. *Science (New York, N.Y.)*, 279(5349), 349–352. doi:10.1126/science.279.5349.349
- Boi, M., Gaudio, E., Bonetti, P., Kwee, I., Bernasconi, E., Tarantelli, C., ... Bertonni, F. (2015). The BET Bromodomain inhibitor OTX015 affects pathogenetic pathways in pre-clinical B-cell tumor models and synergizes with targeted drugs. *Clinical Cancer Research : An Official Journal of the American Association for Cancer Research*, 21(3), 1628–1639. doi:10.1158/1078-0432.CCR-14-1561
- Bozic, I., Antal, T., Ohtsuki, H., Carter, H., Kim, D., Chen, S., ... Nowak, M. a. (2010). Accumulation of driver and passenger mutations during tumor progression. *Proceedings of the National Academy of Sciences of the United States of America*, 107(43), 18545–18550. doi:10.1073/pnas.1010978107
- Brass, A. L., Dykxhoorn, D. M., Benita, Y., Yan, N., Engelman, A., Xavier, R. J., ... Elledge, S. J. (2008). Identification of host proteins required for HIV infection through a functional

- genomic screen. *Science (New York, N.Y.)*, 319(5865), 921–926. doi:10.1542/peds.2008-2139IIII
- Bray, F., Ren, J. S., Masuyer, E., & Ferlay, J. (2013a). Global estimates of cancer prevalence for 27 sites in the adult population in 2008. *International Journal of Cancer*, 132(5), 1133–1145. doi:10.1002/ijc.27711
- Bray, F., Ren, J. S., Masuyer, E., & Ferlay, J. (2013b). Global estimates of cancer prevalence for 27 sites in the adult population in 2008. *International Journal of Cancer*, 132(5), 1133–1145. doi:10.1002/ijc.27711
- Brennan, S. C., Thiem, U., Roth, S., Aggarwal, A., Fetahu, I. S., Tennakoon, S., ... Kallay, E. (2013). Calcium sensing receptor signalling in physiology and cancer. *Biochimica et Biophysica Acta - Molecular Cell Research*, 1833(7), 1732–1744. doi:10.1016/j.bbamcr.2012.12.011
- Brennecke, J., Aravin, A. A., Stark, A., Dus, M., Kellis, M., Sachidanandam, R., & Hannon, G. J. (2007). Discrete Small RNA-Generating Loci as Master Regulators of Transposon Activity in *Drosophila*. *Cell*, 128(6), 1089–1103. doi:10.1016/j.cell.2007.01.043
- Brummelkamp, T. R., Bernards, R., & Agami, R. (2002). A system for stable expression of short interfering RNAs in mammalian cells. *Science (New York, N.Y.)*, 296(5567), 550–553. doi:10.1126/science.1068999
- Brummelkamp, T. R., Berns, K., Hijmans, E. M., Mullenders, J., Fabius, A., Heimerikx, M., ... Beijersbergen, R. L. (2004). Functional identification of cancer-relevant genes through large-scale RNA interference screens in mammalian cells. In *Cold Spring Harbor Symposia on Quantitative Biology* (Vol. 69, pp. 439–445). doi:10.1101/sqb.2004.69.439
- Canté-Barrett, K., Pieters, R., & Meijerink, J. P. P. (2013). Myocyte enhancer factor 2C in hematopoiesis and leukemia. *Oncogene*, (February 2013), 403–410. doi:10.1038/onc.2013.56
- Carthew, R. W., & Sontheimer, E. J. (2009). Origins and Mechanisms of miRNAs and siRNAs. *Cell*. doi:10.1016/j.cell.2009.01.035
- Castanotto, D., Sakurai, K., Lingeman, R., Li, H., Shively, L., Aagaard, L., ... Rossi, J. J. (2007). Combinatorial delivery of small interfering RNAs reduces RNAi efficacy by selective incorporation into RISC. *Nucleic Acids Res*, 35(15), 5154–5164. doi:10.1093/nar/gkm543
- Challen, G. A., Sun, D., Jeong, M., Luo, M., Jelinek, J., Berg, J. S., ... Goodell, M. A. (2011). Dnmt3a is essential for hematopoietic stem cell differentiation. *Nature Genetics*. doi:10.1038/ng.1009

- Chen, C. M., Krohn, J., Bhattacharya, S., & Davies, B. (2011). A comparison of exogenous promoter activity at the ROSA26 locus using a PhiC31 integrase mediated cassette exchange approach in mouse es cells. *PLoS ONE*, 6(8), 6–13. doi:10.1371/journal.pone.0023376
- Chen, J., Odenike, O., & Rowley, J. D. (2010). Leukaemogenesis: more than mutant genes. *Nature Reviews. Cancer*, 10(1), 23–36. doi:10.1038/nrc2765
- Chen, S.-J., Shen, Y., & Chen, Z. (2013). A panoramic view of acute myeloid leukemia. *Nature Genetics*, 45(6), 586–7. doi:10.1038/ng.2651
- Chen, Z., & Chen, S. J. (1992). RARA and PML genes in acute promyelocytic leukemia. *Leukemia & Lymphoma*, 8(4-5), 253–260. doi:10.3109/10428199209051004
- Chen, Z., Xiao, Z., Gu, W. Z., Xue, J., Bui, M. H., Kovar, P., ... Zhang, H. (2006). Selective Chk1 inhibitors differentially sensitize p53-deficient cancer cells to cancer therapeutics. *International Journal of Cancer*, 119(12), 2784–2794. doi:10.1002/ijc.22198
- Chendong, Y., Sudderth, J., Tuyen, D., Bachoo, R. G., McDonald, J. G., & DeBerardinis, R. J. (2009). Glioblastoma cells require glutamate dehydrogenase to survive impairments of glucose metabolism or Akt signaling. *Cancer Research*, 69(20), 7986–7993. doi:10.1158/0008-5472.CAN-09-2266
- Cheng, Z., Gong, Y., Ma, Y., Lu, K., Lu, X., Pierce, L. a., ... Wang, J. (2013). Inhibition of BET bromodomain targets genetically diverse glioblastoma. *Clinical Cancer Research*, 19(7), 1748–1759. doi:10.1158/1078-0432.CCR-12-3066
- Christofk, H. R., Vander Heiden, M. G., Harris, M. H., Ramanathan, A., Gerszten, R. E., Wei, R., ... Cantley, L. C. (2008). The M2 splice isoform of pyruvate kinase is important for cancer metabolism and tumour growth. *Nature*, 452(7184), 230–233. doi:10.1038/nature06734
- Clem, B., Telang, S., Clem, A., Yalcin, A., Meier, J., Simmons, A., ... Chesney, J. (2008). Small-molecule inhibition of 6-phosphofructo-2-kinase activity suppresses glycolytic flux and tumor growth. *Molecular Cancer Therapeutics*, 7(1), 110–120. doi:10.1158/1535-7163.MCT-07-0482
- Cong, L., Ran, F. A., Cox, D., Lin, S., Barretto, R., Habib, N., ... Zhang, F. (2013). Multiplex genome engineering using CRISPR/Cas systems. *Science (New York, N.Y.)*, 339(6121), 819–23. doi:10.1126/science.1231143
- Cortés-Cros, M., Hemmerlin, C., Ferretti, S., Zhang, J., Gounarides, J. S., Yin, H., ... Hofmann, F. (2013). M2 isoform of pyruvate kinase is dispensable for tumor maintenance and growth. *Proceedings of the National Academy of Sciences of the United States of America*, 110(2), 489–94. doi:10.1073/pnas.1212780110

- Coudé, M., Braun, T., Berrou, J., Dupont, M., Bertrand, S., Masse, A., ... Gardin, C. (2015). BET inhibitor OTX015 targets BRD2 and BRD4 and decreases c-MYC in acute leukemia cells. *Oncotarget*. Retrieved from <http://www.ncbi.nlm.nih.gov/pubmed/25989842>
- Cullen, B. R. (2010). Five questions about viruses and microRNAs. *PLoS Pathogens*. doi:10.1371/journal.ppat.1000787
- Czernin, J., & Phelps, M. E. (2002). Positron emission tomography scanning: current and future applications. *Annual Review of Medicine*, 53(1), 89–112. doi:10.1146/annurev.med.53.082901.104028
- Dai, C., Whitesell, L., Rogers, A. B., & Lindquist, S. (2007). Heat Shock Factor 1 Is a Powerful Multifaceted Modifier of Carcinogenesis. *Cell*, 130(6), 1005–1018. doi:10.1016/j.cell.2007.07.020
- Daskalakis, M., Nguyen, T. T., Nguyen, C., Guldberg, P., Köhler, G., Jones, P. a, ... Ko, G. (2013). Demethylation of a hypermethylated P15 / INK4B gene in patients with myelodysplastic syndrome by 5-Aza-2J-deoxycytidine ( decitabine ) treatment, 100(8), 2957–2964. doi:10.1182/blood.V100.8.2957
- Dawson, M. a., & Kouzarides, T. (2012). Cancer epigenetics: From mechanism to therapy. *Cell*. Elsevier Inc. doi:10.1016/j.cell.2012.06.013
- Dawson, M. a., Prinjha, R. K., Dittmann, A., Giotopoulos, G., Bantscheff, M., Chan, W.-I., ... Kouzarides, T. (2011). Inhibition of BET recruitment to chromatin as an effective treatment for MLL-fusion leukaemia. *Nature*, 478(7370), 529–533. doi:10.1038/nature10509
- De Thé, H., & Chen, Z. (2010). Acute promyelocytic leukaemia: novel insights into the mechanisms of cure. *Nature Reviews. Cancer*, 10(11), 775–783. doi:10.1038/nrc2943
- DeBerardinis, R. J., Mancuso, A., Daikhin, E., Nissim, I., Yudkoff, M., Wehrli, S., & Thompson, C. B. (2007). Beyond aerobic glycolysis: transformed cells can engage in glutamine metabolism that exceeds the requirement for protein and nucleotide synthesis. *Proceedings of the National Academy of Sciences of the United States of America*, 104(49), 19345–19350. doi:10.1073/pnas.0709747104
- Delmore, J. E., Issa, G. C., Lemieux, M. E., Rahl, P. B., Shi, J., Jacobs, H. M., ... Mitsiades, C. S. (2011). BET bromodomain inhibition as a therapeutic strategy to target c-Myc. *Cell*, 146(6), 904–917. doi:10.1016/j.cell.2011.08.017
- Demarest, R. M., Dahmane, N., & Capobianco, A. J. (2011). Notch is oncogenic dominant in T-cell acute lymphoblastic leukemia. *Blood*, 117(10), 2901–2909. doi:10.1182/blood-2010-05-286351



- Deng, Y., Gam, J., French, J. B., Zhao, H., An, S., & Benkovic, S. J. (2012). Mapping protein-protein proximity in the purinosome. *Journal of Biological Chemistry*, 287(43), 36201–36207. doi:10.1074/jbc.M112.407056
- Ding, L., Ley, T. J., Larson, D. E., Miller, C. a., Koboldt, D. C., Welch, J. S., ... DiPersio, J. F. (2012). Clonal evolution in relapsed acute myeloid leukaemia revealed by whole-genome sequencing. *Nature*, 481(7382), 506–510. doi:10.1038/nature10738
- Dong, M., Ning, Z.-Q., Xing, P.-Y., Xu, J.-L., Cao, H.-X., Dou, G.-F., ... Feng, F.-Y. (2012). Phase I study of chidamide (CS055/HBI-8000), a new histone deacetylase inhibitor, in patients with advanced solid tumors and lymphomas. *Cancer Chemotherapy and Pharmacology*, 69(6), 1413–1422. doi:10.1007/s00280-012-1847-5
- Donner, L. R., Wainwright, L. M., Zhang, F., & Biegel, J. a. (2007). Mutation of the INI1 gene in composite rhabdoid tumor of the endometrium. *Human Pathology*, 38(6), 935–939. doi:10.1016/j.humpath.2006.12.003
- Druker, B. J., Guilhot, F., O'Brien, S. G., Gathmann, I., Kantarjian, H., Gattermann, N., ... Larson, R. a. (2006). Five-year follow-up of patients receiving imatinib for chronic myeloid leukemia. *The New England Journal of Medicine*, 355(23), 2408–2417. doi:10.1056/NEJMoa062867
- Druker, B. J., Sawyers, C. L., Kantarjian, H., Resta, D. J., Reese, S. F., Ford, J. M., ... Talpaz, M. (2001). Activity of a specific inhibitor of the BCR-ABL tyrosine kinase in the blast crisis of chronic myeloid leukemia and acute lymphoblastic leukemia with the Philadelphia chromosome. *The New England journal of medicine* (Vol. 344). doi:10.1056/NEJM200104053441402
- Duvic, M., Talpur, R., Ni, X., Zhang, C., Hazarika, P., Kelly, C., ... Frankel, S. R. (2007). Phase 2 trial of oral vorinostat (suberoylanilide hydroxamic acid, SAHA) for refractory cutaneous T-cell lymphoma (CTCL). *Blood*, 109(1), 31–39. doi:10.1182/blood-2006-06-025999
- Enns, G. M., Berry, S. A., Berry, G. T., Rhead, W. J., Brusilow, S. W., & Hamosh, A. (2007). Survival after treatment with phenylacetate and benzoate for urea-cycle disorders. *The New England journal of medicine* (Vol. 356). doi:10.1056/NEJMoa066596
- Fantin, V. R., St-Pierre, J., & Leder, P. (2006). Attenuation of LDH-A expression uncovers a link between glycolysis, mitochondrial physiology, and tumor maintenance. *Cancer Cell*, 9(6), 425–434. doi:10.1016/j.ccr.2006.04.023
- FARBER, S., & DIAMOND, L. K. (1948). Temporary remissions in acute leukemia in children produced by folic acid antagonist, 4-aminopteroyl-glutamic acid. *The New England Journal of Medicine*, 238(23), 787–793. doi:10.1056/NEJM194806032382301

- Fearon, E. R., & Vogelstein, B. (1990). A genetic model for colorectal tumorigenesis. *Cell*, 61(5), 759–767. doi:10.1016/0092-8674(90)90186-I
- Fedorov, Y., Anderson, E. M., Birmingham, A., Reynolds, A., Karpilow, J., Robinson, K., ... Khvorova, A. (2006). Off-target effects by siRNA can induce toxic phenotype. *RNA (New York, N.Y.)*, 12(7), 1188–1196. doi:10.1261/rna.28106
- Fellmann, C., Hoffmann, T., Sridhar, V., Hopfgartner, B., Muhar, M., Roth, M., ... Zuber, J. (2013). An optimized microRNA backbone for effective single-copy RNAi. *Cell Reports*, 5(6), 1704–1713. doi:10.1016/j.celrep.2013.11.020
- Fellmann, C., & Lowe, S. W. (2014). Stable RNA interference rules for silencing. *J. Biol. Chem.*, 16(1), 10–8. doi:10.1038/ncb2895
- Fellmann, C., Zuber, J., McJunkin, K., Chang, K., Malone, C. D., Dickins, R. a, ... Lowe, S. W. (2011a). Functional Identification of Optimized RNAi Triggers Using a Massively Parallel Sensor Assay. *Molecular Cell*, 41(6), 733–746. doi:10.1016/j.molcel.2011.02.008
- Fellmann, C., Zuber, J., McJunkin, K., Chang, K., Malone, C. D., Dickins, R. A., ... Lowe, S. W. (2011b). Functional Identification of Optimized RNAi Triggers Using a Massively Parallel Sensor Assay. *Molecular Cell*, 41(6), 733–746. doi:10.1016/j.molcel.2011.02.008
- Figueroa, M. E., Abdel-Wahab, O., Lu, C., Ward, P. S., Patel, J., Shih, A., ... Melnick, A. (2010). Leukemic IDH1 and IDH2 Mutations Result in a Hypermethylation Phenotype, Disrupt TET2 Function, and Impair Hematopoietic Differentiation. *Cancer Cell*, 18(6), 553–567. doi:10.1016/j.ccr.2010.11.015
- Filipowicz, W., Bhattacharyya, S. N., & Sonenberg, N. (2008). Mechanisms of post-transcriptional regulation by microRNAs: are the answers in sight? *Nature Reviews. Genetics*, 9(2), 102–14. doi:10.1038/nrg2290
- Filippakopoulos, P., Qi, J., Picaud, S., Shen, Y., Smith, W. B., Fedorov, O., ... Bradner, J. E. (2010). Selective inhibition of BET bromodomains. *Nature*, 468(7327), 1067–1073. doi:10.1038/nature09504
- Fire, A., Xu, S., Montgomery, M. K., Kostas, S. A., Driver, S. E., & Mello, C. C. (1998). Potent and specific genetic interference by double-stranded RNA in *Caenorhabditis elegans*. *Nature*, 391(6669), 806–811. doi:10.1038/35888
- Forbes, S. A., Beare, D., Gunasekaran, P., Leung, K., Bindal, N., Boutselakis, H., ... Campbell, P. J. (2014). COSMIC: exploring the world's knowledge of somatic mutations in human cancer. *Nucleic Acids Research*, 43(D1), D805–D811. doi:10.1093/nar/gku1075

- Forbes, S. a., Tang, G., Bindal, N., Bamford, S., Dawson, E., Cole, C., ... Futreal, P. A. (2009). COSMIC (the Catalogue of Somatic Mutations In Cancer): A resource to investigate acquired mutations in human cancer. *Nucleic Acids Research*, 38(SUPPL.1), 652–657. doi:10.1093/nar/gkp995
- Friedrich, G., & Soriano, P. (1991). Promoter traps in embryonic stem cells: A genetic screen to identify and mutate developmental genes in mice. *Genes and Development*, 5(9), 1513–1523. doi:10.1101/gad.5.9.1513
- Futreal, P. A., Coin, L., Marshall, M., Down, T., Hubbard, T., Wooster, R., ... Stratton, M. R. (2004). A census of human cancer genes. *Nature Reviews. Cancer*, 4(3), 177–183. doi:10.1038/nrc1299
- Gambhir, S. S. (2002). Molecular imaging of cancer with positron emission tomography. *Nature Reviews. Cancer*, 2(9), 683–693. doi:10.1038/nrc882
- Ganapathy-Kanniappan, S., Kunjithapatham, R., & Geschwind, J.-F. (2012). Glyceraldehyde-3-phosphate dehydrogenase: a promising target for molecular therapy in hepatocellular carcinoma. *Oncotarget*, 3(9), 940–53. Retrieved from <http://www.pubmedcentral.nih.gov/articlerender.fcgi?artid=3660062&tool=pmcentrez&rendertype=abstract>
- Geutjes, E.-J., Bajpe, P. K., & Bernards, R. (2012). Targeting the epigenome for treatment of cancer. *Oncogene*. Nature Publishing Group. doi:10.1038/onc.2011.552
- Gibson, D. G., Young, L., Chuang, R.-Y., Venter, J. C., Hutchison, C. a, & Smith, H. O. (2009). Enzymatic assembly of DNA molecules up to several hundred kilobases. *Nature Methods*, 6(5), 343–345. doi:10.1038/nmeth.1318
- Gilbert, L. a., Larson, M. H., Morsut, L., Liu, Z., Brar, G. a., Torres, S. E., ... Qi, L. S. (2013). CRISPR-mediated modular RNA-guided regulation of transcription in eukaryotes. *Cell*, 154(2), 442–451. doi:10.1016/j.cell.2013.06.044
- Gilliland, D. G., Jordan, C. T., & Felix, C. a. (2004). The molecular basis of leukemia. *Hematology / the Education Program of the American Society of Hematology. American Society of Hematology. Education Program*, 80–97. doi:10.1182/asheducation-2004.1.80
- Glaser, S. P., Lee, E. F., Trounson, E., Bouillet, P., Wei, A., Fairlie, W. D., ... Strasser, A. (2012). Anti-apoptotic mcl-1 is essential for the development and sustained growth of acute myeloid leukemia. *Genes and Development*, 26(2), 120–125. doi:10.1101/gad.182980.111
- Goecks, J., Nekrutenko, A., & Taylor, J. (2010). Galaxy: a comprehensive approach for supporting accessible, reproducible, and transparent computational research in the life sciences. *Genome Biology*, 11(8), R86. doi:10.1186/gb-2010-11-8-r86

- Goldberg, M. S., & Sharp, P. A. (2012). Pyruvate kinase M2-specific siRNA induces apoptosis and tumor regression. *Journal of Experimental Medicine*. doi:10.1084/jem.20111487
- González-Murillo, A., Lozano, M. L., Alvarez, L., Jacome, A., Almarza, E., Navarro, S., ... Río, P. (2010). Development of lentiviral vectors with optimized transcriptional activity for the gene therapy of patients with Fanconi anemia. *Human Gene Therapy*, 21(5), 623–630. doi:10.1089/hum.2009.141
- Gore, L., Rothenberg, M. L., O'Bryant, C. L., Schultz, M. K., Sandler, A. B., Coffin, D., ... Eckhardt, S. G. (2008). A phase I and pharmacokinetic study of the oral histone deacetylase inhibitor, MS-275, in patients with refractory solid tumors and lymphomas. *Clinical Cancer Research*, 14(14), 4517–4525. doi:10.1158/1078-0432.CCR-07-1461
- Govindan, R., Ding, L., Griffith, M., Subramanian, J., Dees, N. D., Kanchi, K. L., ... Wilson, R. K. (2012). Genomic landscape of non-small cell lung cancer in smokers and never-smokers. *Cell*, 150(6), 1121–1134. doi:10.1016/j.cell.2012.08.024
- Greenlee, R. T., Hill-Harmon, M. B., Murray, T., & Thun, M. (2001). Cancer statistics, 2001. *CA: A Cancer Journal for Clinicians*, 51(1), 15–36. doi:10.3322/canjclin.51.1.15
- Grimm, D., Streetz, K. L., Jopling, C. L., Storm, T. A., Pandey, K., Davis, C. R., ... Kay, M. A. (2006). Fatality in mice due to oversaturation of cellular microRNA/short hairpin RNA pathways. *Nature*, 441(7092), 537–41. doi:10.1038/nature04791
- Grindey, G. B., Hertel, L. W., & Plunkett, W. (1990). Cytotoxicity and antitumor activity of 2',2'-difluorodeoxycytidine (Gemcitabine). *Cancer Investigation*, 8(2), 313. doi:10.3109/07357909009017602
- Grossmann, V., Schnittger, S., Poetzinger, F., Kohlmann, a, Stiel, a, Eder, C., ... Haferlach, C. (2013). High incidence of RAS signalling pathway mutations in MLL-rearranged acute myeloid leukemia. *Leukemia*, 27(9), 1933–6. doi:10.1038/leu.2013.90
- Gu, S., Jin, L., Zhang, Y., Huang, Y., Zhang, F., Valdmanis, P. N., & Kay, M. a. (2012). The loop position of shRNAs and pre-miRNAs is critical for the accuracy of dicer processing in vivo. *Cell*, 151(4), 900–911. doi:10.1016/j.cell.2012.09.042
- Guo, S., & Kemphues, K. J. (1995). par-1, a gene required for establishing polarity in *C. elegans* embryos, encodes a putative Ser/Thr kinase that is asymmetrically distributed. *Cell*, 81(4), 611–620. doi:10.1016/0092-8674(95)90082-9
- Haber, D. A., & Settleman, J. (2007). Cancer: drivers and passengers. *Nature*. doi:10.1038/446145a

- Hanahan, D., Weinberg, R. a, & Francisco, S. (2000). The Hallmarks of Cancer Review University of California at San Francisco. *Hormone Research*, 100(1), 57–70. doi:10.1016/S0092-8674(00)81683-9
- Hanahan, D., & Weinberg, R. a. (2011). Hallmarks of cancer: The next generation. *Cell*. Elsevier Inc. doi:10.1016/j.cell.2011.02.013
- Hasle, H., Clemmensen, I. H., & Mikkelsen, M. (2000). Risks of leukaemia and solid tumours in individuals with Down's syndrome. *Lancet*, 355(9199), 165–169. doi:10.1016/S0140-6736(99)05264-2
- Heckl, D., Kowalczyk, M. S., Yudovich, D., Belizaire, R., Puram, R. V, McConkey, M. E., ... Ebert, B. L. (2014). Generation of mouse models of myeloid malignancy with combinatorial genetic lesions using CRISPR-Cas9 genome editing. *Nature Biotechnology*, 32(June). doi:10.1038/nbt.2951
- Hensley, C. T., Wasti, A. T., & Deberardinis, R. J. (2013). Review series Glutamine and cancer : cell biology , physiology , and clinical opportunities, 123(9). doi:10.1172/JCI69600.3678
- Hitzler, J. K. (2007). Acute megakaryoblastic leukemia in down syndrome. *Pediatric Blood and Cancer*. doi:10.1002/pbc.21353
- Hoffman, G. R., Rahal, R., Buxton, F., Xiang, K., McAllister, G., Frias, E., ... Jagani, Z. (2014). Functional epigenetics approach identifies BRM/SMARCA2 as a critical synthetic lethal target in BRG1-deficient cancers. *Proceedings of the National Academy of Sciences of the United States of America*, 111(8), 3128–33. doi:10.1073/pnas.1316793111
- Horton, S. J., Walf-Vorderwülbecke, V., Chatters, S. J., Sebire, N. J., De Boer, J., & Williams, O. (2009). Acute myeloid leukemia induced by MLL-ENL is cured by oncogene ablation despite acquisition of complex genetic abnormalities. *Blood*, 113(20), 4922–4929. doi:10.1182/blood-2008-07-170480
- Huang, M. E., Ye, Y. C., Chen, S. R., Chai, J. R., Lu, J. X., Zhao, L., ... Wang, Z. Y. (1988). Use of all-trans retinoic acid in the treatment of acute promyelocytic leukemia. *Blood*, 72(2), 567–572.
- Hughes, E. D., Qu, Y. Y., Genik, S. J., Lyons, R. H., Pacheco, C. D., Lieberman, A. P., ... Saunders, T. L. (2007). Genetic variation in C57BL/6 ES cell lines and genetic instability in the Bruce4 C57BL/6 ES cell line. *Mammalian Genome*, 18(8), 549–558. doi:10.1007/s00335-007-9054-0
- Inui, M., Miyado, M., Igarashi, M., Tamano, M., Kubo, A., Yamashita, S., ... Takada, S. (2014). Rapid generation of mouse models with defined point mutations by the CRISPR/Cas9 system. *Scientific Reports*, 4, 5396. doi:10.1038/srep05396

- Issa, J. P. J., Garcia-Manero, G., Giles, F. J., Mannari, R., Thomas, D., Faderl, S., ... Kantarjian, H. M. (2004). Phase 1 study of low-dose prolonged exposure schedules of the hypomethylating agent 5-aza-2'-deoxycytidine (decitabine) in hematopoietic malignancies. *Blood*, 103(5), 1635–1640. doi:10.1182/blood-2003-03-0687
- Ivanisevic, J., Zhu, Z. J., Plate, L., Tautenhahn, R., Chen, S., O'Brien, P. J., ... Siuzdak, G. (2013). Toward 'Omic scale metabolite profiling: A dual separation-mass spectrometry approach for coverage of lipid and central carbon metabolism. *Analytical Chemistry*, 85(14), 6876–6884. doi:10.1021/ac401140h
- Jabbour, E., Ottmann, O. G., Deininger, M., & Hochhaus, A. (2014). Targeting the phosphoinositide 3-kinase pathway in hematologic malignancies. *Haematologica*, 99(1), 7–18. doi:10.3324/haematol.2013.087171
- Jackson, A. L., Bartz, S. R., Schelter, J., Kobayashi, S. V, Burchard, J., Mao, M., ... Linsley, P. S. (2003). Expression profiling reveals off-target gene regulation by RNAi. *Nature Biotechnology*, 21(6), 635–637. doi:10.1038/nbt831
- Jackson, A. L., Burchard, J., Schelter, J., Chau, B. N., Cleary, M., Lim, L., & Linsley, P. S. (2006). Widespread siRNA “off-target” transcript silencing mediated by seed region sequence complementarity. *RNA (New York, N.Y.)*, 12(7), 1179–1187. doi:10.1261/rna.25706
- Jang, M., Kim, S. S., & Lee, J. (2013). Cancer cell metabolism: implications for therapeutic targets. *Experimental & Molecular Medicine*, 45(10), e45. doi:10.1038/emm.2013.85
- Jiang, X. R., Jimenez, G., Chang, E., Frolkis, M., Kusler, B., Sage, M., ... Chiu, C. P. (1999). Telomerase expression in human somatic cells does not induce changes associated with a transformed phenotype. *Nature Genetics*, 21(1), 111–114. doi:10.1038/5056
- Ju, H. Y., Hong, C. R., & Shin, H. Y. (2014). Advancements in the treatment of pediatric acute leukemia and brain tumor - continuous efforts for 100% cure. *Korean Journal of Pediatrics*, 57(10), 434–439.
- Jurica, M. S., Mesecar, A., Heath, P. J., Shi, W., Nowak, T., & Stoddard, B. L. (1998). The allosteric regulation of pyruvate kinase by fructose-1,6-bisphosphate. *Structure (London, England : 1993)*, 6(2), 195–210. doi:10.1016/S0969-2126(98)00021-5
- Kennedy, R. D., Chen, C. C., Stuckert, P., Archila, E. M., De La Vega, M. A., Moreau, L. a, ... D'Andrea, A. D. (2007). Fanconi anemia pathway-deficient tumor cells are hypersensitive to inhibition of ataxia telangiectasia mutated. *Journal of Clinical Investigation*, 117(5), 1440–1449. doi:10.1172/JCI31245

- Khalil, H., Tummala, H., Chakarov, S., Zhelev, N., & Lane, D. (2012). Targeting ATM pathway for therapeutic intervention in cancer. *Biodiscovery*, (1), 1–13. doi:10.7750/BioDiscovery.2012.1.3
- Khan, Z. A., Tripathi, R., & Mishra, B. (2012). Methotrexate: a detailed review on drug delivery and clinical aspects. *Expert Opinion on Drug Delivery*. doi:10.1517/17425247.2012.642362
- Kiessling, A., Wiesinger, R., Sperl, B., & Berg, T. (2007). Selective inhibition of c-Myc/Max dimerization by a pyrazolo[1,5-a]pyrimidine. *ChemMedChem*, 2(5), 627–630. doi:10.1002/cmdc.200600294
- Klijn, C., Durinck, S., Stawiski, E. W., Haverty, P. M., Jiang, Z., Liu, H., ... Zhang, Z. (2014). A comprehensive transcriptional portrait of human cancer cell lines. *Nat Biotechnol*, 33(3), 306–312. doi:10.1038/nbt.3080
- Koç, A., Wheeler, L. J., Mathews, C. K., & Merrill, G. F. (2004). Hydroxyurea Arrests DNA Replication by a Mechanism that Preserves Basal dNTP Pools. *Journal of Biological Chemistry*, 279(1), 223–230. doi:10.1074/jbc.M303952200
- Kon, A., Shih, L.-Y., Minamino, M., Sanada, M., Shiraishi, Y., Nagata, Y., ... Ogawa, S. (2013). Recurrent mutations in multiple components of the cohesin complex in myeloid neoplasms. *Nature Genetics*, 45(10), 1232–7. doi:10.1038/ng.2731
- König, R., Zhou, Y., Elleder, D., Diamond, T. L., Bonamy, G. M. C., Irelan, J. T., ... Chanda, S. K. (2008). Global Analysis of Host-Pathogen Interactions that Regulate Early-Stage HIV-1 Replication. *Cell*, 135(1), 49–60. doi:10.1016/j.cell.2008.07.032
- Kosan, C., & Kunz, J. (2002). Identification and characterisation of the gene TWIST NEIGHBOR (TWISTNB) located in the microdeletion syndrome 7p21 region. *Cytogenetic and Genome Research*, 97(3-4), 167–170. doi:10.1159/000066618
- Krivtsov, A. V., Twomey, D., Feng, Z., Stubbs, M. C., Wang, Y., Faber, J., ... Armstrong, S. a. (2006). Transformation from committed progenitor to leukaemia stem cell initiated by MLL-AF9. *Nature*, 442(7104), 818–822. doi:10.1038/nature04980
- Krivtsov, A. V., Feng, Z., Lemieux, M. E., Faber, J., Vempati, S., Sinha, A. U., ... Armstrong, S. a. (2008). H3K79 Methylation Profiles Define Murine and Human MLL-AF4 Leukemias. *Cancer Cell*, 14(5), 355–368. doi:10.1016/j.ccr.2008.10.001
- Kunimoto, H., Fukuchi, Y., Sakurai, M., Sadahira, K., Ikeda, Y., Okamoto, S., & Nakajima, H. (2012). Tet2 disruption leads to enhanced self-renewal and altered differentiation of fetal liver hematopoietic stem cells. *Scientific Reports*, 2, 1–10. doi:10.1038/srep00273

- Kurtoglu, M., Gao, N., Shang, J., Maher, J. C., Lehrman, M. a, Wangpaichitr, M., ... Lampidis, T. J. (2007). Under normoxia, 2-deoxy-D-glucose elicits cell death in select tumor types not by inhibition of glycolysis but by interfering with N-linked glycosylation. *Molecular Cancer Therapeutics*, 6(11), 3049–3058. doi:10.1158/1535-7163.MCT-07-0310
- Lambeth, L. S., Van Hateren, N. J., Wilson, S. a, & Nair, V. (2010). A direct comparison of strategies for combinatorial RNA interference. *BMC Molecular Biology*, 11, 77. doi:10.1186/1471-2199-11-77
- Lan, R., Lin, G., Yin, F., Xu, J., Zhang, X., Wang, J., ... Zhang, H. (2012). Dissecting the phenotypes of Plk1 inhibition in cancer cells using novel kinase inhibitory chemical CBB2001. *Laboratory Investigation*, 92(10), 1503–1514. doi:10.1038/labinvest.2012.114
- Lane, A. a, Chapuy, B., Lin, C. Y., Tivey, T., Li, H., Townsend, E. C., ... Weinstock, D. M. (2014). Triplication of a 21q22 region contributes to B cell transformation through HMGN1 overexpression and loss of histone H3 Lys27 trimethylation. *Nature Genetics*, 46(6), 618–23. doi:10.1038/ng.2949
- Lane, A. N., & Fan, T. W.-M. (2015). Regulation of mammalian nucleotide metabolism and biosynthesis. *Nucleic Acids Research*, 43(4), 2466–85. doi:10.1093/nar/gkv047
- Lau, W. M., Doucet, M., Stadel, R., Huang, D., Weber, K. L., & Kominsky, S. L. (2013). Enpp1: A Potential Facilitator of Breast Cancer Bone Metastasis. *PLoS ONE*, 8(7), 1–5. doi:10.1371/journal.pone.0066752
- Le, A., Cooper, C. R., Gouw, A. M., Dinavahi, R., Maitra, A., Deck, L. M., ... Dang, C. V. (2010). Inhibition of lactate dehydrogenase A induces oxidative stress and inhibits tumor progression. *Proceedings of the National Academy of Sciences of the United States of America*, 107(5), 2037–2042. doi:10.1073/pnas.0914433107
- Lennard, L., & Lilleyman, J. S. (1989). Variable mercaptopurine metabolism and treatment outcome in childhood lymphoblastic leukemia. *Journal of Clinical Oncology*, 7(12), 1816–1823.
- Lew, C. R., & Tolan, D. R. (2012). Targeting of several glycolytic enzymes using RNA interference reveals aldolase affects cancer cell proliferation through a non-glycolytic mechanism. *Journal of Biological Chemistry*, 287(51), 42554–42563. doi:10.1074/jbc.M112.405969
- Ley, T. J., Mardis, E. R., Ding, L., Fulton, B., McLellan, M. D., Chen, K., ... Wilson, R. K. (2008). DNA sequencing of a cytogenetically normal acute myeloid leukaemia genome. *Nature*, 456(7218), 66–72. doi:10.1038/nature07485



- LI, M. C., HERTZ, R., & BERGENSTAL, D. M. (1958). Therapy of choriocarcinoma and related trophoblastic tumors with folic acid and purine antagonists. *The New England Journal of Medicine*, 259(2), 66–74. doi:10.1056/NEJM195807102590204
- Li, Y., Schwab, C., Ryan, S. L., Papaemmanuil, E., Robinson, H. M., Jacobs, P., ... Harrison, C. J. (2014). Constitutional and somatic rearrangement of chromosome 21 in acute lymphoblastic leukaemia. *Nature*, 508(7494), 98–102. doi:10.1038/nature13115
- Liu, P., Cheng, H., Roberts, T. M., & Zhao, J. J. (2009). Targeting the phosphoinositide 3-kinase pathway in cancer. *Nature Reviews. Drug Discovery*, 8(8), 627–644. doi:10.1038/nrd2926
- Liu, Y., Cao, Y., Zhang, W., Bergmeier, S., Qian, Y., Akbar, H., ... Chen, X. (2012). A Small-Molecule Inhibitor of Glucose Transporter 1 Downregulates Glycolysis, Induces Cell-Cycle Arrest, and Inhibits Cancer Cell Growth In Vitro and In Vivo. *Molecular Cancer Therapeutics*. doi:10.1158/1535-7163.MCT-12-0131
- Lockwood, W. W., Zejnullahu, K., Bradner, J. E., & Varmus, H. (2012). Sensitivity of human lung adenocarcinoma cell lines to targeted inhibition of BET epigenetic signaling proteins. *Proceedings of the National Academy of Sciences of the United States of America*, 109(47), 19408–13. doi:10.1073/pnas.1216363109
- Lomax, M. E., Folkes, L. K., & O'Neill, P. (2013). Biological consequences of radiation-induced DNA damage: Relevance to radiotherapy. *Clinical Oncology*, 25(10), 578–585. doi:10.1016/j.clon.2013.06.007
- Lu, J., Pan, Q., Rong, L., He, W., Liu, S.-L., & Liang, C. (2011). The IFITM proteins inhibit HIV-1 infection. *Journal of Virology*, 85(5), 2126–2137. doi:10.1128/JVI.01531-10
- Luo, J., Emanuele, M. J., Li, D., Creighton, C. J., Schlabach, M. R., Westbrook, T. F., ... Elledge, S. J. (2009). A Genome-wide RNAi Screen Identifies Multiple Synthetic Lethal Interactions with the Ras Oncogene. *Cell*, 137(5), 835–848. doi:10.1016/j.cell.2009.05.006
- Luo, J., Solimini, N. L., & Elledge, S. J. (2009). Principles of Cancer Therapy: Oncogene and Non-oncogene Addiction. *Cell*. doi:10.1016/j.cell.2009.02.024
- Luo, T., Masson, K., Jaffe, J. D., Silkworth, W., Ross, N. T., Scherer, C. a., ... Golub, T. R. (2012). STK33 kinase inhibitor BRD-8899 has no effect on KRAS-dependent cancer cell viability. *Proceedings of the National Academy of Sciences*. doi:10.1073/pnas.1120589109
- M. Isomura, K. A. H. F. (1991). Synthesis and antitumor activity of 20(S)-camptothecin derivatives: carbamate-linked, water-soluble derivatives of 7-ethyl-10-hydroxycamptothecin. *Chemical & Pharmaceutical Bulletin*, 39(6), 1446–1450. doi:10.1248/cpb.39.1446

- Maher, J. C., Wangpaichitr, M., Savaraj, N., Kurtoglu, M., & Lampidis, T. J. (2007). Hypoxia-inducible factor-1 confers resistance to the glycolytic inhibitor 2-deoxy-D-glucose. *Molecular Cancer Therapeutics*, 6(2), 732–741. doi:10.1158/1535-7163.MCT-06-0407
- Mali, P., Esvelt, K. M., & Church, G. M. (2013). Cas9 as a versatile tool for engineering biology. *Nat Methods*, 10(10), 957–963. doi:10.1038/nmeth.2649
- Mali, P., Yang, L., Esvelt, K. M., Aach, J., Guell, M., DiCarlo, J. E., ... Church, G. M. (2013). RNA-guided human genome engineering via Cas9. *Science (New York, N.Y.)*, 339(6121), 823–6. doi:10.1126/science.1232033
- Matsuo, Y., MacLeod, R. A., Uphoff, C. C., Drexler, H. G., Nishizaki, C., Katayama, Y., ... Orita, K. Two acute monocytic leukemia (AML-M5a) cell lines (MOLM-13 and MOLM-14) with interclonal phenotypic heterogeneity showing MLL-AF9 fusion resulting from an occult chromosome insertion, ins(11;9)(q23;p22p23)., 11 Leukemia : official journal of the Leukemia Society of America, Leukemia Research Fund, U.K 1469–1477 (1997). doi:10.1038/sj.leu.2400768
- Mazurek, S., Boschek, C. B., Hugo, F., & Eigenbrodt, E. (2005). Pyruvate kinase type M2 and its role in tumor growth and spreading. *Seminars in Cancer Biology*, 15(4), 300–308. doi:10.1016/j.semcancer.2005.04.009
- McBride, J. L., Boudreau, R. L., Harper, S. Q., Staber, P. D., Monteys, A. M., Martins, I., ... Davidson, B. L. (2008). Artificial miRNAs mitigate shRNA-mediated toxicity in the brain: implications for the therapeutic development of RNAi. *PNAS*, 105(15), 5868–5873. doi:10.1073/pnas.0801775105
- McJunkin, K., Mazurek, A., Premssirrut, P. K., Zuber, J., Dow, L. E., Simon, J., ... Lowe, S. W. (2011). Reversible suppression of an essential gene in adult mice using transgenic RNA interference. *Proceedings of the National Academy of Sciences of the United States of America*, 108(17), 7113–7118. doi:10.1073/pnas.1104097108
- Medes, G., Thomas, A., & Weinhouse, S. (1953). Metabolism of neoplastic tissue. IV. A study of lipid synthesis in neoplastic tissue slices in vitro. *Cancer Research*, 13(1), 27–29.
- Meister, G. (2013). Argonaute proteins: functional insights and emerging roles. *Nature Reviews. Genetics*, 14(7), 447–59. doi:10.1038/nrg3462
- Meyer, L. M., Miller, F. R., Rowen, M. J., Bock, G., & Rutzky, J. (1950). Treatment of Acute Leukemia with Amethopterin (4-amino, 10-methyl pteroyl glutamic acid). *Acta Haematologica*, 4(3), 157–167. doi:10.1159/000203749

- Michelakis, E. D., Webster, L., & Mackey, J. R. (2008). Dichloroacetate (DCA) as a potential metabolic-targeting therapy for cancer. *British Journal of Cancer*, 99(7), 989–994. doi:10.1038/sj.bjc.6604554
- Mocellin, S., & Provenzano, M. (2004). RNA interference: learning gene knock-down from cell physiology. *Journal of Translational Medicine*, 2, 39. doi:10.1186/1479-5876-2-39
- Mohr, S. E., Smith, J. a, Shamu, C. E., & Neumüller, R. a. (2014). RNAi screening comes of age : improved techniques and complementary approaches. *Nature Publishing Group*, 15(9), 591–600. doi:10.1038/nrm3860
- Moon, K. J., Mochizuki, K., Zhou, M., Jeong, H. S., Brady, J. N., & Ozato, K. (2005). The bromodomain protein Brd4 is a positive regulatory component of P-TEFb and stimulates RNA polymerase II-dependent transcription. *Molecular Cell*, 19(4), 523–534. doi:10.1016/j.molcel.2005.06.027
- Moreno-Sánchez, R., Rodríguez-Enríquez, S., Marín-Hernández, A., & Saavedra, E. (2007). Energy metabolism in tumor cells. *FEBS Journal*, 274(6), 1393–1418. doi:10.1111/j.1742-4658.2007.05686.x
- Morse, H. C. (1992). Genetic nomenclature for loci controlling surface antigens of mouse hemopoietic cells. *Journal of Immunology (Baltimore, Md. : 1950)*, 149(10), 3129–3134.
- Mottamal, M., Zheng, S., Huang, T., & Wang, G. (2015). Histone Deacetylase Inhibitors in Clinical Studies as Templates for New Anticancer Agents. *Molecules*, 20(3), 3898–3941. doi:10.3390/molecules20033898
- Muhsin, M., Gricks, C., & Kirkpatrick, P. (2004). Pemetrexed disodium. *Nature Reviews. Drug Discovery*. doi:10.1038/nrd1528
- Muvaffak, A., Pan, Q., Yan, H., Fernandez, R., Lim, J., Dolinski, B., ... Wang, Y. (2014). Evaluating TBK1 as a Therapeutic Target in Cancers with Activated IRF3. *Molecular Cancer Research : MCR*, 12(7), 1055–66. doi:10.1158/1541-7786.MCR-13-0642
- Muzny, D. M., Bainbridge, M. N., Chang, K., Dinh, H. H., Drummond, J. a., Fowler, G., ... Thomson., E. (2012). Comprehensive molecular characterization of human colon and rectal cancer. *Nature*, 487(7407), 330–337. doi:10.1038/nature11252
- Napoli, C., Lemieux, C., & Jorgensen, R. (1990). Introduction of a Chimeric Chalcone Synthase Gene into Petunia Results in Reversible Co-Suppression of Homologous Genes in trans. *The Plant Cell*, 2(4), 279–289. doi:10.1105/tpc.2.4.279
- Nelson, J. A., Carpenter, J. W., Rose, L. M., & Adamson, D. J. (1975). Mechanisms of action of 6-thioguanine, 6-mercaptopurine, and 8-azaguanine. *Cancer Research*, 35(10), 2872–2878.

- Noguchi, T., Inoue, H., & Tanaka, T. (1986). The M1- and M2-type isozymes of rat pyruvate kinase are produced from the same gene by alternative RNA splicing. *Journal of Biological Chemistry*.
- Nordling, C. O. (1953). A new theory on cancer-inducing mechanism. *British Journal of Cancer*, 7(1), 68–72. doi:10.1038/bjc.1953.8
- Nowell, P. C. (1976). The clonal evolution of tumor cell populations. *Science (New York, N.Y.)*, 194(4260), 23–28. doi:10.1126/science.959840
- Nyhan, W. L. (2005). Nucleotide Synthesis via Salvage Pathway. In *Encyclopedia of Life Sciences*. Chichester, UK: John Wiley & Sons, Ltd. doi:10.1038/npg.els.0003909
- O Warburg, K Posener, E. N. (1924). Ueber den stoffwechsel der tumoren (The metabolism of tumor cells). *Biochem Zeitschr*. Retrieved from <http://scholar.google.com/scholar?hl=en&btnG=Search&q=intitle:Ueber+den+Stoffwechse+l+der+Tumoren#2>
- O. Warburg, K. Posener, E. N. (1924). Über den Stoffwechsel der Carcinomzelle. *Biochem. Z.* 152, 309.
- Oudard, S., Carpentier, A., Banu, E., Fauchon, F., Celerier, D., Poupon, M. F., ... Delattre, J. Y. (2003). Phase II study of lonidamine and diazepam in the treatment of recurrent glioblastoma multiforme. *Journal of Neuro-Oncology*, 63(1), 81–86. doi:10.1023/A:1023756707900
- Palles, C., Cazier, J.-B., Howarth, K. M., Domingo, E., Jones, A. M., Broderick, P., ... Tomlinson, I. (2013). Germline mutations affecting the proofreading domains of POLE and POLD1 predispose to colorectal adenomas and carcinomas. *Nature Genetics*, 45(2), 136–44. doi:10.1038/ng.2503
- Parker, W. B. (2009). Enzymology of purine and pyrimidine antimetabolites used in the treatment of cancer. *Chemical Reviews*, 109(7), 2880–2893. doi:10.1021/cr900028p
- Parlo, R. A., & Coleman, P. S. (1984). Enhanced rate of citrate export from cholesterol-rich hepatoma mitochondria. The truncated Krebs cycle and other metabolic ramifications of mitochondrial membrane cholesterol. *Journal of Biological Chemistry*, 259(16), 9997–10003.
- Paton, C. M., Ekert, H., Waters, K. D., Matthews, R. N., & Toogood, I. R. (1982). Treatment of acute myeloid leukaemia in children. *Australian and New Zealand Journal of Medicine*, 12(2), 143–146. doi:10.1016/S0140-6736(95)92813-8

- Pedersen-Bjergaard, J., Andersen, M. T., & Andersen, M. K. (2007). Genetic pathways in the pathogenesis of therapy-related myelodysplasia and acute myeloid leukemia. *Hematology / the Education Program of the American Society of Hematology. American Society of Hematology. Education Program*, 392–397. doi:10.1182/asheducation-2007.1.392
- Piekarz, R. L., Frye, R., Turner, M., Wright, J. J., Allen, S. L., Kirschbaum, M. H., ... Bates, S. E. (2009). Phase II multi-institutional trial of the histone deacetylase inhibitor romidepsin as monotherapy for patients with cutaneous T-cell lymphoma. *Journal of Clinical Oncology*, 27(32), 5410–5417. doi:10.1200/JCO.2008.21.6150
- Placke, T., Faber, K., Nonami, A., Putwain, S. L., Salih, H. R., Heidel, F. H., ... Fröhling, S. (2014). Requirement for CDK6 in MLL-rearranged acute myeloid leukemia. *Blood*, 124(1), 13–23. doi:10.1182/blood-2014-02-558114
- Pleasance, E. D., Cheetham, R. K., Stephens, P. J., McBride, D. J., Humphray, S. J., Greenman, C. D., ... Stratton, M. R. (2010). A comprehensive catalogue of somatic mutations from a human cancer genome. *Nature*, 463(7278), 191–196. doi:10.1038/nature08658
- Plunkett, W., Chubb, S., Alexander, L., & Montgomery, J. a. (1980). Comparison of the toxicity and metabolism of 9-beta-D-arabinofuranosyl-2-fluoroadenine and 9-beta-D-arabinofuranosyladenine in human lymphoblastoid cells. *Cancer Research*, 40(7), 2349–2355.
- Polański, R., Hodgkinson, C. L., Fusi, A., Nonaka, D., Priest, L., Kelly, P., ... Morrow, C. J. (2014). Activity of the monocarboxylate transporter 1 inhibitor AZD3965 in small cell lung cancer. *Clinical Cancer Research : An Official Journal of the American Association for Cancer Research*, 20(4), 926–37. doi:10.1158/1078-0432.CCR-13-2270
- Possemato, R., Marks, K. M., Shaul, Y. D., Pacold, M. E., Kim, D., Birsoy, K., ... Sabatini, D. M. (2011). Functional genomics reveal that the serine synthesis pathway is essential in breast cancer. *Nature*, 476(7360), 346–350. doi:10.1038/nature10350
- Premisrirut, P. K., Dow, L. E., Kim, S. Y., Camiolo, M., Malone, C. D., Miething, C., ... Lowe, S. W. (2011). A rapid and scalable system for studying gene function in mice using conditional RNA interference. *Cell*, 145(1), 145–158. doi:10.1016/j.cell.2011.03.012
- Prendergast, G. C., & Ziff, E. B. (1991). Methylation-sensitive sequence-specific DNA binding by the c-Myc basic region. *Science (New York, N.Y.)*, 251(4990), 186–189. doi:10.1126/science.1987636
- Puissant, A., Frumm, S. M., Alexe, G., Bassil, C. F., Qi, J., Chanthery, Y. H., ... Stegmaier, K. (2013). Targeting MYCN in neuroblastoma by BET bromodomain inhibition. *Cancer Discovery*, 3(3), 309–323. doi:10.1158/2159-8290.CD-12-0418

- Qi, L. S., Larson, M. H., Gilbert, L. a, Doudna, J. a, Weissman, J. S., Arkin, A. P., & Lim, W. a. (2013). Repurposing CRISPR as an RNA-guided platform for sequence-specific control of gene expression. *Cell*, 152(5), 1173–83. doi:10.1016/j.cell.2013.02.022
- Raimondi, C., & Falasca, M. (2011). Targeting PDK1 in cancer. *Current Medicinal Chemistry*, 18(18), 2763–2769. doi:10.2174/092986711796011238
- Rajagopalan, P. T. R., Zhang, Z., McCourt, L., Dwyer, M., Benkovic, S. J., & Hammes, G. G. (2002). Interaction of dihydrofolate reductase with methotrexate: ensemble and single-molecule kinetics. *Proceedings of the National Academy of Sciences of the United States of America*, 99(21), 13481–13486. doi:10.1073/pnas.172501499
- Ran, F. A., Hsu, P. D., Lin, C. Y., Gootenberg, J. S., Konermann, S., Trevino, A. E., ... Zhang, F. (2013). Double nicking by RNA-guided CRISPR cas9 for enhanced genome editing specificity. *Cell*, 154(6), 1380–1389. doi:10.1016/j.cell.2013.08.021
- Rand, V., Parker, H., Russell, L. J., Schwab, C., Ensor, H., Irving, J., ... Harrison, C. J. (2011). Genomic characterization implicates iAMP21 as a likely primary genetic event in childhood B-cell precursor acute lymphoblastic leukemia. *Blood*, 117(25), 6848–6855. doi:10.1182/blood-2011-01-329961
- Rato, S., Maia, S., Brito, P. M., Resende, L., Pereira, C. F., Moita, C., ... Goncalves, J. (2010). Novel HIV-1 knockdown targets identified by an enriched kinases/phosphatases shRNA library using a long-term iterative screen in jurkat T-cells. *PLoS ONE*, 5(2). doi:10.1371/journal.pone.0009276
- Reddy, E. P., & Aggarwal, a. K. (2012). The Ins and Outs of Bcr-Abl Inhibition. *Genes & Cancer*. doi:10.1177/1947601912462126
- Reitzer, L. J., Wice, B. M., & Kennell, D. (1979). Evidence that glutamine, not sugar, is the major energy source for cultured HeLa cells. *Journal of Biological Chemistry*, 254(8), 2669–2676. doi:10.1007/s00125-007-0708-y
- Ricci, F., Tedeschi, A., Morra, E., & Montillo, M. (2009). Fludarabine in the treatment of chronic lymphocytic leukemia: A review. *Therapeutics and Clinical Risk Management*, 5(1), 187–207.
- Roberts, J. D., Poplin, E. A., Tombes, M. B., Kyle, B., Spicer, D. V, Grant, S., ... Moran, R. (2000). *Weekly lometrexol with daily oral folic acid is appropriate for phase II evaluation. Cancer chemotherapy and pharmacology* (Vol. 45). doi:10.1007/s002800050017
- Robertson, K. D., & Jones, P. a. (2000). DNA methylation: past, present and future directions. *Carcinogenesis*, 21(3), 461–467. doi:10.1093/carcin/21.3.461

- Romano, N., & Macino, G. (1992). Quelling: Transient inactivation of gene expression in *Neurospora crassa* by transformation with homologous sequences. *Molecular Microbiology*, 6(22), 3343–3353. doi:10.1111/j.1365-2958.1992.tb02202.x
- Rowe, J. M., & Tallman, M. S. (2010). How I treat acute myeloid leukemia. *Blood*, 116(17), 3147–3156. doi:10.1182/blood-2010-05-260117
- Rudolph, D., Steegmaier, M., Hoffmann, M., Grauert, M., Baum, A., Quant, J., ... Adolf, G. R. (2009). BI 6727, a polo-like kinase inhibitor with improved pharmacokinetic profile and broad antitumor activity. *Clinical Cancer Research*, 15(9), 3094–3102. doi:10.1158/1078-0432.CCR-08-2445
- Russo, P., Loprevite, M., Cesario, A., & Ardizzoni, A. (2004). Farnesylated proteins as anticancer drug targets: from laboratory to the clinic. *Current Medicinal Chemistry. Anti-Cancer Agents*, 4(2), 123–138. doi:10.2174/1568011043482098
- Sasaki, M., Knobbe, C. B., Munger, J. C., Lind, E. F., Brenner, D., Brüstle, A., ... Mak, T. W. (2012). IDH1(R132H) mutation increases murine haematopoietic progenitors and alters epigenetics. *Nature*. doi:10.1038/nature11323
- Schindler, T., Bornmann, W., Pellicena, P., Miller, W. T., Clarkson, B., & Kuriyan, J. (2000). Structural mechanism for STI-571 inhibition of abelson tyrosine kinase. *Science (New York, N.Y.)*, 289(5486), 1938–1942. doi:10.1126/science.289.5486.1938
- Schmitt, C. A., Rosenthal, C. T., & Lowe, S. W. (2000). Genetic analysis of chemoresistance in primary murine lymphomas. *Nature Medicine*, 6(9), 1029–1035. doi:10.1038/79542
- Schöffski, P. (2009). Polo-like kinase (PLK) inhibitors in preclinical and early clinical development in oncology. *The Oncologist*, 14(6), 559–570. doi:10.1634/theoncologist.2009-0010
- Scholl, C., Fröhling, S., Dunn, I. F., Schinzel, A. C., Barbie, D. a., Kim, S. Y., ... Gilliland, D. G. (2009). Synthetic Lethal Interaction between Oncogenic KRAS Dependency and STK33 Suppression in Human Cancer Cells. *Cell*, 137(5), 821–834. doi:10.1016/j.cell.2009.03.017
- Schüler, A., Schwieger, M., Engelmann, A., Weber, K., Horn, S., Müller, U., ... Stocking, C. (2008). The MADS transcription factor Mef2c is a pivotal modulator of myeloid cell fate. *Blood*, 111(9), 4532–4541. doi:10.1182/blood-2007-10-116343
- Schweitzer, B. I., Dicker, A. P., & Bertino, J. R. (1990). Dihydrofolate reductase as a therapeutic target. *FASEB Journal : Official Publication of the Federation of American Societies for Experimental Biology*, 4(8), 2441–52. Retrieved from <http://www.ncbi.nlm.nih.gov/pubmed/2185970>

- Schwieger, M., Schüler, A., Forster, M., Engelmann, A., Arnold, M. A., Delwel, R., ... Stocking, C. (2009). Homing and invasiveness of MLL/ENL leukemic cells is regulated by MEF2C. *Blood*, 114(12), 2476–2488. doi:10.1182/blood-2008-05-158196
- Sessa, C., De Jong, J., D’Incalci, M., Hatty, S., Pagani, O., & Cavalli, F. (1996). Phase I study of the antipurine antifolate lometrexol (DDATHF) with folinic acid rescue. *Clinical Cancer Research*, 2(7), 1123–1127.
- Shalem, O., Sanjana, N. E., Hartenian, E., Shi, X., Scott, D. a, Mikkelsen, T. S., ... Zhang, F. (2014). Genome-scale CRISPR-Cas9 knockout screening in human cells. *Science (New York, N.Y.)*, 343(6166), 84–7. doi:10.1126/science.1247005
- Sharma, S. V, Bell, D. W., Settleman, J., & Haber, D. a. (2007). Epidermal growth factor receptor mutations in lung cancer. *Nature Reviews. Cancer*, 7(3), 169–181. doi:10.1038/nrc2088
- Shih, A. H., Abdel-Wahab, O., Patel, J. P., & Levine, R. L. (2012). The role of mutations in epigenetic regulators in myeloid malignancies. *Nature Reviews Cancer*. doi:10.1038/nrc3343
- Shin, C., Chen, V. J., Gossett, L. S., Gates, S. B., MacKellar, W. C., Habeck, L. L., ... Schultz, R. M. (1997). Ly231514, a pyrrolo[2,3-d]pyrimidine-based antifolate that inhibits multiple folate-requiring enzymes. *Cancer Research*, 57(6), 1116–1123.
- Shinkai, Y., Rathbun, G., Lam, K. P., Oltz, E. M., Stewart, V., Mendelsohn, M., ... Stall, a M. (1992). RAG-2-deficient mice lack mature lymphocytes owing to inability to initiate V(D)J rearrangement. *Cell*, 68(5), 855–867. doi:10.1016/0092-8674(92)90029-C
- Sidi Chen, Neville E. Sanjana, Kaijie Zheng, Ophir Shalem, Kyungheon Lee, Xi Shi, David A. Scott, Jun Song, Jen Q. Pan, Ralph Weissleder, Hakho Lee, Feng Zhang, and P. A. S. (2015, March). Genome-wide CRISPR Screen in a Mouse Model of Tumor Growth and Metastasis. *Cell*, 160(6), 1246–1260. doi:10.1016/j.cell.2015.02.038
- Siegel, R. L., Miller, K. D., & Jemal, A. (2015). Cancer statistics, 2015. *CA: A Cancer Journal for Clinicians*, 65(1), 5–29. doi:10.3322/caac.21254
- Silva, J. M., Marran, K., Parker, J. S., Silva, J., Golding, M., Schlabach, M. R., ... Chang, K. (2008). Profiling essential genes in human mammary cells by multiplex RNAi screening. *Science (New York, N.Y.)*, 319(5863), 617–620. doi:10.1126/science.1149185
- Singh, N., Promkan, M., Liu, G., Varani, J., & Chakrabarty, S. (2013). Role of Calcium sensing receptor (CaSR) in tumorigenesis. *Best Practice and Research: Clinical Endocrinology and Metabolism*, 27(3), 455–463. doi:10.1016/j.beem.2013.04.00113



- Snyder, R. C., Ray, R., Blume, S., & Miller, D. M. (1991). Mithramycin blocks transcriptional initiation of the c-myc P1 and P2 promoters. *Biochemistry*, 30(17), 4290–4297.
- Solimini, N. L., Luo, J., & Elledge, S. J. (2007). Non-Oncogene Addiction and the Stress Phenotype of Cancer Cells. *Cell*. doi:10.1016/j.cell.2007.09.007
- Solimini, N. L., Xu, Q., Mermel, C. H., Liang, A. C., Schlabach, M. R., Luo, J., ... Elledge, S. J. (2012). Recurrent Hemizygous Deletions in Cancers May Optimize Proliferative Potential. *Science*. doi:10.1126/science.1219580
- Sroczyńska, P., Cruickshank, V. A., Bukowski, J. P., Miyagi, S., Bagger, F. O., Walfridsson, J., ... Helin, K. (2014). ShRNA screening identifies JMJD1C as being required for leukemia maintenance. *Blood*, 123(12), 1870–1882. doi:10.1182/blood-2013-08-522094
- Stegmeier, F., Hu, G., Rickles, R. J., Hannon, G. J., & Elledge, S. J. (2005). A lentiviral microRNA-based system for single-copy polymerase II-regulated RNA interference in mammalian cells. *Proceedings of the National Academy of Sciences of the United States of America*, 102(37), 13212–13217. doi:10.1073/pnas.0506306102
- Stratton, M. R., Campbell, P. J., & Futreal, P. A. (2009). The cancer genome. *Nature*, 458(7239), 719–724. doi:10.1038/nature07943
- Sun, C., Wang, L., Huang, S., Heynen, G. J. J. E., Prahallad, A., Robert, C., ... Bernards, R. (2014). Reversible and adaptive resistance to BRAF(V600E) inhibition in melanoma. *Nature*, 508(7494), 118–22. doi:10.1038/nature13121
- Tallman, M. S., & Altman, J. K. (2008). Curative strategies in acute promyelocytic leukemia. *Hematology / the Education Program of the American Society of Hematology. American Society of Hematology. Education Program*, 391–399. doi:10.1182/asheducation-2008.1.391
- Tang, S.-T., Shen, X.-R., Tang, H.-Q., Wang, C.-J., Wei, W., Zhang, Q., & Wang, Y. (2014). Association of the ENPP1 K121Q polymorphism with susceptibility to type 2 diabetes in different populations: evidence based on 40 studies. *Endocrine Journal*, 61(11), 1093–103. Retrieved from <http://www.ncbi.nlm.nih.gov/pubmed/25109753>
- Taylor, E. C., Kuhnt, D., Shih, C., Rinzel, S. M., Grindey, G. B., Barredo, J., ... Moran, R. G. (1992). A dideazatetrahydrofolate analogue lacking a chiral center at C-6, N-[4-[2-(2-amino-3,4-dihydro-4-oxo-7H-pyrrolo[2,3-d]pyrimidin-5-yl)ethyl]benzoyl]-L-glutamic acid, is an inhibitor of thymidylate synthase. *Journal of Medicinal Chemistry*, 35(23), 4450–4454.
- Tennant, D. a, Durán, R. V, & Gottlieb, E. (2010). Targeting metabolic transformation for cancer therapy. *Nature Reviews. Cancer*, 10(4), 267–277. doi:10.1038/nrc2817

- Thol, F., Bollin, R., Gehlhaar, M., Walter, C., Dugas, M., Suchanek, K. J., ... Heuser, M. (2014). Mutations in the cohesin complex in acute myeloid leukemia: Clinical and prognostic implications. *Blood*, 123(6), 914–920. doi:10.1182/blood-2013-07-518746
- Tomasetti, C., Marchionni, L., Nowak, M. a., Parmigiani, G., & Vogelstein, B. (2015). Only three driver gene mutations are required for the development of lung and colorectal cancers. *Pnas*, 112(1). doi:10.1073/pnas.1421839112
- Townsend, D., Witkop, C. J., & Mattson, J. (1981). Tyrosinase subcellular distribution and kinetic parameters in wild type and C-locus mutant C57BL/6J mice. *The Journal of Experimental Zoology*, 216(1), 113–119. doi:10.1002/jez.1402160112
- Toyoshima, M., Howie, H. L., Imakura, M., Walsh, R. M., Annis, J. E., Chang, a. N., ... Grandori, C. (2012). Functional genomics identifies therapeutic targets for MYC-driven cancer. *Proceedings of the National Academy of Sciences*. doi:10.1073/pnas.1121119109
- Tucker, K. L., Wang, Y., Dausman, J., & Jaenisch, R. (1997). A transgenic mouse strain expressing four drug-selectable marker genes. *Nucleic Acids Research*, 25(18), 3745–3746. doi:10.1093/nar/25.18.3745
- Vander Heiden, M. G. (2011). Targeting cancer metabolism: a therapeutic window opens. *Nature Reviews. Drug Discovery*, 10(9), 671–684. doi:10.1038/nrd3504
- Vander Heiden, M. G., Christofk, H. R., Schuman, E., Subtelny, A. O., Sharfi, H., Harlow, E. E., ... Cantley, L. C. (2010). Identification of small molecule inhibitors of pyruvate kinase M2. *Biochemical Pharmacology*, 79(8), 1118–1124. doi:10.1016/j.bcp.2009.12.003
- Vander Heiden, M. G., Cantley, L.C., Thompson, C. B. (2009). Understanding the Warburg Effect: the metabolic requirements of cells proliferation. *Science*, 324(5930), 1029–1033. doi:10.1126/science.1160809.Understanding
- Vazquez, A., Liu, J., Zhou, Y., & Oltvai, Z. N. (2010). Catabolic efficiency of aerobic glycolysis: the Warburg effect revisited. *BMC Systems Biology*, 4, 58. doi:10.1186/1752-0509-4-58
- Villa, R., Pasini, D., Gutierrez, A., Morey, L., Occhionorelli, M., Viré, E., ... Di Croce, L. (2007). Role of the Polycomb Repressive Complex 2 in Acute Promyelocytic Leukemia. *Cancer Cell*, 11(6), 513–525. doi:10.1016/j.ccr.2007.04.009
- Vivanco, I. (2014). Targeting molecular addictions in cancer. *British Journal of Cancer*, 111(11), 2033–2038. doi:10.1038/bjc.2014.461
- Walter, M. J., Shen, D., Ding, L., Shao, J., Koboldt, D. C., Chen, K., ... Graubert, T. a. (2012). Clonal Architecture of Secondary Acute Myeloid Leukemia. *New England Journal of Medicine*. doi:10.1056/NEJMoa1106968

- Wang, J. Bin, Erickson, J. W., Fuji, R., Ramachandran, S., Gao, P., Dinavahi, R., ... Cerione, R. a. (2010). Targeting mitochondrial glutaminase activity inhibits oncogenic transformation. *Cancer Cell*, 18(3), 207–219. doi:10.1016/j.ccr.2010.08.009
- Wang, H., Hammoudeh, D. I., Follis, A. V., Reese, B. E., Lazo, J. S., Metallo, S. J., & Prochownik, E. V. (2007). Improved low molecular weight Myc-Max inhibitors. *Molecular Cancer Therapeutics*, 6(9), 2399–2408. doi:10.1158/1535-7163.MCT-07-0005
- Wang, H., Mannava, S., & Grachtchouk, V. (2007). c-Myc depletion inhibits proliferation of human tumor cells at various stages of the cell cycle. *Oncogene*, 27(13), 1905–1915. doi:10.1038/sj.onc.1210823.c-Myc
- Wang, J. C. (2002). Cellular roles of DNA topoisomerases: a molecular perspective. *Nature Reviews. Molecular Cell Biology*, 3(6), 430–440. doi:10.1038/nrm831
- Wang, J., Hoshino, T., Redner, R. L., Kajigaya, S., & Liu, J. M. (1998). ETO, fusion partner in t(8;21) acute myeloid leukemia, represses transcription by interaction with the human N-CoR/mSin3/HDAC1 complex. *Proceedings of the National Academy of Sciences of the United States of America*, 95(18), 10860–10865. doi:10.1073/pnas.95.18.10860
- Wang, S. S., Hsiao, R., Limpar, M. M., Lomahan, S., Tran, T. A., Maloney, N. J., ... Tang, X. X. (2014). Destabilization of MYC/MYCIN by the mitochondrial inhibitors, metaiodobenzylguanidine, metformin and phenformin. *International Journal of Molecular Medicine*, 33(1), 35–42. doi:10.3892/ijmm.2013.1545
- Wang, T., Wei, J. J., Sabatini, D. M., & Lander, E. S. (2014). Genetic screens in human cells using the CRISPR-Cas9 system. *Science (New York, N.Y.)*, 343(6166), 80–4. doi:10.1126/science.1246981
- Wang, Y., & Leung, F. C. C. (2004). An evaluation of new criteria for CpG islands in the human genome as gene markers. *Bioinformatics*, 20(7), 1170–1177. doi:10.1093/bioinformatics/bth059
- Warburg, O. (1956). Injuring of Respiration the Origin of Cancer Cells. *Science*, 123(3191), 309–14. doi:10.1126/science.123.3191.309
- Weinstein, I. B., & Joe, A. (2008). Oncogene addiction. *Cancer Research*. doi:10.1158/0008-5472.CAN-07-3293
- Welch, J. S., Ley, T. J., Link, D. C., Miller, C. a., Larson, D. E., Koboldt, D. C., ... Wilson, R. K. (2012). The origin and evolution of mutations in acute myeloid leukemia. *Cell*, 150(2), 264–278. doi:10.1016/j.cell.2012.06.023

- Welin, M., Grossmann, J. G., Flodin, S., Nyman, T., Stenmark, P., Trésaugues, L., ... Lehtiö, L. (2010). Structural studies of tri-functional human GART. *Nucleic Acids Research*, 38(20), 7308–7319. doi:10.1093/nar/gkq595
- West, A. C., & Johnstone, R. W. (2014). New and emerging HDAC inhibitors for cancer treatment. *Journal of Clinical Investigation*. doi:10.1172/JCI69738
- Wheeler, D. a, Srinivasan, M., Egholm, M., Shen, Y., Chen, L., McGuire, A., ... Rothberg, J. M. (2008). The complete genome of an individual by massively parallel DNA sequencing. *Nature*, 452(7189), 872–876. doi:10.1038/nature06884
- Whitehurst, A. W., Bodemann, B. O., Cardenas, J., Ferguson, D., Girard, L., Peyton, M., ... White, M. a. (2007). Synthetic lethal screen identification of chemosensitizer loci in cancer cells. *Nature*, 446(7137), 815–819. doi:10.1038/nature05697
- Whittaker, S. R., Theurillat, J. P., Van Allen, E., Wagle, N., Hsiao, J., Cowley, G. S., ... Garraway, L. a. (2013). A genome-scale RNA interference screen implicates NF1 loss in resistance to RAF inhibition. *Cancer Discovery*, 3(3), 350–362. doi:10.1158/2159-8290.CD-12-0470
- Wijermans, P., Lübbert, M., Verhoef, G., Bosly, A., Ravoet, C., Andre, M., & Ferrant, A. (2000). Low-dose 5-Aza-2'-deoxycytidine, a DNA hypomethylating agent, for the treatment of high-risk myelodysplastic syndrome: A multicenter phase II study in elderly patients. *Journal of Clinical Oncology*, 18(5), 956–962.
- Wijermans, P. W., Lübbert, M., Verhoef, G., Klimek, V., & Bosly, a. (2005). An epigenetic approach to the treatment of advanced MDS; the experience with the DNA demethylating agent 5-aza-2'-deoxycytidine (decitabine) in 177 patients. *Annals of Hematology, Supplement*, 84(13), 9–17. doi:10.1007/s00277-005-0012-1
- Winding, P., & Berchtold, M. W. (2001). The chicken B cell line DT40: A novel tool for gene disruption experiments. *Journal of Immunological Methods*, 249(1-2), 1–16. doi:10.1016/S0022-1759(00)00333-1
- Xiang, Y., Stine, Z. E., Xia, J., Lu, Y., O'Connor, R. S., Altman, B. J., ... Dang, C. V. (2015). Targeted inhibition of tumor-specific glutaminase diminishes cell-autonomous tumorigenesis. *The Journal of Clinical Investigation*, 125(6), 2293–306. doi:10.1172/JCI75836
- Xue, W., Chen, S., Yin, H., Tammela, T., Papagiannakopoulos, T., Joshi, N. S., ... Jacks, T. (2014). CRISPR-mediated direct mutation of cancer genes in the mouse liver. *Nature*, 3–7. doi:10.1038/nature13589
- Yang, S., Tutton, S., Pierce, E., & Yoon, K. (2001). Specific double-stranded RNA interference in undifferentiated mouse embryonic stem cells. *Molecular and Cellular Biology*, 21(22), 7807–7816. doi:10.1128/MCB.21.22.7807-7816.2001

- Younes, A., Sureda, A., Ben-Yehuda, D., Zinzani, P. L., Ong, T. C., Prince, H. M., ... Engert, A. (2012). Panobinostat in patients with relapsed/refractory Hodgkin's lymphoma after autologous stem-cell transplantation: Results of a phase II study. *Journal of Clinical Oncology*, 30(18), 2197–2203. doi:10.1200/JCO.2011.38.1350
- Zaza, G., Cheok, M., Krynetskaia, N., Thorn, C., Stocco, G., Hebert, J. M., ... Altman, R. B. (2010). Thiopurine pathway. *Pharmacogenetics and Genomics*, 20(9), 573–574. doi:10.1097/FPC.0b013e328334338f
- Zeng, Y., Wagner, E. J., Cullen, B. R., & Carolina, N. (2002). Both natural and designed micro RNAs can inhibit the expression of cognate mRNAs when expressed in human cells. *Mol Cell*, 9(6), 1327–1333. doi:10.1016/S1097-2765(02)00541-5
- Zhang, J., Ding, L., Holmfeldt, L., Wu, G., Heatley, S. L., Payne-Turner, D., ... Mullighan, C. G. (2012). The genetic basis of early T-cell precursor acute lymphoblastic leukaemia. *Nature*. doi:10.1038/nature10725
- Zhong, D., Liu, X., Schafer-Hales, K., Marcus, A. I., Khuri, F. R., Sun, S.-Y., & Zhou, W. (2008). 2-Deoxyglucose induces Akt phosphorylation via a mechanism independent of LKB1/AMP-activated protein kinase signaling activation or glycolysis inhibition. *Molecular Cancer Therapeutics*, 7(4), 809–817. doi:10.1158/1535-7163.MCT-07-0559
- Zhong, D., Xiong, L., Liu, T., Liu, X., Liu, X., Chen, J., ... Zhou, W. (2009). The glycolytic inhibitor 2-deoxyglucose activates multiple prosurvival pathways through IGF1R. *Journal of Biological Chemistry*, 284(35), 23225–23233. doi:10.1074/jbc.M109.005280
- Zhou, H., Xu, M., Huang, Q., Gates, A. T., Zhang, X. D., Castle, J. C., ... Espeseth, A. S. (2008). Genome-scale RNAi screen for host factors required for HIV replication. *Cell Host & Microbe*, 4(5), 495–504. doi:10.1016/j.chom.2008.10.004
- Zhou, M., Zhao, Y., Ding, Y., Liu, H., Liu, Z., Fodstad, O., ... Tan, M. (2010). Warburg effect in chemosensitivity: targeting lactate dehydrogenase-A re-sensitizes taxol-resistant cancer cells to taxol. *Molecular Cancer*, 9, 33. doi:10.1186/1476-4598-9-33
- Zhu, X., Dai, Y., Chen, Z., Xie, J., Zeng, W., Lin, Y., & Tan, Q. (2013). Knockdown of ECHS1 protein expression inhibits hepatocellular carcinoma cell proliferation via suppression of Akt activity. *Critical Reviews in Eukaryotic Gene Expression*, 23(3), 275–82. Retrieved from <http://www.ncbi.nlm.nih.gov/pubmed/23879543>
- Zhu, X.-S., Gao, P., Dai, Y.-C., Xie, J.-P., Zeng, W., & Lian, Q.-N. (2014). Attenuation of enoyl coenzyme A hydratase short chain 1 expression in gastric cancer cells inhibits cell proliferation and migration in vitro. *Cellular and Molecular Biology Letters*, 19(4). doi:10.2478/s11658-014-0213-5

- Zielke, H. R., Zielke, C. L., & Ozand, P. T. (1984). Glutamine: a major energy source for cultured mammalian cells. *Federation Proceedings*, 43(1), 121–125.
- Zimmermann, J., Buchdunger, E., Mett, H., Meyer, T., & Lydon, N. B. (1997). Potent and selective inhibitors of the Abl-kinase: Phenylaminopyrimidine (PAP) derivatives. *Bioorganic and Medicinal Chemistry Letters*, 7(2), 187–192. doi:10.1016/S0960-894X(96)00601-4
- Zogg, C. K. (2014). Phosphoglycerate dehydrogenase: potential therapeutic target and putative metabolic oncogene. *Journal of Oncology*, 2014, 524101. doi:10.1155/2014/524101
- Zuber, J., McJunkin, K., Fellmann, C., Dow, L. E., Taylor, M. J., Hannon, G. J., & Lowe, S. W. (2011). Toolkit for evaluating genes required for proliferation and survival using tetracycline-regulated RNAi. *Nature Biotechnology*, 29, 79–83. doi:10.1038/nbt.1720
- Zuber, J., Radtke, I., Pardee, T. S., Zhao, Z., Rappaport, A. R., Luo, W., ... Lowe, S. W. (2009). Mouse models of human AML accurately predict chemotherapy response. *Genes & Development*, 23(7), 877–89. doi:10.1101/gad.1771409
- Zuber, J., Rappaport, A. R., Luo, W., Wang, E., Chen, C., Vaseva, A. V., ... Lowe, S. W. (2011). An integrated approach to dissecting oncogene addiction implicates a Myb-coordinated self-renewal program as essential for leukemia maintenance. *Genes Dev*, 25(15), 1628–1640. doi:10.1101/gad.17269211
- Zuber, J., Rappaport, A. R., Luo, W., Wang, E., Chen, C., Vaseva, A. V., ... Lowe, S. W. (2011). An integrated approach to dissecting oncogene addiction implicates a Myb-coordinated self-renewal program as essential for leukemia maintenance. *Genes & Development*, 25(15), 1628–40. doi:10.1101/gad.17269211
- Zuber, J., Shi, J., Wang, E., Rappaport, A. R., Herrmann, H., Sison, E. a, ... Vakoc, C. R. (2011). RNAi screen identifies Brd4 as a therapeutic target in acute myeloid leukaemia. *Nature*, 478(7370), 524–8. doi:10.1038/nature10334

I endeavored to ascertain the copyright holders of all illustrations and secure their consent to the utilization of their illustrations in the present paper. If, in spite of my efforts, a copyright infringement should have occurred, I kindly request the relevant parties to contact me.

## 7 CV

### **Curriculum vitae**

Name: Thomas Hoffmann

Place of birth: Vienna, Austria

Nationality: Austrian

### **Education**

2011 – 2015 PhD thesis (IMP Vienna PhD Program)

2010 – 2011 Diploma thesis, Ludwig Boltzmann Institute for Cancer research, in the Group of Prof. Dr. Robert Eferl

2010 – 2006 Master studies of Molecular Biology, University of Vienna, Austria; main subjects: Cell Biology & Molecular Medicine & Immunology

2000 – 2005 HTL Rosensteingasse, Biochemistry and Biotechnology

## Publications

B. Grabner, L. Blaas, M. Musteanu, T. Hoffmann, A. Birbach, R. Eferl, and E. Casanova, "A mouse tool for conditional mutagenesis in ovarian granulosa cells," *Genesis*, vol. 48, no. 10, pp. 612–617, Oct. 2010.

M. Musteanu, L. Blaas, R. Zenz, J. Svinka, T. Hoffmann, B. Grabner, D. Schramek, H.-P. Kantner, M. Müller, T. Kolbe, T. Rülcke, R. Moriggl, L. Kenner, D. Stoiber, J. M. Penninger, H. Popper, E. Casanova, and R. Eferl, "A mouse model to identify cooperating signaling pathways in cancer," *Nature Methods*, vol. 9, no. 9, pp. 897–900, Sep-2012.

C. Fellmann, T. Hoffmann, V. Sridhar, B. Hopfgartner, M. Muhar, M. Roth, D. Y. Lai, I. a M. Barbosa, J. S. Kwon, Y. Guan, N. Sinha, and J. Zuber, "An optimized microRNA backbone for effective single-copy RNAi," *Cell Rep.*, vol. 5, no. 6, pp. 1704–1713, 2013.

J. Jurkin, T. Henkel, A. F. Nielsen, M. Minnich, J. Popow, T. Kaufmann, K. Heindl, T. Hoffmann, M. Busslinger, and J. Martinez, "The mammalian tRNA ligase complex mediates splicing of XBP1 mRNA and controls antibody secretion in plasma cells.," *EMBO J.*, pp. 1–16, 2014.

B. Grabner, D. Schramek, K. M. Mueller, H. P. Moll, J. Svinka, T. Hoffmann, E. Bauer, L. Blaas, N. Hruschka, K. Zboray, P. Stiedl, H. Nivarthi, E. Bogner, W. Gruber, T. Mohr, R. H. Zwick, L. Kenner, V. Poli, F. Aberger, D. Stoiber, G. Egger, H. Esterbauer, J. Zuber, R. Moriggl, R. Eferl, B. Györfy, J. M. Penninger, H. Popper, and E. Casanova, "Disruption of STAT3 signalling promotes KRAS-induced lung tumorigenesis.," *Nat. Commun.*, vol. 6, p. 6285, 2015.

P. Pathria, D. Gotthardt, M. Prchal-Murphy, E. Putz, M. Holcman, M. Schlederer, B. Grabner, I. Crncec, J. Svinka, M. Musteanu, T. Hoffmann, M. Filipits, W. Berger, V. Poli, L. Kenner, M. Bilban, E. Casanova, M. Müller, B. Strobl, E. Bayer, T. Mohr, V. Sexl, and R. Eferl, "Myeloid STAT3 promotes formation of colitis-associated colorectal cancer in mice," *Oncoimmunology*, vol. 4, no. 4, p. e998529, 2015.

G. Wedeh, S. Cerny-Reiterer, G. Eisenwort, H. Herrmann, K. Blatt, E. Hadzijusufovic, I. Sadovnik, L. Müllauer, J. Schwaab, T. Hoffmann, J. E. Bradner, D. Radia, W. R. Sperr, G. Hoermann, A. Reiter, H.-P. Horny, J. Zuber, M. Arock, and P. Valent, "Identification of bromodomain-containing protein 4 (BRD4) as a novel marker and epigenetic target in mast cell leukemia," *Leukemia*, vol. 4, no. April, 2015.



P. Rathert, M. Roth, T. Neumann, F. Muerdter, J. Roe, M. Muhar, S. Deswal, S. Cerny-Reiterer, B. Peter, J. Jude, T. Hoffmann, Ł. M. Boryń, E. Axelsson, N. Schweifer, U. Tontsch-Grunt, L. E. Dow, D. Gianni, M. Pearson, P. Valent, A. Stark, N. Kraut, C. R. Vakoc, and J. Zuber, „Transcriptional plasticity promotes primary and acquired resistance to BET inhibition,” Nature, in Press 07/2015.

## Conferences

**42nd Annual Scientific Meeting of the ISEH** – Society for Hematology and Stem Cells  
August 22 - August 25, 2013, The Imperial Riding School Renaissance Hotel Vienna, Austria

**MECHANISMS & MODELS OF CANCER** - August 12 – August 16, 2014, Cold spring harbor laboratories, Cold Spring Harbor Laboratory & CSH-Asia 1 Bungtown Road Cold Spring Harbor, NY 11724

## Undergraduate laboratory internships and employments

Genetics: “Analysis of putative tmt-Opsin homologs in teleosts” (2 month, Group of K. Tessmar-Raible, MFPL)

Immunology: “Production of specific probes to characterize Alzheimer’s disease in an animal model” (2 month, Group of M. Mandler, AFFiRiS AG)

Molecular Medicine: “Applications of NextGen Sequencing (Solexa Sequencing) in Molecular Medicine: Massive parallel sequencing of SNPs and genome wide sequencing of transcription factor binding sites (ChIPSeq)” (2 month, Genomics Department IMP/IMBA, A. Sommer, P. Steinlein)

AFFiRiS AG: During all my undergraduate studies I was working 10 hours per week at AFFiRiS AG, a company developing vaccines against Alzheimer’s disease, Parkinson’s disease and Atherosclerosis. I was responsible for fixation, embedding and sectioning of mouse brains. In the following, I did several immunohistochemical stainings on the sections.

**Supervised students**

Anna Łabno, summer student, July - August 2011

Richard Pentz, Diploma student, February 2013 – January 2014